TNFalpha-signaling in drug-induced liver injury

Fredriksson, L.E.

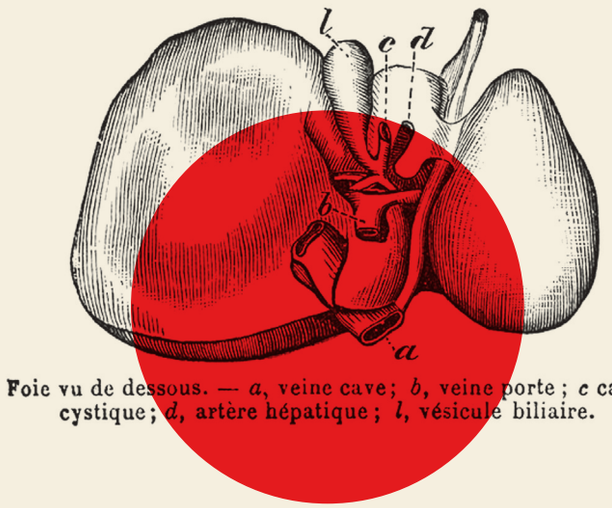

Foie vu de dessous. — *a*, veine cave; *b*, veine porte ; *c* canal cystique ; *d*, artère hépatique ; *l*, vésicule biliaire.

TNFα-SIGNALING IN DRUG-INDUCED LIVER INJURY

Lisa Fredriksson

2012

TNFα-SIGNALING IN DRUG-INDUCED LIVER INJURY

Lisa Fredriksson

2012

Stellingen

behorende bij het proefschrift

TNFα-signaling in drug-induced liver injury

1. Chemicals that show strong Nrf2 activation as well as a perturbation of NF-κB signaling have a significant drug-cytokine cytotoxic synergy, which is predictive for DILI (*this thesis*).

2. Enhanced drug-induced translation processes initiate PERK-mediated CHOP signaling, thereby sensitizing towards caspase-8-dependent TNFα-induced apoptosis (*this thesis*).

3. The de(ubiquitinase) A20 is a master regulator in the life-death decision upon TNFα stimulation in drug-induced hepatotoxic responses, which, in turn, is kept under control by a network of genes that control its expression level (*this thesis*).

4. TNFα enhancement of diclofenac cytotoxicity in HepG2 cells is an excellent model system to study the detailed molecular mechanism(s) of inflammatory stress signaling in DILI (*this thesis*).

5. Early gene expression is not dependent on the inducing signal intensity, whereas the expression of later genes requires persistent nuclear localizations of the transcription factor (NF-κB) (Tay *et al*, Nature 2010).

6. Increased activation of hepatic Nrf2 is more important for the detoxification and elimination of electrophiles than reactive oxygen species (Reisman *et al*, Toxicological Sciences, 2009).

7. The liver injury induced by drug/LPS co-exposure can be reproduced by substituting TNFα administration for LPS, which supports the critical importance of this cytokine in the pathogenesis (Shaw *et al*, Journal of Pharmacology and Experimental Therapeutics, 2009).

8. Hepatic cytotoxicity responses are governed by multi-pathway signaling network balance (Cosgrove *et al*, Molecular Biosystems, 2010).

9. One has to dare exposing him-/herself to the unknown in order to be successful and be able to move forward, both in science and in life.

10. Patience is a virtue…also when trypsinizing HepG2 cells.

11. It is fascinating how many and complex processes are needed for life to exist. But it is even more fascinating how seldom they actually fail.

12. It is wise to know what you are looking for, before you start looking for it (Winnie the Pooh).

Lisa Fredriksson, Leiden, 6 December 2012

TNFα-signaling in drug-induced liver injury

Lisa Fredriksson

TNFα-signaling in drug-induced liver injury
Lisa Fredriksson
December 2012

ISBN: 978-94-6182-196-6

Cover: Ramon Garriga Caamaño, www.gratstudio.com

Printed by Off Page, Amsterdam, the Netherlands

TNFα-signaling in drug-induced liver injury

Proefschrift

ter verkrijging van
de graad van Doctor aan de Universiteit Leiden,
op gezag van Rector Magnificus prof. mr. P.F. van der Heijden,
volgens besluit van het College voor Promoties
te verdedigen op donderdag 6 December 2012
klokke 15.00 uur

door

Lisa Emilia Fredriksson

geboren te Uppsala, Zweden
in 1984

PROMOTION COMMITTEE

Promotor:

Prof. Dr. B. van de Water	LACDR, Leiden

Overige leden:

Prof. Dr. M. Danhof	LACDR, Leiden
Prof. Dr. J. Kuiper	LACDR, Leiden
Prof. Dr. A. Ijzerman	LACDR, Leiden
Prof. Dr. N. Vermeulen	LACDR, Amsterdam
Prof. Dr. J.G. Hengstler	IfADo, Dortmund, Germany

The investigations described in this thesis were performed at the Division of Toxicology of the Leiden/Amsterdam Center for Drug Research, Leiden University, Leiden, the Netherlands

Till mina föräldrar

TABLE OF CONTENTS

1

Intracellular signaling in drug-induced liver injury

Lisa Fredriksson and Bob van de Water

1. ADVERSE DRUG REACTIONS

Adverse drug reactions (ADRs) constitute an important issue both in clinic and for the drug-industry. 5% of the hospital admissions in Europe are due to adverse drug reactions and in 2008 this was estimated to cost the society a total of €79 billion (source: Annex 2 of the report on the impact assessment of strengthening and rationalizing EU Pharmacovigilance, 2008).

Some decades ago, the major reasons for drug attrition were based on poor pharmacokinetic and bioavailability. While these drug development problems were tackled, 10 years ago this had shifted towards increased issues with clinical safety and toxicology, which was the underlying reason for ~30% of the compound withdrawals (1).

The development of a new drug is estimated to cost about 1 billion dollars (2), the cost for the society is significant if adverse drug reactions lead to hospitalization and, even more importantly, the ADRs cause a lot of suffering for the individuals affected. Therefore it is of outmost importance to improve our understanding of the underlying mechanisms of adverse drug reactions and integrate this knowledge in pre-clinical safety testing strategies of new medicines.

The most common type of adverse drug reactions, and the most common cause of drug withdrawal is drug-induced liver injury (DILI) (3,4). Moreover, DILI is the leading cause of acute liver failure in the Unites States with paracetamol (acetaminophen) accounting for about 50% of those cases and other adverse drug reactions (mostly idiosyncratic; see below) accounting for another 10% (5). This thesis will focus on mechanisms of DILI.

2. DRUG-INDUCED LIVER INJURY (DILI)

The reason why the liver is a critical target organ for adverse drug reactions is not surprising. The liver has the highest exposure to oxygen and nutrient rich blood, it is equipped with highest drug metabolizing capacity in the body to enhance excretion of xenobiotics. The first-pass effect ensures that the liver is the first organ exposed to anything that is ingested.

In addition to the drug metabolism capacity, the liver is an essential organ for clearance of circulating pathogens and products thereof. Thus, the liver contains the largest amount of resident macrophages (in the liver called Kupffer cells) and natural killer cells, which upon activation can produce large amounts of cytokines and chemokines (6) to activate the systemic immune systems. As a consequence the liver cells may also be exposed to not only toxic drug metabolites but also inflammatory cytokines, which potentially could act synergistically to increase the risk for the DILI.

DILI can roughly be classified into two types, intrinsic and idiosyncratic. Intrinsic DILI is generally dose-dependent, predictable and related to the pharmacological action of the drug, with an example being hepatotoxicity after paracetamol overdose. But only

a minority of the clinically associated DILIs is dose-dependent and predictable. In a pharmacological and toxicological context ''idiosyncratic'' DILI (iDILI) means that the adverse reaction to a drug is particular to a certain individual, involving risk factors such as gender, age, concomitant disease and genetic background (4). In concrete terms this means that the adverse drug reaction in question is unexplainable, rare (about 1 in 10,000-100,000 people who take the drug), occurring with variable times of onset and that it is typically non-related to the dose, although this can be discussed since drugs with a dosing of more than 50 mg/day is related to a higher incidence of iDILI (7-9). For the drug-industry iDILI is extremely difficult to foresee and prevent. The rarity and the unpredictability often lead to the adverse reactions only being recognized after the release of the drug to the market when many patients have been exposed. This commonly results in the withdrawal of the product or a restricted use. This causes both financial harm to the industry and unmet needs for patients that would otherwise benefit from this medication (7). Examples of drugs that induce iDILI are carbamazepine, diclofenac, ketoconazole and nefazodone (3,10). The mechanisms behind idiosyncratic DILI are incompletely understood but there are however, several hypotheses behind their incidence.

3. MECHANISTIC WORKING MODELS FOR IDILI

The formation of reactive intermediates during drug metabolism on the one hand and the activation of the immune system (innate and/or adaptive) on the other, are thought to represent the two most critical events in the pathogenesis of DILI (4,9,11). The hapten, danger and pharmacologic interaction (p-i) hypothesis has long been described as the primary working models for iDILI. These working models for iDILI will be discussed below also taking additional cellular stress responses and inflammatory stress conditions into consideration.

3.1 Adaptive immunity – allergic hepatotoxicity

3.1.1 Hapten hypothesis

Small molecules with a mass of less than 1,000 daltons are unable to induce an immune response unless they are bound to macromolecules, including proteins. Landsteiner already proposed this in 1935 (12) and it forms the basis of the hapten hypothesis to describe the occurrence of iDILI. This hypothesis also has its foundation in the fact that some DILIs are presented with an allergic response including fever, rash and the presence of circulating autoantibodies (3).

In the context of DILI, reactive drug metabolites formed in the liver can bind to cellular proteins that can subsequently act as haptens causing initiation of an adaptive immune response. In a first exposure, the immune system recognizes such a hapten and becomes sensitized towards it. Upon re-challenge, the hapten-exposing tissue is attacked by the immune system involving a strong sterile inflammation reaction and exposure

of target cells to for example reactive oxygen species (ROS), cytotoxic cytokines and proteases, thereby causing severe tissue damage (11). A classical example is the allergic reaction to penicillin. The penicillin molecule contains a reactive group that can bind to proteins and in some patients this result in an immune response against the penicillin-protein complex (11,13).

Idiosyncratic DILIs, such as the one caused by diclofenac and carbamazepine, have also been associated with T-cell activation and production of antibodies against drug-adducted proteins, which would support the role of haptenization and activation of the adaptive immune system in iDILI (11,14-16). As individuals may vary in the way they develop an adaptive immune response to a specific antigen this could explain the rarity of iDILI, and make the adaptive immune system an attractive target to understand iDILI.

3.1.2 P-i concept

The p-i concept (direct pharmacological interaction of drugs with immune receptors) is an alternative to the hapten hypothesis. According to this theory, iDILI is the result of a drug's ability to stimulate the T-cell receptor without hapten-protein formation and subsequent antigen presentation by antigen presenting cells (APCs) (17). The p-i concept was first developed after the observation that T-cells from sulfamethoxazole-sensitive patients, recognized the drug itself and not a protein adducted by the drug (18). Nowadays more drugs have been associated with this hypothesis, including carbamazepine (19). In some cases, the immunological evidence can not be explained by drug metabolism and the hapten model (20). The p-i concept then favors a iDILI working model whereby drugs do not require drug metabolism followed by covalent modification of target proteins to cause an immune response.

3.1.3 Danger hypothesis

The danger hypothesis is a modified version of the hapten hypothesis and it was first described by Matzinger in 1994 (21). It proposes that the major determinant whether an immune response is elicited against a drug or not is if this drug induces some type of cell damage by itself already (22). The fundamental step leading to an adaptive immune response is recognition by T-cells of processed antigens presented on the major histocompatibility complex (MHC; in humans human leukocyte antigen [HLA]) of APCs, for example macrophages. In addition to this first signal, a second one is needed for a fulminant immune response. If this is not presented, the result is tolerance to the presented antigen.

Activation of APCs leads to up-regulation of co-stimulatory molecules that would induce this second, activating signal. The activation of APCs can occur via several mechanisms but the most attractive one, in this context, is indeed that injured cells (by drugs and drug metabolites) provide the APCs a "danger signal". This danger signal could include the secretion of heatshock proteins, the nuclear protein high mobility group box 1 (HMGB1) and the calcium binding S100 proteins (23-25). However, other examples of danger signals, non-related to cellular damage, could be concomitant bacterial or viral

infections, or secreted cytokines (26). This type of allergic hepatotoxicity is for example more common in HIV patients (27) and especially in patients with concomitant hepatitis B or C infection (28), which would further support the need for a danger signal in the induction of DILI as well as generally supporting the hypothesis that an activated immune system might affect the drug toxicity (9).

Due to frequent exposure to circulating and absorbed antigens in the liver, and the large amount of immune cells present in this organ, adaptation is crucial to avoid a hyper-activated immune system. Importantly, the response in the liver is usually adaptation (4,6). Yet, failure of an adaptation response could be another susceptibility factor for the development of iDILI. It is likely that cytokines play an important role in the balance of either promoting a tolerogenic or a pathogenic response to drug-protein adducts (26).

3.2 Mitochondrial dysfunction hypothesis

The mitochondria can be the direct intracellular target of drug toxicity as well as the reason for patient susceptibility to DILI (29). Gradual accumulating mitochondrial damage could explain the temporal onset of iDILI; it might happen faster in certain individuals than in others due to genetic or acquired mitochondrial abnormalities (30). Moreover, mutations in mitochondrial DNA seem associated with DILI caused by certain drugs (9,29).

As an example, superoxide dismutase (SOD2) is a protein that is located in the mitochondria where it plays a critical role in detoxifying superoxide anion radicals that are constantly being formed during electron transport in the respiratory chain, an essential step for cellular energy production. Heterozygous $SOD2^{+/-}$ mice exhibit a similar phenotype to susceptible humans in the sense that the “mutation” goes unnoticed until there is a drug exposure leading to mitochondrial damage by enhanced mitochondrial oxidative stress. Troglitazone-induced hepatotoxicity, which goes typically unnoticed in “normal” animal models, has been shown to involve mitochondrial damage in this mouse-model and drug exposure led to a late onset of hepatic necrosis, mimicking a human iDILI process (31).

For mitochondria to get fatally damaged, certain thresholds need to be reached at multiple levels. For example inhibition of the different complexes in the electron transport chain needs to reach more than 50% to affect the ATP production, and about 60% of the mitochondrial DNA must be deleted before this has an overt effect (30). This is called the mitochondrial threshold effect and might also explain the lag time of iDILI since it will likely take a long time for the critical thresholds to be reached after drug exposure. The results obtained with the $SOD^{+/-}$ mice described above represents an interesting model for studying the role of the threshold effect in iDILI.

3.3 Inflammatory stress hypothesis

Inflammatory infiltrates are common in patients suffering from iDILI. This raised the possibility that some idiosyncratic reactions might be explained by episodes of modest

inflammation (32,33). Conditions associated with inflammation include arthritis, atherosclerosis, infection by bacteria and virus, immune responses to certain antigens etc. However, activation of the innate immune response could also be elicited by apoptotic and necrotic hepatocytes and their release of so-called damage-associated molecular pattern molecules such as heat shock proteins (4), as described above in the section about the danger hypothesis, and thereby lead to inflammatory stress.

The underlying mechanism of sensitization to DILI by viral infections remains unknown. Possibly the mechanism includes activation of the innate immune system, whereby secreted cytokines and chemokines are important components of an anti-viral response (34). These cytokines might then modulate the extent of inflammation and, thereby, control the levels of injury (26).

The balance between the secretion of protective cytokines like IL-6 and IL-10 and injurious ones like TNFα, FasL, IL-1β and IFN-γ have also been implicated in the development of iDILI and genetic circumstances that could make the balance tip one way or the other could be detrimental (3,4).

Another source of innate immune system activation are bacterial endotoxins released from the intestines into the circulation. The magnitude of such endotoxin release may vary depending on different factors such as diet and alcohol consumption (33). This could also explain the random temporal onset of iDILI as well as the rare incidence. Animal models have been developed to simulate this scenario using the Gram-negative bacterial endotoxin lipopolysaccharide (LPS). Injection of LPS to animals in this model has rendered an otherwise non-toxic dose of a drug known to cause iDILI in humans, toxic (7). This LPS co-exposure model is also the first animal model to mimic the pronounced liver injury seen in patients with iDILI (7). Examples of drugs that have been used and proven toxic in such a model include diclofenac, amiodarone, sulindac and trovafloxacin (35-38). Importantly, the pro-inflammatory cytokine tumor necrosis factor alpha (TNFα) has been determined the most important mediator of the toxicities observed. Inhibition of TNFα transcription significantly reduced trovafloxacin/LPS induced liver injury indicating that the hepatotoxicity is largely TNFα dependent (38) and the same was shown for sulindac using a soluble TNFα-receptor to inactivate the cytokine, etanercept (37), emphasizing the important role for cytokines and cytokine-induced signaling in iDILI.

3.4 Multiple-determinant hypothesis

The above hypotheses are not mutually exclusive. It is more likely that they are all individual parts of a complex puzzle that provides a complete mechanistic understanding of human iDILI. A combination of many factors would support the sporadic occurrence of iDILI, and provide a condition whereby the risk of developing iDILI would be the product of all the different mechanistic risk factors taken together (3,34). As a summary of this we foresee an overall working model whereby the main susceptibility determinants for the development of iDILI include the biochemical properties of the drug, environmental factors, genetic factors, and immune system components.

Potential genetic factors include for example polymorphisms in drug-metabolizing enzymes and mutations that determine sensitivity to mitochondrial damage and to inflammatory stresses. Environmental factors could include exposures to inducers of drug metabolism and viral/bacterial products (7).

Because of their rarity and unpredictability, iDILIs are thought to depend largely on genetic variation (9). The most apparent example is provided by the highly variable human leukocyte antigen (HLA) system. This plays a key role in delayed immune-mediated adverse drug reactions, including DILI, since it is involved in the T-cell recognition of the drug-induced antigen (9,39,40). For some reactions, for example abacavir hypersensitivity, one single gene locus (HLA-B*5701) can provide adequate predictive accuracy to allow the gene to be used in a clinical setting as a biomarker for the risk of idiosyncratic adverse drug reactions (41,42). A correlation with HLA polymorphism has also been found for more drugs, including the antibiotics amoxicillin-clavulanate and flucloxacillin (40). For most other drugs there are likely correlations between polymorphisms in single gene and specific adverse drug reactions. Yet, it seems more plausible that such individual gene polymorphism are insufficient to significantly increase the susceptibility for ADR, but rather would act in combination with other genes (43).

4. INTRACELLULAR STRESS SIGNALING IN IDILI

Since both drug metabolism-dependent cell injury responses as well as immune-mediated responses are critical components of iDILI, a cross-talk between drug-induced and cytokine-induced intracellular signaling events that enhances the drug-toxicity in certain individuals is likely to occur. In the following paragraphs these two responses and their cellular consequences will be described.

4.1 Drug-induced intracellular stress signaling

4.1.1 The role of drug-metabolism

Drugs are generally designed as hydrophobic molecules to allow proper absorption into the body after oral intake. Biotransformation reactions are essential to metabolize these molecules into more hydrophilic compounds that can easily be eliminated via the urine or the bile. Most of this xenobiotic metabolism occurs in the liver. The primary biotransformation of drugs involves the cytochrome P450 (CYP450) oxidase system, consisting of over 100 different family members (44). Typically, drug metabolism leads to their inactivation and ultimate elimination. But alternatively it leads to the formation of reactive moieties that can then covalently bind to cellular macromolecules, and as a consequence disturb the intracellular homeostasis or induce oxidative stress and thereby cause cellular damage (3,45).

Drugs that are being metabolized have a significantly higher risk of causing iDILI (46) and the formation of harmful reactive metabolites is an anticipated main mechanism behind DILI (4,11,45,47). In addition, polymorphisms in drug metabolizing and detoxifying

enzymes are related to increased incidence of this type of adverse drug reactions (9,48). Further support for biotransformation as a mechanism is based on the association of iDILI with dosages higher than 50 mg/day, which would result in higher absolute levels of metabolites formed than with a lower daily dosing. However, importantly, inability to metabolize can also lead to toxicity as this most likely leads to decreased elimination, and thereby the possibility for enhanced, toxic, levels of the parent drug (47).

Not only oxidative metabolism by CYP450s has been shown to form reactive intermediates, but also conjugation reactions (phase II metabolism). Thus, acyl-glucuronide formation has been linked to DILI (45,49). Diclofenac is a good example here since the acyl-glucuronides and not the CYP produced hydroxyl-metabolites are linked to diclofenac-induced iDILI (15,49). In addition, a genetic variant of the enzyme that produces the diclofenac acyl-glucuronide, uridine diphosphate glucuronosyl-transferase 2B7 (UGT2B7), has been shown to significantly contribute to the risk of developing diclofenac-induced DILI (50).

Many drugs are being metabolized into reactive species, however, clearly not all of them cause hepatotoxicity. The reason for this is the tight association between bioactivation and detoxifying enzyme systems. Examples of inactivation systems are glutathione *S*-transferases (GSTs) and their conjugation of glutathione (GSH) to reactive molecules as well as other reactive oxygen species (ROS) involved in downstream hepatotoxic mechanisms. Interestingly, double mutations in two relevant GSTs (GSTT1 and GSTM1) have been linked to troglitazone hepatotoxicity in Japanese patients (51). In the case of reactive metabolite formation cytotoxicity will only occur when the (adaptive) detoxifying defense systems are saturated or fail (45).

Formation of protein adducts is implicated in the toxicity of many drugs including paracetamol. Moreover, protein adduct formation seems correlated with higher incidence of iDILI (52). If the adducts are formed on proteins critical for certain cellular functions and signaling pathways, it increases the likelihood of inhibiting/activating critical cellular functions eventually resulting in cytotoxicity (45,53). Additionally, if adduct formation occurs on proteins that are subsequently presented to the immune system, an adaptive immune response can be elicited (see above). However, protein adduction does not *per se* mean enhanced toxicity. A good example of this is the difference observed between paracetamol and its regioisomer 3'-hydroxyacetanilide (AMAP). Parecetamol is liver toxic while AMAP is not, but interestingly, both drugs cause similar levels of total cellular protein adduction. However, paracetamol causes mitochondrial protein adduct formation, while AMAP does not, which possibly explains their difference in toxicity (54). This underlines the critical requirement of gaining more mechanistic information about the exact cellular targets modified by covalent binding (45) and the resulting cellular injury such as mitochondrial damage or oxidative stress (4). Although, it might be tempting to completely abandon the chemical entities in (candidate) drugs that show covalent binding, this will not always offer a solution since some drugs, like penicillins and omeprazole, are dependent on covalent binding for their efficacy (45).

New techniques involving mass spectrometry and glutathione trapping are

fruitful in identifying the structures of reactive intermediates that are formed in the course of drug metabolism and their intrinsic potential to cause hepatotoxicity (55). In addition, identifying critical residues within proteins that become adducted and that leads to protein inactivation, as well as which proteins become adducted, adds another importance to these types of studies (45,56,57).

4.1.2 Mitochondrial damage

The role of mitochondria in hepatocellular death can be either direct by drug accumulation, inhibition of electron transport or depletion of antioxidant defense mechanisms, or indirect by the activation of different signaling pathway that affect the mitochondrial integrity and, thereby, the cell survival outcome (30).

Hepatocytes have many mitochondria that besides taking care of the energy supply of the cell ensuring cell survival, play a role in the control of cell death. Mitochondria are unique organelles involved in the control of both apoptosis and necrosis. For example high pH, pro-oxidants and activation of the pro-apoptotic Bcl-2 family member Bax can lead a so-called mitochondrial membrane permeability transition (mPT) (30).

The induction of mPT leads to loss of the transmembrane potential, which is essential for ATP production. Moreover, mPT makes the mitochondria release a large pool of mitochondrial free calcium resulting in cellular calcium-overload and related cytotoxicity (58). The direct toxic targeting of all mitochondria followed by the induction of mPT is in general believed to lead to necrosis as a result of loss of cellular energy. On the contrary, more subtle mitochondrial perturbation, as described in the following paragraph, would most likely favor apoptosis (3).

Selective permeabilization of the outer mitochondrial membrane, MOMP, is induced by translocation and binding of the two pro-apoptotic Bcl-2 family members Bax and Bak to the membrane pore, leading to the release of pro-apoptotic factors that are normally located in the inter-membrane space, such as cytochrome c, apoptosis-inducing factor (AIF) and Smac/Diablo, (29,59-61). The release of cytochrome c from the mitochondrial inner membrane space leads to activation of pro-caspase-9 via formation of the so called apoptosome, which includes cytochrome c and apoptosis protease-activating factor 1 (APAF1) (62). Caspase-9 subsequently activates the effector capase-3 which cleaves several cytosolic and nuclear proteins to trigger apoptosis (63). Importantly, for the cell to undergo apoptosis the mitochondrial membrane potential needs to be retained thus ensuring enough energy for the active apoptotic process to proceed. The two factors that determine if the cell will undergo apoptosis or necrosis, is the amount of mitochondria affected and the extent of ATP depletion.

The integrity of the mitochondrial membrane is thus in large parts determined by the Bcl-2 family members. This family of proteins is composed of both pro- and anti-apoptotic members, with the former group including the already introduced Bax and Bak, and the latter for example Bcl-2 itself and Bcl-xL. The anti-apoptotic Bcl-2 family members act by binding to the pro-apoptotic ones and thereby inhibiting the release of pro-apoptotic factors (61). The Bcl-2 family members are consequently very important for

the control of life or death.

Oxidant stress is a crucial regulator of mitochondria-mediated cell death. Under normal conditions the large amount of antioxidant systems in the mitochondria will prevent any damage, but if this protective system is compromised due to genetic defects or for example drug exposure, the cellular organelles and substructures will get damaged (29). Oxidant stress can also lead to damage of the mitochondrial DNA. Since this DNA encodes specific subunits of the electron transport chain, long term problems here may involve further increased production of ROS and additional cellular damage, thus causing a vicious cycle (29). In addition, mutations in mitochondrial DNA are not uncommon in the population, although this normally does not result in damage since there are so many mitochondria present in one cell. However, under particular stress conditions, as after drug exposure, this might change if the drug of interest also targets the mitochondria (29).

Many hepatotoxic drugs, or the metabolites thereof, can interfere with the mitochondrial function (58) and this is also common with drugs associated with iDILI. Interestingly, in a study by Xu and colleagues (64), 50-60% of the 300 drugs associated with iDILI showed mitochondrial changes while 0-5% of the negative controls did not. Moreover, drugs like carbamazepine, known to cause iDILI, interferes with the mitochondrial respiration, mitochondrial membrane potential and ATP synthesis (10). Diclofenac on the other hand, is known to cause mitochondrial damage by for example the uncoupling of the oxidative phosphorylation and inhibition of complex I/III which leads to an increased mitochondrial-derived oxidative stress due to enhanced superoxide formation (29,65,66)

Mitochondrial inhibition is most likely not by itself the cause of cellular injury, however it might increase the susceptibility to other damaging factors. This includes for example depletion of the reduced glutathione (GSH) storage (34) or by stress kinases increased susceptibility of the mitochondria to induction of cell death (30). It is likely that underlying defects in mitochondrial function, possibly genetic, amplify the risk of iDILI development in certain susceptible individuals.

4.1.3 Oxidative stress

Formation of reactive oxygen species (ROS) is one of the most commonly cited cell death mechanisms in organ toxicity, including DILI (59). The most apparent sources of intracellular ROS are the electron transport chain in the mitochondria, the drug metabolizing CYP450 system, and intracellular oxidases (59). In addition, reactive metabolites originating from drug metabolism can by themselves induce oxidative stress (45). This either directly through redox cycling, or indirectly through glutathione depletion, increases the amount of reactive oxygen species as observed with APAP and diclofenac exposure (45,49,67).

Extensive ROS formation bares a problem to the cells since it increases the damage to macromolecules through protein oxidation, lipid peroxidation and DNA damage (4). Superoxides are the most reactive ROS and their main source is the mitochondrial

electron transport chain. Alternatively, drug metabolism can result in superoxide formation through the development of unstable radicals by P450 reductases, which then reacts with molecular oxygen (30).

Because of the damage that can be caused by oxidative stress, the cell has a well-developed system to deal with ROS. Superoxide dismutases (SOD1 and SOD2) are responsible for detoxifying superoxides, and glutathione peroxidases (GPXs) take care of reducing hydrogen peroxides, where the isoform GPX4 is specialized in reducing fatty acid hydroperoxides (59). In addition, small antioxidant molecules such as glutathione (GSH) constitute a very important anti-oxidant defense system by scavenging different types of ROS (59). Emphasizing the importance of this small molecule, the toxicity of drugs such as paracetamol and nevirapine can be diminished by supplementing with the glutathione precursor N-acetyl-cysteine (68). The mitochondria have their own separate GSH pool and especially depletion of this one upon drug exposure has been linked to enhanced toxicity (69). The reason for this is enhanced reactive metabolite-mediated impairment of the electron transport chain, or by other means enhanced ROS generation by mitochondria since GSH is especially important in hydrogen peroxide detoxification as a conjugation molecule for GPX (70).

Another consequence of reduced GSH levels is alterations of the protein redox status, possibly leading to altered protein function (71). However, such post-translational redox modifications of proteins can also be an important mechanism for activating or inactivating signaling pathways in hepatocytes following drug exposure. As an example, ROS can lead to inhibition of JNK phosphatases crucial for the inactivation of this pro-apoptotic stress-kinase (72). Yet, ROS also activates the anti-oxidant adaptive response through the activation of the transcription factor nuclear factor-erythroid 2 (NF-E2)-related factor 2 (Nrf2).

Factors that influence drug metabolism and detoxification are likely all critical components in iDILI. A major pathway regulating both of these processes is Nrf2-signaling. Nrf2 initiates transcription of both drug metabolizing enzymes, detoxifying enzymes and molecules, such as sulfiredoxin (SRXN1), GSTs and GSH (73,74), and is as such the most important transcription factor in the anti-oxidant response system. Under non-stressed conditions, Nrf2 is kept in the cytosol by its endogenous inhibitor Kelch-like ECH-associated protein 1 (Keap1) and thereby guided to proteasomal degradation as Keap1 acts as a substrate adaptor for the ubiquitination complex responsible for the polyubiquitination of Nrf2 (75). Many reactive drug metabolites and intermediates as well as ROS activate the Nrf2 response by reacting with the many critical cysteine residues on Keap1 (74,76-78) and thereby allowing newly synthesized Nrf2 to translocate to the nucleus. In the nucleus Nrf2 heterodimerizes with small Maf proteins and subsequently binds with high affinity to the so-called antioxidant response elements (ARE) in the promoter region of antioxidant genes (79). In support of the Keap1/Nrf2 system in the control of DILI, $Nrf2^{-/-}$ mice have been shown to be more susceptible towards paracetamol toxicity (80) while liver specific Keap1 knockout resulted in resistance against the organ damage (73).

Although overwhelming oxidative stress and mitochondrial dysfunction due to reactive metabolite formation can lead to hepatocyte death, ROS can also initiate cell injury by (in)activation of intracellular (stress) signaling (30,81,82). Whether the hepatocyte survives or dies, either by controlled apoptosis or by necrosis, is in great part determined by the balance between pro-death and pro-survival signaling pathways activated (81).

ROS has been shown to induce JNK activation, and when sustained, this activity causes cell death (82,83). Inhibition or knockdown of JNK showed protection against paracetamol-induced hepatotoxicity in mice (84) and troglitazone-induced apoptosis in cultured hepatocytes (HepG2) (85). JNK can actively promote hepatocyte cell death by translocating to the mitochondria and there promote membrane permeabilization resulting in the release of pro-apoptotic factors (30,81,86) (see above). However, active JNK does not *per se* induce mitochondrial permeabilization and cell death; most likely the mitochondria must first suffer redox-related damage (30,81). In addition, the exact mechanism by which JNK induces mitochondrial membrane permeabilisation has not been determined, but JNK has been shown to translocate to the mitochondria, and there anti-apoptotic Bcl-xL and pro-apoptotic Bax are known downstream targets of JNK (30,84,87).

Supportive for the role of extensive ROS production in iDILI is the genotypic variation in SOD2 and GPX1 in humans suffering from this drug-induced damage (48,88). This would lead to enhanced production/reduced detoxification of ROS within the mitochondria upon drug exposure leading to enhanced mitochondrial damage. In addition to this, combined deficiency of GSTT1 and GSTM1, enzymes important for catalyzing the conjugation of GSH to ROS and reactive metabolites, has been linked to troglitazone hepatotoxicity and other iDILI-inducing compounds in humans (51,89,90).

In addition to mitochondrial effects of oxidative stress, the activity of heat shock proteins (HSPs) is also enhanced after this type of stress induction. Pre-treatment with hyperthermia, which up-regulates heat shock proteins, has been shown to protect against paracetamol-induced hepatotoxicity while HSP70 knockout induced it (91), illustrating the role of these proteins in drug-induced toxicity. Heat shock proteins are chaperones that ensure proper folding of proteins, which is likely altered as a consequence of covalent binding and redox changes after drug exposure. A central organelle in which protein folding is continuously taking place is the endoplasmic reticulum.

4.1.4 Endoplasmic reticulum stress

The endoplasmic reticulum (ER) is mostly recognized for its role in protein synthesis and folding and as intracellular calcium storage. However the endoplasmic reticulum is also involved in many processes that are important in drug-induced toxicity. It is in the membrane of this organelle that the P450 enzymes, the UDP-glucuronosyltransferases (UGTs) and some GSTs that are so important in drug metabolism reside (92,93). Furthermore, the ER is now recognized as a target of reactive intermediate-mediated damage through covalent binding and the induction of oxidative stress. In addition, it is

involved in the signaling induced after such damage determining the fate of the affected cell (94).

The ER lumen has two unique properties that are relevant to drug toxicity (94). Firstly, it has an oxidizing environment relative to the cytosol, something that is critical in the oxidative protein folding but that can also contribute to the generation of oxidative stress (95). Secondly, the ER contains a much higher concentration of calcium and thereby serves as a storage for calcium which is needed for intracellular signaling (96). Severe ER stress can lead to calcium release, thereby increasing cytosolic calcium levels which enters the mitochondria to trigger mPT and MOMP and thereby cell death (97).

The ER lumen also contains proteins that are involved in ER function. The most prominent protein, which is also important in the sensing of ER stress, is the glucose-regulated protein 78 (GRP78; a heat shock protein family member also known as BiP) (98,99). This stress protein is expressed under normal conditions but the expression is enhanced by insults that disrupts ER-function and causes accumulation of unfolded proteins. GRP78 plays a crucial role in initiation of the so called unfolded protein response (UPR) in ER stress (99).

The UPR functions to counteract the ER stress in three major ways: 1) by decreasing protein synthesis to decrease the protein load in the ER (100); 2) by up-regulating chaperones (such as GRP78) to enhance the protein folding capacity (100); and 3) by increasing the activity of ER-associated degradation pathways to remove unfolded proteins (101). The initiating step to the UPR is the binding of GRP78 to the unfolded proteins in the lumen of the ER. This releases and thereby activates the signaling molecules that then transmit the intracellular signals of the UPR (102).

The UPR signaling is transduced by three ER resident proteins, which are inhibited by GRP78 in a non-stressed state; protein kinase R-like ER kinase (PERK), inositol-requiring enzyme 1-alpha (IRE-1α) and activating transcription factor 6 (ATF6). The reduction in protein synthesis is mediated by PERK-induced eIF2α phosphorylation (103). This attenuates global translation but favors translation of activating transcription factor 4 (ATF4) that induces production of proteins involved in amino acid transport and protection against oxidative stress, but most importantly, also C/EBP-homologous protein (CHOP; also known as GADD153 and DDIT3) which is an important transcription factor in ER-stress dependent apoptosis (104). The transcriptional up-regulation of genes involved in the protein processing is mediated by activation of the other ER-resident kinase and endonuclease, IRE-1α (105). Once activated IRE-1α splices X-box binding protein 1 (XBP1) mRNA yielding a mature mRNA that encodes the required transcription factor (106). The last ER stress signal transducing protein that resides in the ER membrane is ATF6. After translocating to the Golgi apparatus where it gets cleaved, ATF6 induces genes involved in for example quality control in the ER (107). These three pathways of the UPR are critical for the cell to be able to withstand disruption of normal ER homeostasis. However, if the stress is too immense the apoptotic program will be initiated.

The mitochondrial death pathway mediates ER stress-induced apoptosis, and a central modulator of this pathway is the transcription factor CHOP (104). Importantly,

CHOP overexpression by itself does not cause apoptosis (108). However, CHOP sensitizes mitochondria to pro-apoptotic signals by inhibiting the transcription of anti-apoptotic Bcl-2 (108), by transcribing pro-apoptotic Bim (109) and by disturbing the cellular redox state including depletion of cellular GSH (108). The activity of IRE-1α has also been implicated in the apoptosis induction downstream of ER-stress-induction. However, the importance of this pathway is less clear than that of CHOP (110), although it has been shown to involve the activation of JNK which results in apoptosis (111). More importantly, XBP1 splicing and protein levels decline with time of ER stress, which is associated with enhanced apoptosis, and reconstitution of IRE-1α protects against cytotoxicity (112). Also ATF6 was shown to have a protective effect, while prolonged activation of PERK including CHOP expression is what caused the ER-stress-induced apoptosis (112).

Since drugs are being metabolized and potentially bioactivated by P450 enzymes in the ER, the ER-resident proteins also serve a high risk of getting covalently adducted by these metabolites. This has been reported for both CYP-enzymes themselves, but also for other ER-related proteins such as UGTs (94,113). This binding has also been shown associated to the formation of antibodies targeting ER proteins suggesting a resulting immune related response (94).

4.2. Cytokine-induced intracellular stress signaling

Cytokines are small soluble messenger molecules that can be secreted by all types of cells in the body, although they are mainly used by the immune system and the main function of the cytokines is to regulate inflammatory responses (26). The liver can produce both hepatotoxic and -protective cytokines in response to injury and it is believed that the balance between these is what affects an individual's susceptibility to DILI. The secretion of cytokines has even been proposed as potential biomarkers of DILI, although an increased understanding of their role in the actual damage induction is required before this can be implemented (114,115).

4.2.1 The role of TNFα in DILI

TNFα is a cytokine that is mainly secreted by monocytes and activated macrophages but also T-cells (26), and in hepatic inflammation, TNFα release is one of the earliest events observed. Moreover, TNFα is secreted by the liver stationary macrophages, Kupffer cells, after contact with bacterial factors absorbed via the gastrointestinal tract to activate an immunological response as a defense mechanism (6). Interestingly, polymorphisms within the promoter region of the gene encoding this cytokine has been linked to the severity of inflammatory reactions in humans (116) although this has so far not been shown to correlate with the risk of developing DILI (117).

TNFα has been implicated in liver injuries induced by several types of drugs including paracetamol (118), trovafloxacin (38), ranitidine (119) and sulindac (37) and its role in DILI has been demonstrated using neutralizing antibodies (38,119). Other cytokines including IFNγ, also seem to play a role in DILI since neutralizing antibodies

against IFNγ as well as IFNγ$^{-/-}$ mice protected against paracetamol-induced toxicity (120). However, the proposed mechanism underlying this observation was down-regulation of other cytokines including TNFα, which further emphasizes the role of the latter cytokine in DILI.

TNFα is especially interesting in the context of toxicity due to the nature of its receptor, which can induce both direct pro-apoptotic signaling via its death domain and pro-survival signaling via activation of the nuclear factor kappa B (NF-κB) pathway. These two signaling pathways will be further discussed in the following paragraphs.

4.2.2 NF-κB signaling

Hepatocytes, like most cells are resistant to TNFα exposure due to their activation of NF-κB. NF-κB is an important transcription factor that promotes expression of anti-apoptotic genes such as Bcl-xL, cellular FLICE inhibitory protein (cFLIP) and inhibitor of apoptosis proteins (IAPs), although it is mostly recognized as a master regulator of the immune response due to its transcription of for example cytokines and adhesion molecules (121).

The NF-κB proteins are dimeric transcription factors composed of five different subunits, p65 (RelA), RelB, cRel, p50 and p52 (121,122). Under normal conditions the transcription factor is kept in the cytoplasm through masking of its nuclear localization sequence by the inhibitor of kappa B (IκB) proteins. There are two routes through which NF-κB can be activated, the classical or canonical activation route and the alternative, non-canonical route. After TNFα binding to its receptor, it is the canonical pathway that gets activated, and therefore this pathway will be in focus here. An overview of the signaling pathway can be seen in Figure 1.

After TNFα binding to its receptor, the adaptor protein TNF receptor-associated death domain (TRADD) connects with the cytoplasmic tail of the receptor, and so does the kinase receptor-interacting protein 1 (RIP1) (122,123). This leads to the recruitment of the TNF receptor associated factor 2 (TRAF2) adaptor protein (124), which in turn promotes cellular (c) IAP1 and cIAP2 association to the complex. This is an essential event for the IκB kinase (IKK) activation since this promotes the K63-linked ubiquitination of RIP1 (125) needed for IKK and TGF-β-activated kinase-1 (TAK1)/ TAK1 binding protein (TAB) complex recruitment (126). In the canonical pathway, the IKK complex consist of the catalytic subunits IKKβ (IKK2 or IKBKB), IKKα (IKK1 or CHUK) and the regulatory component IKKγ (NEMO or IKBKG). The latter is important for the binding to the K63 ubiquitin chain on RIP1 needed for activation (127). This subsequently leads to the rate-limiting and crucial step of (IKK) complex activation (128) via TAK1-mediated or auto-phosphorylation of IKK (126). The activated IKK complex then phosphorylates IκB proteins, for the canonical p65/p50 dimer the IκB-protein IκBα, resulting in its K48-linked polyubiquitination and proteasomal degradation, which subsequently leads to the nuclear translocation of NF-κB (126).

The activation of the NF-κB pathway is clearly tightly regulated by different post-translational modification steps, as illustrated above. However, this pathway is also regulated by transcriptionally mediated feedback mechanisms. IκBα is one of the

target genes of NF-κB and constitutes the most important inhibitory protein of NF-κB signaling: the newly synthesized IκBα protein transports NF-κB from the nucleus back into the cytoplasm (129). A20 is another NF-κB target gene and an important regulator of NF-κB activation by its effect on RIP1 ubiquitination (130). A20 deubiquitinates the K63-linked activating ubiquitin chains on RIP1 and it also promotes K48-linked poly-ubiquitinations that targets the protein for proteasomal degradation, resulting in inhibited NF-κB activation (131).

NF-κB and the proteins involved in NF-κB activation all contain critical cysteine residues that are important for proper function. Non-hepatotoxic doses of APAP alter the redox environment of hepatocytes which lead to the inhibition of NF-κB activation, sensitizing primary hepatocytes to TNFα-induced apoptosis (132). Also other compounds, such as hydrogen peroxide and antimycin, that affect the redox status of cells, cause hepatocyte sensitization to TNFα (133). Additionally, glutathione depletion has been linked to inhibition of NF-κB activation (134,135).

The reason why inhibition of NF-κB renders TNFα-exposure cytotoxic is due to the dual role of the TNF receptor 1. The pro-apoptotic role of this receptor will be introduced in the following section.

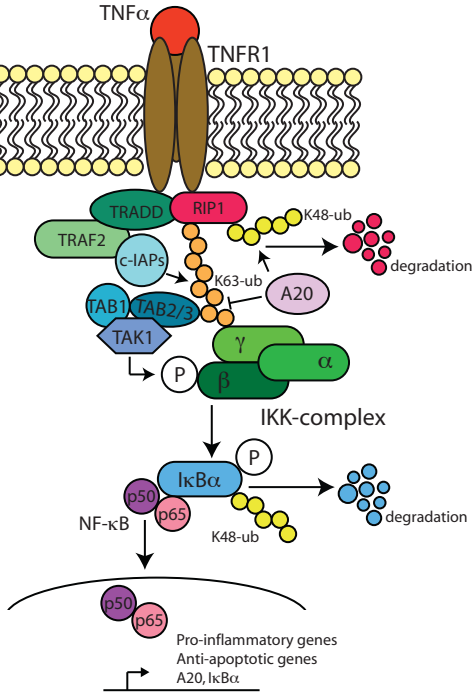

Figure 1. *NF-κB signaling downstream of TNFR1.* Upon TNFα binding to its receptor a complex sequence of protein recruitment and posttranslational modification events is initiated, ultimately leading to the rate-limiting step of IKK-complex activation by phosphorylation. The activated IKKβ then phosphorylates the inhibitor of NF-κB, IκBα, which is followed by its polyubiquitination and proteasomal degradation. This unmasks the nuclear localization signal in NF-κB, allowing nuclear translocation of the transcription factor and transcription of genes involved in for example inflammation, suppression of apoptosis and, importantly, the inhibitors of NF-signaling, IκBα and A20.

4.2.2 Pro-apoptotic death receptor signaling

There are six TNF receptor (TNFR) family death receptors, including TNFR1, and they are characterized by the presence of a death domain (DD) in their cytosolic segments (136). Under normal conditions, the pro-apoptotic signaling is not induced by TNFα exposure as the NF-κB-mediated activation of gene transcription leads to production of proteins that inhibit this pathway, such as cIAP1/2 and cFLIP (121).

RIP1 is essential for the activation of NF-κB and it is hypothesized that when RIP1 gets degraded, or not ubiquitinated by cIAP1/2 (137), this results in activation of the pro-apoptotic pathway. However, this hypothesis has not fully been proven and it is still a mystery how and when TNFα-induced signaling switches from pro-survival to pro-apoptotic (138).

What is known, though, is the basic compilation of proteins leading to the formation of the pro-apoptotic complex (see Fig. 2). Upon induction of pro-apoptotic TNFR1 signaling the TRADD adaptor protein, which is also essential for activation of the NF-κB pathway, recruits Fas-associated death domain (FADD) together with pro-caspase-8 to form the cytoplasmic pro-apoptotic complex. In the case of functional NF-κB signaling, cFLIP is also present in this complex inhibiting the activation of caspase-8 (139). Although caspase-8 can lead to direct activation of caspase-3 (140) the apoptotic signal usually needs amplification. This is achieved by caspase-8 mediated cleavage of the Bcl-2 family member Bid (141). tBid then promotes the disruption of the mitochondrial membrane integrity by Bax and Bak oligomerization (see above in the section about the role of mitochondria in DILI).

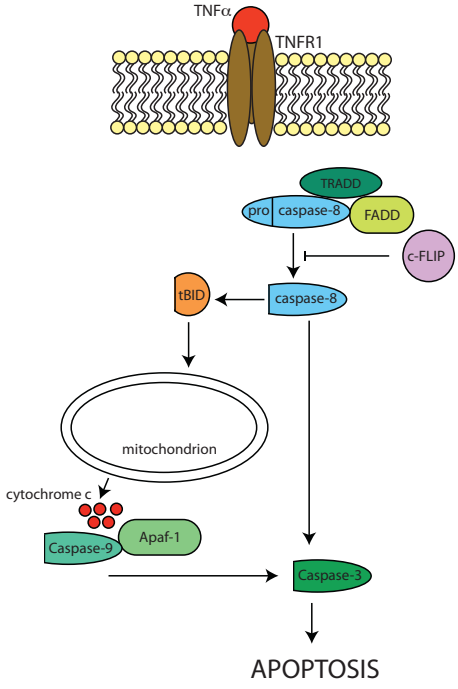

Figure 2. *Pro-apoptotic signaling downstream of TNFR1.* Unless inhibited by NF-κB transcribed genes, such as cIAPs and cFLIP, intracellular signaling induced by TNFα also leads to apoptosis. This event is initiated by TRADD dissociation from the receptor leading to FADD and pro-caspase-8 recruitment. This is followed by activation of caspase-8, which can then induce apoptosis either directly by caspase-3 cleavage or by involvement of the mitochondrial death pathway via activation of the Bcl2-family protein Bid.

5. METHODS TO STUDY CROSS-TALK BETWEEN DRUG- AND CYTOKINE-INDUCED SIGNALING IN LIVER INJURY

As already mentioned in the beginning of this chapter, it is of outmost importance to integrate a complete molecular mechanistic understanding of iDILI in advanced pre-clinical cell and animal models to identify candidate drugs that are at high risk to induce DILI. Of course relevant models to uncover these molecular mechanisms are essential to bring this project forward.

5.1 Existing *in vivo* and *in vitro* models

It has been suggested that only animal models should be able to model the complexities that iDILIs constitute (7). However, as iDILI is expected to be as rare in animal models as in humans, not any animal model would be sufficient to get a complete mechanistic understanding of these rare but serious adverse drug reactions. Most likely, a first step is to move away from healthy animal models towards more intrinsically stressed ones, especially since humans on drug treatment have at least one condition, their illness, that potentially makes them more susceptible to adverse drug reactions (142). Two animal models have received special attention in this aspect, the $SOD2^{+/-}$ heterozygous mice, used to study the role of latent mitochondrial susceptibility (143), and the LPS co-exposure model, to address the role of inflammatory stress in iDILI (7).

As animals cannot be used for drug safety screening campaigns, there is also a need for in vitro mechanism based high throughput tests that could be used in an even earlier preclinical toxicity testing phase (7). Cosgrove and colleagues presented such a model, which is analogous to the *in vivo* LPS co-exposure model developed by Roth and Ganey (144). By exposing different cell types (HepG2 cell line and primary rat as well as human hepatocytes) to known hepatotoxicants and their non-toxic counterparts, together with pro-inflammatory cytokines, they demonstrated that primarily drugs known to cause idiosyncratic DILI, displayed synergism in cytotoxicity when combined with cytokines. Important in the context of the studies presented in this thesis, TNFα was one of the cytokines that contributed most to the observed toxicity.

5.2 High content imaging

High content cellular imaging techniques provides an in vitro platform to investigate the toxicity-inducing potential of many drugs and it provides an outstanding method to determine the mechanisms behind such toxicity. The most beneficial aspects is the possibility to see what is happening to the cells in time after drug exposure in a non-invasive way that does not require many sample preparation steps which could result in the outcome deviating more than necessary to reality.

One example of non-invasive measurement of apoptosis is the use of AnnexinV-

mediated fluorescence staining in combination of automated imaging (145). This method does not only provide the amount of apoptosis induced as an end-point, but can also provide information on the kinetics of the apoptosis induced, something that could potentially provide a more mechanistic insight.

The use of fluorescent fusion proteins has opened up a whole new field of mechanistic research as it makes it possible to for example follow the translocation of crucial transcription factors from the cytoplasm to the nucleus in real time, or the induction of certain stresses by following the induction of typical target genes such as SRXN1 that is induced upon oxidative stress and the activation of Nrf2 (146).

Another way to follow the induction cytotoxic stress, such as glutathione depletion and mitochondrial damage proven important for the induction of idiosyncratic DILI (see above), is by the use of fluorescent probes indicative of the particular damage. Using this technique Xu and colleagues were able to develop an in vitro screening method, with a true-positive rate of 50-60% and a false-positive rate of 0-5%, for the identification of hepatotoxicants (64). This technique gives a good example of how high content imaging can prove very useful, not only for mechanistic insight, but also for the pre-clinical screening of novel compounds in pharmaceutical companies.

5.3 Pharmacogenetics

As genetic variations are important determining factors for the development of iDILI, pharmacogenetics constitutes an important method in the study of these adverse drug reactions.

The most common way of studying relationships between genes and adverse events is by a targeted candidate gene association studies (CGAS) (40). However as it, due to the low incidence of iDILI, is rather unlikely to find a one-gene-association, genome wide association studies (GWAS) is a better approach as they are more likely to identify a combination of genetic risk factors associated to one adverse drug reaction (40). However, important for both the CGAS and the GWAS approach, is a more mechanistic insights to the iDILI in question. It is a prerequisite for the targeted CGAS study but it has also been proven more fruitful for GWAS studies as this helps to narrow down the target genes by only focusing on certain functional areas (40). This approach was nicely demonstrated when identifying genetic variation of the glucuronidation enzyme UGT2B7 as a risk factor for diclofenac induced DILI (50).

Apart from the use of pharmacogenetics in identifying single or small groups of genes that can be linked to the development of iDILI, gene expression analysis is an important method to identify signaling pathways that are activated in the cellular stress response to a toxic insult (147). To achieve this, the development of dedicated and commercially available pathway analysis software such as Ingenuity Pathway Analysis® and MetacoreTM has been a major accomplishment (148,149).

Although informative in the search for transcriptionally regulated genes, transcriptomics provides little information about the functional role of the genes that are

differentially expressed. Furthermore, transcriptional up-or down-regulation does not per se mean a functional change relevant for the phenotype studied. Small interfering RNAs (siRNAs) were first discovered in the early 2000s and they constitute an outstanding method for targeted silencing of individual genes for the study of their function (150). siRNA screening is now widely used by both academia and drug-industry for the discovery of novel drug targets affecting a certain intracellular system or for example for fundamental studies of mechanisms behind certain cellular processes (151,152). In addition, siRNA technology comprises an invaluable resource for the study of the functional roles of differentially expressed genes identified in GWAS studies.

6. AIM AND SCOPE OF THIS THESIS

It has been anticipated that *in vitro* studies of idiosyncratic drug reactions cannot simply mimic all the complex interactions that occur *in vivo* (22). Rather, animal models could be better used to support hypothesis coming from clinical observations. However, in depth mechanistic *in vitro* studies at the molecular level are still essential to gain more detailed insight. Where appropriate the gathered knowledge could be integrated in improved pre-clinical *in vitro* toxicity screening.

In this thesis I used an *in vitro* approach for the mechanistic studies of DILI by investigating the hypothesis that cross–talk between drug (metabolite)-induced and cytokine-induced intracellular stress signaling is a likely critical event that leads to an enhanced toxic response in susceptible individuals (Fig. 3). This hypothesis does not exclude either the innate or the adaptive immune system activation, as cytokines are the mediators of both. The focus is here on TNFα since this is a major mediator of inflammation-induced toxicity.

Diclofenac-induced liver injury has been termed a "paradigm of idiosyncratic drug toxicity" (49). In **chapter 2** I first used this drug in combination with a non-toxic dose of TNFα to provide a proof-of-concept for our working hypothesis. The apoptotic mechanism behind the enhanced drug-induced toxicity seen with the addition of TNFα was further studied using siRNA-screening technology and high-content imaging of apoptosis as described above. Using this methodology, the enhanced apoptosis was shown to originate from the TNF receptor, suggesting that diclofenac enhances the pro-apoptotic properties of TNFα and not the other way around. Furthermore, I showed that this enhanced toxicity is related to diclofenac's ability to inhibit the oscillatory pattern of NF-κB translocation. This is in line with the observation that TNFα can only be cytotoxic in the case of NF-κB inhibition.

In **chapter 3** the concept of TNFα enhancing the apoptotic outcome of drugs associated with idiosyncratic DILI was further investigated using a panel of 15 drugs, involving drugs linked to iDILI, DILI without an inflammatory component as well as non-liver-toxic compounds. Here I show that the synergistic response with TNFα addition is not only linked to the inhibition of NF-κB as this could also be observed following the exposure to non-toxic compounds as well, but also dependent on induction of oxidative stress by the drug. The kinetics of oxidative stress induction was determined using high content imaging of Srxn1-GFP, a reporter for the activation of Nrf2-mediated oxidative stress response. I anticipate that the use of these three high content imaging methods can be used as a part of a toxicity-screening panel for the identification of compounds in a pre-clinical setting with a potential risk for human iDILI.

In **chapter 4** the mechanism behind the synergistic apoptotic response seen with certain drugs and TNFα addition was further investigated using a transcriptomics and subsequent functional genomics approach. In addition to diclofenac, carbamazepine was shown, both in this chapter and in chapter 2, to have a clear apoptotic synergism with TNFα. Using Ingenuity Pathway Analysis (IPA®), genes related to the death receptor, oxidative

stress and ER stress pathways were shown to be significantly regulated with diclofenac and carbamazepine, but not with the non-toxic drug methotrexate. The involvement of these pathways could be confirmed using RNA interference. Moreover, a critical role for translation initiation mediated by RNA helicase EIF4A1 was shown for diclofenac/TNFα- and carbamazepine/TNFα-induced apoptosis. Potentially this gene could be used as a susceptibility marker to identify individual with a higher risk of developing iDILI.

As the nuclear translocation of NF-κB was found important for the toxic outcome of drug/TNFα exposure, the role of individual proteins involved in post-translational modifications in this response was investigated in **chapter 5** using an siRNA screening approach and high content imaging of GFP-p65 translocation following TNFα exposure. Knockdown of genes that resulted in a faster, slower or blocked translocation response were identified. Further attention was given to the knockdowns that stopped the TNFα response and unexpectedly this was related to a protective response in a drug/TNFα exposure condition. Interestingly, both the translocation and the apoptosis outcomes were related to enhanced expression of the (de)ubiquitinase A20, a critical component in the NF-κB feedback loop, by the knockdowns themselves.

Finally, **chapter 6** provides a summary and a general discussion on the findings and implications of the work in this thesis.

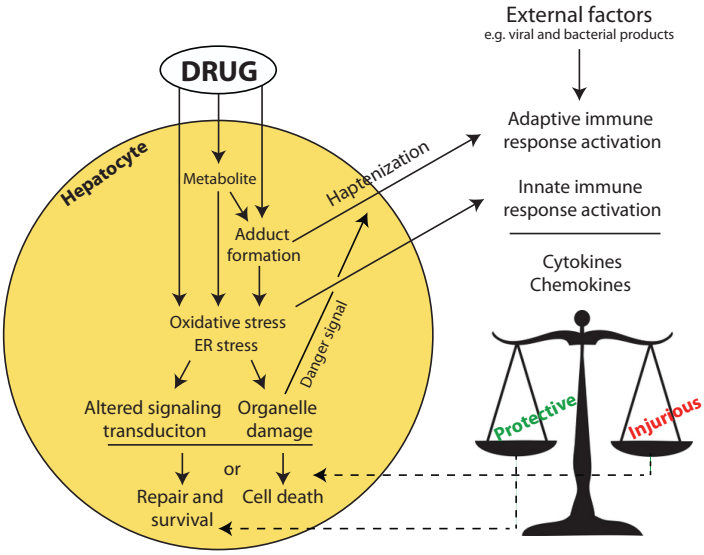

Figure 3. *Summary of the hypothesized interplay between drug- and cytokine-induced stress signaling in the hepatocyte.* A drug, when taken up by the hepatocyte, may induce intracellular stress either by itself or by the formation of reactive metabolites. This can alter the intracellular signaling pattern or cause organelle damage resulting in increased susceptibility of the cell. The hepatocyte damage, or external factors such as exposure to bacterial or vial products, can lead to activation of the innate and/or adaptive immune system. These exert their response by secretion of cytokines and chemokines, which either allow repair and survival of the already susceptible hepatocyte in the case of protective cytokines, or enhanced cellular injury and ultimately cell death in the case of secretion of injurious ones.

REFERENCES

1. Kola I, Landis J. Can the pharmaceutical industry reduce attrition rates? Nat Rev Drug Discov 2004;3:711–715.
2. Adams CP, Brantner VV. Spending on new drug development1. Health Econ 2010;19:130–141.
3. Kaplowitz N. Idiosyncratic drug hepatotoxicity. Nat Rev Drug Discov 2005;4:489–499.
4. Holt M, Ju C. Drug-induced liver injury. Handb Exp Pharmacol 2010;:3–27.
5. Lee WM. Acute liver failure. Semin Respir Crit Care Med 2012;33:36–45.
6. Nemeth E, Baird AW, O'Farrelly C. Microanatomy of the liver immune system. Semin Immunopathol 2009;31:333–343.
7. Roth RA, Ganey PE. Animal models of idiosyncratic drug-induced liver injury--current status. Crit Rev Toxicol 2011;41:723–739.
8. Lammert C, Einarsson S, Saha C, Niklasson A, Björnsson E, Chalasani N. Relationship between daily dose of oral medications and idiosyncratic drug-induced liver injury: search for signals. Hepatology 2008;47:2003–2009.
9. Chalasani N, Björnsson E. Risk factors for idiosyncratic drug-induced liver injury. Gastroenterology 2010;138:2246–2259.
10. Santos NAG, Medina WSG, Martins NM, Mingatto FE, Curti C, Santos AC. Aromatic antiepileptic drugs and mitochondrial toxicity: effects on mitochondria isolated from rat liver. Toxicol In Vitro 2008;22:1143–1152.
11. Uetrecht J. Idiosyncratic drug reactions: past, present, and future. Chem Res Toxicol 2008;21:84–92.
12. Landsteiner K, Jacobs J. Studies on the sensitization of animals with simple chemical compounds. J Exp Med 1935;61:643–656.
13. Antunez C, Martin E, Cornejo-Garcia JA, Blanca-Lopez N, R-Pena R, Mayorga C, et al. Immediate hypersensitivity reactions to penicillins and other betalactams. Curr Pharm Des 2006;12:3327–3333.
14. Aithal GP, Ramsay L, Daly AK, Sonchit N, Leathart JBS, Alexander G, et al. Hepatic adducts, circulating antibodies, and cytokine polymorphisms in patients with diclofenac hepatotoxicity. Hepatology 2004;39:1430–1440.
15. Boelsterli UA, Zimmerman HJ, Kretz-Rommel A. Idiosyncratic liver toxicity of nonsteroidal antiinflammatory drugs: molecular mechanisms and pathology. Crit Rev Toxicol 1995;25:207–235.
16. Wu Y, Farrell J, Pirmohamed M, Park BK, Naisbitt DJ. Generation and characterization of antigen-specific CD4+, CD8+, and CD4+CD8+ T-cell clones from patients with carbamazepine hypersensitivity. J Allergy Clin Immunol 2007;119:973–981.
17. Pichler WJ. Pharmacological interaction of drugs with antigen-specific immune receptors: the p-i concept. Curr Opin Allergy Clin Immunol 2002;2:301–305.
18. Schnyder B, Burkhart C, Schnyder-Frutig K, Greyerz von S, Naisbitt DJ, Pirmohamed M, et al. Recognition of sulfamethoxazole and its reactive metabolites by drug-specific CD4+ T cells from allergic individuals. J Immunol 2000;164:6647–6654.
19. Naisbitt DJ, Britschgi M, Wong G, Farrell J, Depta JPH, Chadwick DW, et al. Hypersensitivity reactions to carbamazepine: characterization of the specificity, phenotype, and cytokine profile of drug-specific T cell clones. Mol Pharmacol 2003;63:732–741.
20. Adam J, Pichler WJ, Yerly D. Delayed drug hypersensitivity: models of T-cell stimulation. Br. J Clin Pharmacol 2011;71:701–707.
21. Matzinger P. Tolerance, danger, and the extended family. Annu Rev Immunol 1994;12:991–1045.
22. Li J, Uetrecht JP. The danger hypothesis applied to idiosyncratic drug reactions. Handb Exp Pharmacol 2010;:493–509.
23. Bianchi ME. DAMPs, PAMPs and alarmins: all we need to know about danger. J Leukoc Biol 2007;81:1–5.
24. Calderwood SK, Mambula SS, Gray PJ. Extracellular heat shock proteins in cell signaling and immunity. Ann N Y Acad Sci 2007;1113:28–39.
25. Klune JR, Dhupar R, Cardinal J, Billiar TR, Tsung A. HMGB1: endogenous danger signaling. Mol Med 2008;14:476–484.
26. Masson MJ, Collins LA, Pohl LR. The role of cytokines in the mechanism of adverse drug reactions. Handb Exp Pharmacol 2010:195–231.
27. Levy M. Role of viral infections in the induction of adverse drug reactions. Drug Saf 1997;16:1–8.
28. Brinker den M, Wit FW, Wertheim-van Dillen PM, Jurriaans S, Weel J, van Leeuwen R, et al. Hepatitis B and C virus co-infection and the risk for hepatotoxicity of highly active antiretroviral therapy in HIV-1 infection. AIDS 2000;14:2895–2902.
29. Boelsterli UA, Lim PLK. Mitochondrial abnormalities--a link to idiosyncratic drug hepatotoxicity? Toxicol Appl Pharmacol 2007;220:92–107.
30. Jones DP, Lemasters JJ, Han D, Boelsterli UA, Kaplowitz N. Mechanisms of pathogenesis in drug

hepatotoxicity putting the stress on mitochondria. Mol Interv 2010;10:98–111.
31. Ong MMK, Latchoumycandane C, Boelsterli UA. Troglitazone-induced hepatic necrosis in an animal model of silent genetic mitochondrial abnormalities. Toxicol Sci 2007;97:205–213.
32. Ganey PE, Luyendyk JP, Maddox JF, Roth RA. Adverse hepatic drug reactions: inflammatory episodes as consequence and contributor. Chem Biol Interact 2004;150:35–51.
33. Ganey PE, Roth RA. Concurrent inflammation as a determinant of susceptibility to toxicity from xenobiotic agents. Toxicology. 2001;169:195–208.
34. Ulrich RG. Idiosyncratic toxicity: a convergence of risk factors. Annu Rev Med 2007;58:17–34.
35. Deng X, Stachlewitz RF, Liguori MJ, Blomme EAG, Waring JF, Luyendyk JP, et al. Modest inflammation enhances diclofenac hepatotoxicity in rats: role of neutrophils and bacterial translocation. J Pharmacol Exp Ther 2006;319:1191–1199.
36. Lu J, Jones AD, Harkema JR, Roth RA, Ganey PE. Amiodarone exposure during modest inflammation induces idiosyncrasy-like liver injury in rats: role of tumor necrosis factor-alpha. Toxicol Sci 2012;125:126–133.
37. Zou W, Beggs KM, Sparkenbaugh EM, Jones AD, Younis HS, Roth RA, et al. Sulindac metabolism and synergy with tumor necrosis factor-alpha in a drug-inflammation interaction model of idiosyncratic liver injury. J Pharmacol Exp Ther 2009;331:114–121.
38. Shaw PJ, Hopfensperger MJ, Ganey PE, Roth RA. Lipopolysaccharide and trovafloxacin coexposure in mice causes idiosyncrasy-like liver injury dependent on tumor necrosis factor-alpha. Toxicol Sci 2007;100:259–266.
39. Posadas SJ, Pichler WJ. Delayed drug hypersensitivity reactions - new concepts. Clin Exp Allergy 2007;37:989–999.
40. Russmann S, Jetter A, Kullak-Ublick GA. Pharmacogenetics of drug-induced liver injury. Hepatology 2010;52:748–761.
41. Mallal S, Nolan D, Witt C, Masel G, Martin AM, Moore C, et al. Association between presence of HLA-B*5701, HLA-DR7, and HLA-DQ3 and hypersensitivity to HIV-1 reverse-transcriptase inhibitor abacavir. Lancet 2002;359:727–732.
42. Phillips E, Mallal S. Successful translation of pharmacogenetics into the clinic: the abacavir example. Mol Diagn Ther 2009;13:1–9.
43. Pirmohamed M, Park BK. Genetic susceptibility to adverse drug reactions. Trends Pharmacol Sci 2001;22:298–305.
44. Zhou S-F, Liu J-P, Chowbay B. Polymorphism of human cytochrome P450 enzymes and its clinical impact. Drug Metab Rev 2009;41:89–295.
45. Srivastava A, Maggs JL, Antoine DJ, Williams DP, Smith DA, Park BK. Role of reactive metabolites in drug-induced hepatotoxicity. Handb Exp Pharmacol 2010:165–194.
46. Lammert C, Björnsson E, Niklasson A, Chalasani N. Oral medications with significant hepatic metabolism at higher risk for hepatic adverse events. Hepatology 2010;51:615–620.
47. Park BK, Kitteringham NR, Maggs JL, Pirmohamed M, Williams DP. The role of metabolic activation in drug-induced hepatotoxicity. Annu Rev Pharmacol Toxicol 2005;45:177–202.
48. Huang Y-S, Su W-J, Huang Y-H, Chen C-Y, Chang F-Y, Lin H-C, et al. Genetic polymorphisms of manganese superoxide dismutase, NAD(P)H:quinone oxidoreductase, glutathione S-transferase M1 and T1, and the susceptibility to drug-induced liver injury. J Hepatol 2007;47:128–134.
49. Boelsterli UA. Diclofenac-induced liver injury: a paradigm of idiosyncratic drug toxicity. Toxicol Appl Pharmacol 2003;192:307–322.
50. Daly AK, Aithal GP, Leathart JBS, Swainsbury RA, Dang TS, Day CP. Genetic susceptibility to diclofenac-induced hepatotoxicity: contribution of UGT2B7, CYP2C8, and ABCC2 genotypes. Gastroenterology 2007;132:272–281.
51. Watanabe I, Tomita A, Shimizu M, Sugawara M, Yasumo H, Koishi R, et al. A study to survey susceptible genetic factors responsible for troglitazone-associated hepatotoxicity in Japanese patients with type 2 diabetes mellitus. Clin Pharmacol Ther 2003;73:435–455.
52. Takakusa H, Masumoto H, Yukinaga H, Makino C, Nakayama S, Okazaki O, et al. Covalent binding and tissue distribution/retention assessment of drugs associated with idiosyncratic drug toxicity. Drug Metab Dispos 2008;36:1770–1779.
53. Roth RA, Ganey PE. Intrinsic versus idiosyncratic drug-induced hepatotoxicity--two villains or one? J Pharmacol Exp Ther 2010;332:692–697.
54. Tirmenstein MA, Nelson SD. Subcellular binding and effects on calcium homeostasis produced by acetaminophen and a nonhepatotoxic regioisomer, 3'-hydroxyacetanilide, in mouse liver. J Biol Chem 1989;264:9814–9819.
55. Wen B, Ma L, Nelson SD, Zhu M. High-throughput screening and characterization of reactive metabolites using polarity switching of hybrid triple quadrupole linear ion trap mass spectrometry. Anal Chem 2008;80:1788–1799.
56. Liebler DC. Protein damage by reactive electrophiles: targets and consequences. Chem Res Toxicol

2008;21:117–128.
57. Kumar S, Mitra K, Kassahun K, Baillie TA. Approaches for minimizing metabolic activation of new drug candidates in drug discovery. Handb Exp Pharmacol 2010:511–544.
58. Kass GEN. Mitochondrial involvement in drug-induced hepatic injury. Chem Biol Interact 2006;163:145–159.
59. Jaeschke H, McGill MR, Ramachandran A. Oxidant stress, mitochondria, and cell death mechanisms in drug-induced liver injury: lessons learned from acetaminophen hepatotoxicity. Drug Metab Rev 2012;44:88–106.
60. Newmeyer DD, Ferguson-Miller S. Mitochondria: releasing power for life and unleashing the machineries of death. Cell 2003;112:481–490.
61. Youle RJ, Strasser A. The BCL-2 protein family: opposing activities that mediate cell death. Nat Rev Mol Cell Biol 2008;9:47–59.
62. Bratton SB, Salvesen GS. Regulation of the Apaf-1-caspase-9 apoptosome. J Cell Sci 2010;123:3209–3214.
63. Pessayre D, Mansouri A, Berson A, Fromenty B. Mitochondrial involvement in drug-induced liver injury. Handb Exp Pharmacol 2010:311–365.
64. Xu JJ, Henstock PV, Dunn MC, Smith AR, Chabot JR, de Graaf D. Cellular imaging predictions of clinical drug-induced liver injury. Toxicol Sci 2008;105:97–105.
65. Siu WP, Pun PBL, Latchoumycandane C, Boelsterli UA. Bax-mediated mitochondrial outer membrane permeabilization (MOMP), distinct from the mitochondrial permeability transition, is a key mechanism in diclofenac-induced hepatocyte injury: Multiple protective roles of cyclosporin A. Toxicol Appl Pharmacol 2008;227:451–461.
66. Gómez-Lechón MJ, Ponsoda X, O'Connor E, Donato T, Castell JV, Jover R. Diclofenac induces apoptosis in hepatocytes by alteration of mitochondrial function and generation of ROS. Biochem Pharmacol 2003;66:2155–2167.
67. Lores Arnaiz S, Llesuy S, Cutrín JC, Boveris A. Oxidative stress by acute acetaminophen administration in mouse liver. Free Radic Biol Med 1995;19:303–310.
68. Atkuri KR, Mantovani JJ, Herzenberg LA, Herzenberg LA. N-Acetylcysteine--a safe antidote for cysteine/glutathione deficiency. Curr Opin Pharmacol 2007;7:355–359.
69. Shan X, Jones DP, Hashmi M, Anders MW. Selective depletion of mitochondrial glutathione concentrations by (R,S)-3-hydroxy-4-pentenoate potentiates oxidative cell death. Chem Res Toxicol 1993;6:75–81.
70. Han D, Canali R, Rettori D, Kaplowitz N. Effect of glutathione depletion on sites and topology of superoxide and hydrogen peroxide production in mitochondria. Mol Pharmacol 2003;64:1136–1144.
71. Han D. Mechanisms of Liver Injury. III. Role of glutathione redox status in liver injury. Am J Physiol Gastrointest Liver Physiol 2006;291:G1–G7.
72. Kamata H, Honda S-I, Maeda S, Chang L, Hirata H, Karin M. Reactive oxygen species promote TNFalpha-induced death and sustained JNK activation by inhibiting MAP kinase phosphatases. Cell 2005;120:649–661.
73. Okawa H, Motohashi H, Kobayashi A, Aburatani H, Kensler TW, Yamamoto M. Hepatocyte-specific deletion of the keap1 gene activates Nrf2 and confers potent resistance against acute drug toxicity. Biochem Biophys Res Commun 2006;339:79–88.
74. Copple IM, Goldring CE, Kitteringham NR, Park BK. The keap1-nrf2 cellular defense pathway: mechanisms of regulation and role in protection against drug-induced toxicity. Handb Exp Pharmacol 2010:233–266.
75. Kobayashi A, Kang M-I, Okawa H, Ohtsuji M, Zenke Y, Chiba T, et al. Oxidative stress sensor Keap1 functions as an adaptor for Cul3-based E3 ligase to regulate proteasomal degradation of Nrf2. Mol Cell Biol 2004;24:7130–7139.
76. Copple IM, Goldring CE, Kitteringham NR, Park BK. The Nrf2-Keap1 defence pathway: role in protection against drug-induced toxicity. Toxicology 2008;246:24–33.
77. Dinkova-Kostova AT, Holtzclaw WD, Cole RN, Itoh K, Wakabayashi N, Katoh Y, et al. Direct evidence that sulfhydryl groups of Keap1 are the sensors regulating induction of phase 2 enzymes that protect against carcinogens and oxidants. Proc Natl Acad Sci U S A 2002;99:11908–11913.
78. Itoh K, Tong KI, Yamamoto M. Molecular mechanism activating Nrf2-Keap1 pathway in regulation of adaptive response to electrophiles. Free Radic Biol Med 2004;36:1208–1213.
79. Itoh K, Chiba T, Takahashi S, Ishii T, Igarashi K, Katoh Y, et al. An Nrf2/small Maf heterodimer mediates the induction of phase II detoxifying enzyme genes through antioxidant response elements. Biochem Biophys Res Commun 1997;236:313–322.
80. Chan K, Han XD, Kan YW. An important function of Nrf2 in combating oxidative stress: detoxification of acetaminophen. Proc Natl Acad Sci U S A 2001;98:4611–4616.
81. Han D, Shinohara M, Ybanez MD, Saberi B, Kaplowitz N. Signal transduction pathways involved in drug-induced liver injury. Handb Exp Pharmacol 2010:267–310.
82. Singh R, Czaja MJ. Regulation of hepatocyte apoptosis by oxidative stress. J Gastroenterol Hepatol

2007;22 Suppl 1:S45–8.
83. Liu H, Lo CR, Czaja MJ. NF-kappaB inhibition sensitizes hepatocytes to TNF-induced apoptosis through a sustained activation of JNK and c-Jun. Hepatology 2002;35:772–778.
84. Gunawan BK, Liu ZX, Han D, Hanawa N, Gaarde WA, Kaplowitz N. c-Jun N-terminal kinase plays a major role in murine acetaminophen hepatotoxicity. Gastroenterology. 2006;131:165–178.
85. Bae M-A, Song BJ. Critical role of c-Jun N-terminal protein kinase activation in troglitazone-induced apoptosis of human HepG2 hepatoma cells. Mol Pharmacol 2003;63:401–408.
86. Hanawa N, Shinohara M, Saberi B, Gaarde WA, Han D, Kaplowitz N. Role of JNK translocation to mitochondria leading to inhibition of mitochondria bioenergetics in acetaminophen-induced liver injury. J Biol Chem 2008;283:13565–13577.
87. Kim B-J, Ryu S-W, Song B-J. JNK- and p38 kinase-mediated phosphorylation of Bax leads to its activation and mitochondrial translocation and to apoptosis of human hepatoma HepG2 cells. J Biol Chem 2006;281:21256–21265.
88. Lucena MI, García-Martín E, Andrade RJ, Martínez C, Stephens C, Ruiz JD, et al. Mitochondrial superoxide dismutase and glutathione peroxidase in idiosyncratic drug-induced liver injury. Hepatology 2010;52:303–312.
89. Lucena MI, Andrade RJ, Martínez C, Ulzurrun E, García-Martín E, Borraz Y, et al. Glutathione S-transferase m1 and t1 null genotypes increase susceptibility to idiosyncratic drug-induced liver injury. Hepatology 2008;48:588–596.
90. Leiro V, Fernández-Villar A, Valverde D, Constenla L, Vázquez R, Piñeiro L, et al. Influence of glutathione S-transferase M1 and T1 homozygous null mutations on the risk of antituberculosis drug-induced hepatotoxicity in a Caucasian population. Liver Int 2008;28:835–839.
91. Tolson JK, Dix DJ, Voellmy RW, Roberts SM. Increased hepatotoxicity of acetaminophen in Hsp70i knockout mice. Toxicol Appl Pharmacol 2006;210:157–162.
92. de Waziers I, Cugnenc PH, Yang CS, Leroux JP, Beaune PH. Cytochrome P 450 isoenzymes, epoxide hydrolase and glutathione transferases in rat and human hepatic and extrahepatic tissues. J Pharmacol Exp Ther 1990;253:387–394.
93. Meech R, Mackenzie PI. Determinants of UDP glucuronosyltransferase membrane association and residency in the endoplasmic reticulum. Arch Biochem Biophys 1998;356:77–85.
94. Cribb AE, Peyrou M, Muruganandan S, Schneider L. The endoplasmic reticulum in xenobiotic toxicity. Drug Metab Rev 2005;37:405–442.
95. Tu BP, Weissman JS. Oxidative protein folding in eukaryotes: mechanisms and consequences. J Cell Biol 2004;164:341–346.
96. Groenendyk J, Lynch J, Michalak M. Calreticulin, Ca2+, and calcineurin - signaling from the endoplasmic reticulum. Mol Cells 2004;17:383–389.
97. Deniaud A, Sharaf el dein O, Maillier E, Poncet D, Kroemer G, Lemaire C, et al. Endoplasmic reticulum stress induces calcium-dependent permeability transition, mitochondrial outer membrane permeabilization and apoptosis. Oncogene 2008;27:285–299.
98. Lee AS. The glucose-regulated proteins: stress induction and clinical applications. Trends Biochem Sci 2001;26:504–510.
99. Little E, Ramakrishnan M, Roy B, Gazit G, Lee AS. The glucose-regulated proteins (GRP78 and GRP94): functions, gene regulation, and applications. Crit Rev Eukaryot Gene Expr 1994;4:1–18.
100. Harding HP, Calfon M, Urano F, Novoa I, Ron D. Transcriptional and translational control in the Mammalian unfolded protein response. Annu Rev Cell Dev Biol 2002;18:575–599.
101. Meusser B, Hirsch C, Jarosch E, Sommer T. ERAD: the long road to destruction. Nat Cell Biol 2005;7:766–772.
102. Bertolotti A, Zhang Y, Hendershot LM, Harding HP, Ron D. Dynamic interaction of BiP and ER stress transducers in the unfolded-protein response. Nat Cell Biol 2000;2:326–332.
103. Harding HP, Zhang Y, Ron D. Protein translation and folding are coupled by an endoplasmic-reticulum-resident kinase. Nature 1999;397:271–274.
104. Oyadomari S, Mori M. Roles of CHOP/GADD153 in endoplasmic reticulum stress. Cell Death Differ 2004;11:381–389.
105. Urano F, Bertolotti A, Ron D. IRE1 and efferent signaling from the endoplasmic reticulum. J Cell Sci 2000;113 Pt 21:3697–3702.
106. Yoshida H, Matsui T, Yamamoto A, Okada T, Mori K. XBP1 mRNA is induced by ATF6 and spliced by IRE1 in response to ER stress to produce a highly active transcription factor. Cell 2001;107:881–891.
107. Adachi Y, Yamamoto K, Okada T, Yoshida H, Harada A, Mori K. ATF6 is a transcription factor specializing in the regulation of quality control proteins in the endoplasmic reticulum. Cell Struct Funct 2008;33:75–89.
108. McCullough KD, Martindale JL, Klotz LO, Aw TY, Holbrook NJ. Gadd153 sensitizes cells to endoplasmic reticulum stress by down-regulating Bcl2 and perturbing the cellular redox state. Mol Cell Biol 2001;21:1249–1259.

109. Puthalakath H, O'Reilly LA, Gunn P, Lee L, Kelly PN, Huntington ND, et al. ER stress triggers apoptosis by activating BH3-only protein Bim. Cell 2007;129:1337–1349.
110. Malhi H, Kaufman RJ. Endoplasmic reticulum stress in liver disease. J Hepatol 2011;54:795–809.
111. Nishitoh H, Matsuzawa A, Tobiume K, Saegusa K, Takeda K, Inoue K, et al. ASK1 is essential for endoplasmic reticulum stress-induced neuronal cell death triggered by expanded polyglutamine repeats. Genes Dev 2002;16:1345–1355.
112. Lin JH, Li H, Yasumura D, Cohen HR, Zhang C, Panning B, et al. IRE1 signaling affects cell fate during the unfolded protein response. Science 2007;318:944–949.
113. Terrier N, Benoit E, Senay C, Lapicque F, Radominska-Pandya A, Magdalou J, et al. Human and rat liver UDP-glucuronosyltransferases are targets of ketoprofen acylglucuronide. Mol Pharmacol 1999;56:226–234.
114. Lacour S, Gautier J-C, Pallardy M, Roberts R. Cytokines as potential biomarkers of liver toxicity. Cancer Biomark 2005;1:29–39.
115. Laverty HG, Antoine DJ, Benson C, Chaponda M, Williams D, Kevin Park B. The potential of cytokines as safety biomarkers for drug-induced liver injury. Eur J Clin Pharmacol 2010;66:961–976.
116. Stuber F, Petersen M, Bokelmann F, Schade U. A genomic polymorphism within the tumor necrosis factor locus influences plasma tumor necrosis factor-alpha concentrations and outcome of patients with severe sepsis. Crit Care Med 1996;24:381–384.
117. Pachkoria K, Lucena MI, Crespo E, Ruiz-Cabello F, Lopez-Ortega S, Fernandez MAC, et al. Analysis of IL-10, IL-4 and TNF-alpha polymorphisms in drug-induced liver injury (DILI) and its outcome. J Hepatol 2008;49:107–114.
118. Blazka ME, Wilmer JL, Holladay SD, Wilson RE, Luster MI. Role of proinflammatory cytokines in acetaminophen hepatotoxicity. Toxicol Appl Pharmacol 1995;133:43–52.
119. Tukov FF, Luyendyk JP, Ganey PE, Roth RA. The role of tumor necrosis factor alpha in lipopolysaccharide/ranitidine-induced inflammatory liver injury. Toxicol Sci 2007;100:267–280.
120. Ishida Y, Kondo T, Ohshima T, Fujiwara H, Iwakura Y, Mukaida N. A pivotal involvement of IFN-gamma in the pathogenesis of acetaminophen-induced acute liver injury. FASEB J 2002;16:1227–1236.
121. Hayden MS, Ghosh S. Shared principles in NF-kappaB signaling. Cell 2008;132:344–362.
122. Wajant H, Scheurich P. TNFR1-induced activation of the classical NF-κB pathway. FEBS J 2011;278:862–876.
123. Kelliher MA, Grimm S, Ishida Y, Kuo F, Stanger BZ, Leder P. The death domain kinase RIP mediates the TNF-induced NF-kappaB signal. Immunity 1998;8:297–303.
124. Hsu H, Shu HB, Pan MG, Goeddel DV. TRADD-TRAF2 and TRADD-FADD interactions define two distinct TNF receptor 1 signal transduction pathways. Cell 1996;84:299–308.
125. Yin Q, Lamothe B, Darnay BG, Wu H. Structural basis for the lack of E2 interaction in the RING domain of TRAF2. Biochemistry 2009;48:10558–10567.
126. Hayden MS, Ghosh S. NF-κB, the first quarter-century: remarkable progress and outstanding questions. Genes Dev 2012;26:203–234.
127. Poyet JL, Srinivasula SM, Lin JH, Fernandes-Alnemri T, Yamaoka S, Tsichlis PN, et al. Activation of the Ikappa B kinases by RIP via IKKgamma /NEMO-mediated oligomerization. J Biol Chem 2000;275:37966–37977.
128. Li Q, Estepa G, Memet S, Israel A, Verma IM. Complete lack of NF-kappaB activity in IKK1 and IKK2 double-deficient mice: additional defect in neurulation. Genes Dev 2000;14:1729–1733.
129. Brown K, Park S, Kanno T, Franzoso G, Siebenlist U. Mutual regulation of the transcriptional activator NF-kappa B and its inhibitor, I kappa B-alpha. Proc Natl Acad Sci U S A 1993;90:2532–2536.
130. Lee EG, Boone DL, Chai S, Libby SL, Chien M, Lodolce JP, et al. Failure to regulate TNF-induced NF-kappaB and cell death responses in A20-deficient mice. Science 2000;289:2350–2354.
131. Wertz IE, ORourke KM, Zhou H, Eby M, Aravind L, Seshagiri S, et al. De-ubiquitination and ubiquitin ligase domains of A20 downregulate NF-kappaB signaling. Nature 2004;430:694–699.
132. Nagai H, Matsumaru K, Feng G, Kaplowitz N. Reduced glutathione depletion causes necrosis and sensitization to tumor necrosis factor-alpha-induced apoptosis in cultured mouse hepatocytes. Hepatology 2002;36:55–64.
133. Han D, Hanawa N, Saberi B, Kaplowitz N. Hydrogen peroxide and redox modulation sensitize primary mouse hepatocytes to TNF-induced apoptosis. Free Radic Biol Med 2006;41:627–639.
134. Lou H, Kaplowitz N. Glutathione depletion down-regulates tumor necrosis factor alpha-induced NF-kappaB activity via IkappaB kinase-dependent and -independent mechanisms. J Biol Chem 2007;282:29470–29481.
135. Matsumaru K, Ji C, Kaplowitz N. Mechanisms for sensitization to TNF-induced apoptosis by acute glutathione depletion in murine hepatocytes. Hepatology 2003;37:1425–1434.
136. Ashkenazi A, Dixit VM. Death receptors: signaling and modulation. Science 1998;281:1305–1308.
137. Bertrand MJM, Milutinovic S, Dickson KM, Ho WC, Boudreault A, Durkin J, et al. cIAP1 and cIAP2 facilitate cancer cell survival by functioning as E3 ligases that promote RIP1 ubiquitination. Mol Cell

2008;30:689–700.
138. Wertz IE, Dixit VM. Regulation of death receptor signaling by the ubiquitin system. Cell Death Differ 2010;17:14–24.
139. Micheau O, Tschopp J. Induction of TNF receptor I-mediated apoptosis via two sequential signaling complexes. Cell 2003;114:181–190.
140. Fischer U, Janicke RU, Schulze-Osthoff K. Many cuts to ruin: a comprehensive update of caspase substrates. Cell Death Differ 2003;10:76–100.
141. Luo X, Budihardjo I, Zou H, Slaughter C, Wang X. Bid, a Bcl2 interacting protein, mediates cytochrome c release from mitochondria in response to activation of cell surface death receptors. Cell 1998;94:481–490.
142. Dixit R, Boelsterli UA. Healthy animals and animal models of human disease(s) in safety assessment of human pharmaceuticals, including therapeutic antibodies. Drug Discov Today 2007;12:336–342.
143. Boelsterli UA, Hsiao C-JJ. The heterozygous Sod2(+/-) mouse: modeling the mitochondrial role in drug toxicity. Drug Discov Today 2008;13:982–988.
144. Cosgrove BD, King BM, Hasan MA, Alexopoulos LG, Farazi PA, Hendriks BS, et al. Synergistic drug-cytokine induction of hepatocellular death as an in vitro approach for the study of inflammation-associated idiosyncratic drug hepatotoxicity. Toxicol Appl Pharmacol 2009;237:317–330.
145. Puigvert JC, de Bont H, van de Water B, Danen EHJ. High-throughput live cell imaging of apoptosis. Curr Protoc Cell Biol 2010;Chapter 18:Unit 18.10.1–13.
146. Hendriks G, Atallah M, Morolli B, Calléja F, Ras-Verloop N, Huijskens I, et al. The ToxTracker assay: novel GFP reporter systems that provide mechanistic insight into the genotoxic properties of chemicals. Toxicol Sci 2012;125:285–298.
147. Cui Y, Paules RS. Use of transcriptomics in understanding mechanisms of drug-induced toxicity. Pharmacogenomics 2010;11:573–585.
148. Sivachenko AY, Yuryev A. Pathway analysis software as a tool for drug target selection, prioritization and validation of drug mechanism. Expert Opin Ther Targets 2007;11:411–421.
149. Ganter B, Zidek N, Hewitt PR, Müller D, Vladimirova A. Pathway analysis tools and toxicogenomics reference databases for risk assessment. Pharmacogenomics 2008;9:35–54.
150. Fjose A, Ellingsen S, Wargelius A, Seo HC. RNA interference: mechanisms and applications. Biotechnol Annu Rev 2001;7:31–57.
151. Haney SA. RNAi and high-content screening in target identification and validation. IDrugs 2005;8:997–1001.
152. Rausch O. High content cellular screening. Curr Opin Chem Biol 2006;10:316–320.

2

Diclofenac inhibits TNFα-induced NF-κB activation causing synergistic hepatocyte apoptosis

Lisa Fredriksson*, Bram Herpers*, Giulia Benedetti, Quraisha Matadin, Jordi C. Puigvert, Hans de Bont, Sanja Dragovic, Nico P.E. Vermeulen, Jan N.M. Commandeur, Erik Danen, Marjo de Graauw and Bob van de Water

Published in Heptology 2011

ABSTRACT

Drug-induced liver injury (DILI) is an important clinical problem. It involves a crosstalk between drug toxicity and the immune system, but the exact mechanism at the cellular hepatocyte level is not well understood. Here we studied the mechanism of crosstalk in hepatocyte apoptosis caused by diclofenac and the pro-inflammatory cytokine tumor necrosis factor α (TNFα). HepG2 cells were treated with diclofenac followed by TNFα challenge and subsequent evaluation of necrosis and apoptosis. Diclofenac caused a mild apoptosis of HepG2 cells, which was strongly potentiated by TNFα. A focused apoptosis machinery short interference RNA (siRNA) library screen identified that this TNFα-mediated enhancement involved activation of caspase-3 through a caspase-8/Bid/APAF1 pathway. Diclofenac itself induced sustained activation of c-Jun N-terminal kinase (JNK) and inhibition of JNK decreased both diclofenac and diclofenac/TNFα-induced apoptosis. Live cell imaging of GFPp65/RelA showed that diclofenac dampened the TNFα-mediated nuclear NF-κB translocation oscillation in association with reduced NF-κB transcriptional activity. This was associated with inhibition by diclofenac of the TNFα-induced phosphorylation of the inhibitor of nuclear factor κB (NF-κB) alpha (IκBα). Finally, inhibition of IκB kinase β (IKKβ) with BMS-345541 as well as stable lentiviral short hairpin RNA (shRNA)-based knockdown of p65/RelA sensitized hepatocytes towards diclofenac/TNFα-induced cytotoxicity. Conclusion: Together our data suggest a model whereby diclofenac-mediated stress signaling suppresses TNFα-induced survival signaling routes and sensitizes cells to apoptosis.

INTRODUCTION

Adverse drug reactions are an important cause of morbidity and mortality in humans and drug-induced liver injuries (DILIs) are the leading cause of acute liver failure (1). In addition, DILI accounts for most of the drug attritions (2) and more than 10 % of the occurring liver failures happen due to idiosyncratic DILIs (1). We propose that the crosstalk between drug reactive metabolite-mediated stress responses and cytokine-mediated pro- and anti-apoptotic signaling is an important component in the pathophysiology of DILI.

Diclofenac is one of the most commonly used drugs causing idiosyncratic DILI (3). Diclofenac is a non-steroidal anti-inflammatory drug (NSAID) widely prescribed to treat for example pain and rheumatoid arthritis. Although the most frequently occurring ADR associated with use of diclofenac is gastrointestinal ulceration (4), severe idiosyncratic liver injuries are reported and due to the drug's frequent clinical use, the total number of affected patients is significant (3).

The underlying cellular mechanisms that determine the susceptibility towards developing DILI are incompletely understood. Due to their relatively rare occurrence, it is expected that multiple factors are involved. Increasing evidence points towards a role for the formation of reactive metabolites and the (innate) immune system (2, 5, 6). In the liver, diclofenac is metabolized into three main metabolites, 4'-OH-diclofenac, 5-OH-diclofenac and diclofenac acylglucuronide, that are reactive towards protein thiol-groups, associated with formation of reactive oxygen species (ROS) and causally related to DILI (7). Covalent protein modifications and ROS cause cellular injury and activation of different stress signaling pathways, including c-Jun N-terminal kinase (JNK) (8).

The largest pool of stationary immune cells in the liver is the liver-specific macrophages, the Kupffer cells. Through intercellular communication between hepatocytes and Kupffer cells or due to direct endotoxin exposure from the intestine, Kupffer cells secrete pro-inflammatory cytokines, of which tumor necrosis factor-α (TNFα) is the major component (9). TNFα severely enhances liver damage caused by different xenobiotics (10-12). Although an involvement of the immune system in diclofenac hepatotoxicity is clear from an in vivo rat model (13), the exact role of cytokine signaling and the molecular mechanism of such an interaction are poorly defined.

TNFα induces both pro- and anti-apoptotic signaling. By formation of the complex I signalosome after TNFα binding to its receptor (TNFR-1), the transcription factor nuclear factor kappa-B (NF-κB) is activated (14). Nuclear translocation of NF-κB occur in an oscillatory manner following degradation of the inhibitor of NF-κB, IκBα, to induce transcription of its target genes which primarily encode survival proteins, e.g. cellular FLICE-like inhibitory protein (c-FLIP) and inhibitor of apoptosis proteins (IAPs), and proteins that negatively regulate the activation of complex I, e.g. A20 and IκBα (15). Depending on the cellular signaling context, from complex I an apoptosis activating complex II can be formed, which results in activation of caspase-8 and induction of the apoptotic pathway (15, 16). In addition to activation of transcription factor NF-κB, signaling from complex I can lead to activation of mitogen activated protein kinases

(MAPKs). Activation of c-Jun N-terminal kinase (JNK) can either lead to survival or apoptosis, depending on whether the activation is transient or prolonged (17). Activation of caspases and prolonged JNK signaling are under normal conditions antagonized by different NF-κB target genes (16, 18).

Here we used a human HepG2 cell-based model to study the diclofenac/cytokine interaction. We show that the concentration-dependent toxicity of diclofenac is enhanced in the presence of the cytokine TNFα, which is dependent on the activation of JNK1. Consistent with signaling from the TNFR-I downstream pro-apoptotic response, using an RNA interference approach targeting all apoptotic machinery components, we identified a key role for the capase-8/Bid/APAF1 route in the diclofenac/TNFα-induced apoptosis. TNFα-induced IκBα phosphorylation was inhibited by diclofenac in association with attenuation of the nuclear translocation of NF-κB. Inhibition of IKKβ or RNA interference-based silencing of the NF-κB subunit p65/RelA further sensitized cells to diclofenac/TNFα-induced apoptosis. Our findings support a model whereby diclofenac perturbs pro-survival NF-κB responses during periods of inflammation, which favours pro-apoptotic signaling via capase-8 and JNK upon cytokine exposure, ultimately increasing the likelihood of liver cell death.

MATERIALS AND METHODS

Reagents and antibodies

Diclofenac sodium, naproxen sodium and the selective IKK2-inhibitor BMS-345541 were obtained from Sigma (Zwijndrecht, the Netherlands). Human and mouse recombinant TNFα were acquired from R&D Systems (Abingdon, United Kingdom). The selective JNK-inhibitor SP600125 was from Enzo Life Sciences (Zandhoven, Belgium). The irreversible pan-caspase inhibitor z-VAD-fmk was from Bachem (Weil am Rhein, Germany). The irreversible inhibitors of caspases z-DEVD-fmk (caspase-3), z-IETD-fmk (caspase-8) and z-LEHD-fmk (caspase-9) were from Calbiochem (Merck KGaA, Darmstadt, Germany). AnnexinV-Alexa633 was made as previously described (19). The antibodies against active caspase-3 and phospho-specific JNK antibody were from New England Biolabs (Leusden, the Netherlands). The antibodies against caspase-8, caspase-9, cleaved PARP, JNK1/2, IκBα and the phospho-specific cJun and IκBα antibodies were from Cell Signaling (Bioké, Leiden, Netherlands). The antibody against tubulin was from Sigma and the antibody against NF-κB (p65) was from Santa Cruz (Tebu-Bio, Heerhugowaard, the Netherlands).

Cell lines

Human hepatoma HepG2 cells and mouse hepatoma Hepa1c1c7 cells were obtained from American Type Culture Collection (ATCC, Wesel, Germany), cultured in DMEM supplemented with 10% (v/v) FBS, 25 U/mL penicillin and 25 μg/mL streptomycin and used for experiments between passage 5 and 20.

RNA interference

Stable HepG2 cell lines with p65/RelA knocked down were produced using lenti-viral shRNA vectors (Sigma-Aldrich, collaboration with dr. Hoeben, Leiden University Medical Centre, the Netherlands) and selection with puromycin (2.5 μg/mL). The sequence for the non-targeting control shRNA was CCGGTCCGCAGGTATGCACGCGTGAATTC and the shRelA sequence was CCGGCACCATCAACTATGATGAGTTCTCGAGAACTCATCATAGTTGATGGTGTTTTT. Transient knockdowns of individual target genes were achieved using siGENOME SMARTpool siRNA reagents in the primary screen or single siRNA sequences in the secondary deconvolution screen (50 nM; Dharmacon Thermo Fisher Scientific, Landsmeer, the Netherlands). The negative control was siGENOME non-targeting pool #1. HepG2 cells were transfected using INTERFERin™ siRNA transfection reagent according to the manufacturer's procedures (Polyplus transfection, Leusden, the Netherlands) and left for 72 hours to achieve maximal knockdown before treatment.

Cell death analysis assays

Apoptosis was determined by cell cycle analysis using 4',6-diamidino-2-phenylindole (DAPI) and flow cytometry (FACSCanto II; Becton Dickinson, Erembodegem, Belgium). The amount of cells in sub G0/G1 was calculated using the BD FACSDiva software (Becton Dickinson). Overall cell death (loss of membrane integrity) was determined by lactate dehydrogenase (LDH) release in the medium in essentially the same manner as previously described (20). Induction of apoptosis in real time was quantified using a live cell apoptosis assay previously described (19). Briefly, binding of annexin V-Alexa633 conjugate to phosphatidyl serine on the membranes of apoptotic cells was followed in time by imaging every 30 minutes after drug exposure with a BD PathwayTM 855 imager (Becton Dickinson). The total fluorescent intensity per image or the relative fluorescence intensity per cell area was quantified using Image ProTM (Media Cybernetics, Bethesda, MD, USA). Caspase-3 activity was determined as previously described (21).

Western blot analysis and immunofluorescence

Western blot analysis and immunofluorescent staining were essentially performed as previously described (20). For the immunofluorescence, cells were stained for NF-κB p65 followed by goat anti-mouse Alexa488- (Molecular probes, Breda, the Netherlands) or Cy3-labeled (Jackson, Amsterdam, the Netherlands) secondary antibodies. Hoechst 33258 (2 μg/ml) was used to visualize the nuclei. Cells were imaged using a BD PathwayTM 855 imager (Becton Dickinson) and the NF-κB translocation was quantified as an intensity-ratio of NF-κB (nucleus): NF-κB (cytoplasm) using the AttoVisionTM software (Becton Dickinson). Images were processed in Adobe Photoshop CS2 (Adobe, Amsterdam, the Netherlands).

Live cell imaging of GFPp65 in HepG2 cells

HepG2 cells stably expressing GFPp65 (NF-κB subunit) were created by 400 mg/

mL G418 selection upon pEGFP-C1-p65 transfection using LipofectamineTM 2000 (Invitrogen, Breda, the Netherlands). Prior to imaging, nuclei were stained with 100 ng/ml Hoechst 33342 in complete DMEM. The GFPp65 nuclear translocation response upon 10 ng/mL human TNFα challenge was followed for a period of 6 hours, by automated confocal imaging (Nikon TiE2000, Nikon, Amstelveen, the Netherlands). Quantification of the nuclear/cytoplasmic ratio of GFPp65 intensity in individual cells was performed using an algorithm for ImageJ (Di *et al*, submitted).

Luciferase reporter assay

To determine the effect of diclofenac exposure and RelA inhibition/knockdown on TNFα-induced NF-κB transcriptional activity, HepG2 cells were transiently transfected with an NF-κB promoter-luciferase reporter plasmid (Clontech, Saint-Germain-en-Laye, France) using LipofectamineTM 2000 reagent according to the manufacturer's procedures (Invitrogen, Breda, the Netherlands) and incubated for 16-18 hours. The Dual-Luciferase® luciferase assay kit (Promega, Leiden, the Netherlands) and a microplate luminometer (Centro XS3 LB960, Berthold Technologies) was used to monitor luciferase activity.

Statistical analysis

All numerical results are expressed as the mean ± standard error of the mean (S.E.M.) and represent data from three independent experiments, unless otherwise stated. Calculations were made using GraphPad Prism 4.00 (GraphPad software, La Jolla, USA). Significance levels were calculated using unpaired student's t-test or 2-way ANOVA in the case of multiple comparisons, * = $P < .05$, ** = $P < .01$, *** = $P < .0001$.

RESULTS

TNFα enhances diclofenac induced cell death in hepatocytes

To investigate a role for TNFα signaling in enhancement of diclofenac-induced hepatotoxicity, we first pre-treated human hepatoma HepG2 cells with increasing concentrations of diclofenac for 8 hours to allow formation of reactive metabolites (supplementary data S1), followed by treatment with TNFα (10 ng/mL). Importantly, during this 8-hour period diclofenac was metabolized into both acylglucuronide and hydroxymetabolites (Supporting Data S1) which further accumulated in time. After 24 hours, cells were collected to determine cell death. Diclofenac alone induced a mild concentration dependent increase in cell death and while no apoptosis was observed by TNFα alone, in combination with diclofenac, TNFα-addition resulted in a two-fold increase of apoptosis (Fig. 1 A). This enhancement effect could be abrogated by co-treatment with the pan-caspase inhibitor z-VAD-fmk (50 μM), indicating that the TNFα-enhanced diclofenac-induced DNA-fragmentation is a caspase-executed apoptotic process (Fig. 1 A). A structurally different non-steroid anti-inflammatory compound, naproxen, did not lead to concentration-dependent induction of apoptosis after 24 hours of exposure, even

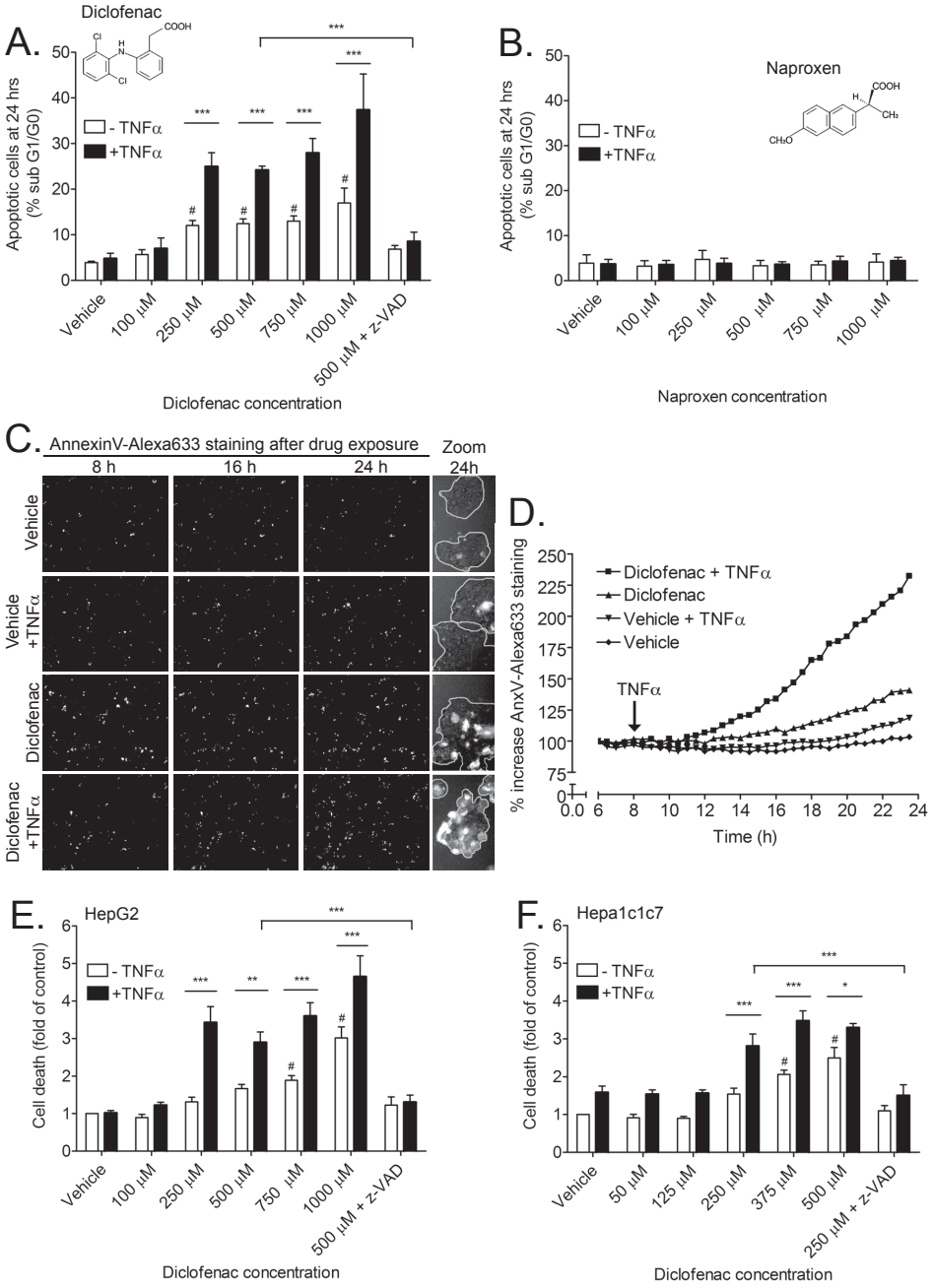

Figure 1. *TNFα enhances diclofenac-induced apoptosis in hepatocytes.* Treatment with diclofenac (A), but not the structurally different non-steroidal anti-inflammatory drug naproxen (B), induces apoptosis in HepG2 cells after 24 hours, which is significantly enhanced by addition of tumour necrosis factor α (TNFα; 10 ng/mL) after 8 hours of drug exposure. The apoptosis was determined by cell cycle analysis (A and B) or followed in time using AnnexinV (AnxV)-Alexa633 staining and automated imaging (500 μM diclofenac; C and D). Lactate dehydrogenase (LDH) activity in the medium after 24 hours of diclofenac exposure +/- TNFα was used as a measurement of overall cytotoxicity in human (E) and mouse hepatocytes (F; 1 ng/mL TNFα added after 8 hours). The data are presented as means of at least three independent experiments +/- S.E.M. The percentage of total LDH-activity under control conditions is <5 % and z-VAD-fmk (50 μM) was included where indicated. *** P < .001, ** P < .01, * P < .05, # P < .05 compared to Vehicle treated cells

in presence of TNFα (Fig. 1 B). This indicates that the diclofenac/TNFα induced apoptosis is independent from cyclooxygenase inhibition.

To gain insight in the temporal onset of the TNFα-enhanced diclofenac-induced apoptosis, we applied a live apoptosis microscopy assay, based on Alexa633-labeled annexin V (AnxV) binding to cells that present phosphatidyl-serine in the outer layer of their plasma-membrane (19). The diclofenac/TNFα-induced apoptotic response was initiated 4 hours after addition of TNFα (Fig. 1 D). This enhanced accumulation of AnxV positive cells correlated with enhanced release of lactate dehydrogenase (LDH) in the medium, which was prevented by z-VAD-fmk treatment (Fig. 1 E), supporting a model whereby TNFα promotes diclofenac-exposed HepG2 cell-killing by primarily apoptosis, followed later by secondary necrosis. Importantly, the apoptosis-inducing synergism between diclofenac and TNFα was not restricted to HepG2 cells, since the mouse hepatoma cell line Hepa1c1c7 was also susceptible to the combined treatment (Fig. 1 F).

The induced apoptosis by TNFα in diclofenac treated HepG2 cells is dependent on the extrinsic apoptotic pathway

Diclofenac alone can induce apoptosis in hepatocytes via the intrinsic, mitochondrial, apoptotic pathway involving caspase-9 (22). However, TNFα is well known to induce the apoptotic cascade via the extrinsic, death receptor-mediated pathway involving caspase-8 (16). To investigate which initial apoptotic process dominates in diclofenac/TNFα co-exposed HepG2 cells, we assessed the activation of initiator caspases -8, -9 and effector caspase-3. Diclofenac-induced apoptosis involved activation of caspase-8 which started at 16 hours after drug exposure. Activation of caspase-8 by TNFα co-exposure was already observed between 10 and 12 hours after drug treatment (Fig. 2 A). However, whereas enhanced initiation of caspase-8 cleavage correlated with caspase-3 activation and cleavage of the endogenous caspase-3 substrate poly (ADP-ribose) polymerase (PARP), caspase-9 activation was not significantly affected. Caspase-inhibition by z-VAD-fmk blocked activation of caspase-3 and PARP cleavage (Fig. 2 A) as well as caspase-3 activity (Ac-DEVD-AMC cleavage) (Fig. 2 B). Caspase-8 and caspase-9 cleavage was also partially inhibited by z-VAD-fmk and diclofenac/TNFα co-exposure (Fig. 2 A, right panel). Together these data indicate that under diclofenac conditions, TNFα induces direct cleavage of caspase-8, which is the essential step in promoting the diclofenac-induced apoptotic response.

To further determine the individual roles of caspase-8, -9 and -3, we exposed HepG2 cells with selective irreversible inhibitors (z-IETD-fmk, z-LEHD-fmk and z-DEVD-fmk, respectively) and measured the onset of apoptosis by AnxV-Alexa633 live cell imaging (Fig. 2 C). All three caspase-inhibitors delayed the initiation of the diclofenac/TNFα-induced apoptotic process (Fig. 2 D). At the 24-hour timepoint, the inhibition of caspase-3 and caspase-8 significantly reduced the apoptotic response to diclofenac/TNFα treatment, while the capase-9 inhibitor z-LEHD-fmk did not (Fig. 2 E).

To get further insight into which players in the apoptotic pathways have important

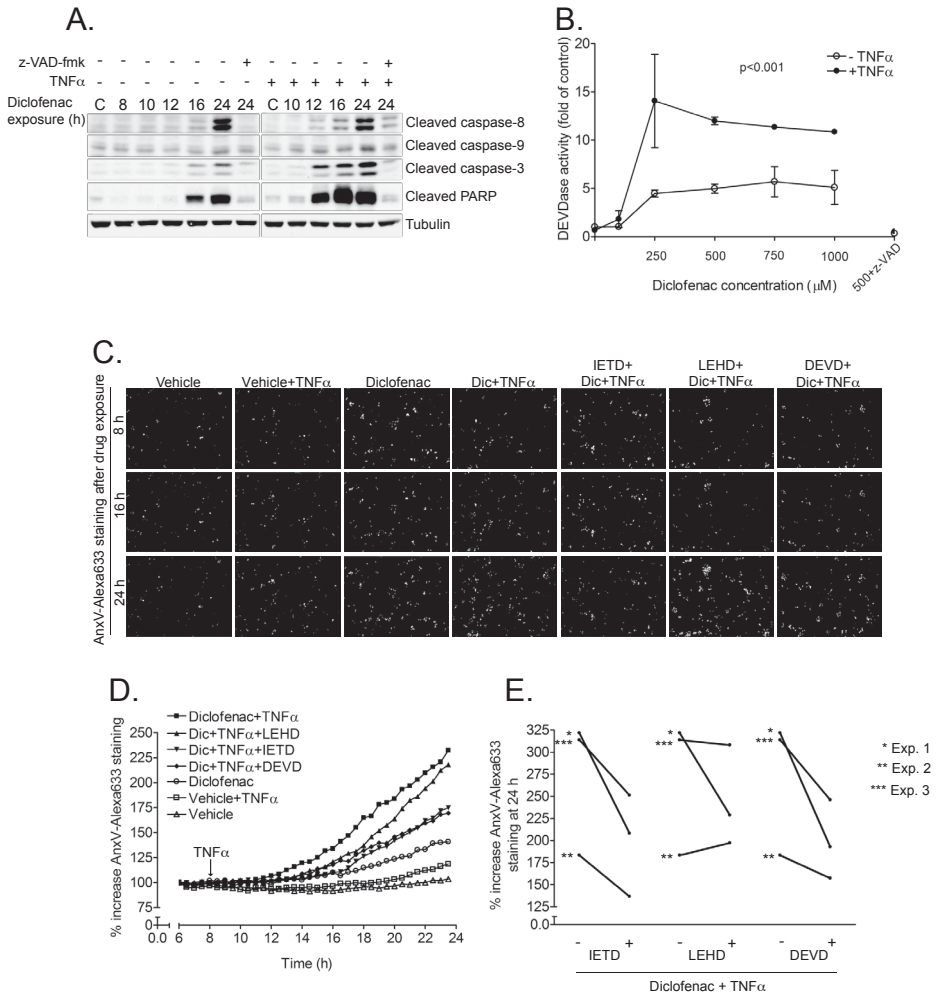

Figure 2. *Diclofenac/TNFα-induced apoptosis is dependent on caspase-8 and -3 activities.* (A) Expression levels of the active forms of caspase-8, -9, and -3 and the cleavage of poly (ADP-ribose) polymerase (PARP) after 500 μM diclofenac exposure +/- TNFα (10 ng/mL) were measured by Western blot analysis. "C" : controls exposed to vehicle for 24 hours +/- TNFα after 8 hours. (B) Activity of effector caspase-3 after exposure to diclofenac +/- TNFα (10 ng/mL), was measured by Ac-DEVD-AMC cleavage assay. The activity is presented as fold of control where the control activity is ~1 pmol AMC/min/mg protein. (C, D and E) The effect of specific caspase inhibitors on apoptosis induced by 500 μM diclofenac +/- TNFα (10 ng/mL) was investigated by following AnxV-Alexa633 binding to apoptotic cells in time using automated imaging. (C) Images, representative of three independent experiments (see supplementary information for complete movies M1-M7); IETD = caspase-8 inhibitor z-IETD-fmk, LEHD = caspase-9 inhibitor z-LEHD-fmk, DEVD = caspase-3 inhibitor z-DEVD-fmk. (D) Quantification of the fluorescent AnxV-Alexa633 labelled apoptotic cells. (E) The difference in % increase in AnxV-Alexa633 staining after 24 hours of drug exposure (+TNFα) is shown, with the three independent experiments illustrated separately.

roles in the induction of diclofenac/TNFα-induced apoptosis, we created a siRNA SMARTpool library containing 50 siRNAs against known pro- and anti-apoptotic genes (Supporting Data S2). Following knockdown in three independent experiments, as a primary screen, HepG2 cells were treated with diclofenac/TNFα, and onset of apoptosis was analyzed by live cell imaging. Candidate gene knockdown resulting in a >2.0 fold

reduction in apoptosis after 24 hours of diclofenac/TNFα exposure were defined as target genes involved in the onset of diclofenac/TNFα-induced apoptosis (Fig. 3 A and Supporting Data S2); knockdown resulting in a >2.0 fold increase in apoptosis were defined as apoptosis suppressors (Fig. 3 B and Supporting Data S2). Knockdown of caspase-8, Bid, p53 up-regulated modulator of apoptosis (PUMA), apoptosis inducing factor (AIF) and apoptotic protease activating factor 1 (APAF1) inhibited diclofenac/TNFα-induced apoptosis; knockdown of cellular FLICE-like inhibitory protein (c-FLIP), Bcl10, Bcl-B and RIP-associated protein with a death domain (RAIDD) enhanced the apoptosis. Knockdown of caspase-9 and -3 partially inhibited apoptosis (Supporting Data S2). To

A.

	Primary screen				Secondary screen	
	Exp 1	Exp 2	Exp 3	Average	Deconvolution	True? (≥2/4)
Caspase-8	0.0	0.08	0.19	**0.07**	4/4	Yes
Bid	0.22	0.40	0.42	**0.32**	3/4	Yes
APAF1	0.30	0.34	0.55	**0.38**	2/4	Yes
AIF	0.40	0.34	0.55	**0.42**	1/4	No
PUMA	0.38	0.56	0.63	**0.50**	2/4	Yes
Caspase-9	0.43	0.90	0.58	0.60	2/4	Yes
Caspase-3	0.58	0.57	0.87	0.66	4/4	Yes

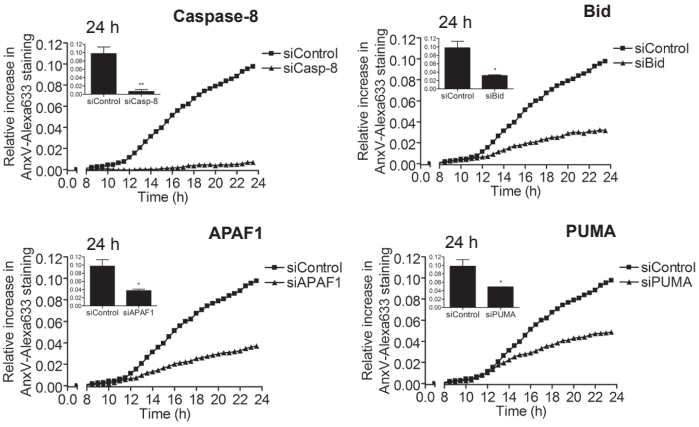

B.

	Primary screen				Secondary screen	
	Exp 1	Exp 2	Exp 3	Average	Deconvolution	True? (≥2/4)
c-FLIP	2.01	3.77	4.32	3.14	2/4	Yes
Bcl10	1.87	4.29	3.53	3.02	1/4	No
Bcl-B	1.60	2.71	2.50	2.17	1/4	No
RAIDD	1.80	2.64	2.01	2.10	1/4	No

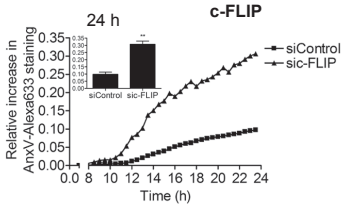

Figure 3. *siRNA-mediated knockdown of central apoptotic machinery components.* siRNAs targeting 50 apoptotic machinery genes were used to investigate their individual roles in diclofenac/TNFα-induced apoptosis (500 μM/10 ng/mL). AnxV-Alexa633 staining was followed in time using automated imaging. (A) Genes defined as pro-apoptotic regulators of diclofenac/TNFα based on the average > 2.0-fold decrease compared to siControl transfected cells in the primary screen and 2 out of 4 single siRNA sequences showing the phenotype in the secondary deconvolution screen. (B) Genes defined as anti-apoptotic components of diclofenac/TNFα-induced apoptosis based on average > 2.0-fold increase compared to siControl transfected cells in the primary screen and 2 out of 4 single siRNA sequences showing the phenotype in the secondary deconvolution screen. For both (A) and (B), the tables present the fold-change induction of apoptosis in the primary screen compared to siControl transfected HepG2 cells from three independent experiments as well as from averages of all three and the number of constructs in the secondary screen that resulted in the expected phenotype. The graphs present the average time-dependent diclofenac/TNFα-induced apoptosis as well as the averages of the 24 hour timepoints for the hits from the primary screen that could also be validated in the secondary deconvolution screen. Data are the means of three independent experiments +/- S.E.M. ** P < .01, * P < .05

further validate the effect of the knockdown of the mentioned genes, a deconvolution secondary screen was performed with the four individual siRNA sequences that were present in the siRNA SMARTpool mix used in the primary screen. Deconvolution analysis of caspase-3 and -9 were also included, to verify the mitochondrial-dependent APAF1-mediated apoptosome formation resulting in caspase-3 activation. Knockdown that resulted in a >1.5 fold increase or decrease in apoptosis compared to siControl transfected cells after 24 hours exposure of diclofenac/TNFα in at least 2 out of 4 individual siRNA sequences were considered as true mediators of diclofenac/TNFα-induced apoptosis (Fig. 3 A and B; Supporting Data S3). These included caspases-8, -3 and -9, Bid, APAF1 and PUMA. The caspase-8 inhibitory protein c-FLIP was indentified as a reducer of diclofenac/TNFα apoptosis.

Altogether these data indicate that the route of apoptosis-induction after diclofenac/TNFα exposure is dependent on the extrinsic apoptotic pathway involving caspase-8. In addition, the siRNA screen revealed that the apoptosis was dependent on the mitochondrial apoptotic pathway initiated by the activation of Bid and including the release of APAF1-dependent activation of caspase-9 and -3.

Diclofenac and diclofenac/TNFα co-exposure leads to JNK-activation in HepG2 cells

Diclofenac-induced small intestinal injury is dependent on JNK-activation (23). In addition, TNFα-induced apoptosis can result from sustained JNK activation (24). Therefore we determined the activation status of JNK after diclofenac and diclofenac/TNFα treatment. Both diclofenac alone and diclofenac/TNFα co-exposure caused sustained JNK phosphorylation although only little sustained activation was seen with TNFα alone (Fig. 4 A). The diclofenac/TNFα-induced JNK activity was associated with increased phosphorylation of c-Jun, an important downstream target of JNK (Fig. 4 A). Inhibition of JNK-activation by a specific inhibitor of JNK, SP600125, almost completely inhibited the onset of diclofenac/TNFα-induced apoptosis (Fig. 4 B-D).

TNFα-induced apoptosis is associated with prolonged activation of JNK1 (25). However, other studies demonstrated a role for JNK2 as well (26, 27). We performed knockdown of the two major JNK isoforms, JNK1 and JNK2. Knockdown was verified by Western blotting (Supporting Data S2). Live cell imaging of the apoptosis onset identified JNK1 as the main JNK isoform involved in diclofenac/TNFα-induced apoptosis (Fig. 4 E-F). Altogether these data suggest an important role for JNK1 activation by diclofenac in sensitizing HepG2 cells towards enhanced cell injury induced by TNFα.

Diclofenac inhibits TNFα-induced NF-κB signaling

Under normal physiological conditions hepatocytes are resistant to TNFα-induced apoptosis due to NF-κB mediated transcriptional regulation of anti-apoptotic target genes such as c-FLIP, thereby suppressing TNF-R-mediated caspase-8 activation (16). Activation of the IKK-complex by TNFα causes phosphorylation of the inhibitor of NF-κB,

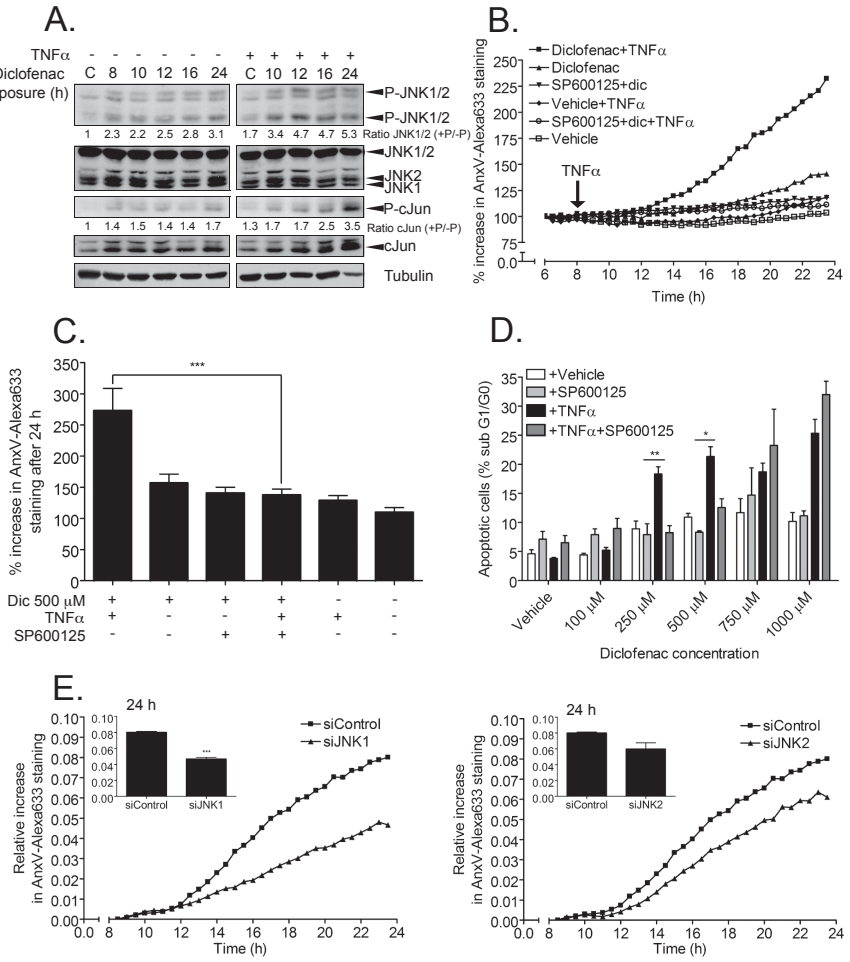

Figure 4. *Diclofenac/TNFα-induced apoptosis is dependent on JNK activity.* (A) JNK activation in time after diclofenac exposure +/- TNFα was assessed by Western blot analysis. Tubulin was used as loading control. "C": controls exposed to vehicle for 24 hours +/- TNFα after 8 hours. The ratios represent the fold increase of phosphorylated protein expression over total protein compared to C (-TNFα). (B, C and D) Cells were treated with the cJun N-terminal kinase (JNK)-specific inhibitor SP-600125 (20 μM) and its effect on apoptosis induced by 500 μM diclofenac +/- TNFα was followed by AnxV-Alexa633 staining and automated imaging (B) and by cell cycle analysis after 24 h drug exposure (D). End-point quantification of the AnxV-Alexa633 signal increase after 24 hours of drug exposure in the live apoptosis assay (B) is shown in (C). (E) Effect of siRNA-mediated knockdown of the individual isoforms JNK1 and JNK2 on apoptosis induction by diclofenac/TNFα was followed by AnxV-Alexa633 staining and automated imaging. Data are the means of three independent experiments +/- S.E.M. *** P < .001, ** P < .01, * P < .05

IκBα, followed by its degradation by the proteasome allowing translocation of NF-κB to the nucleus. Since caspase-8 was central in diclofenac/TNFα-induced apoptosis (see Fig. 2 and Fig. 3), we next investigated whether the NF-κB signaling induced by TNFα was affected by diclofenac. Diclofenac caused a concentration dependent disturbance of the TNFα-induced NF-κB signaling (Fig. 5). Diclofenac both decreased and delayed IκBα phosphorylation in association with an inhibition of its degradation (Fig. 5 A, top and middle panel respectively). The delay in IκBα degradation was associated with a disruption of NF-κB nuclear translocation shown by immunofluorescence staining of

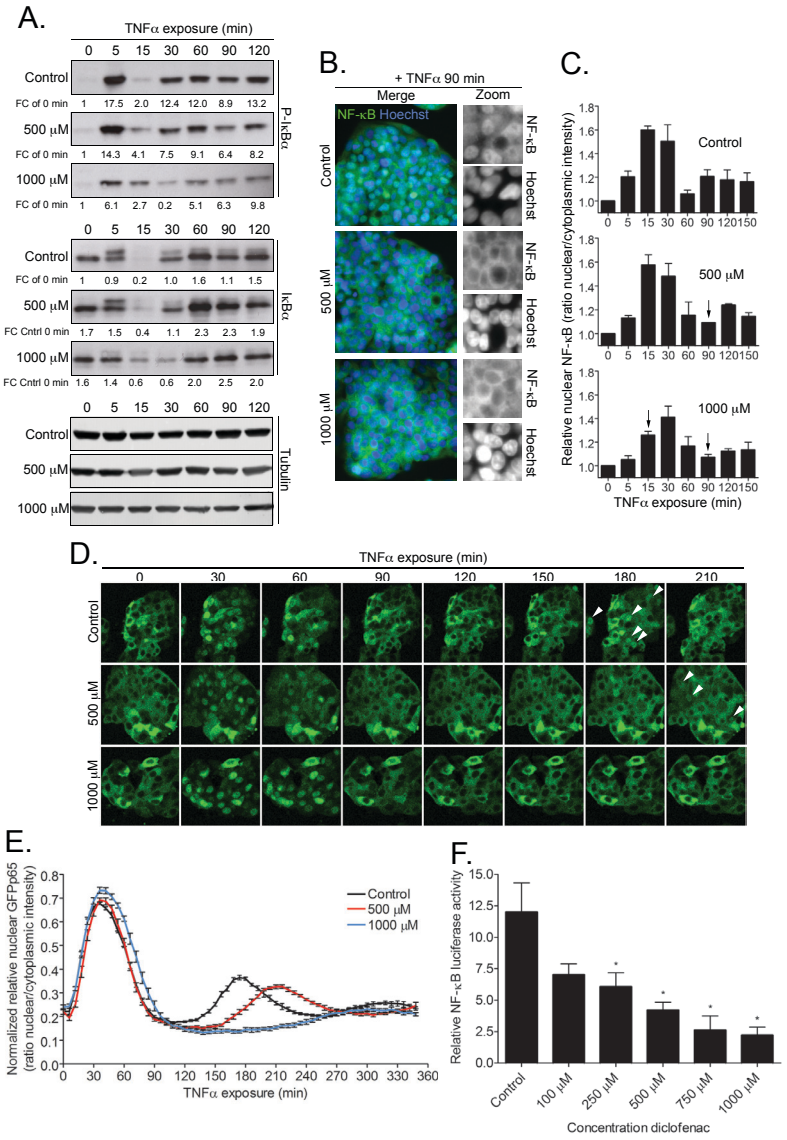

Figure 5. *Diclofenac inhibits NF-κB signalling induced by TNFα.* (A) HepG2 cells were pre-exposed to diclofenac for 8 hours before adding TNFα (10 ng/mL). The phosphorylation status of inhibitor of NF-κB (IκBα) and the subsequent degradation of the IκBα protein, were determined by Western blot analysis. Tubulin staining was used as loading control. Results are representative of three independent experiments and the fold changes (FC) represent the tubulin-normalized FC in protein expression compared to 0 minutes of TNFα exposure. (B) The effect of 8 hours diclofenac exposure on nuclear factor κB (NF-κB) (p65) translocation into the nucleus was investigated in time by immunofluorescence staining of p65 (green). The nuclei were stained with Hoechst 33258 (blue). The cells were imaged using a BD PathwayTM 855 imager. The results are representative for three independent experiments. (C) The nuclear translocation pattern of NF-κB was determined using the BD AttoVisionTM software. The graphs represent the means of three independent experiments +/- S.E.M. (D and E) HepG2 GFPp65 cells were used to follow the translocation of NF-κB after TNFα exposure live +/- diclofenac pre-treatment using automated confocal imaging with pictures taken every 6 minutes. (E) The graph represents the quantification of the GFPp65 nuclear/cytoplasmic intensity ratio normalized to the highest intensity/cell. (F) NF-κB transcriptional activity was investigated using a NF-κB luciferase reporter construct. The luciferase activity was measured after 12 hours drug exposure +/- 10 ng/mL TNFα for the last 4 hours. Results are expressed as ratios of the luciferase activity measured after TNFα exposure in non-pre-exposed cells over diclofenac pre-exposed cells and represent the means from three independent experiments +/- S.E.M. * $P < .05$

wildtype HepG2 cells and live cell imaging of HepG2 cells stably expressing the NF-κB subunit p65 coupled to GFP (GFPp65) (Fig. 5 B and D). Automated image quantification of the p65 signal intensity ratio of nucleus/cytoplasm, showed that diclofenac delays the onset of the second nuclear entry of NF-κB (Fig. 5 C and E). This diclofenac-induced reduction of the TNFα-induced NF-κB nuclear translocation response was associated with a decrease in the transcriptional NF-κB activity after TNFα treatment (Fig. 5 F). These data indicate that diclofenac interferes with the TNFα-mediated NF-κB response dynamics.

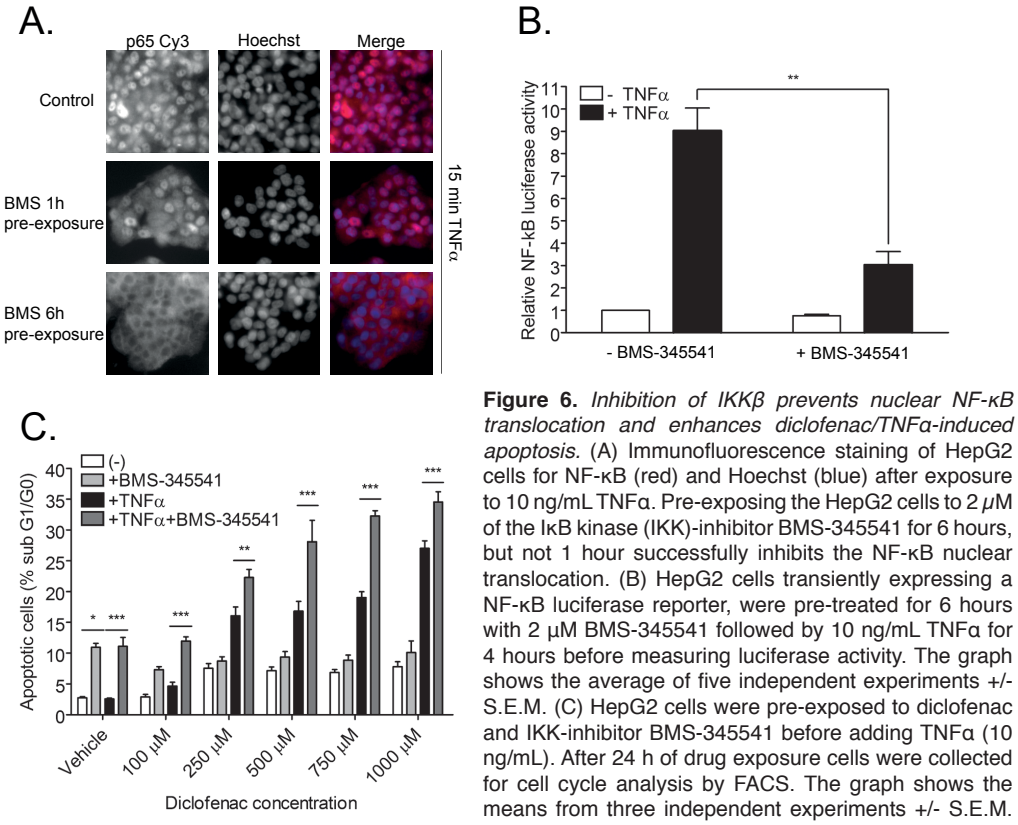

Figure 6. *Inhibition of IKKβ prevents nuclear NF-κB translocation and enhances diclofenac/TNFα-induced apoptosis.* (A) Immunofluorescence staining of HepG2 cells for NF-κB (red) and Hoechst (blue) after exposure to 10 ng/mL TNFα. Pre-exposing the HepG2 cells to 2 μM of the IκB kinase (IKK)-inhibitor BMS-345541 for 6 hours, but not 1 hour successfully inhibits the NF-κB nuclear translocation. (B) HepG2 cells transiently expressing a NF-κB luciferase reporter, were pre-treated for 6 hours with 2 μM BMS-345541 followed by 10 ng/mL TNFα for 4 hours before measuring luciferase activity. The graph shows the average of five independent experiments +/- S.E.M. (C) HepG2 cells were pre-exposed to diclofenac and IKK-inhibitor BMS-345541 before adding TNFα (10 ng/mL). After 24 h of drug exposure cells were collected for cell cycle analysis by FACS. The graph shows the means from three independent experiments +/- S.E.M. *** P < .001, ** P < .01, * P < .05

NF-κB signaling is essential to prevent TNFα-mediated enhancement of diclofenac-induced apoptosis

We anticipated that interference of the NF-κB signalling pathway is causally associated with diclofenac/TNFα-induced apoptosis. To inhibit NF-κB activation we used an inhibitor of IKKβ, BMS-345541 (BMS, 2 μM). Pre-treatment with BMS for 6 hours prevented the TNFα-induced nuclear entry of NF-κB (Fig. 6 A) in association with decreased NF-κB transcriptional activity (Fig. 6 B). Under these conditions, BMS strongly sensitized the HepG2 cells for diclofenac/TNFα-induced apoptosis (Fig. 6 C).

Next we determined whether knockdown of the NF-κB subunit p65 affected diclofenac/TNFα cell killing. Lentiviral shRNA-based stable knockdown of p65/RelA reduced the levels of p65 as determined by immunofluorescence and Western blotting NF-κB (Fig. 7 A and B). Moreover, importantly, TNFα-induced activation of a NF-κB-luciferase reporter construct was inhibited in shRelA-HepG2 cells to approximately the same extent as pre-exposure to the IKKβ inhibitor BMS (compare Fig. 6 B and Fig. 7 C). Knockdown of p65/RelA did not affect the basic level of apoptosis under both control and TNFα conditions (Fig. 7 D and E, respectively). Next, we exposed the different cell lines to a concentration range of diclofenac for 8 hours followed by TNFα treatment. Loss of p65/RelA did not significantly enhance the induction of apoptosis by diclofenac alone

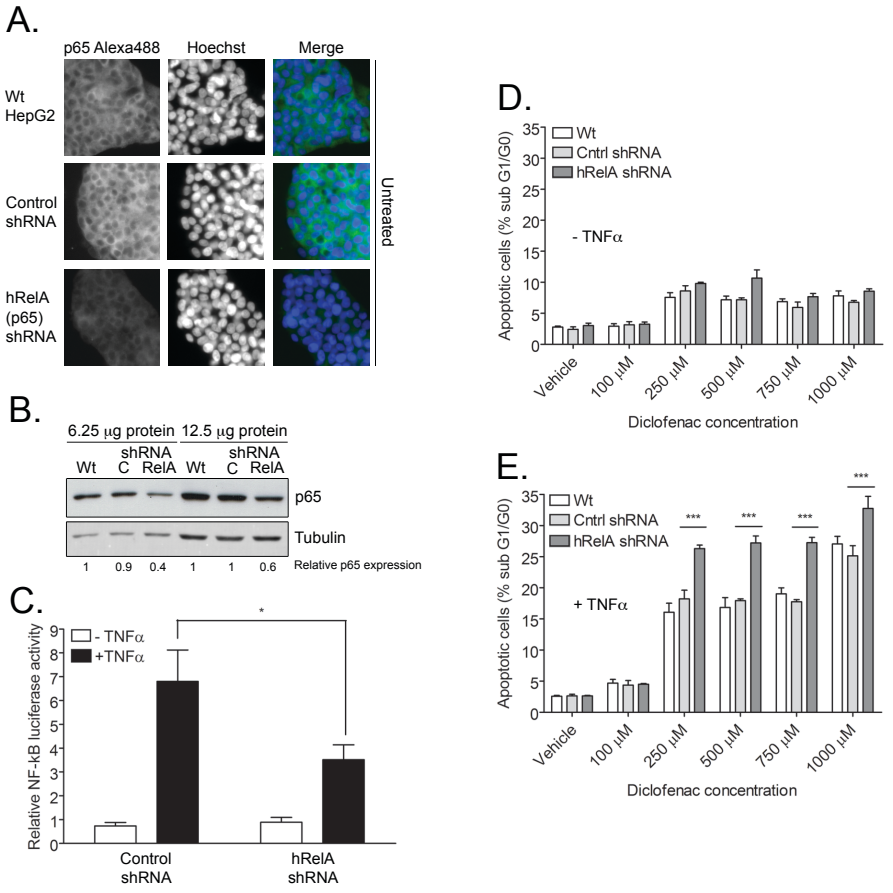

Figure 7. *Knockdown of p65 sensitizes HepG2 cells for TNFα-enhanced diclofenac-induced apoptosis.* (A) Immunofluorescence staining of NF-κB (green) on untreated wild-type (Wt) HepG2 cells and cells stably transduced with control or human RelA short hairpin RNA (shRNA) constructs. Nuclei were detected with Hoechst 33258 (blue). (B) Quantification of RelA/p65 levels in Wt, shControl and shRelA HepG2 cells by Western blot analysis. (C) Control shRNA and p65/hRelA shRNA transduced HepG2 cells transiently expressing a NF-κB luciferase reporter, were treated with 10 ng/mL TNFα for 4 hours before measuring luciferase activity. The graph shows the average of five independent experiments +/- S.E.M. (C and D) Wt, control shRNA transduced and HepG2 cells stably knocked down for p65 (hRelA shRNA), were exposed to diclofenac for 24 hours without (C) or in the presence of TNFα (10 ng/mL; D). The graphs represent the percentage of apoptosis detected by cell cycle analysis and shows the means from three independent experiments +/- S.E.M. *** P < .001, * P < .05

(Fig. 7 D). However, knockdown of p65/RelA sensitized HepG2 cells towards diclofenac/TNFα-induced apoptosis (Fig. 7 E). Together, these data confirm the important role of functional NF-κB signalling and nuclear translocation in protecting hepatocytes from TNFα-enhanced diclofenac-induced apoptosis.

DISCUSSION

Drug-induced liver injuries are a significant problem in clinical practice as well as during drug development. There is increasing evidence for a role of the innate immune system in the pathophysiology of drug-induced liver injury which seems to involve an interaction between reactive metabolite formation and cytokine signaling (2, 5, 6). Diclofenac can cause drug-induced liver injury in an idiosyncratic manner. Here we studied in detail the role and mechanism of diclofenac/cytokine-induced stress signaling on the onset of hepatocyte apoptotic cell death. Our data indicate that: 1) TNFα enhances diclofenac-induced cell death of HepG2 cells; 2) this cell death involves the onset of apoptosis which is dependent on a caspase-8/Bid/APAF1 cascade and the activity of caspase-3; 3) the diclofenac/TNFα synergy involves an inhibition of TNFα-induced NF-κB activity which is related to a disruption of IκBα phosphorylation and degradation and subsequent differential translocation of NF-κB to the nuclear compartment. Our results support a model in which diclofenac affects the TNFα signaling program, thereby preventing the anti-apoptotic actions of NF-κB and allowing a JNK- and death receptor-mediated mitochondrial onset of apoptosis.

Our data demonstrate that TNFα enhances the cytotoxicity of diclofenac in both human HepG2 and mouse Hepa1c1c7 cells. Our data fit with a model whereby activated Kupffer cells in the liver release TNFα and thereby aggravate liver injury (10-12). Although a role for TNFα in diclofenac-induced liver injury has not previously been demonstrated, LPS treatment severely enhances liver failure induced by diclofenac (13). Since LPS induces direct activation of Kupffer cells with the subsequent release of high levels of TNFα (9), a direct interaction between diclofenac and TNFα in the liver can be anticipated. Importantly, oral administration of diclofenac can cause severe injury to the intestine (28), thus creating a condition for increased systemic levels of endotoxins and activation of liver macrophages with a subsequent deleterious interaction with diclofenac in the liver. A role of polymorphonuclear neutrophils (PMNs) infiltration in the above mentioned animal model of diclofenac/LPS-induced liver injury was demonstrated by PMN-depleting antiserum (13). We suggest that this observation does not exclude the importance of (LPS-induced) TNFα secretion in this model, as we simulate in our *in vitro* system. Thus, the PMN-depletion only provided partial protection against diclofenac/LPS liver injury, while the deleterious effect of the PMNs themselves could involve the release of TNFα by these cells within the liver (28).

The concentrations of diclofenac used to achieve diclofenac/TNFα synergy (>100 μM) in this *in vitro* study exceed the maximal plasma concentration reached in humans after a single dose of 50 mg, 5-10 μM (29; with the potentially higher concentration in the liver

after oral intake). This is also expected since HepG2 cells are poor in drug metabolizing capacity, but do form identical relevant diclofenac metabolites (see Supporting Data S1). Indeed, using HepG2 cells that express GFP-Nrf2, we could demonstrate stabilization of Nrf2 upon diclofenac treatment in a time and concentration dependent manner supportive for drug reactive metabolite formation that has cell biological consequences (Herpers, Fredriksson and van de Water, unpublished observation). Although the observed patient concentrations are well below the concentration used in our studies, higher levels of drug metabolism in hepatocytes in the liver as well as chronic treatment of patients with diclofenac is likely to lead to equal levels of drug metabolite formation as well as accumulation of diclofenac metabolite covalent modification of cellular proteins in hepatocytes, in particular after overdosing, conditions of liver function insufficiency or reduced capacity of systemic diclofenac excretion.

Our data indicate that diclofenac/TNFα-induced apoptosis involves a mitochondrial pathway. This is in accordance with previous observations that diclofenac alone can induce apoptosis via the mitochondrial death route, which involves an increase in free cytosolic calcium and induction of the mitochondrial pore transition (mPT) (31) most likely through Bax-mediated mitochondrial outer membrane permeabilization (MOMP) (22). We used a small siRNA library that targets all individual components of the apoptotic machinery. Thereby, we identified two Bcl-2 family members that contribute to the control of diclofenac/TNFα-induced apoptosis, Bid and PUMA, two pro-apoptotic family members (32). Bid is activated through direct caspase-8-mediated cleavage, thereby inducing onset of the MOMP in mitochondria (33). Indeed, diclofenac/TNFα activates caspase-8 and knockdown of caspase-8 as well as an inhibitor of caspase-8 effectively inhibited diclofenac/TNFα-induced apoptosis (Fig. 2 and Fig. 3 A). Furthermore, knockdown of c-FLIP, an endogenous inhibitor of caspase-8, strongly enhances the apoptosis (Fig. 3 B). Diclofenac-induced permeabilization of the mitochondria is followed by release of pro-apoptotic factors which results in activation of caspase-9 and caspases-3 mediated apoptosis (22, 31, 34). In our hands only a weak activation of caspase-9 could be seen with diclofenac and diclofenac/TNFα exposure (Fig. 2 A), and in accordance with this, the specific caspase-9 inhibitor was not fully effective in inhibiting diclofenac/TNFα-induced apoptosis (Fig. 2 C-E). Nevertheless, knockdown of caspase-9 as well as of APAF1 was confirmed as essential for the diclofenac/TNFα-induced apoptosis (Fig. 3 A and Supporting Data S3). Together this suggests a clear role for the apoptosome formation in this process..

We show that diclofenac directly affected the efficient TNFα-induced activation of NF-κB. Diclofenac inhibited the TNFα-mediated phosphorylation and degradation of the inhibitor of NF-κB, IκBα. This was directly associated with a shift in the oscillatory NF-κB translocation pattern and a reduced TNFα-induced NF-κB transcriptional activity (Fig. 5 and Fig. 6). In our model, NF-κB signalling is essential in the control of diclofenac/TNFα-induced apoptosis. Thus, inhibition of the NF-κB activation using an IKKβ-inhibitor, BMS-345541, or stable shRNA-based RelA knockdown increases the cell death induced by diclofenac/TNFα (Fig. 6 C and Fig. 7 E). The inhibition of NF-κB signaling by diclofenac

most likely affects the anti-apoptotic program typically induced by TNFα in normal cells (15). This would result in the reduced expression of anti-apoptotic molecules. Indeed, in cutaneous squamous cell carcinoma cells, diclofenac enhances death ligand-induced apoptosis which was associated with downregulation of c-FLIP (35), an NF-κB target gene that inhibits caspase-8 (36). Knockdown of c-FLIP in our hands enhances diclofenac/TNFα induced apoptosis (Fig. 3 B). TNFα alone did not cause apoptosis when NF-κB signaling was inhibited by BMS-345541 or RelA knockdown (Fig. 6 C and Fig. 7 E). This indicates that TNFα signaling itself is not the main contributor to the onset of apoptosis, further supporting a synergistic action between TNFα and the toxic properties of diclofenac, most likely involving formation of diclofenac reactive metabolites (2, 5, 6; Supporting Data S1).

In summary, we show that TNFα enhances hepatocyte injury caused by diclofenac. We propose a mechanism by which diclofenac inhibits the TNFα-induced nuclear translocation of NF-κB thereby affecting the transcriptional activation of anti-apoptotic molecules and allowing a caspase-8/Bid/APAF1 dependent onset of apoptosis (see Fig. 8). These results shed new light on the interaction of hepatotoxic drugs and pro-inflammatory cytokines in drug-induced liver cell injury.

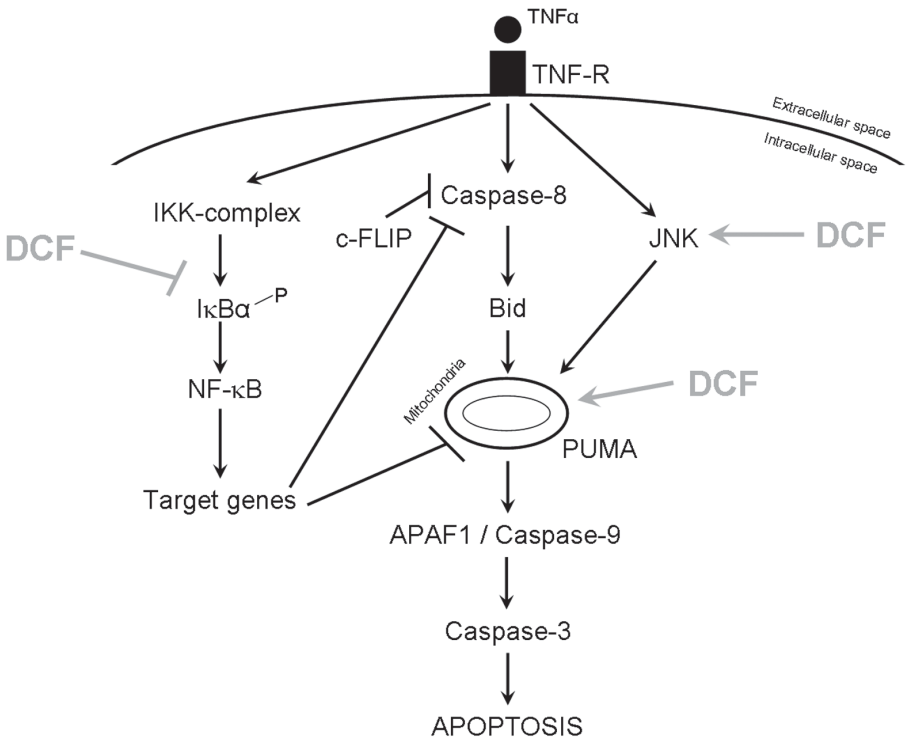

Figure 8. *Working model for diclofenac-TNFα hepatotoxicity synergy.* Reactive metabolites formed by diclofenac (DCF) metabolism inhibits IκBα phosphorylation in association with the NF-κB nuclear translocation oscillatory response and transcriptional activity. In the absence of the anti-apoptotic NF-κB signaling, the synergistic activation of both the death receptor pathway and JNK signaling pathway, mediate the onset of apoptotic cell death. This apoptosis is dependent on the caspase-8/Bid/Apaf-1/caspase-9/3 pathway with an additional involvement of the pro-apoptotic Bcl-2 family member PUMA.

REFERENCES

1. Lee WM. Etiologies of acute liver failure. Semin Liver Dis 2008;28:142-152.
2. Antoine DJ, Williams DP, Park BK. Understanding the role of reactive metabolites in drug-induced hepatotoxicity: state of the science. Expert Opin Drug Metab Toxicol 2008;4:1415-1427.
3. Aithal GP, Day CP. Nonsteroidal anti-inflammatory drug-induced hepatotoxicity. Clin Liver Dis 2007;11:563-575, vi-vii.
4. Laine L, Smith R, Min K, Chen C, Dubois RW. Systematic review: the lower gastrointestinal adverse effects of non-steroidal anti-inflammatory drugs. Aliment Pharmacol Ther 2006;24:751-767.
5. Kaplowitz N. Drug-induced liver injury. Clin Infect Dis 2004;38 Suppl 2:S44-48.
6. Ulrich RG. Idiosyncratic toxicity: a convergence of risk factors. Annu Rev Med 2007;58:17-34.
7. Boelsterli UA. Diclofenac-induced liver injury: a paradigm of idiosyncratic drug toxicity. Toxicol Appl Pharmacol 2003;192:307-322.
8. Han D, Shinohara M, Ybanez MD, Saberi B, Kaplowitz N: Signal transduction pathways involved in drug-induced liver injury. In: Uetrecht J, ed. Handb Exp Pharmacol. Volume 196. 2009/12/19 ed. Heidelberg: Springer, 2010; 267-310.
9. Roberts RA, Ganey PE, Ju C, Kamendulis LM, Rusyn I, Klaunig JE. Role of the kupffer cell in mediating hepatic toxicity and carcinogenesis. Toxicol. Sci. 2007;96:2-15.
10. Shaw PJ, Hopfensperger MJ, Ganey PE, Roth RA. Lipopolysaccharide and trovafloxacin coexposure in mice causes idiosyncrasy-like liver injury dependent on tumor necrosis factor-alpha. Toxicol Sci 2007;100:259-266.
11. Barton CC, Barton EX, Ganey PE, Kunkel SL, Roth RA. Bacterial lipopolysaccharide enhances aflatoxin B1 hepatotoxicity in rats by a mechanism that depends on tumor necrosis factor alpha. Hepatology 2001;33:66-73.
12. Shaw PJ, Ganey PE, Roth RA. Tumor necrosis factor alpha is a proximal mediator of synergistic hepatotoxicity from trovafloxacin/lipopolysaccharide coexposure. J Pharmacol Exp Ther 2009;328:62-68.
13. Deng X, Stachlewitz RF, Liguori MJ, Blomme EA, Waring JF, Luyendyk JP, et al. Modest inflammation enhances diclofenac hepatotoxicity in rats: role of neutrophils and bacterial translocation. J Pharmacol Exp Ther 2006;319:1191-1199.
14. Hoffmann A, Baltimore D. Circuitry of nuclear factor kappaB signaling. Immunol Rev 2006;210:171-186.
15. Beyaert R, Van Loo G, Heyninck K, Vandenabeele P. Signaling to gene activation and cell death by tumor necrosis factor receptors and Fas. Int Rev Cytol 2002;214:225-272.
16. Micheau O, Tschopp J. Induction of TNF receptor I-mediated apoptosis via two sequential signaling complexes. Cell 2003;114:181-190.
17. Wullaert A, Heyninck K, Beyaert R. Mechanisms of crosstalk between TNF-induced NF-kappaB and JNK activation in hepatocytes. Biochem Pharmacol 2006;72:1090-1101.
18. Papa S, Bubici C, Zazzeroni F, Franzoso G. Mechanisms of liver disease: cross-talk between the NF-kappaB and JNK pathways. Biol Chem 2009;390:965-976.
19. Puigvert JC, de Bont H, van de Water B, Danen EH. High-throughput live cell imaging of apoptosis. Curr Protoc Cell Biol 2010;47:18.10.11-18.10.13.
20. van de Water B, Houtepen F, Huigsloot M, Tijdens IB. Suppression of chemically induced apoptosis but not necrosis of renal proximal tubular epithelial (LLC-PK1) cells by focal adhesion kinase (FAK). Role of FAK in maintaining focal adhesion organization after acute renal cell injury. J Biol Chem 2001;276:36183-36193.
21. de Graauw M, Tijdens I, Cramer R, Corless S, Timms JF, van de Water B. Heat shock protein 27 is the major differentially phosphorylated protein involved in renal epithelial cellular stress response and controls focal adhesion organization and apoptosis. J Biol Chem 2005;280:29885-29898.
22. Siu WP, Pun PB, Latchoumycandane C, Boelsterli UA. Bax-mediated mitochondrial outer membrane permeabilization (MOMP), distinct from the mitochondrial permeability transition, is a key mechanism in diclofenac-induced hepatocyte injury: Multiple protective roles of cyclosporin A. Toxicol Appl Pharmacol 2008;227:451-461.
23. Ramirez-Alcantara V, Loguidice A, Boelsterli UA. Protection from diclofenac-induced small intestinal injury by the JNK inhibitor SP600125 in a mouse model of NSAID-associated enteropathy. Am J Physiol Gastrointest Liver Physiol 2009;297:G990-G998.
24. Deng Y, Ren X, Yang L, Lin Y, Wu X. A JNK-dependent pathway is required for TNFalpha-induced apoptosis. Cell 2003;115:61-70.
25. Chang L, Kamata H, Solinas G, Luo JL, Maeda S, Venuprasad K, et al. The E3 ubiquitin ligase itch couples JNK activation to TNFalpha-induced cell death by inducing c-FLIP(L) turnover. Cell 2006;124:601-613.
26. Kodama Y, Taura K, Miura K, Schnabl B, Osawa Y, Brenner DA. Antiapoptotic effect of c-Jun N-terminal Kinase-1 through Mcl-1 stabilization in TNF-induced hepatocyte apoptosis. Gastroenterology

2009;136:1423-1434.
27. Wang Y, Singh R, Lefkowitch JH, Rigoli RM, Czaja MJ. Tumor necrosis factor-induced toxic liver injury results from JNK2-dependent activation of caspase-8 and the mitochondrial death pathway. J Biol Chem 2006;281:15258-15267.
28. Cassatella M. Neutrophil-derived proteins: selling cytokines by the pound. Adv Immunol 1999;73:369-509
29. J. V. Willis, M. J. Kendall, R. M. Flinn, D. P. Thornhill, P. G. Welling The pharmacokinetics of diclofenac sodium following intravenous and oral administration. Eur J Clin Pharmacol 1979;16:405-410
30. Bjarnason I, Hayllar J, MacPherson AJ, Russell AS. Side effects of nonsteroidal anti-inflammatory drugs on the small and large intestine in humans. Gastroenterology 1993;104:1832-1847.
31. Lim MS, Lim PL, Gupta R, Boelsterli UA. Critical role of free cytosolic calcium, but not uncoupling, in mitochondrial permeability transition and cell death induced by diclofenac oxidative metabolites in immortalized human hepatocytes. Toxicol Appl Pharmacol 2006;217:322-331.
32. Willis SN, Adams JM. Life in the balance: how BH3-only proteins induce apoptosis. Curr Opin Cell Biol 2005;17:617-625.
33. Garrido C, Galluzzi L, Brunet M, Puig PE, Didelot C, Kroemer G. Mechanisms of cytochrome c release from mitochondria. Cell Death Differ 2006;13:1423-1433.
34. Gomez-Lechon MJ, Ponsoda X, O'Connor E, Donato T, Castell JV, Jover R. Diclofenac induces apoptosis in hepatocytes by alteration of mitochondrial function and generation of ROS. Biochem Pharmacol 2003;66:2155-2167.
35. Fecker LF, Stockfleth E, Braun FK, Rodust PM, Schwarz C, Kohler A, et al. Enhanced death ligand-induced apoptosis in cutaneous SCC cells by treatment with diclofenac/hyaluronic acid correlates with downregulation of c-FLIP. J Invest Dermatol 2010;130:2098-2109.
36. Karin M, Lin A. NF-kappaB at the crossroads of life and death. Nat Immunol 2002;3:221-227.

SUPPORTING MATERIALS AND METHODS

Metabolite measurements

HepG2 cells were grown until confluency in TC-75 flasks and incubated with 500 μM diclofenac in 15 mL complete DMEM for 8, 16 or 24 hours. After incubation, 15 mL ice-cold methanol (MeOH) was added and the total volume with cells was collected in 50 mL falcon tubes and stored at -80°C until analysis. The incubations were first centrifuged for 15 minutes at 4000 rpm to remove the cells. Solid phase extraction (SPE) was used for the isolation and purification of the metabolites. StrataTM-X C-18 SPE columns (Phenomenex, Torrance, CA, USA) were first conditioned according the manufacturer's instructions. A 6 mL aliquot of the supernatant for each time point was then applied to the column and washed with 6 mL of water. Diclofenac and its metabolites were eluted using 2 x 1 mL of MeOH. Samples were evaporated to dryness under a stream of nitrogen and reconstituted in 300 µL of methanol/water (1:1, v/v). Samples were analyzed using LC-MS/MS for identification and UV/VIS detector on 254 nm for quantification with the assumption that the extinction coefficients of the formed metabolites are equal to that of diclofenac. A SymmetryShieldTM RP18 3.5 µm column (100 mm x 4.6 mm i.d.) from Waters Corporation (Milford, Massachusetts, USA) was used as stationary phase using previously described HPLC conditions for diclofenac metabolites separation (1). An Agilent 1200 Series Rapid resolution LC system was connected to a hybrid quadrupole-time-of-flight (Q-TOF) Agilent 6520 mass spectrometer (Agilent Technologies, Waldbronn, Germany), equipped with electrospray ionization (ESI) source and operating in the positive mode with the MS ion source parameters previously described (2).

SUPPORTING REFERENCES

1. Damsten MC, van Vugt-Lussenburg BM, Zeldenthuis T, de Vlieger JS, Commandeur JN, Vermeulen NP, Application of drug metabolising mutants of cytochrome P450 BM3 (CYP102A1) as biocatalysts for the generation of reactive metabolites, Chem Biol Interact. 2008 Jan 10;171(1):96-107.
2. Dragovic S, Boerma JS, van Bergen L, Vermeulen NP, Commandeur JN, Role of human glutathione S-transferases in the inactivation of reactive metabolites of clozapine, Chem Res Toxicol. 2010 Sep 20;23(9):1467-76.

A.

i)

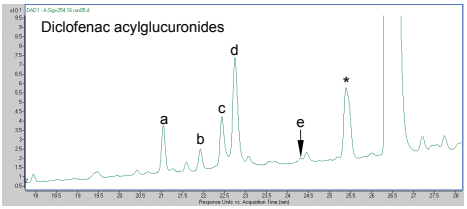

ii)

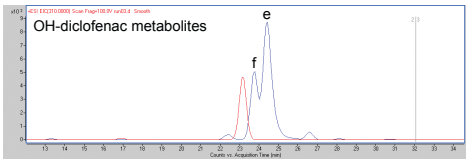

B.

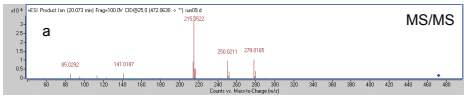

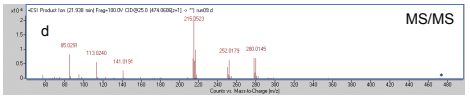

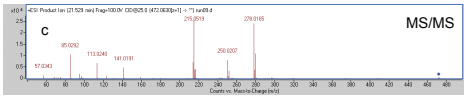

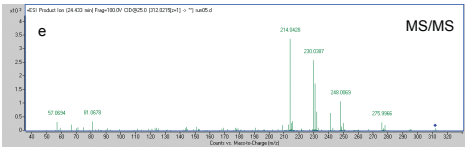

C.

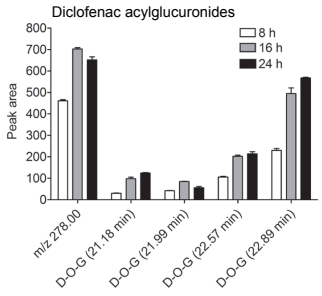

Supporting Data S1. *Diclofenac metabolites accumulate in HepG2 cells.* (A) i) Chromatogram of diclofenac metabolite spectrum. Four different diclofenac acylglucuronides (D-O-G) were identified with retention times 21.18 minutes, 21.99 minutes, 22.57 minutes and 22.89 minutes (a-d). The star (*) at 25.44 minutes indicates m/z 278, a diclofenac metabolite which results form intramolecular cyclization of the acylglucuronide. The arrow (e) points at 4'-OH-diclofenac (m/z 312, 24.44 minutes). 5-OH-diclofenac (m/z 312, 23.78 minutes) and 5-OH-Quinone-Imine-diclofenac (m/z 310, 23.13 minutes) are not indicated, as these are not UV-detectable. ii) Extracted Ion Chromatogram (EIC) of the hydroxy-metabolites. Red indicates 5-OH-QI-diclofenac, blue 5-OH (f) and 4'-OH-diclofenac (e). (B) MS/MS spectra that identifies the respective peaks from panel A. (C) Quantification of the different diclofenac acylglucuronide metabolites in HepG2 cells at 8 hours, 16 hours and 24 hours of incubation.

Supporting Data S2. *List of genes included in the primary apoptosis siRNA screen.* The table presents all the short interfering RNAs (siRNAs) included in the screen, as well as the fold change in apoptosis endpoint that each individual siRNA resulted in after diclofenac/TNFα (500 μM/10 ng/mL) treatment in HepG2 cells compared to siControl. The mean apoptosis endpoint of all three experiments, expressed as fold change over siControl, is given under "Average". Blue indicates the genes that are identified as apoptosis inducers (≥ 2.0-fold reduction in endpoint compared to siControl) and in Red the genes that are identified as apoptosis suppressors (≥ 2.0-fold induction of endpoint compared to siControl transfected cells).

Table S2:

	Exp. 1	Exp. 2	Exp. 3	Average
CASP1	1.07	1.85	1.38	1.38
CASP10	1.16	1.98	1.46	1.48
CASP14	1.12	1.98	1.09	1.36
CASP2	0.58	0.99	0.93	0.79
CASP3	0.58	0.57	0.87	0.66
CASP4	1.46	1.97	**2.23**	1.82
CASP6	0.73	0.87	0.96	0.83
CASP7	0.93	1.14	1.42	1.12
CASP8	**-0.02**	**0.08**	**0.19**	**0.07**
CASP9	**0.43**	0.90	0.58	0.60
BCL10	1.87	**4.29**	**3.53**	**3.02**
BCL2	0.60	0.72	0.94	0.72
BCL2A1	0.73	0.94	0.72	0.79
BCL2L1	0.75	0.95	1.00	0.87
BCL2L10	1.60	**2.71**	**2.50**	**2.17**
BCL2L11	0.62	0.71	0.53	0.62
BCL2L14	0.60	1.07	0.95	0.83
BCL2L2	1.06	1.61	1.39	1.31
BAD	0.63	1.07	1.42	0.97
BAG1	0.51	0.95	0.85	0.73
BAG4	1.05	-	1.01	1.10
BAG5	0.63	0.66	0.74	0.67
BAK1	1.10	1.04	1.25	1.12
BAX	0.70	0.94	1.57	1.00
BBC3	**0.38**	0.56	0.63	**0.50**
BMF	0.78	1.29	1.33	1.07
BOK	0.74	**2.13**	1.73	1.41
MCL1	0.68	1.32	1.64	1.13
BID	**0.22**	**0.40**	**0.42**	**0.32**
HRK	**0.23**	0.76	0.79	0.53
PMAIP1	0.82	1.03	1.04	0.94
BIK	1.08	1.93	1.14	1.34
API5	0.84	0.70	0.96	0.83
BIRC1	**0.48**	1.19	1.04	0.84
BIRC2	1.07	1.82	**2.09**	1.56
BIRC3	0.75	**0.45**	0.85	0.69
BIRC5	**0.29**	1.06	1.07	0.72
BIRC6	1.01	1.71	1.53	1.36
DIABLO	1.50	**2.32**	1.79	1.82
BIRC4	1.05	1.91	1.53	1.43
PDCD8	**0.40**	**0.34**	0.55	**0.42**
APAF1	**0.30**	**0.34**	0.55	**0.38**
AVEN	1.17	**2.28**	1.73	1.64
BFAR	0.55	1.06	1.30	0.90
CFLAR	**2.01**	**3.77**	**4.32**	**3.14**
CRADD	1.80	**2.64**	**2.01**	**2.10**
CYCS	0.96	1.48	1.08	1.14
DEDD	0.66	0.82	1.21	0.85
TOSO	0.75	1.16	1.05	0.95
MOAP1	0.80	1.92	1.11	1.21

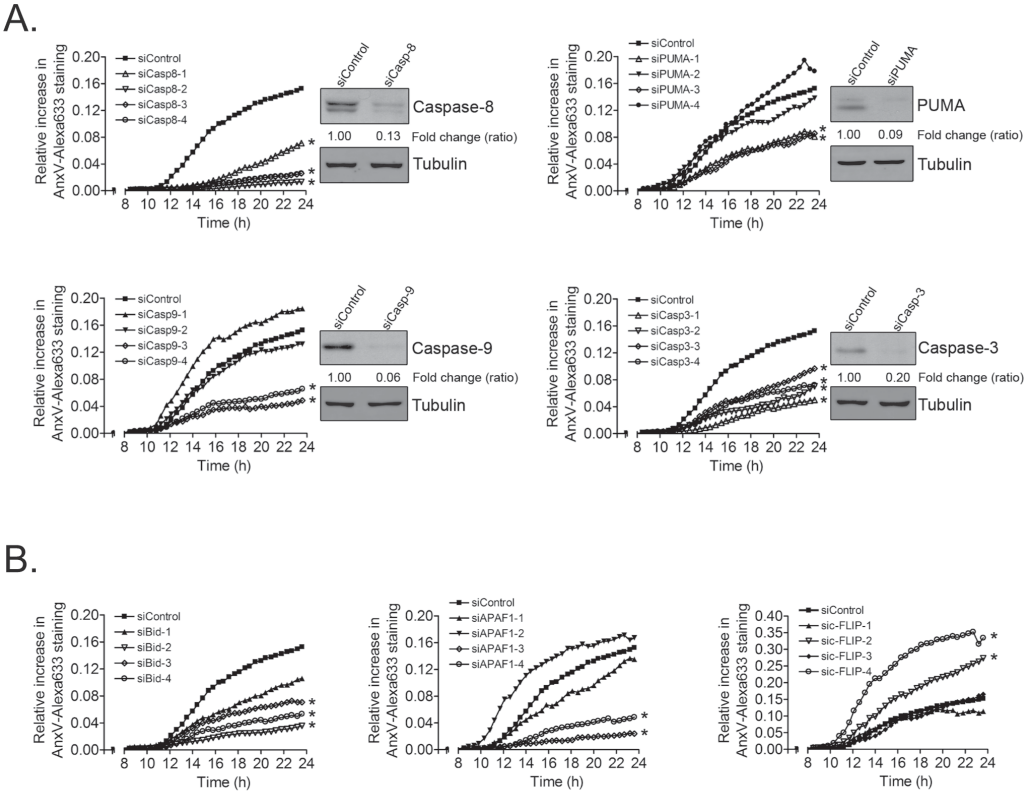

Supporting Data S3. *Graphical representation of hits from the secondary siRNA screen.* (A) Confirmed inducers of diclofenac/TNFα-caused apoptosis in HepG2 cells for which knockdown could also be verified by western blotting. The knockdown confirmed by western blotting was achieved by transfection with siRNA smartpools as used in the primary screen. The fold change of protein expression after knockdown was determined by comparing tubulin normalized band intensities from the knockdown to the one of siControl transfected cells. (B) Confirmed inducers and inhibitor of diclofenac/TNFα-caused apoptosis that were not verified by western blotting. (A and B) The constructs that caused >1.5 fold increase or decrease in apoptosis compared to siControl transfected cells after 24 h diclofenac/TNFα treatment were identified as confirmed hits from the primary screen. The individual apoptosis time curves from the effective siRNA sequences are represented by open symbols and stars (*).

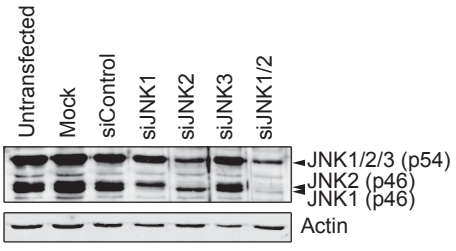

Supporting Data S4. *Protein levels of JNK1/2 after JNK1 and JNK2 knockdown.* HepG2 cells were transfected with cJun N-terminal kinase (JNK)-1, JNK2, JNK3 and Control siRNA before collecting lysates from those cells to confirm knockdown by Western blot analysis 96 hours after transfection. The data shown is representative of 3 independent experiments corresponding to the results shown in Figure 4E.

3

High content imaging of Nrf2 and NF-κB activation as markers for the prediction of drug-induced liver injury

Lisa Fredriksson*, Bram Herpers*, Zi Di, Giel Hendriks, Harry Vrieling, Hans de Bont and Bob van de Water

Submitted to Journal of Hepatology

ABSTRACT

Drug-induced liver injury (DILI) is an important clinical problem, yet predicting human DILI for novel candidate drugs remains difficult. Current models indicate that in many cases DILI is linked to reactive metabolite formation and involves activation of innate immune responses.Here we systematically evaluated the combined application of high content live cell imaging-based analysis of 1) Nrf2 activation as a measure for reactive metabolite stress; 2) perturbations of the normal NF-κB activation mediated by TNFα; and 3) synergistic induction of apoptosis by DILI compounds and TNFα. Fifteen drugs associated with DILI were evaluated. Most DILI compounds induced Nrf2 stabilization-dependent activation of the downstream target SRXN1 (11 out of 15). Various DILI compounds diminished the TNFα-induced activation of NF-κB (6 out of 15), which strongly correlated to the strength of Nrf2 activation. In particular for those compounds that show strong Nrf2 activation and perturbation of NF-κB signaling, a significant drug-cytokine synergy for apoptosis was observed, which included carbamazepine, diclofenac and ketoconazole, and to a lesser extent clozapine, nefazodone and amiodarone. Together, our data support that mechanism-based high content imaging strategies involving combined analyses of cellular stress responses contribute to DILI hazard identification.

INTRODUCTION

Adverse drug reactions are difficult to predict because of a lack in the understanding of the underlying mechanisms (1). Evidence points at the formation of chemically reactive metabolites being one of the initial causes of drug-induced liver injury (DILI) (1, 2), leading to oxidative stress and mitochondrial dysfunction (3). In addition, DILI involves an immune component (4) largely involving the innate immune system with the liver Kupffer cells as critical players (5-8). Activated immune cells release pro-inflammatory cytokines (9) which act on the hepatocytes undergoing reactive metabolite stress. This combination of toxicant and cytokine-induced stress signals may activate a pro-apoptotic response. Indeed, in mouse models non-hepatotoxic drugs (with DILI association in humans) can become hepatotoxic by co-treatment with lipopolysaccharide (LPS) which is dependent on the pro-inflammatory cytokine TNFα (10, 11). This critical role of TNFα in adverse drug-cytokine synergy can be reconstituted in an *in vitro* model by co-exposing liver epithelial cells to drugs linked to DILI in combination with TNFα (12, 13).

Reactive drug metabolite-mediated intracellular perturbations of the cellular redox potential are counterbalanced by the anti-oxidant response under control of the transcription factor Nrf2 (14, 15). Under low oxidative stress conditions Nrf2 is degraded by the proteasome, due to ubiquitination by its inhibitory protein Keap1 (or INrf2) (14). During toxic stress the soft electrophilic reactive metabolites and/or increased levels of reactive oxygen species (ROS) target the cysteine residues in Keap1 (16, 17), allowing Nrf2 to evade the Keap1-mediated repression, and accumulates in the nucleus to activate a diversity of cytoprotective antioxidant target genes (18). Nrf2 is an essential transcription factor for defense against DILI (18), e.g. for the detoxification of acetaminophen (APAP) (19, 20). Interestingly, activation of Nrf2 is also influenced by the p53-p21 axis, autophagy, HSP90 and NF-κB signaling (21). This indicates that oxidative stress signaling, apoptosis regulation and immune signaling are tightly linked biological programs to accurately control the cell fate decision after toxicant exposure.

TNFα binding to its receptor leads to activation of the tri-partite inhibitor of kappa-B kinase (IKK-) complex (IKKα, IKKβ and NEMO). This kinase complex phosphorylates the inhibitor of kappa B (IκBα), leading to rapid ubiquitination and degradation of this inhibitor directly followed by the release of NF-κB and nuclear translocation to activate its target genes. A primary early transcriptional target of NF-κB is IκBα (NFKBIA), which recruits NF-κB back into the cytoplasm (resting state), creating an autoregulatory negative feedback loop (22). Hence, NF-κB activation follows an oscillating nuclear translocation pattern, dependent on the persistence of the cytokine signal and intracellular responses (23). Its periodicity is influenced by redox regulation and dictates the outcome of the genetic response (24). Importantly, we recently established that the hepatotoxicant diclofenac interferes with the NF-κB oscillatory response in association with a synergy between diclofenac and TNFα to induce apoptosis in liver cells (13). Whether this holds true for other DILI compounds is investigated here.

We established a high content imaging-based strategy using HepG2 cells as

a model to quantitatively follow the onset of apoptosis, Nrf2-dependent activation of Sulfiredoxin (Srxn1) expression, and nuclear oscillation of NF-κB. These assays were used for concentration- and time-course experiments with a panel of fifteen drugs associated to human DILI: acetaminophen (APAP), 3'-hydroxyacetanilide (AMAP), amiodarone (AMI), carbamazepine (CBZ), clozapine (CLZ), diclofenac (DCF), isoniazid (INH), ketoconazole (KTZ), methotrexate (MTX), nefazodone (NFZ), naproxen (NPX), nitrofurantoin (NTF), ofloxacin (OFX), simvastatin (SN) and troglitazone (TGZ). We studied their effect on cell stress in relation to co-exposure with TNFα. Our results indicate that a strong correlation between Nrf2 activation and inhibition of TNFα-induced NF-κB nuclear translocation responses. When both of these response pathways are affected, TNFα and DILI compounds synergize to enhance the onset of cell killing.

MATERIALS AND METHODS

Reagents

All drugs were acquired from Sigma-Aldrich and freshly dissolved in DMSO, except for menadione and naproxen (in PBS). Human TNFα was purchased from R&D systems and stored as 10 µg/mL in 0.1% BSA in PBS aliquots.

Cell culture

Human hepatoma HepG2 cells were acquired from ATCC (clone HB8065) and maintained and exposed to drugs in DMEM high glucose supplemented with 10% (v/v) FBS, 25 U/mL penicillin and 25 µg/mL streptomycin. The cells were used between passage 5 and 20. For live cell imaging, the cells were seeded in Greiner black µ-clear 96-well plates, at 20,000 cells per well.

Generation of GFP-tagged cell lines

HepG2 cells stably expressing human GFP-p65 as in (13). Mouse Sulfiredoxin (Srxn1) was tagged with GFP at the C-terminus using BAC recombineering (25) and stably introduced into HepG2 cells by transfection and 500 µg/ml G-418 selection.

RNA interference

siRNAs against human NFE2L2 and KEAP1 were acquired from Dharmacon (ThermoFisher Scientific) as siGENOME SMARTpool reagents, as well as in the form of four individual siRNAs. HepG2 cells were transiently transfected with the siRNAs (50 nM) using INTERFERin (Polyplus).

Western blotting

Samples were collected by direct cell lysis (including pelleted apoptotic cells) in 1x Sample Buffer supplemented with 5% v/v β-mercaptoethanol and heat-denatured at 95°C for 10 minutes. The separated proteins were blotted onto PVDF membranes before antibody incubation in 1% BSA in TBS-Tween20. Antibodies: mouse-anti-GFP (Roche); rabbit-

anti-IκBα (Cell Signaling); rabbit-anti-Nrf2 (H300, Santa-Cruz); mouse-anti-caspase-8 (Cell Signaling); rabbit-anti-cleaved PARP (Cell Signaling); mouse-anti-Tubulin (Sigma).

Microscopy

Real-time apoptosis induction was determined by monitoring the accumulation of Annexin-V-Alexa633 labeled cells over a 24 hour time period (26). For this, transmission and Alexa633 images of the same area with cells were taken automatically every 30 minutes using a BD Pathway™ 855 bioimager and a 10x Olympus PlanApo lens.

Stabilization of Srxn1-GFP or nuclear oscillation of GFP-p65 was monitored using a Nikon TiE2000 confocal laser microscope (lasers: 488nm and 408nm), equipped with an automated stage and perfect focus system. Prior to imaging at 20x magnification, HepG2 cells were loaded for 45 minutes with 100ng/mL $Hoechst_{33342}$ to visualize the nuclei, upon which the Hoechst-containing medium was washed away to avoid Hoechst phototoxicity (27). Srxn1-GFP cells were imaged every 30 minutes across a 24 hour time span, GFP-p65 cells every 6 minutes for 6 hours.

Image quantification

To quantify the total pixel area occupied by cells or the number of cells per field imaged, transmission images and Hoechst images respectively were analyzed using ImagePro 7.0 (Media Cybernetics). The accumulation of apoptotic cells or the appearance of Srxn1-GFP positive cells was quantified as the total number of pixels above background. The apoptotic pixel total was normalized for the total cell area. The number of adjacent fluorescent Srxn1-GFP pixels above background (with a minimum size of 45 pixels) was multiplied by the average density of those pixels as a measure for the GFP signal-intensity increase and normalized for the amount of nuclei.

To quantify the nuclear translocation of GFP-p65, nuclei (Hoechst) masks are segmented and tracked in ImageJ to define the GFP-p65 nuclear intensity, followed by cytoplasm segmentation. The normalized nuclear / cytoplasmic intensity ratio for each cell is recorded and further analyzed for different oscillation features, also using ImageJ, including the number of translocations, time period of each individual peak, intensity of the peaks, delay between peaks, and nuclear entry and exit rates (Di Z., Herpers B., Fredriksson L., *et al*., submitted for publication).

Statistics

All experiments are performed at least in triplicate. Error bars indicate Standard Error, unless indicated otherwise. Statistical comparisons were done in a one-way ANOVA. P-value indications: $P<0.05$ (*); $P<0.01$ (**); $P<0.001$ (***).

RESULTS

Drug-induced cell death of human HepG2 cells

To establish a strategy for a mechanism-based evaluation of adverse drug liver toxicities in *in vitro* models we assembled a list of 15 compounds linked to various types of adverse drug liver toxicity (Supporting Table 1). HepG2 cells were chosen as a model system since genetic manipulation allows the integration of fluorescent reporter constructs for live cell imaging approaches. First we incubated cells in presence of Alexa633-labeled AnnexinV and used live cell imaging to determine the concentration-dependent onset of apoptotic cell death. While none of the compounds induced an overwhelming amount of cell death, our sensitive and robust method allowed us to identify a concentration-dependent HepG2 cell apoptosis for AMI, AMAP, APAP, CBZ, CLZ, DCF, KTZ, NFZ, NTF and SN. Little apoptosis was observed for INH, MTX, NPX, OFX and TGZ. For further experiments for each compounds we defined a concentration that is mildly cytotoxic (indicated in Fig. 1 A) to establish the effect on Nrf2 activation, NF-κB signaling and in relation to co-exposure to the pro-inflammatory cytokine TNFα.

A BAC-Srxn1-GFP HepG2 cell line reports xenobiotic-mediated Nrf2 activation

Rising levels of oxidative stress leads to activation of the antioxidant pathway, controlled by the transcription factor Nrf2. We first monitored the dynamics of Nrf2 stabilization in our HepG2 model. Menadione (20 μM, MEN), di-ethyl maleate (100 μM, DEM) and iodoacetamide (10 μM, IAA) are potent pro-oxidant xenobiotics that time-dependently stabilize Nrf2 in HepG2 cells (Fig. 1 B). Also KTZ and DCF for which phase I and II metabolism has been demonstrated in HepG2 cells (13, 28) caused stabilization of Nrf2. To visualize the Nrf2 activation in real time, we generated HepG2 reporter cells expressing the Nrf2 target gene Sulfiredoxin (Srxn1) coupled to GFP, controlled by its own promoter, by BAC recombineering (25). Under normal conditions, the Srxn1-GFP reporter is not expressed, but exposure to MEN, DEM, IAA, H2O2, DCF and KTZ induced a strong time-dependent expression of GFP-Srxn1 (Fig. 1 C) which was easily detected by confocal microscopy live-cell imaging (Fig. 1 D-E). Quantification of the Srxn1-GFP signal shows that activation of the Nrf2 response by the different Nrf2-inducing compounds follows differential activation patterns. All compounds activated the Srxn1-GFP expression within 8 hours. However, while MEN, DEM, IAA and H2O2 induce acute Srxn1-GFP expression upon a lag-phase of 4 hours, the hepatotoxicants DCF and KTZ induce a gradual increase of the Nrf2 activity reporter over time (Fig. 1 E), possibly related to reactive metabolite formation. Importantly, the Srxn1-GFP expression in our model is Nrf2-dependent, since transfection with siRNA oligos targeting Nrf2 inhibits the expression of Srxn1-GFP after exposure to MEN, DEM, DCF and KTZ (Fig. 1 F). Moreover, also Keap1 knockdown which caused an expected stabilization of Nrf2, strongly induced Srxn1-GFP levels.

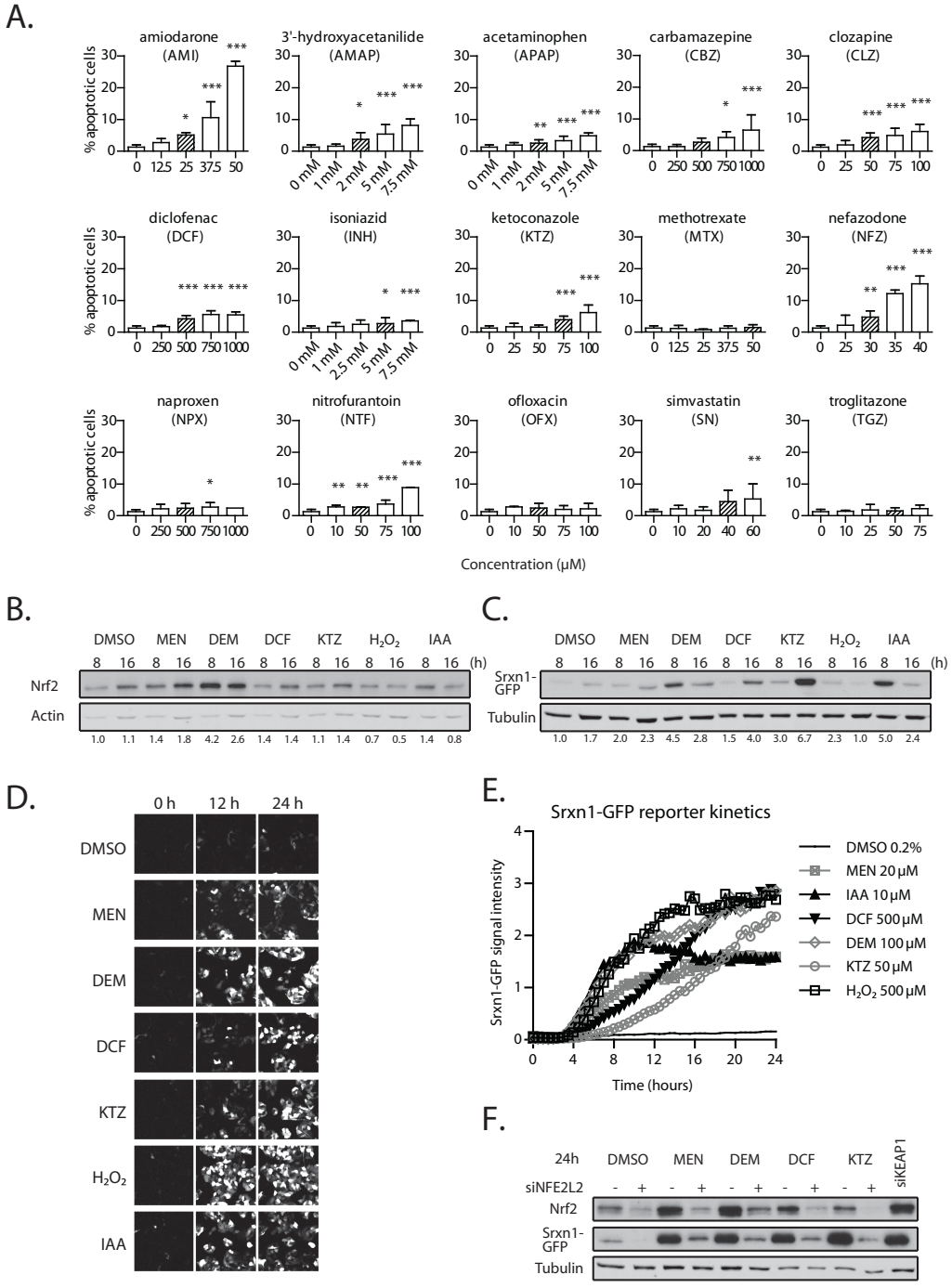

Figure 1. *Drug-induced apoptosis and oxidative stress* (A) Percentage of apoptotic HepG2 cells at 24 hours after exposure to fifteen different drugs. Concentrations are indicated in µM, except for AMAP, APAP and INH: in mM. "0": 0.2% (v/v) DMSO. Shaded bars: concentration used in subsequent assays. (B) Western blot of Nrf2 expression in HepG2 cells exposed for 8 or 16 hours. (C) Western blot of GFP expression in HepG2 Srxn1-GFP cells. (D) Stills of time-lapse image series of HepG2 Srxn1-GFP cells exposed to Nrf2 inducers. (E) Quantification of the Srxn1-GFP reporter response kinetics. (F) Knockdown of Nrf2 (siNFE2L2) and Keap1 (siKEAP1) in HepG2 Srxn1-GFP cells upon 24h treatment.

DILI compounds activate the Nrf2 stress response independent of TNFR activation

Next, we systematically tested the panel of liver toxicants on the HepG2 Srxn1-GFP reporter cells and monitored the increase of the GFP signal by live-cell imaging (Fig. 2 A-B). We observed that APAP and its regioisomer AMAP potently induce the oxidative stress reporter, as soon as 4 hours after compound exposure. The drugs CBZ, CLZ, DCF, KTZ, NFZ and NTF strongly induced the Srxn1-GFP reporter 8 hours after compound exposure. AMI, MTX and NPX are weak oxidative stress inducers, and Srxn1-GFP induction was observed with delayed kinetics, at 16 hours after compound exposure. The drugs INH, OFX, SN and TGZ did not lead to oxidative stress induction within the 24-hour imaging period in our cell system. These results were confirmed by Western blot (Fig. 2 C-D).

Next, we addressed the question whether TNFα (10 ng/ml) co-exposure increases the rate of Nrf2 stabilization. TNFα has been reported to induce ROS formation, which can be counterbalanced by NF-κB driven production of anti-oxidant genes (29). However, as an anti-oxidant transcription factor, Nrf2 is potentially involved in this process as well. We observed no significant rise in Nrf2 stabilization or Srxn1-GFP expression when the HepG2 Srxn1-GFP cells were exposed to TNFα alone (Fig. 2 C and D). Since most of our test drugs induced activation of the Nrf2 response 8 hours after drug exposure, we pre-incubated for 8 hours before addition of 10 ng/ml TNFα and assessed the effect of TNFα on the activity of the oxidative stress response 24 hours after the start of the exposure. No significant increase in Nrf2 responses by compound-TNFα combination was observed (Fig. 2 C and D).

Multiparametric analysis of HepG2/GFP-p65 cells to monitor spatio-temporal NF-κB responses

TNFα promotes liver cell injury under hepatotoxicant treatment conditions. We previously demonstrated that this is related to perturbations of NF-κB signaling by TNFα (13). To monitor the effect of the hepatotoxicants on the execution of the NF-κB response, we used a previously established HepG2 cell line expressing GFP-tagged p65/RelA, a subunit of the dimeric transcription factor NF-κB. This GFP-p65 reporter allows us to follow and quantify the spatio-temporal nuclear translocation of NF-κB. TNFα promotes phosphorylation and subsequent degradation of the NF-κB inhibitor IκBα in an oscillatory manner (Fig. 3 A) which is followed by nuclear translocation of NF-κB that oscillates in time (Fig. 3 B: top panel). This activity is IKK-dependent, because an 8 hour pre-incubation with 2 μM BMS-345541, a potent IKKβ inhibitor, resulted in inhibition of the NF-κB oscillation response (Fig. 3 B). Quantification of the nuclear/cytoplasmic ratio of the GFP-p65 NF-κB reporter construct (based on ~1000 individual cells per condition) revealed that BMS-345541 not only inhibits the NF-κB response in relation to the number of nuclear translocation events at 0.5 μM, but also the translocation amplitude of the GFP-p65 signal (Fig. 3 C). Extraction of multiple parameters from the oscillation pattern of all individual cells

within the observed population revealed that the IKKβ inhibition caused a concentration-dependent decrease in the number of cells oscillating upon TNFα stimulation, together with an increase in the time of the second nuclear translocation maximum (150 minutes

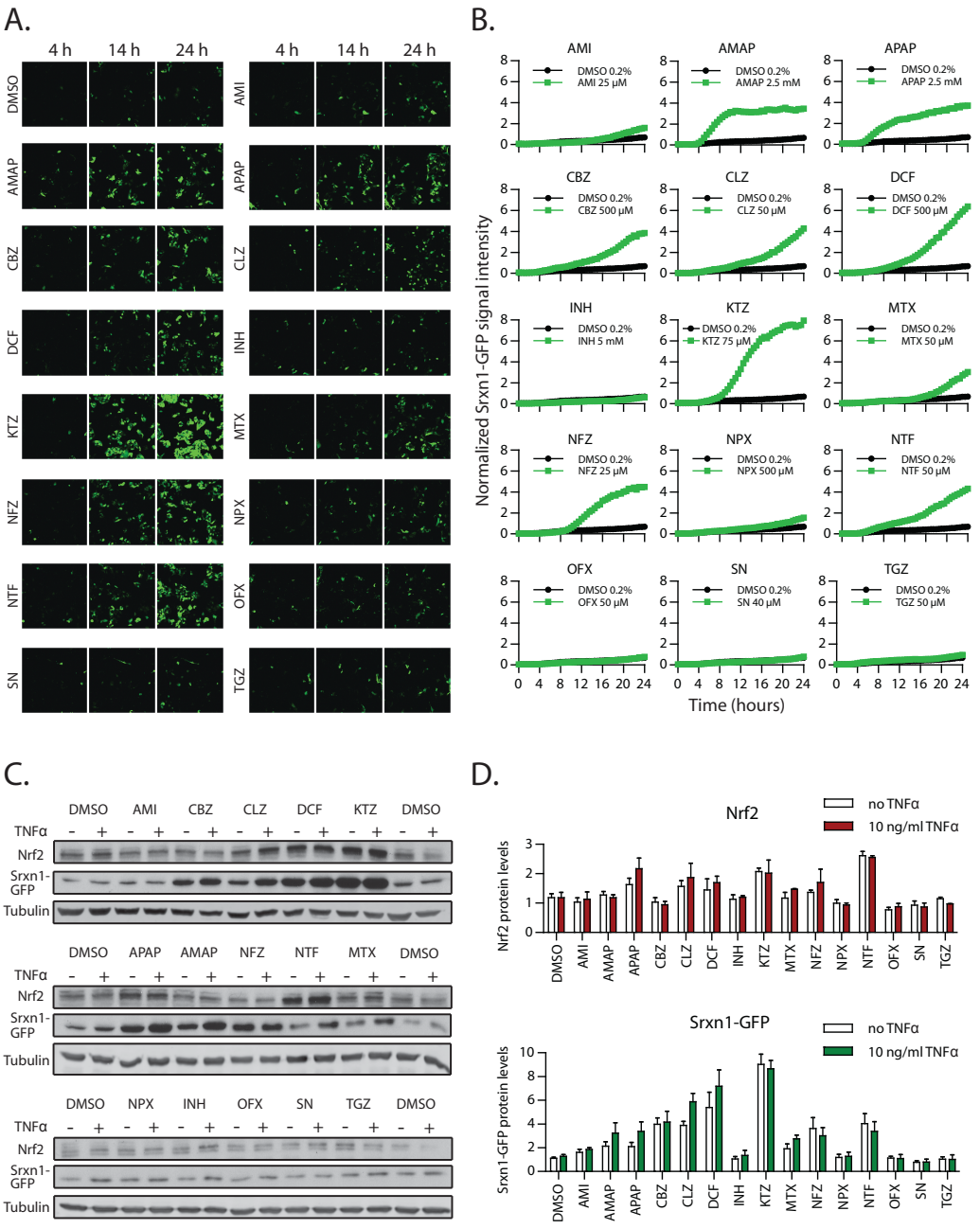

Figure 2. *Drug exposure induces dynamically divergent Nrf2 responses.* (A) Stills of live-cell imaging on HepG2 Srxn1-GFP cells upon drug exposure (shown are 4, 14 and 24 hours). (B) Quantification of the Srxn1-GFP signal appearing upon drug exposure. (C) Western-blots for Nrf2 and GFP expression after 24 hour drug exposure in HepG2 Srxn1-GFP cells, either with or without co-exposure to 10ng/ml TNFα. (D) Quantification of the Nrf2 and Srxn1-GFP protein levels, 24h after drug +/- TNFα exposure.

in control conditions, 186 minutes at low BMS-345541 concentrations, and 216 minutes at the highest concentration) (Fig. 3 D). These data indicate that this GFP-p65 HepG2 reporter cell line in combination with high content imaging provides thorough insight in the perturbations of the NF-κB signaling that fit with the biochemistry.

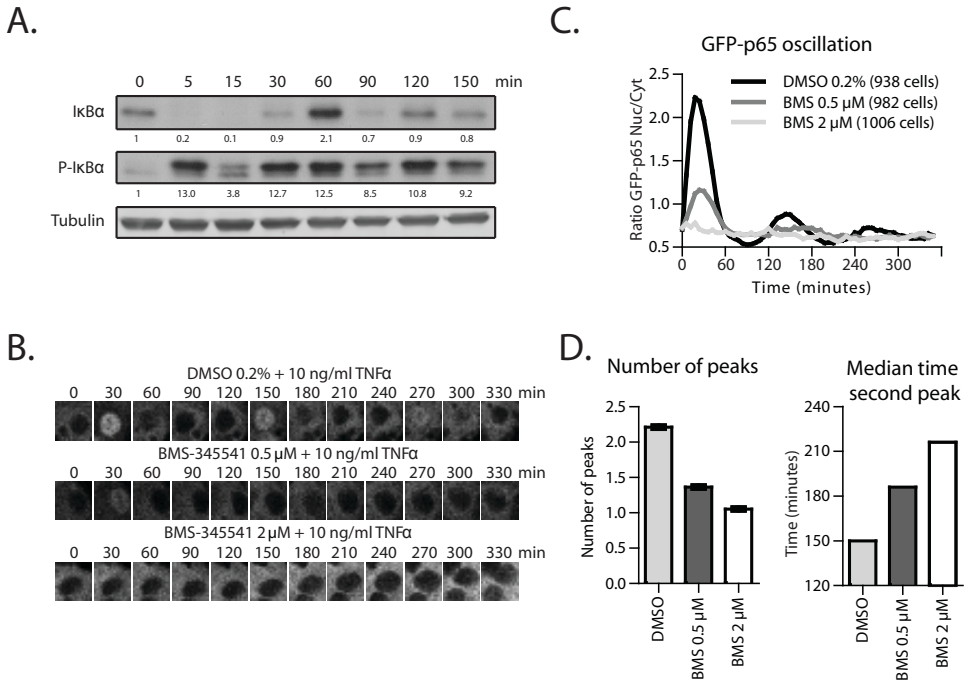

Figure 3. *TNFα stimulation induces IKKβ-dependent NF-κB oscillations.* (A) 10 ng/ml TNFα stimulation induces IκBα phosphorylation and degradation, followed by IκBα re-synthesis and degradation. (B) HepG2 GFP-p65 (NF-κB reporter) cells treated for 8 hours with the IKKβ-inhibitor BMS-345541 before TNFα exposure show impaired NF-κB nuclear translocation. (C) Quantification of the nuclear/cytoplasmic GFP-p65 intensity ratio in control (0.2% DMSO) and BMS-345541 treated cells upon TNFα stimulation. (D) Statistical analysis of the HepG2 GFP-p65 cell population under control versus BMS-345541 conditions.

DILI compounds cause a perturbation of NF-κB signaling

Next we tested the effect of DILI compound treatment on TNFα-induced NF-κB activation. We selected an 8-hour drug pre-incubation period before the addition of TNFα. As reported previously, DCF delayed the second translocation event (+20 min) (Fig. 4 A). AMI (+20 minutes), CBZ (+20 minutes) and NTF (+20 minutes) delayed the oscillation to a similar extent as DCF. Already at 25 µM KTZ strongly delayed the oscillation by 37 minutes. NFZ delayed the oscillation by 30 minutes. Pretreatment with CLZ and MTX only weakly perturbed the appearance of the second translocation response with a delay of 10 and 16 min, respectively. Neither AMAP, APAP, INH, OFX, SN nor TGZ significantly influenced the translocation maximum of the second nuclear translocation event.

Detailed cell population-based quantitative analysis of the translocation response

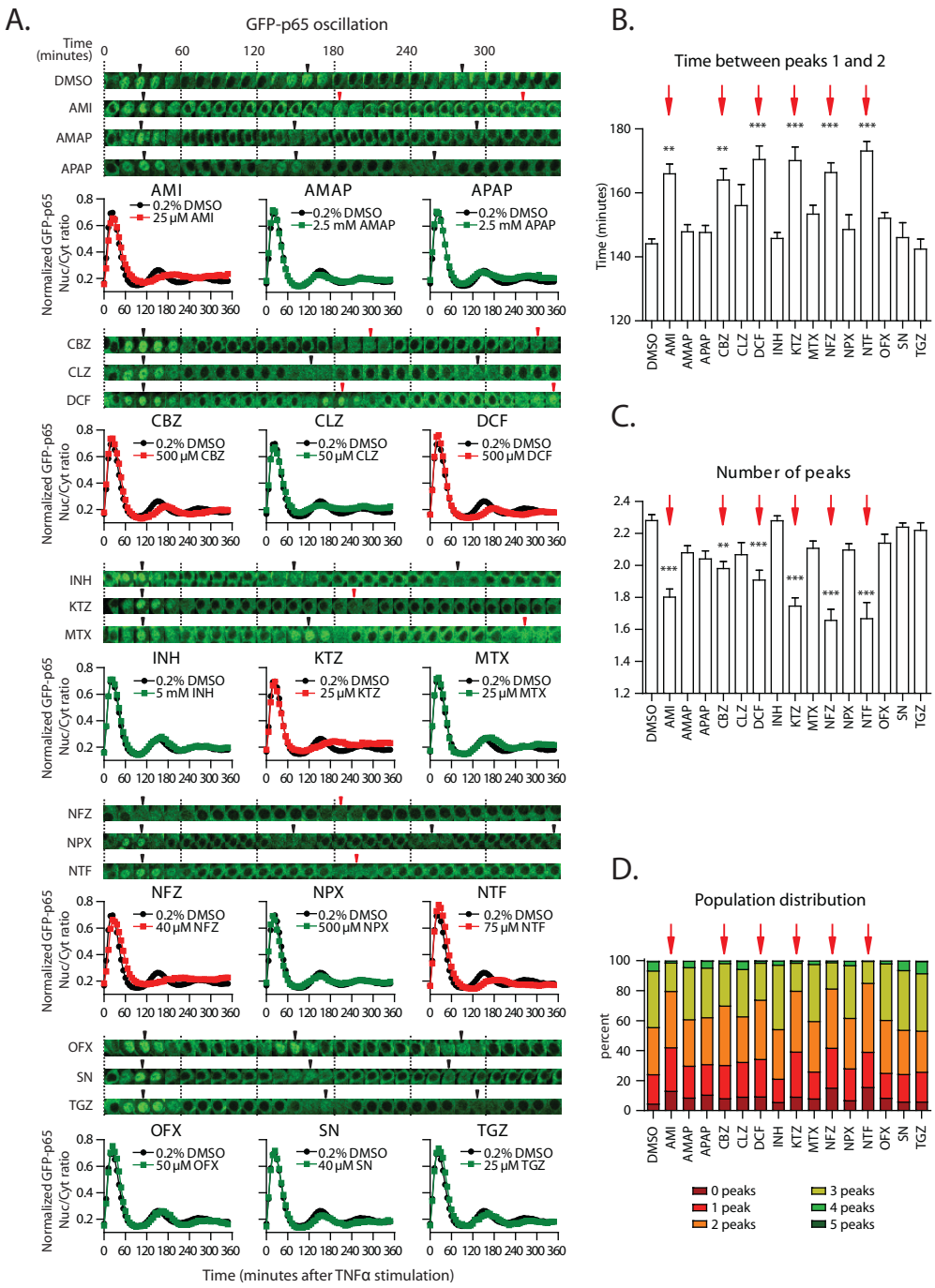

Figure 4. *Drug-impaired NF-κB activation.* (A) Time-lapse images of one representative cell showing NF-κB oscillation upon 10 ng/ml TNFα stimulation after an 8-hour drug pre-incubation period. Arrowheads point at the local nuclear translocation maxima. Quantified average of the GFP-p65 nuclear/cytoplasmic intensity ratio, normalized between 0 and 1 to focus on the appearance of the nuclear translocation maxima (peaks). (B) Analysis of the NF-κB response: time between peaks 1 and 2. (C) Analysis of the NF-κB response: assessment of the number of peaks. (D) Distribution of the TNFα-stimulated, drug pre-exposed cell population, classified for showing 0 to 5 peaks within the 6-hour imaging period.

allows extraction of various parameters that describe the NF-κB oscillation response to TNFα. Indeed, pre-treatment with AMI, CBZ, DCF, KTZ, NFZ or NTF significantly affects the time between the translocation maxima 1 and 2 (Fig. 4 B) and thereby reduces the average number of translocation events within the 6-hour imaging window (Fig. 4 C). Importantly, by evaluating the cell distribution of on average ~1000 cells per condition, we identified that AMI, CBZ, DCF, KTZ, NFZ and NTF in general increased the percentage

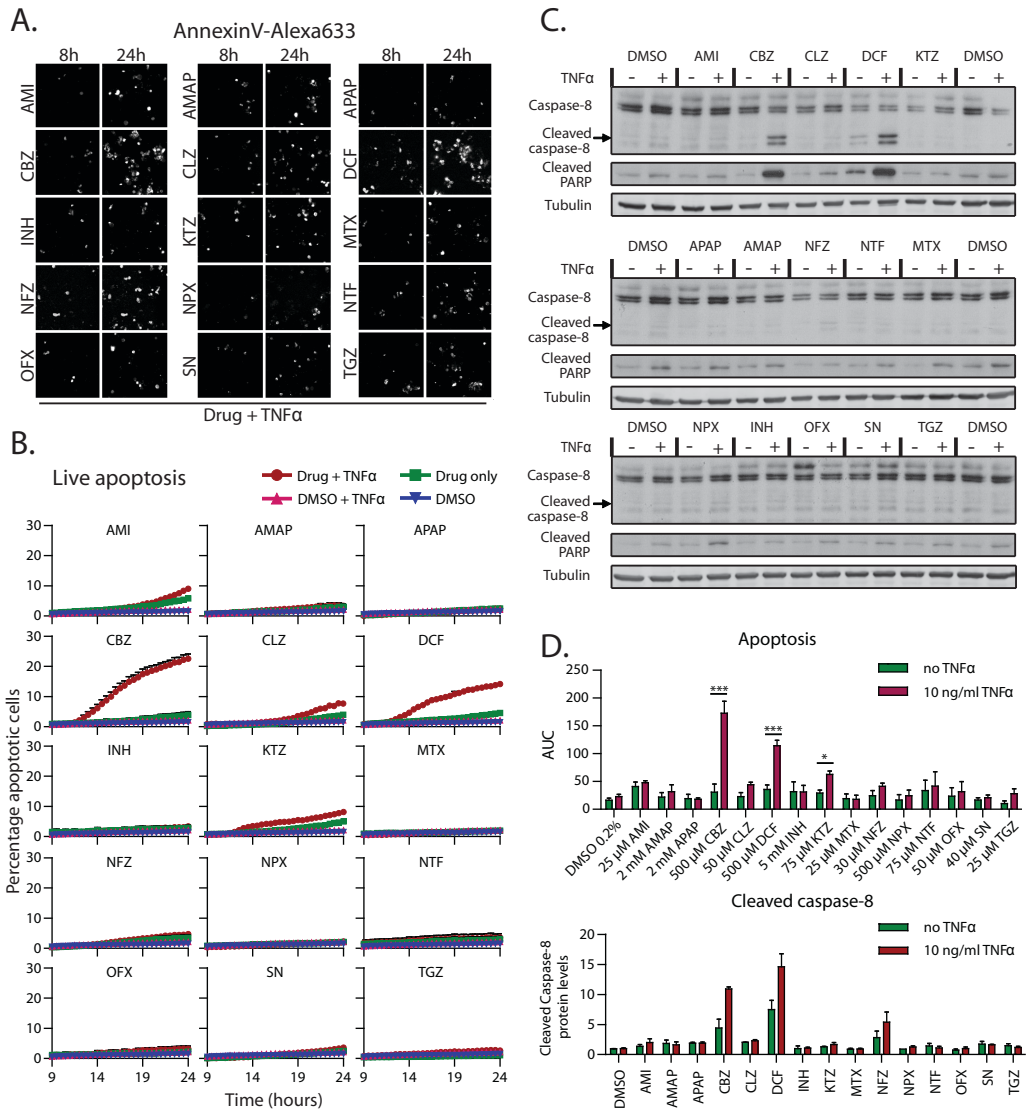

Figure 5. *Drug pre-incubation followed by TNFα may induce adverse drug-cytokine synergy.* (A) Still images of time-lapse movies of HepG2 cells exposed to the drugs in co-presence of Annexin-V-Alexa-633, taken at 8 hours (before 10 ng/ml TNFα addition) and at 24 hours (16 hours TNFα). (B) Quantification of the percentage apoptotic cells appearing upon drug only exposure, or in combination with TNFα. (C) Western-blot for cleaved caspase-8 and the caspase substrate PARP induction by drug alone or drug-TNFα co-treatment. (D) Comparison of the quantified percentage apoptotic cells 24 hours after drug (+TNFα) exposure, the area under the curve (AUC) and cleaved caspase-8 protein levels.

of cells with only one or two nuclear translocation peaks, and thereby decreased the percentage of cells with three or more NF-κB nuclear translocation events (Fig. 4 D).

DILI compound and TNFα synergy towards apoptosis

Since TNFα drives a NF-κB-dependent pro-survival response we anticipated that the inhibitory effect of drug pre-exposure on the NF-κB response might sensitize HepG2 cells towards apoptosis. To address this we systematically analyzed the compound-TNFα apoptosis synergy upon 8-hour drug pre-treatment followed by TNFα treatment. We monitored the onset of apoptosis within a 24-hour time period by live-cell imaging of AnnexinV-Alexa633 (Fig. 5 A). TNFα clearly enhanced the cell killing for CBZ, DCF and KTZ compared to the drugs alone. The cell killing for the other compounds was low, yet a significant increase in apoptosis under drug/TNFα conditions could be observed for AMI, CLZ and NFZ (Fig. 5 B). To further evaluate the onset of apoptosis, we monitored caspase-8 activation and PARP cleavage as markers of death receptor mediated cell killing. In accordance with the live apoptosis assay, we found a marked increase in cleaved caspase-8 and caspase-cleaved PARP under DCF/TNFα and CBZ/TNFα co-exposure conditions (Fig. 5 C and D).

Integrated analysis of Nrf2, NF-κB and apoptosis high content live cell imaging assays

Finally we evaluated the relationship between Nrf2 activation, NF-κB signaling perturbations and compound/TNFα synergy. For all markers we defined the response from absent to very strong and accordingly ranked the compounds based on their synergy response (Table 1). Firstly, the data indicate that there is not a necessary correlation between Nrf2 activation and NF-κB inhibition, since both AMAP and APAP have a strong Srxn1-GFP induction but hardly affect the NF-κB response. In this situation also no cytotoxic synergy is observed. Yet for almost all compounds that show some synergy response for apoptosis, a strong Srxn1-GFP induction as well as a delayed NF-κB nuclear oscillation is observed.

DISCUSSION

Whether a candidate drug in the development phase harbors an increased risk for liver failure remains difficult to predict due to the lack of adequate biomarkers and predictive *in vitro* and *in vivo* models. In this manuscript we propose the integration of three high content quantitative microscopy live cell imaging-based *in vitro* approaches to systematically analyze and classify the effect of drug exposure over time by addressing the biochemical mechanism (oxidative stress-based Nrf2 activation), the immune response mechanism (NF-κB signaling) and the cell death response (apoptosis).

Drug metabolism can create reactive soft electrophiles which are eradicated by

Table 1. Overview of the test results derived from the Srxn1-GFP assay (Nrf2 response), the GFP-p65 assay (NF-κB response) and the Annexin-V apoptosis assay (TNFα-enhanced apoptosis).

	Nrf2 response		NF-κB response		TNFα-enhanced apoptosis			
Drug	Fold increase Srxn1-GFP	Initiation (hours)	delay 2nd peak (minutes)	Oscillations (#)	24h drug only (%)	24h drug + TNFα (%)	Difference (%)	Synergy initiation (hours)
CBZ	3.2	10	20	1.98	2.8	21.8	18.9	12
DCF	5.7	10	20	1.91	3.8	13.6	9.8	12
KTZ	7.3	8	37	1.75	4.1	6.7	2.7	12
CLZ	3.6	11	10	2.07	3.3	5.3	2.0	22
NFZ	3.8	10	20	1.66	2.8	4.4	1.6	23
AMI	0.9	19	20	1.8	5.0	7.1	2.1	23
NTF	3.6	8	30	1.67	1.5	1.8	0.3	>24
AMAP	3.0	5	5	2.11	1.3	2.6	1.3	19
APAP	3.0	5	6	2.04	2.1	2.4	0.4	>24
MTX	2.3	17	16	2.11	1.0	1.4	0.5	>24
NPX	0.8	20	0	2.1	1.0	1.9	0.9	>24
TGZ	0.3	>24	0	2.22	0.7	1.8	1.1	19
SN	0.1	>24	3	2.24	1.8	1.8	0	>24
OFX	0.1	>24	6	2.14	1.1	2.1	1.0	24
INH	0.0	>24	0	2.28	1.4	2.4	1.1	24
DMSO	0.0	>24	0	2.28	0.8	1.3	0.5	>24

further phase 2 drug metabolism or scavenged by glutathione (GSH). GSH depletion is sensed by the Nrf2-Keap1 system, which responds by Nrf2-driven increases in GSH production. Alternatively, reactive metabolites may covalently modify free cysteine moieties in Keap1. To monitor activation of the Nrf2-Keap1 as a measure for reactive metabolite formation, we made advantage of a bacterial artificial chromosome-based Sulfiredoxin (Srxn1)-GFP reporter, driven by the endogenous promoter of Srxn1, which is fully dependent on Nrf2. Most DILI compounds showed activation of the Nrf2 response suggesting that reactive metabolites are formed by these compounds. Indeed in an earlier study we demonstrated metabolite formation for DCF (13). We observed for APAP and its regioisomer AMAP a fast Srxn1-GFP induction, similar to the GSH-depleting agents DEM and IAA, suggesting a direct effect for GSH depletion on the Nrf2 induction. Sustained Nrf2 stabilization, indicating persistent Nrf2 activation, was found for CLZ, DCF, KTZ, NFZ and NTF, possibly modifying Keap1 through reactive metabolites, which correlated with Srxn1-GFP induction. No effect was found on the Nrf2 response or the Nrf2 reporter in HepG2 cells for the drugs INH, NPX, OFX, SN and TGZ. This effect might be due to the low expression of cytochrome P450 enzymes in HepG2 cells, compared to primary hepatocytes (30), the FBS concentration (10 %) used (31), the duration of the experiments, or the chosen concentration (32). Since the redox-cycling agent MEN as well as H_2O_2 also activated Srxn1-GFP expression, at this moment we cannot entirely exclude that the observed effect for the DILI compounds is (partly) related to secondary oxidative stress, possibly derived from mitochondrial toxicity. Further research is required to identify the exact mechanism of Nrf2 activation for the different DILI compounds.

Stimulation of HepG2 cells with TNFα activates the IKK complex, which is essential for the activation of the downstream NF-κB response. We showed that a strong

drug-induced Nrf2 activation for the drugs AMI, CBZ, DCF, KTZ, NFZ and NTF closely correlated with a delay in the timing of the nuclear translocation peaks of NF-κB. Yet, while APAP also caused Nrf2 activation, this was not associated to a delay in the NF-κB oscillation. We speculate that the crosstalk between the Nrf2 and NF-κB signaling is apparently not mediated through Nrf2 activation *per se*. Alternatively, the reactive metabolites derived from AMI, CBZ, DCF, KTZ, NFZ and NTF likely affect a broader set of intracellular sensors and, thereby, affect alternative signaling pathways, including Nrf2 and NF-κB signaling. APAP-derived metabolites presumably only affect the Nrf2 pathway. This difference in response is likely related to different reactivity of the metabolites and/or the intracellular sites where they are generated. More work is required to identify the levels of metabolite formation and their cellular targets for the DILI compounds we used. Moreover, it will be highly relevant to determine which compounds directly affect the Nrf2 activation through covalent modification of Keap1.

In case of combined Nrf2 activation and NF-κB suppression an increased risk for drug-cytokine cytotoxic synergy may be present. The working model for immune-related DILI suggests the imbalance between pro-inflammatory cytokine and anti-inflammatory cytokine signaling as a critical initiator of hepatocyte cell killing (11, 12). We observed the strongest TNFα-enhanced drug-induced apoptosis for CBZ, DCF and KTZ, and more weakly for NFZ, AMI and CLZ. These six drugs activate both the Srxn1-GFP reporter and induce a delay in the NF-κB response, albeit that the effect of CLZ at 50 μM on NF-κB oscillation was not significant (10-minute delay), yet at 75 μM the effect became significant (20 minutes). This suggests that monitoring the ability of drugs to activate the Nrf2 response and determining the drug effect on NF-κB oscillations can be indicative for sensitization towards pro-inflammatory cytokines during drug exposure, as a sign for increased risk of DILI potential. We are currently investigating the underlying molecular mechanisms through RNA-interference-based functional genomics strategies and our findings indicate a critical role for the translational control component EIF4A1 in close relationship to the expression of the pro-apoptotic unfolded protein response gene CHOP/DDIT3 (Fredriksson *et al.*, submitted).

In conclusion, we have established a systems microscopy approach using high content confocal microscopy live-cell imaging in combination with automated multiparametric quantitative image analysis to monitor in parallel the kinetics of apoptosis, Nrf2 activation and the NF-κB oscillatory response. Our systems microscopy assays are more quantitative, robust, reliable and more informative than standard protein quantification, because single cells within a large population can be monitored across time. Furthermore, the approach can be multiplexed: the Srxn1-GFP reporter can be combined with Annexin-V or propidium-iodide to monitor oxidative stress simultaneously with apoptosis or necrosis induction, respectively. We are aware that our current strategy does not positively identify all DILI compounds. Given the diversity of molecular mechanisms for DILI, we would not expect this. Although the monolayer cultures of our HepG2 reporter cells provide greater speed and accuracy, we understand that their limited differentiation status is posing some limitations. Currently we are establishing 3D

spheroid cultures of HepG2 cells to increase their differentiation status and increase the levels of phase 1 and 2 metabolism. Preliminary results using 3D HepG2-Srxn1-GFP cells for high content imaging shows induction of Srxn1-GFP expression by TGZ. While we have limited ourselves to Nrf2 and NF-κB signaling in this study, further development of additional cell injury reporters (e.g. mitochondrial function, ER-stress and DNA damage) is ongoing. We anticipate that the application of such models in combination with DILI compound, cytokine and siRNA screening will greatly contribute to the mechanistic understanding of adverse drug reactions.

ACKNOWLEDGEMENTS

The authors like to thank the TI-Pharma consortium for critically reading the manuscript and members of the division of Toxicology for help and scientific discussions.

FUNDING

This work was funded by the TI-Pharma project D3-201 and IMI-MIP-DILI project to BvdW and the NGI Horizon project 9351008 to BH.

REFERENCES

1. Park BK, Laverty H, Srivastava A, Antoine DJ, Naisbitt D, Williams DP. Drug bioactivation and protein adduct formation in the pathogenesis of drug-induced toxicity. Chem Biol Interact 2010.
2. Srivastava A, Maggs JL, Antoine DJ, Williams DP, Smith DA, Park BK. Role of reactive metabolites in drug-induced hepatotoxicity. Handb Exp Pharmacol 2010:165-194.
3. Jones DP, Lemasters JJ, Han D, Boelsterli UA, Kaplowitz N. Mechanisms of pathogenesis in drug hepatotoxicity putting the stress on mitochondria. Mol Interv 2010;10:98-111.
4. Uetrecht J. Immunoallergic drug-induced liver injury in humans. Semin Liver Dis 2009;29:383-392.
5. Li J, Uetrecht JP. The danger hypothesis applied to idiosyncratic drug reactions. Handb Exp Pharmacol 2010:493-509.
6. Naisbitt DJ, Williams DP, Pirmohamed M, Kitteringham NR, Park BK. Reactive metabolites and their role in drug reactions. Curr Opin Allergy Clin Immunol 2001;1:317-325.
7. Pichler WJ, Beeler A, Keller M, Lerch M, Posadas S, Schmid D, Spanou Z, et al. Pharmacological interaction of drugs with immune receptors: the p-i concept. Allergol Int 2006;55:17-25.
8. Pirmohamed M, Naisbitt DJ, Gordon F, Park BK. The danger hypothesis--potential role in idiosyncratic drug reactions. Toxicology 2002;181-182:55-63.
9. Lucas M, Stuart LM, Savill J, Lacy-Hulbert A. Apoptotic cells and innate immune stimuli combine to regulate macrophage cytokine secretion. J Immunol 2003;171:2610-2615.
10. Deng X, Stachlewitz RF, Liguori MJ, Blomme EA, Waring JF, Luyendyk JP, Maddox JF, et al. Modest inflammation enhances diclofenac hepatotoxicity in rats: role of neutrophils and bacterial translocation. J Pharmacol Exp Ther 2006;319:1191-1199.
11. Shaw PJ, Ganey PE, Roth RA. Idiosyncratic drug-induced liver injury and the role of inflammatory stress with an emphasis on an animal model of trovafloxacin hepatotoxicity. Toxicol Sci 2010;118:7-18.
12. Cosgrove BD, King BM, Hasan MA, Alexopoulos LG, Farazi PA, Hendriks BS, Griffith LG, et al. Synergistic drug-cytokine induction of hepatocellular death as an in vitro approach for the study of inflammation-associated idiosyncratic drug hepatotoxicity. Toxicol Appl Pharmacol 2009;237:317-330.
13. Fredriksson L, Herpers B, Benedetti G, Matadin Q, Puigvert JC, de Bont H, Dragovic S, et al. Diclofenac inhibits tumor necrosis factor-alpha-induced nuclear factor-kappaB activation causing synergistic hepatocyte apoptosis. Hepatology 2011;53:2027-2041.
14. Kaspar JW, Niture SK, Jaiswal AK. Nrf2:INrf2 (Keap1) signaling in oxidative stress. Free Radic Biol Med 2009;47:1304-1309.
15. Copple IM, Goldring CE, Kitteringham NR, Park BK. The Nrf2-Keap1 defence pathway: role in protection against drug-induced toxicity. Toxicology 2008;246:24-33.
16. Zhang DD, Hannink M. Distinct cysteine residues in Keap1 are required for Keap1-dependent ubiquitination of Nrf2 and for stabilization of Nrf2 by chemopreventive agents and oxidative stress. Mol Cell Biol 2003;23:8137-8151.
17. McMahon M, Lamont DJ, Beattie KA, Hayes JD. Keap1 perceives stress via three sensors for the endogenous signaling molecules nitric oxide, zinc, and alkenals. Proceedings of the National Academy of Sciences of the United States of America 2010;107:18838-18843.
18. Copple IM, Goldring CE, Kitteringham NR, Park BK. The keap1-Nrf2 cellular defense pathway: mechanisms of regulation and role in protection against drug-induced toxicity. Handb Exp Pharmacol 2010:233-266.
19. Chan K, Han XD, Kan YW. An important function of Nrf2 in combating oxidative stress: detoxification of acetaminophen. Proc Natl Acad Sci U S A 2001;98:4611-4616.
20. Copple IM, Goldring CE, Jenkins RE, Chia AJ, Randle LE, Hayes JD, Kitteringham NR, et al. The hepatotoxic metabolite of acetaminophen directly activates the Keap1-Nrf2 cell defense system. Hepatology 2008;48:1292-1301.
21. Liguori MJ, Ditewig AC, Maddox JF, Luyendyk JP, Lehman-McKeeman LD, Nelson DM, Bhaskaran VM, et al. Comparison of TNFalpha to Lipopolysaccharide as an Inflammagen to Characterize the Idiosyncratic Hepatotoxicity Potential of Drugs: Trovafloxacin as an Example. International journal of molecular sciences 2010;11:4697-4714.
22. Wullaert A, Heyninck K, Beyaert R. Mechanisms of crosstalk between TNF-induced NF-kappaB and JNK activation in hepatocytes. Biochem Pharmacol 2006;72:1090-1101.
23. Ashall L, Horton CA, Nelson DE, Paszek P, Harper CV, Sillitoe K, Ryan S, et al. Pulsatile stimulation determines timing and specificity of NF-kappaB-dependent transcription. Science 2009;324:242-246.
24. Enesa K, Ito K, Luong le A, Thorbjornsen I, Phua C, To Y, Dean J, et al. Hydrogen peroxide prolongs nuclear localization of NF-kappaB in activated cells by suppressing negative regulatory mechanisms. J Biol Chem 2008;283:18582-18590.
25. Hendriks G, Atallah M, Morolli B, Calleja F, Ras-Verloop N, Huijskens I, Raamsman M, et al. The ToxTracker assay: novel GFP reporter systems that provide mechanistic insight into the genotoxic

properties of chemicals. Toxicol Sci 2012;125:285-298.
26. Puigvert JC, de Bont H, van de Water B, Danen EH. High-throughput live cell imaging of apoptosis. Curr Protoc Cell Biol 2010;Chapter 18:Unit 18 10 11-13.
27. Purschke M, Rubio N, Held KD, Redmond RW. Phototoxicity of Hoechst 33342 in time-lapse fluorescence microscopy. Photochem Photobiol Sci 2010;9:1634-1639.
28. Gerets HH, Tilmant K, Gerin B, Chanteux H, Depelchin BO, Dhalluin S, Atienzar FA. Characterization of primary human hepatocytes, HepG2 cells, and HepaRG cells at the mRNA level and CYP activity in response to inducers and their predictivity for the detection of human hepatotoxins. Cell biology and toxicology 2012;28:69-87.
29. Trachootham D, Alexandre J, Huang P. Targeting cancer cells by ROS-mediated mechanisms: a radical therapeutic approach? Nature reviews. Drug discovery 2009;8:579-591.
30. Westerink WM, Schoonen WG. Cytochrome P450 enzyme levels in HepG2 cells and cryopreserved primary human hepatocytes and their induction in HepG2 cells. Toxicol In Vitro 2007;21:1581-1591.
31. Yamamoto Y, Nakajima M, Yamazaki H, Yokoi T. Cytotoxicity and apoptosis produced by troglitazone in human hepatoma cells. Life Sci 2001;70:471-482.
32. Nicod L, Viollon C, Regnier A, Jacqueson A, Richert L. Rifampicin and isoniazid increase acetaminophen and isoniazid cytotoxicity in human HepG2 hepatoma cells. Hum Exp Toxicol 1997;16:28-34.

Supporting Table 1. Drugs used in this study and their reported adverse effects on the liver

Drug name	Abbreviation	Function	Metabolizing enzymes	Adverse drug reactions in the liver	References
amiodarone	AMI	antiarrhythmic agent	CYP3A4; 1A2	ALT/AST elevations; cirrhosis; jaundice; hepatomegaly; hepatitis; phospholipidosis; steatohepatitis; cholestasis	(1, 2)
3'-hydroxyacetanilide	AMAP	regioisomer of paracetamol	CYP2E1	Does not cause liver failure in mice	(3, 4)
paracetamol / acetaminophen	APAP	analgesic and antipyretic	CYP2E1; 1A2; 2D6; 3A4	DRESS syndrome; acute liver failure; necrosis	(5-7)
carbamazepine	CBZ	antiepileptic drug	CYP3A4; 2C9; induces CYP3A4	SJS/TEN (Stevens-Johnson syndrome / toxic epidermal necrolysis); chronic hepatitis	(8-11)
clozapine	CLZ	antipsychotic drug	CYP3A4; 1A2; 2D6	ALT/AST elevations; hepatitis; jaundice; necrosis	(12-16)
diclofenac	DCF	NSAID	CYP3A4; 2C9 ; 2C8; UGT2B7	SJS; acute hepatitis; necrosis; autoimmune chronic liver injury	(17-19)
isoniazid	INH	anti-tuberculosis drug	CYP2E1; inhibits CYP2C9 and 3A4	ALT/AST elevation; acute hepatitis; chronic hepatitis; necrosis	(20-22)
ketoconazole	KTZ	antifungal antibiotic	CYP3A4; inhibits CYP3A4 and UGT2B7	acute hepatitis; cholestasis; necrosis	(23-25)
methotrexate	MTX	chemotherapeutic agent	aldehyde oxidase; CYP2E1	ALT/AST elevations; fibrosis; cirrhosis; chronic hepatitis; NASH	(26, 27)
nefazodone	NFZ	antidepressant	CYP3A4; inhibits CYP3A4	liver failure; jaundice; hepatitis; hepatocellular necrosis	(28, 29)
naproxen	NPX	NSAID	CYP2C9	ALT/AST elevations; cholestasis; acute hepatitis	(30)
nitrofurantoin	NTF	antibiotic against urinary tract infections	CYP1A	autoimmune hepatitis; chronic active hepatitis; necrosis	(31, 32)
ofloxacin	OFX	antibiotic	CYP1A2; 2C19	SJS/TEN; hepatocellular necrosis; jaundice; hepatitis	(33)
simvastatin	SN	statin	CYP3A4	ALT/AST elevations; jaundice; hepatitis	(34, 35)
troglitazone	TGZ	antidiabetic	CYP1A1; 2C8; 2C19; 3A4	fulminant hepatitis; ALF	(36, 37)

SUPPORTING REFERENCES

1. Lu J, Jones AD, Harkema JR, Roth RA, Ganey PE. Amiodarone exposure during modest inflammation induces idiosyncrasy-like liver injury in rats: role of tumor necrosis factor-alpha. Toxicol Sci 2012;125:126-133.
2. Pollak PT, Shafer SL. Use of population modeling to define rational monitoring of amiodarone hepatic effects. Clin Pharmacol Ther 2004;75:342-351.
3. Stamper BD, Bammler TK, Beyer RP, Farin FM, Nelson SD. Differential regulation of mitogen-activated protein kinase pathways by acetaminophen and its nonhepatotoxic regioisomer 3'-hydroxyacetanilide in TAMH cells. Toxicol Sci 2010;116:164-173.
4. Halmes NC, Samokyszyn VM, Hinton TW, Hinson JA, Pumford NR. The acetaminophen regioisomer 3'-hydroxyacetanilide inhibits and covalently binds to cytochrome P450 2E1. Toxicol Lett 1998;94:65-71.
5. Jaeschke H, Williams CD, Ramachandran A, Bajt ML. Acetaminophen hepatotoxicity and repair: the role of sterile inflammation and innate immunity. Liver Int 2012;32:8-20.
6. Manyike PT, Kharasch ED, Kalhorn TF, Slattery JT. Contribution of CYP2E1 and CYP3A to acetaminophen reactive metabolite formation. Clin Pharmacol Ther 2000;67:275-282.
7. Pirmohamed M, Madden S, Park BK. Idiosyncratic drug reactions. Metabolic bioactivation as a pathogenic mechanism. Clin Pharmacokinet 1996;31:215-230.
8. Daly AK. Using genome-wide association studies to identify genes important in serious adverse drug reactions. Annu Rev Pharmacol Toxicol 2012;52:21-35.
9. Phillips EJ, Mallal SA. HLA-B*1502 screening and toxic effects of carbamazepine. N Engl J Med 2011;365:672; author reply 673.
10. Bjornsson E. Hepatotoxicity associated with antiepileptic drugs. Acta Neurol Scand 2008;118:281-290.
11. Syn WK, Naisbitt DJ, Holt AP, Pirmohamed M, Mutimer DJ. Carbamazepine-induced acute liver failure as part of the DRESS syndrome. Int J Clin Pract 2005;59:988-991.
12. McKnight C, Guirgis H, Votolato N. Clozapine rechallenge after excluding the high-risk clozapine-induced agranulocytosis genotype of HLA-DQB1 6672G>C. Am J Psychiatry 2011;168:1120.
13. Dragovic S, Boerma JS, van Bergen L, Vermeulen NP, Commandeur JN. Role of human glutathione s-transferases in the inactivation of reactive metabolites of clozapine. Chem Res Toxicol 2010;23:1467-1476.
14. Damsten MC, van Vugt-Lussenburg BM, Zeldenthuis T, de Vlieger JS, Commandeur JN, Vermeulen NP. Application of drug metabolising mutants of cytochrome P450 BM3 (CYP102A1) as biocatalysts for the generation of reactive metabolites. Chem Biol Interact 2008;171:96-107.
15. Valevski A, Klein T, Gazit E, Meged S, Stein D, Elizur A, et al. HLA-B38 and clozapine-induced agranulocytosis in Israeli Jewish schizophrenic patients. Eur J Immunogenet 1998;25:11-13.
16. Hummer M, Kurz M, Kurzthaler I, Oberbauer H, Miller C, Fleischhacker WW. Hepatotoxicity of clozapine. J Clin Psychopharmacol 1997;17:314-317.
17. Fredriksson L, Herpers B, Benedetti G, Matadin Q, Puigvert JC, de Bont H, et al. Diclofenac inhibits tumor necrosis factor-alpha-induced nuclear factor-kappaB activation causing synergistic hepatocyte apoptosis. Hepatology 2011;53:2027-2041.
18. Deng X, Luyendyk JP, Ganey PE, Roth RA. Inflammatory stress and idiosyncratic hepatotoxicity: hints from animal models. Pharmacol Rev 2009;61:262-282.
19. Boelsterli UA. Diclofenac-induced liver injury: a paradigm of idiosyncratic drug toxicity. Toxicol Appl Pharmacol 2003;192:307-322.
20. Daly AK, Day CP. Genetic association studies in drug-induced liver injury. Drug Metab Rev 2012;44:116-126.
21. Srivastava A, Maggs JL, Antoine DJ, Williams DP, Smith DA, Park BK. Role of reactive metabolites in drug-induced hepatotoxicity. Handb Exp Pharmacol 2010:165-194.
22. Zand R, Nelson SD, Slattery JT, Thummel KE, Kalhorn TF, Adams SP, et al. Inhibition and induction of cytochrome P4502E1-catalyzed oxidation by isoniazid in humans. Clin Pharmacol Ther 1993;54:142-149.
23. Lin CL, Hu JT, Yang SS, Shin CY, Huang SH. Unexpected emergence of acute hepatic injury in patients treated repeatedly with ketoconazole. J Clin Gastroenterol 2008;42:432-433.
24. Kim TH, Kim BH, Kim YW, Yang DM, Han YS, Dong SH, et al. Liver cirrhosis developed after ketoconazole-induced acute hepatic injury. J Gastroenterol Hepatol 2003;18:1426-1429.
25. Bernuau J, Durand F, Pessayre D. Ketoconazole-induced hepatotoxicity. Hepatology 1997;26:802.
26. Aithal GP. Hepatotoxicity related to antirheumatic drugs. Nat Rev Rheumatol 2011;7:139-150.
27. West SG. Methotrexate hepatotoxicity. Rheum Dis Clin North Am 1997;23:883-915.
28. Xu JJ, Henstock PV, Dunn MC, Smith AR, Chabot JR, de Graaf D. Cellular imaging predictions of clinical drug-induced liver injury. Toxicol Sci 2008;105:97-105.
29. Stewart DE. Hepatic adverse reactions associated with nefazodone. Can J Psychiatry 2002;47:375-377.

30. Ali S, Pimentel JD, Ma C. Naproxen-induced liver injury. Hepatobiliary Pancreat Dis Int 2011;10:552-556.
31. Czaja AJ. Drug-induced autoimmune-like hepatitis. Dig Dis Sci 2011;56:958-976.
32. Boelsterli UA, Ho HK, Zhou S, Leow KY. Bioactivation and hepatotoxicity of nitroaromatic drugs. Curr Drug Metab 2006;7:715-727.
33. Blum A. Ofloxacin-induced acute severe hepatitis. South Med J 1991;84:1158.
34. Bjornsson E, Jacobsen EI, Kalaitzakis E. Hepatotoxicity associated with statins: reports of idiosyncratic liver injury post-marketing. J Hepatol 2012;56:374-380.
35. Law M, Rudnicka AR. Statin safety: a systematic review. Am J Cardiol 2006;97:52C-60C.
36. Jaeschke H. Troglitazone hepatotoxicity: are we getting closer to understanding idiosyncratic liver injury? Toxicol Sci 2007;97:1-3.
37. Kaplowitz N. Idiosyncratic drug hepatotoxicity. Nat Rev Drug Discov 2005;4:489-499.

4

Translation initiation factor EIF4A1 determines TNFα-mediated apoptosis in drug-induced liver injury through the stress protein CHOP

Lisa Fredriksson*, Bram Herpers*, Steven Wink, Giulia Benedetti, Hans de Bont, Erik Danen, Mirjam Luijten, Marjo de Graauw, John Meerman and Bob van de Water

Submitted to Hepatology

ABSTRACT

Drug-induced liver injury (DILI) is an important clinical problem. Here we used a functional genomics approach to establish the critical drug-induced toxicity pathways that act in synergy with the pro-inflammatory cytokine tumor necrosis factor α (TNFα) to cause apoptosis of liver HepG2 cells. Transcriptomics-based analysis of the toxicity response pathways activated by diclofenac (DCF), carbamazepine (CBZ), ketoconazole and nefazodone revealed activation of death-receptor/apoptosis pathway signaling, nuclear factor-erythroid 2 (NF-E2)-related factor 2 (Nrf2) oxidative stress response, and endoplasmic reticulum (ER) stress/translational initiation signaling, independent of TNFα signaling. Systematic siRNA-mediated knockdown of the individual toxicity pathway determinants established the critical role of caspase-8, Bid, Bim and APAF1 for the drug/TNFα-induced apoptosis. Cell death involved an oxidative stress component since pre-induction of the Nrf2 pathway by knockdown of its negative regulator Kelch-like ECH-associated protein 1 (Keap1) suppressed the drug/TNFα synergy and down-regulation of the glutathione reductase and peroxidase enhanced cell killing independent of TNFα. While ER stress signaling through inositol-requiring enzyme 1-alpha (IRE1α) and activating transcription factor 6 (ATF6) acted cytoprotective, CBZ- and DCF-induced activation of protein kinase R-like ER kinase (PERK) and subsequent expression of C/EBP-homologous protein (CHOP) was crucial in the onset of drug/TNFα-induced apoptosis independent of drug-induced oxidative stress. CBZ and DCF caused a strong expression of the translational initiation factor EIF4A1. Importantly, depletion of EIF4A1 almost completely inhibited CHOP expression in association with protection against the drug/TNFα-mediated cell killing. Conclusion: We propose a model in which enhanced drug-induced translation initiates PERK-mediated CHOP signaling thereby sensitizing towards caspase-8-dependent TNFα-induced apoptosis.

INTRODUCTION

Drug-induced liver injuries (DILIs) constitute an important problem both in the clinic as well as during drug development (1). The underlying cellular mechanisms that determine the susceptibility towards developing DILI are incompletely understood. Recent data indicate that the crosstalk between drug reactive metabolite-mediated intracellular stress responses and cytokine-mediated pro-apoptotic signaling are important components in the pathophysiology of DILI (2,3). Tumor necrosis factor-α (TNFα) severely enhances liver damage caused by various xenobiotics (2,4-6) and it is the major cytokine to be excreted by the liver stationary macrophages (Kupffer cells) upon exposure to bacterial endotoxins or as a response to hepatocyte damage (7). In addition, reactive drug metabolites covalently modify cellular macromolecules leading to intracellular biochemical perturbations and the induction of various intracellular stress signaling pathways. It is likely that these stress pathways are causal for the sensitization of the crosstalk with the cytokine signaling. So far it remains unclear which toxicity pathways modulate the pro-apoptotic activity of TNFα signaling.

The Kelch-like ECH-associated protein 1 (Keap1)/ nuclear factor-erythroid 2 (NF-E2)-related factor 2 (Nrf2) pathway is important in the recognition of reactive metabolites and/or cellular oxidative stress (8). Under normal conditions Nrf2 is maintained in the cytoplasm and guided towards proteasomal degradation by Keap1 (9). Nucleophilic reactions with the redox-sensitive cysteine residues of Keap1 releases Nrf2 followed by its nuclear entry and transcriptional activation of antioxidant genes (8,10). Nrf2 signaling is critical in the cytoprotective response against reactive metabolites both in vitro and in vivo (11,12), but its role in regulating TNFα pro-apoptotic signaling relation to DILI is unclear.

The endoplasmic reticulum (ER) unfolded protein response is an adaptive stress response to ER protein overload due to enhanced translation and/or perturbed protein folding. It involves expression of molecular chaperones such as the heat shock family member HSPA5 (also known as BiP or Grp78) (13). When adaptation fails, a pro-apoptotic program to eliminate the injured cell is initiated (14). The ER stress response contains three signaling arms: the protein kinase R-like ER kinase (PERK), the activating transcription factor 6 (ATF6) and the inositol-requiring enzyme 1α (IRE1α) (13). Activation of IRE1α and ATF6 initiates protective responses, while activation of PERK leads to attenuation of global protein synthesis and favored translation of activating transcription factor 4 (ATF4) by phosphorylation of eIF2α, resulting in expression of the ATF4 downstream target gene DDIT3 encoding the C/EBP homologous protein (CHOP) (15). CHOP initiates a pro-apoptotic program by modulation of Bcl2-family proteins (13,14). The role and mechanism of ER stress in controlling DILI in relation to TNFα-induced apoptosis and its relation to drug-induced oxidative stress remains undefined.

We show that different hepatotoxic drugs including diclofenac, carbamazepine, and ketoconazole show a synergistic apoptotic response with the pro-inflammatory cytokine TNFα. Genome-wide transcriptomics analysis revealed an activation of the Nrf2-

related oxidative stress response, the ER stress response as well as the death receptor-signaling pathway as critical cell toxicity pathways independent of, and preceding TNFα-mediated cell killing. A systematic short interfering RNA (siRNA) mediated knockdown approach of genes related to these stress-induced pathways allowed a detailed functional evaluation of the mechanism by which oxidative stress, ER stress and translational regulation are interrelated in the sensitization towards pro-apoptotic TNFα signaling during DILI.

MATERIALS AND METHODS

Reagents and antibodies

Diclofenac sodium, carbamazepine, nefazodone and ketoconazole were obtained from Sigma (Zwijndrecht, the Netherlands). Methotrexate was from Acros Organics (Geel, Belgium). Human recombinant TNFα was acquired from R&D Systems (Abingdon, United Kingdom). AnnexinV-Alexa633 was made as previously described (16). The antibody against caspase-8, cleaved PARP, and CHOP were from Cell Signaling (Bioké, Leiden, Netherlands). The antibody against tubulin was from Sigma and the antibody against P-Thr 981-PERK was from Santa Cruz (Tebu-Bio, Heerhugowaard, the Netherlands). The antibody against Nrf2 was a kind gift from Dr. Goldring (Liverpool University, United Kingdom).

Cell line

Human hepatoma HepG2 cells were obtained from American Type Culture Collection (ATCC, Wesel, Germany), cultured in DMEM supplemented with 10 % (v/v) FBS, 25 U/mL penicillin and 25 μg/mL streptomycin and used for experiments between passage 5 and 20.

RNA isolation and cRNA microarrays

After drug exposure for 8, 14 or 8 hours followed by the addition of 10 ng/mL TNFα for 6 hours, RNA was isolated from HepG2 cells using the RNeasy® Plus Mini Kit (Qiagen, Venlo, the Netherlands). RNA integrity and quality was assessed using the Agilent bioanalyser (Agilent Technologies, Palo Alto, CA, USA).

The synthesis of labeled cRNA and hybridization steps were performed by Service XS (Leiden, The Netherlands) using the Affymetrix 3' IVT-Express Labeling Kit (#901229) and the Affymetrix Human Genome U133 plus PM arrays. Scanning of the Array Plates was performed using the Affymetrix GeneTitan scanner. BRB Array Tools software (developed by Dr. Richard Simon and BRB-ArrayTools Development Team) was used to normalize the .cel data using the Robust Multichip Average (RMA) method. Significantly differentially expressed genes (p-value < 0.001) between the various experimental conditions were identified with an ANOVA test followed by calculation of the false discovery rate according to Benjamini and Hochberg (17). Classification of the selected genes according to their biological and toxicological functions was performed

using the Ingenuity Pathway Analysis (IPA®) software (Ingenuity® Systems, Redwood, CA, USA). Heatmap representations and hierarchical clustering (using Pearson correlation) were performed using the MultiExperiment Viewer software (18).

RNA interference

Transient knockdowns (72 hrs) of individual target genes were achieved using siGENOME SMARTpool siRNA reagents and siGENOME single siRNA sequences (50 nM; Dharmacon Thermo Fisher Scientific, Landsmeer, the Netherlands) with INTERFERin™ siRNA transfection reagent (Polyplus transfection, Leusden, the Netherlands). The negative controls were siGFP or mock transfection. The single siRNA sequences were used to exclude any off target effects of the SMARTpools resulting in a significant biological effect. The SMARTpool was considered on target when 2 or more of the 4 singles showed a similar significant effect. All siRNA-targeted genes can be found in Supplemental Data S5.

Cell death analysis assays

Induction of apoptosis in real time was quantified using a live cell apoptosis assay previously described (16). Briefly, binding of Annexin V-Alexa633 conjugate to apoptotic cells was followed in time by imaging every 30 minutes after drug exposure with a BD PathwayTM 855 imager (Becton Dickinson). The relative fluorescence intensity per cell area was quantified using Image ProTM (Media Cybernetics, Bethesda, MD, USA). When siRNA-based knockdown resulted in a difference in the area under cell death curve (AUC) larger than 2 standard deviations from the negative control, the effect was considered biologically significant.

Western blot analysis

Western blot analysis was essentially performed as previously described (2) using above-mentioned antibodies.

Live cell imaging of GFP-tagged proteins in HepG2 cells

Reporter HepG2 cells for Nrf2 activity (Srxn1 [mouse]) and ER-stress (HSPA5 [BiP/Grp78; human]) were generated by bacterial artificial chromosome (BAC) recombineering (19,20). Upon validation of correct C-terminal integration of the green fluorescent protein (GFP)-cassette by PCR, the BAC-GFP constructs were transfected using LipofectamineTM 2000 (Invitrogen, Breda, the Netherlands). Stable HepG2 BAC-GFP reporters were obtained by 500 μg/mL G418 selection. Prior to imaging, nuclei were stained with 100 ng/ml Hoechst 33342 in complete DMEM. The induction of Srxn1-GFP and HSPA5-GFP expression was followed for a period of 24 hours, by automated confocal imaging (Nikon TiE2000, Nikon, Amstelveen, the Netherlands). Quantification of the GFP intensity in individual cells was performed using Image ProTM.

Statistical analysis

All numerical results are expressed as the mean ± standard error of the mean (S.E.M.) and represent data from three independent experiments. The statistical analyses were made using GraphPad Prism 5.00 (GraphPad software, La Jolla, USA). Significance levels were calculated using 2-way ANOVA with Bonferroni post-test, * = P < .05, ** = P < .01, *** = P < .001.

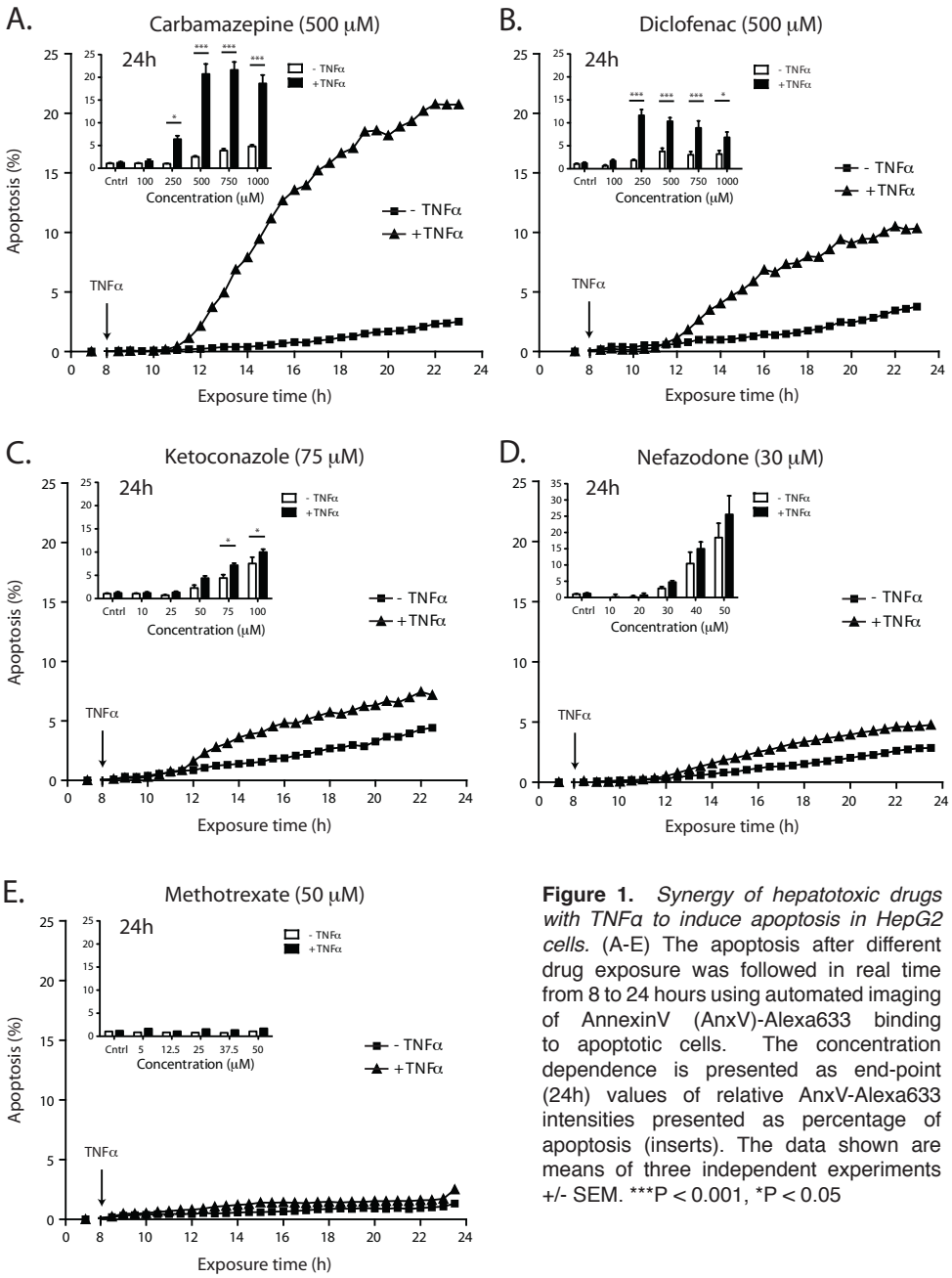

Figure 1. *Synergy of hepatotoxic drugs with TNFa to induce apoptosis in HepG2 cells.* (A-E) The apoptosis after different drug exposure was followed in real time from 8 to 24 hours using automated imaging of AnnexinV (AnxV)-Alexa633 binding to apoptotic cells. The concentration dependence is presented as end-point (24h) values of relative AnxV-Alexa633 intensities presented as percentage of apoptosis (inserts). The data shown are means of three independent experiments +/- SEM. ***P < 0.001, *P < 0.05

RESULTS

Hepatotoxic drug synergy with TNFα is preceded by oxidative stress, ER stress and death receptor signaling gene expression networks

We have previously shown that TNFα enhances the apoptosis induced by diclofenac (DCF) (2). To determine whether synergism with TNFα to induce apoptosis is a more general effect with compounds that cause drug-induced liver injury (DILI), we treated HepG2 cells for 8 hours with different compounds associated with unpredictable idiosyncratic DILI in humans, diclofenac (DCF), carbamazepine (CBZ), ketoconazole (KTZ), nefazodone (NFZ) and methotrexate (MTX), followed by an additional incubation with or without TNFα (10 ng/ml) for 16 hrs. DCF, CBZ and KTZ showed a significant enhanced apoptosis when combined with TNFα (Fig. 1 A-C). Only a trend to towards synergy was observed for NFZ (Fig. 1 D), while hardly any toxicity was observed for MTX (Fig. 1 E). Importantly, TNFα itself did not induce any apoptosis ("Control" in Fig. 1 A-E).

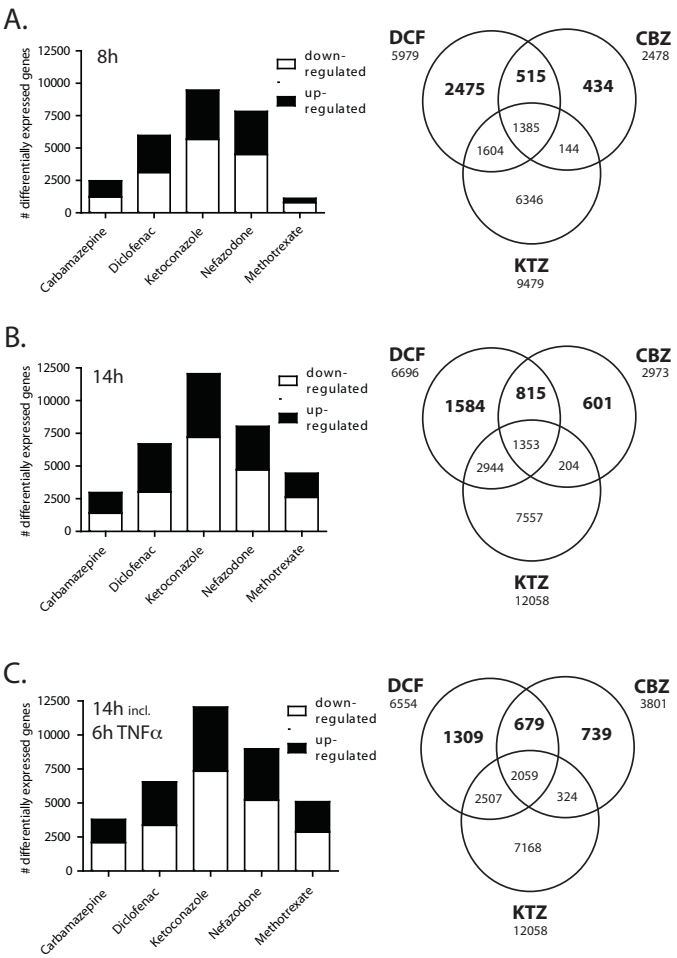

Figure 2. *Differentially expressed genes after exposure to hepatotoxic drugs.* The gene expression after 8 (A), 14 (B) and 14 hours including 6 hours of TNFα (10 ng/mL; C) exposure to diclofenac (DCF; 500 μM), carbamazepine (CBZ; 500 μM), ketoconazole (KTZ; 75 μM), nefazodone (NFZ; 30 μM) and methotrexate (MTX; 50 μM) is presented as number of genes differentially up- (black) or down-regulated (white) compared to control ($p<0.001$). The total number of genes overlapping among the TNFα-synergizing drugs is show in the corresponding Venn-diagrams.

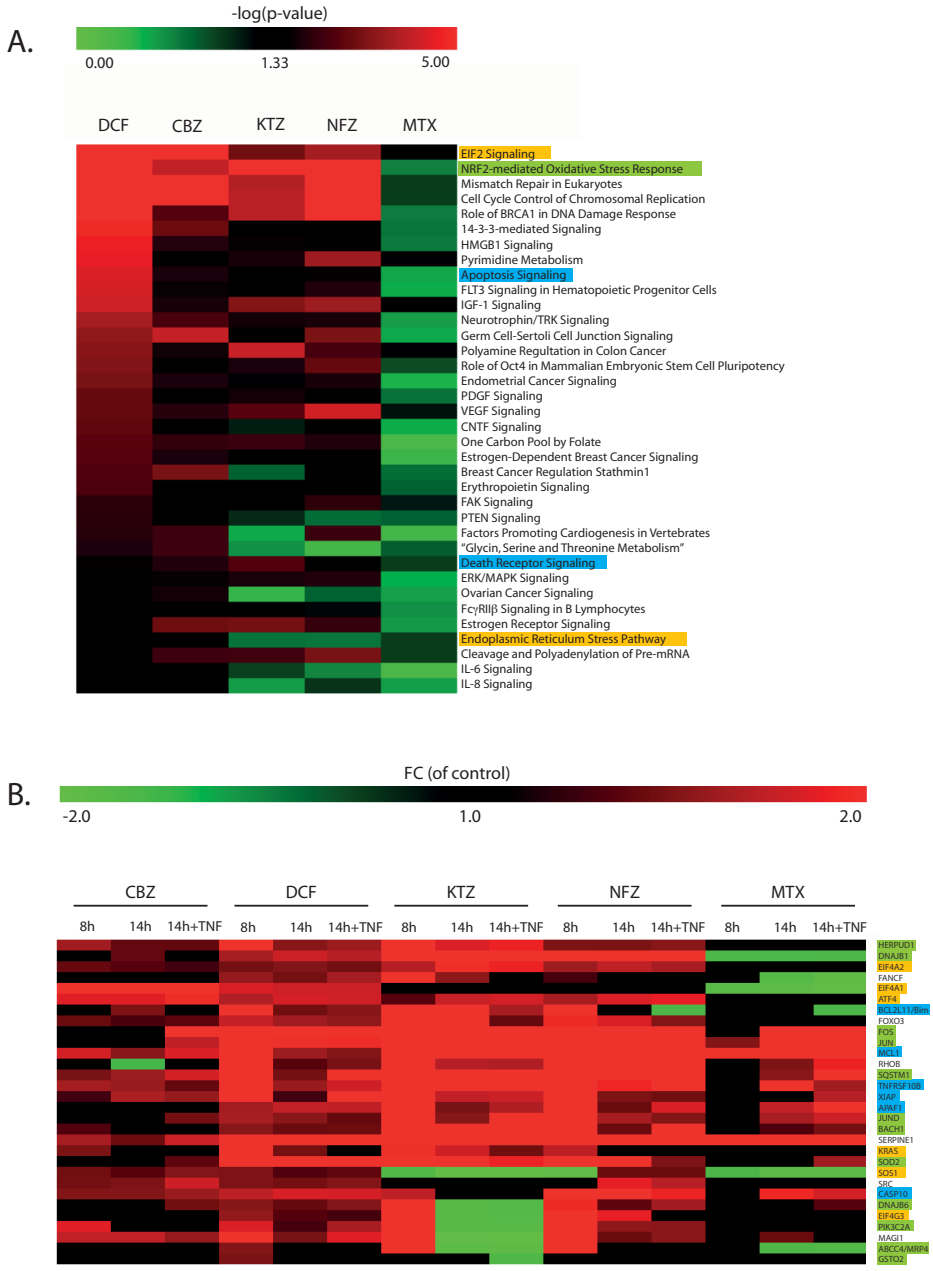

Figure 3. *Ingenuity Pathway Analysis (IPA) of common differentially expressed genes.* (A) Using IPA® the canonical pathways being significantly affected following exposure to diclofenac (DCF; 500 μM), carbamazepine (CBZ; 500 μM), ketoconazole (KTZ; 75 μM), nefazodone (NFZ; 30 μM) and methotrexate (MTX; 50 μM) for 8 hours were determined. The pathways are ranked by the criteria of being significantly regulated after DCF and CBZ, but not after MTX treatment. The most striking toxicity pathways are highlighted as follows: EIF2 Signaling/Endoplasmic Reticulum Stress Pathways are marked in yellow, Nrf2-mediated Oxidative Stress response is marked in green and Apoptosis/Death Receptor Signalling is marked in blue. (B) After hierarchical clustering using Pearson correlation and average linkage of the genes representing the pathways in A, the three clusters showing most genes up-regulated under DCF and CBZ conditions but not MTX are shown. The colours indicate the corresponding pathways from A.

To gain further insight into the toxicity pathways that may sensitize towards TNFα-mediated cell killing, we first performed a gene expression analysis on HepG2 cells exposed to DCF, CBZ, KTZ, NFZ and MTX for 8 hours (Fig. 2 A). While MTX only mildly affected the gene expression (1121 differentially expressed genes [DEGs] at 8 hours), which was related to the mild cytotoxicity (Fig. 1 E), KTZ caused the strongest gene expression changes (9479 DEGs at 8 hours; Fig. 2 A) in association with greater onset of cell death (Fig. 1 C). Not many additional changes in DEGs were observed after treatment for an additional 6 hours with the compounds either in presence or absence of TNFα (Fig. 2 B and C).

To identify likely candidate genes that contribute to this synergy we determined the overlap in DEGs for all synergizing drugs (DCF, CBZ and KTZ; see Venn-diagrams in Fig. 2). Since the most significant TNFα synergy was observed for CBZ (Fig. 1 A) we considered this a relevant model compound. DCF showed the highest overlap with CBZ in DEGs (Fig. 2 A-C). Due to this and the fact that KTZ showed marked cytotoxicity with the compound alone accompanied by only a slight, though significant, synergism with TNFα, we chose to focus on CBZ and DCF alone from here onwards.

Next we employed Ingenuity Pathway Analysis (IPA®) software to identify the signaling pathways that were affected by both CBZ and DCF (Fig. 3 A). Three prominent toxicity pathways were found: “EIF2-signaling/Endoplasmic reticulum stress pathway”, “Nrf2-mediated oxidative stress response”, and “Apoptosis/Death receptor signaling”. Subsequently we identified all the individual genes that determined these significant pathways (Supporting Data S1). Hierarchical clustering of these selected genes allowed identification of three main gene clusters that were up-regulated after 8 hours CBZ and/or DCF but not MTX treatment (Supporting Data S2). Interestingly, these contained almost exclusively genes representing the above-mentioned significantly affected pathways (compare Fig. 3 A and Supporting Data S2). For further gene selection we used a threshold of 1.5-fold change for any CBZ or DCF treatment time point (Fig. 3 B). Importantly, we confirmed the regulation of the Nrf2-mediated stress response and ER stress by DCF in primary hepatocytes (Supporting Data S3).

The death receptor pathway is critical in the drug/TNFα-induced apoptosis

Previously we showed that DCF/TNFα-induced apoptosis is dependent on the death receptor pathway (2). Next we systematically analyzed whether the CBZ/TNFα-induced apoptosis was using an identical apoptotic pathway. We observed the 41/43 kDa cleavage products of caspase-8, the most proximal initiator caspase downstream of the death receptor signaling complex, in CBZ/TNFα conditions already at 12 hours, but not for CBZ alone (Fig. 4 A). This correlated with the cleavage of caspase-3 substrate PARP (Fig. 4 A). Importantly, successful siRNA-mediated knockdown of caspase-8 (Supporting Data S4 A and S5) demonstrated that CBZ/TNFα-induced apoptosis was almost fully dependent on caspase-8 (Fig. 4 B).

Next we investigated the functional roles of the genes in the apoptotic and

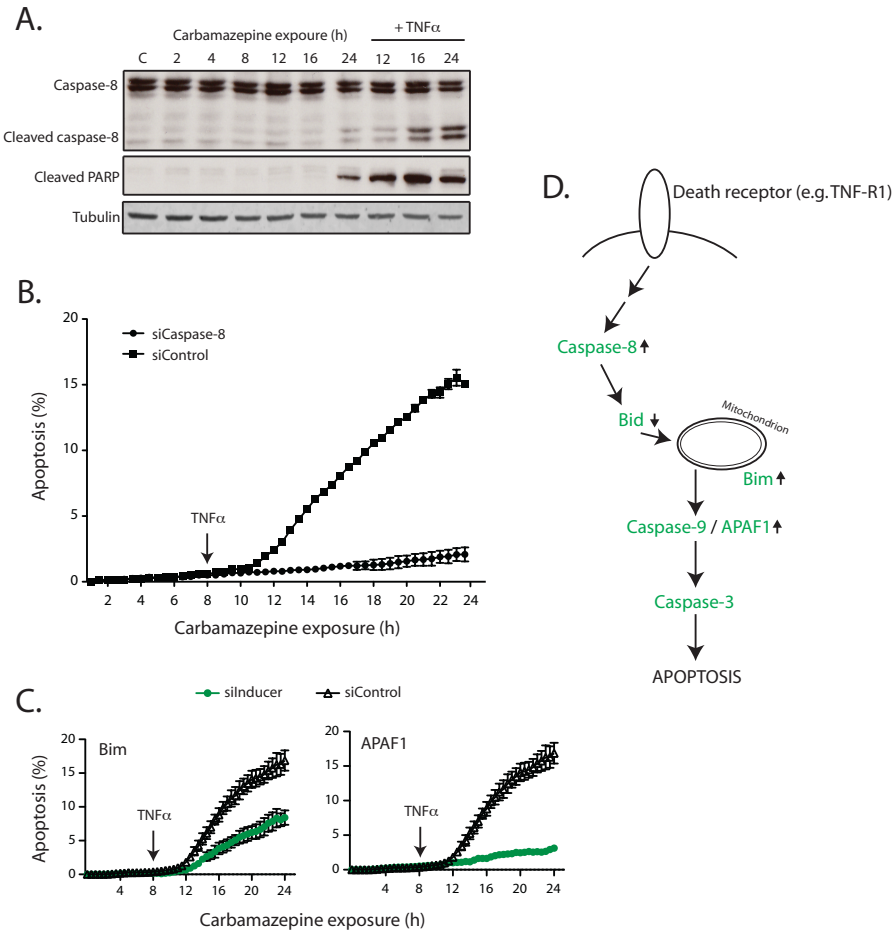

Figure 4. *Carbamazepine (CBZ)/TNFα-induced apoptosis is dependent on the extrinsic apoptotic pathway.* (A) Caspase-8 and PARP cleavage after exposure to CBZ +/- TNFα after 8 hours of exposure was assessed by western blot analysis. "C", controls exposed to vehicle for 12 hours. (B) Apoptosis was followed by AnnexinV (AnxV)-Alexa633 binding to apoptotic cells using automated microscopy after siRNA-mediated knockdown of caspase-8 and CBZ/TNFα-exposure. (C) AnxV-Alexa633 staining followed in time after knockdown of APAF1 and Bim/BCL2L11 and CBZ/TNFα-exposure. (D) Schematic representation of the pro-apoptotic pathway activated by CBZ/TNFα-exposure. Identified inducers of apoptosis are shown in green and the arrows indicate an up-or down-regulation after DCF and/or CBZ exposure on a transcriptional level (p-value ≤ 0.001) after 8 hours exposure. The data are presented as means of three independent experiments +/- SEM.

death receptor-related pathways that were up-regulated after both DCF and CBZ exposure conditions (see Fig. 3 B, blue highlight) using siRNA-mediated knockdowns of the individual genes. Knockdown of Bim/BCL2L11, a BH3 domain-containing Bcl2-family member, significantly decreased CBZ/TNFα apoptosis (Fig. 4 C). In addition, knockdown of apoptotic protease activating factor 1 (APAF1), a critical component of the apoptosome formed upon mitochondrial release of cytochrome c, led to an inhibition of apoptosis (Fig. 4 C and Supporting Data S5). We anticipated that the onset of apoptosis followed a caspase-8/Bid/APAF1/caspase-9/caspase-3 route. Indeed, knockdown of Bid, caspase-9 and caspase-3 all significantly decreased CBZ/TNFα-induced apoptosis

(Supporting Data S4 B). Collectively, these data support the involvement of the death receptor/apoptotic pathway in the induction of CBZ/TNFα-induced apoptosis (Fig. 4 D) and is therefore similar to DCF/TNFα-mediated apoptosis (2).

Oxidative stress sensitizes in the diclofenac and carbamazepine mediated apoptosis

The Nrf2-mediated oxidative stress response was significantly affected by CBZ and DCF treatment (Fig. 3), likely in relation to the formation of reactive metabolites of these compounds in our cell model (2). Modification of critical cysteine residues on Keap1, leads to the liberation of Nrf2 followed by its nuclear translocation and transcriptional activation of antioxidant genes (8,10,21). We first investigated the Nrf2 levels after CBZ and DCF treatment. DCF caused a stabilization of Nrf2, which was associated with increased levels of the Nrf2 target gene γGCSm (Fig. 5 A). Little effect of CBZ was observed on Nrf2 levels. Sulfiredoxin 1 (Srxn1) is a direct target of Nrf2 (22) and we monitored the activity of Nrf2 using live cell imaging of a BAC-Srnx1-GFP HepG2 reporter cell line. Srxn1-GFP expression was near absent under control conditions but increased over time following DCF and CBZ treatment independent of TNFα (Fig. 5 B and C). Importantly, siRNA-mediated knockdown of Nrf2 completely inhibited the Srnx1-GFP expression after CBZ, supporting Nrf2 activation (Fig. 5 C).

The antioxidant N,N'-diphenylbenzene-1,4-diamine (DPPD) drastically decreased both CBZ and CBZ/TNFα-mediated cell death (Fig. 5 D) as well as for DCF and DCF/TNFα treatment (Supporting Data S6 A), indicating a role for oxidative stress in drug/TNFα-induced apoptosis. The Nrf2 pathway and its related gene targets identified in the CBZ and DCF stress response (Fig. 3 B, green highlight) were also critically involved in the protection against drug/TNFα-mediated cell killing. Knockdown of Keap1 led to enhanced protein levels of Nrf2 (Supporting Data S6 B), which was associated with a protection against CBZ/TNFα- and DCF/TNFα-induced cytotoxicity (CBZ: Fig. 5 E and DCF: Supporting Data S7). Importantly, knockdown of Nrf2 itself (Supporting Data S6 B) led to enhancement of the apoptosis (Fig. 5 E and Supporting Data S7). In addition, depletion of two key antioxidant enzymes GSR and GPX4 that are involved in the detoxification of reactive oxygen species, led to enhancement of the cytotoxic response following drug/TNFα-exposure (Fig. 5 E). In contrast, depletion of a negative regulator of Nrf2-dependent transcription, BACH1 (23,24), which was found up-regulated following CBZ and DCF exposure in our gene array (Fig. 3 B), had a cytoprotective effect (Fig. 5 F and Supporting Data S7). Somewhat unexpected, knockdown of the multi-drug resistance protein MRP4, the glutathione S-transferase GSTO2 and the anti-oxidant gene inducer JUND also protected against the cell killing (Fig. 5 F and Supporting Data S7). All functionally relevant antioxidant components that we tested were validated by single siRNAs (Supporting data S 5). Altogether these data indicate the functional involvement of an Nrf2-dependent antioxidative stress pathway activation to protect against CBZ/TNFα as well as DCF/TNFα induced cell death.

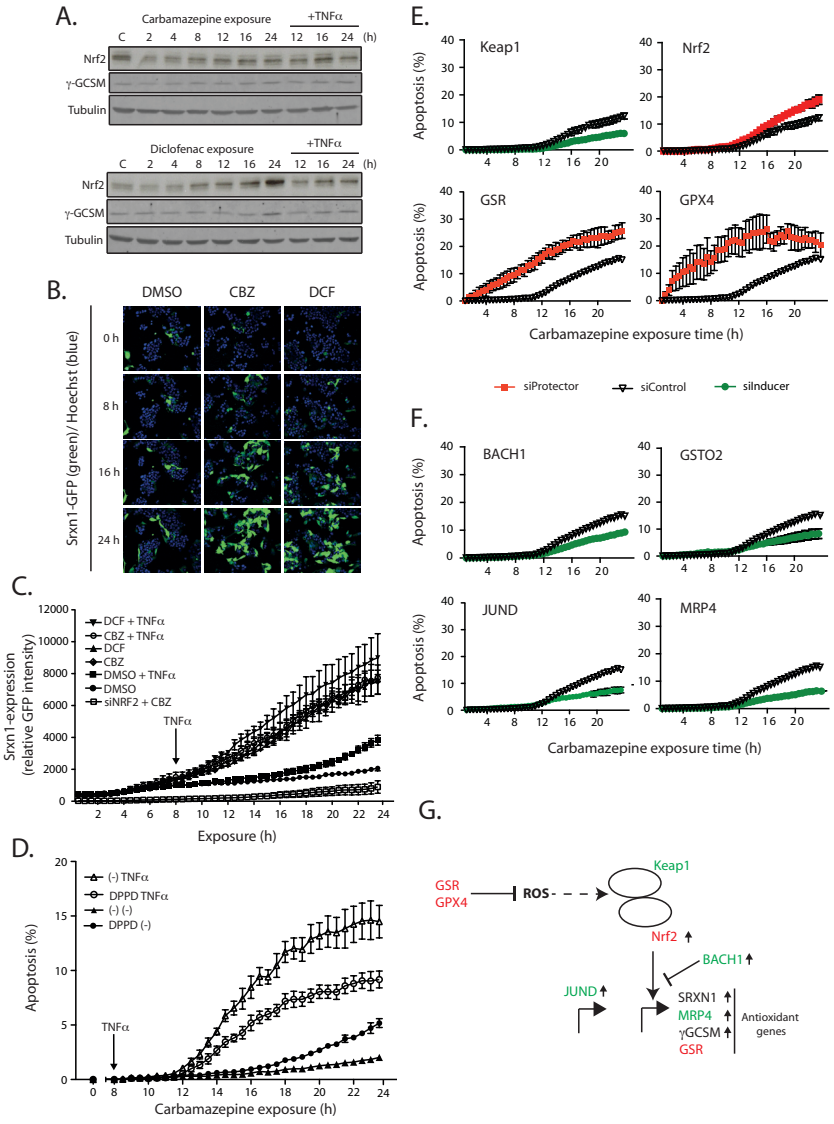

Figure 5. *Carbamazepine (CBZ) and diclofenac (DCF) induces an Nrf2-response affecting the drug/TNFα-induced apoptosis.* (A) Nrf2 and γ-GCSM protein levels were investigated by western blot analysis following DCF and CBZ exposure +/- TNFα addition. "C", controls exposed to vehicle for 12 hours. (B and C) Nrf2-responsive Srxn1-GFP levels were followed using automated confocal microscopy. Shown are representative images of Srxn1-GFP HepG2 cells exposed to vehicle (DMSO), DCF or CBZ (B) and the quantification of GFP-intensity in time normalized to the area occupied by the nuclei (Hoechst; C). (D) AnxV-Alexa633 staining of HepG2 cells +/- pre-exposure to antioxidant DPPD (10 μM) followed by CBZ-exposure +/- addition of TNFα (10 ng/mL) after 8 hours. (E) The effect on CBZ/TNFα induced apoptosis was investigated using live cell imaging of apoptosis after knockdown of crucial players in the oxidative stress response using siRNAs targeting Keap1, Nrf2, GSR and GPX4. Green indicates knockdown of inducers of oxidative stress and red protectors against oxidative stress. (F) The effect of knockdown of genes up-regulated in Fig. 3B and involved in an Nrf2-mediated oxidative stress response on the apoptosis induced by CBZ/TNFα measured by AnxV-Alexa633 staining and automated microscopy. (G) Schematic representation of the Nrf2-mediated oxidative stress response. Oxidative stress related protectors in E are shown in red, oxidative stress related inducers in F are shown in green and the arrows indicate an up-regulation on a transcriptional level (p-value ≤ 0.001) following DCF and/or CBZ exposure for 8 hours. The data are presented as means of three independent experiments +/- SEM.

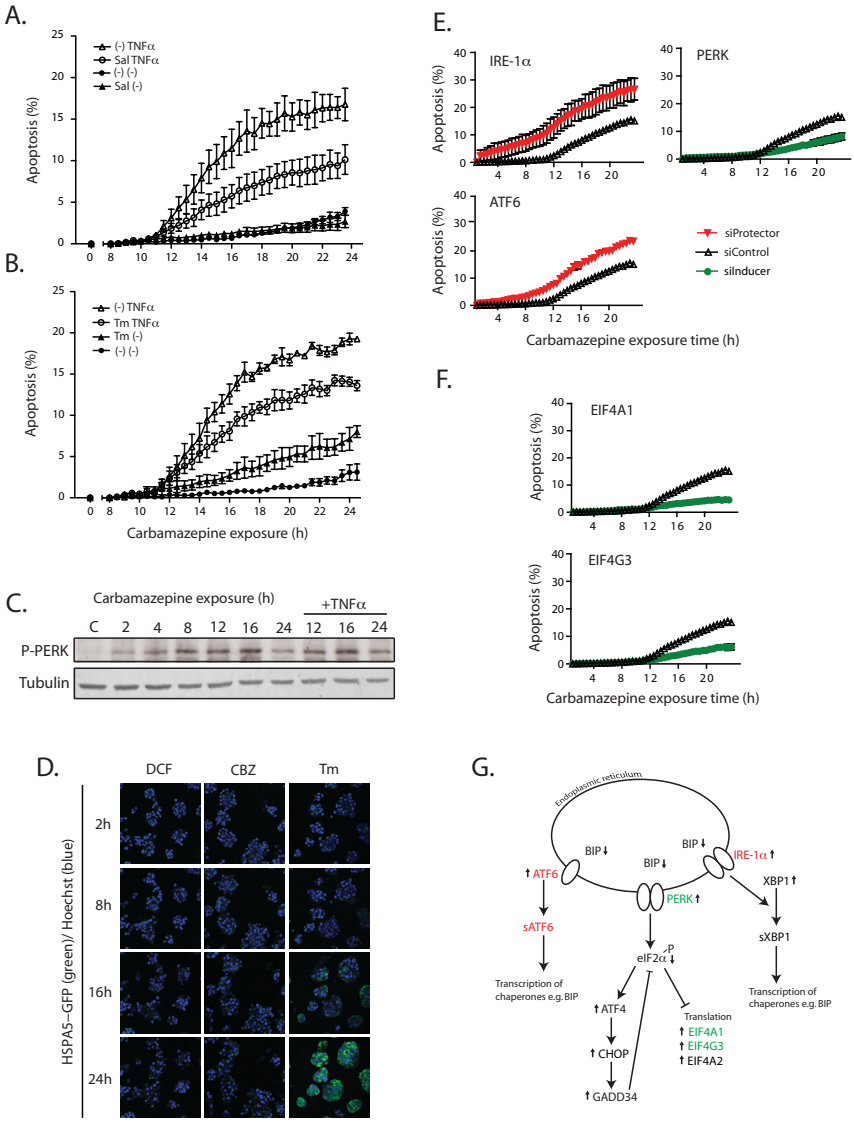

Figure 6. *Carbamazepine (CBZ) induces an ER stress-response affecting the drug/TNFα-induced apoptosis.* (A and B) HepG2 cells were pre-treated with eIF2α phosphatase inhibitor salubrinal (Sal; 50 μM; A) or ER-stressor tunicamycin (Tm; 10 μg/mL; B) for 16 hours before treatment with 500 μM CBZ. TNFα (10 ng/mL) was added 8 hours after drug exposure. (C) PERK activation was followed in time by western blotting for phosphorylated PERK (P-PERK). "C", control exposed to vehicle for 12 hours. (D) HepG2 cells expressing HSPA5-GFP (BiP) were followed in time after exposure to diclofenac (DCF; 500 μM), carbamazepine (CBZ; 500 μM), or Tm (10 μg/mL) using automated confocal microscopy. Shown are representative merged images of HSPA5-GFP (green) and Hoechst (blue) at 2, 8, 16 and 24 hours after drug exposure. (E) The effect of knockdown of the three arms of the UPR on the apoptosis induced by CBZ/TNFα was measured by AnxV-Alexa633 staining and automated microscopy. An enhanced apoptosis response is shown in red and a reduced response in green. (F) The effect of knockdown of genes involved in translational initiation (found up-regulated on expression level in Fig. 3B) on the apoptosis induced by CBZ/TNFα was measured by AnxV-Alexa633 staining and automated microscopy. (G) Schematic representation of the ER stress response. ER stress related protectors in E are shown in red, ER stress- and translation-related inducers in F are shown in green and the arrows indicate an up- or down-regulation on a transcriptional level (p-value ≤ 0.001) following DCF and/or CBZ exposure for 8 hours. The data are presented as means of three independent experiments +/- SEM.

PERK activation determines ER stress-mediated hepatotoxicant/TNF synergistic cell death

EIF2-signaling in the context of translational initiation was identified as the most significantly affected pathway by CBZ and DCF, which was associated with endoplasmic reticulum (ER) stress or unfolded protein response (UPR) pathway regulation (Fig. 3, yellow highlight). First we pre-treated cells with an inhibitor of the de-phosphorylation of eIF2α, salubrinal, thereby prolonging the translational inhibition (25). This resulted in a protection against CBZ/TNF and DCF/TNF cell death (Fig. 6 A and Supporting Data S8 A). Also pre-treatment of cells with an ER-stressor, tunicamycin, to induce a protective adaptive response (26), inhibited the apoptosis induced by CBZ/TNFα as well as DCF/TNFα (Fig. 6 B and Supporting Data S8 B). ER stress/UPR induces the activation of PERK-ATF4, IRE1α-XBP1 and ATF6 target gene expression (13). Using IPA® pathway analysis of the DEGs after 8 hours of CBZ and DCF exposure, we investigated the expression of downstream targets of ATF4, XBP1 and ATF6. ATF4 showed the strongest upregulation of downstream targets indicating an important role for PERK/ATF4 signaling (Supporting Data S9). Indeed, PERK was activated after both CBZ and DCF treatment (Fig. 6 C and Supporting Data S10). Importantly, addition of TNFα did not enhance the levels of phosphorylated PERK.

Next we systematically analyzed the critical signaling components of the ER stress/UPR in regulation of the cytotoxicity. The UPR induces expression of BiP/HSPA5 through the activation of IRE1α and ATF6 (13). Using a BAC-HSPA5-GFP reporter HepG2 cell line we demonstrated a strong induction of HSPA5 after tunicamycin treatment. Although no obvious induction was observed after CBZ and DCF (Fig. 6 D), knockdown of IRE1α and ATF6 by siRNA, sensitized cells against apoptosis, indicating a role for the IRE1α/ATF6 adaptive response in the protection against cell death (Fig. 6 E and Supporting Data S11 A). In contrast, PERK knockdown led to reduction of apoptosis-induction following CBZ/TNFα (Fig. 6 E) and DCF/TNFα (Supporting Data S11 A).

The protective effect of salubrinal suggested a central role for the translational program in the onset of apoptosis. To further test this hypothesis we performed a knockdown of the DEGs that determined the strong significance of the “EIF2 signaling” pathway (Fig. 3): the RNA helicase EIF4A1 and translation facilitator EIF4G3. Depletion of EIF4A1 and EIF4G3 provided an almost complete protection against both CBZ/TNF- and DCF/TNF-induced apoptosis (Fig. 6 F and Supporting Data S11 B). All functionally relevant ER stress-translation initiation components that we tested were validated by single siRNAs (Supporting Data S5).

Together these data support a role for the ER stress/UPR pathway and translational control in the regulation of the observed cytotoxicity (Fig. 6 G).

EIF4A1 controls CHOP expression and thereby apoptosis onset

Finally we investigated the mechanism of the PERK-mediated cytoprotection. PERK-

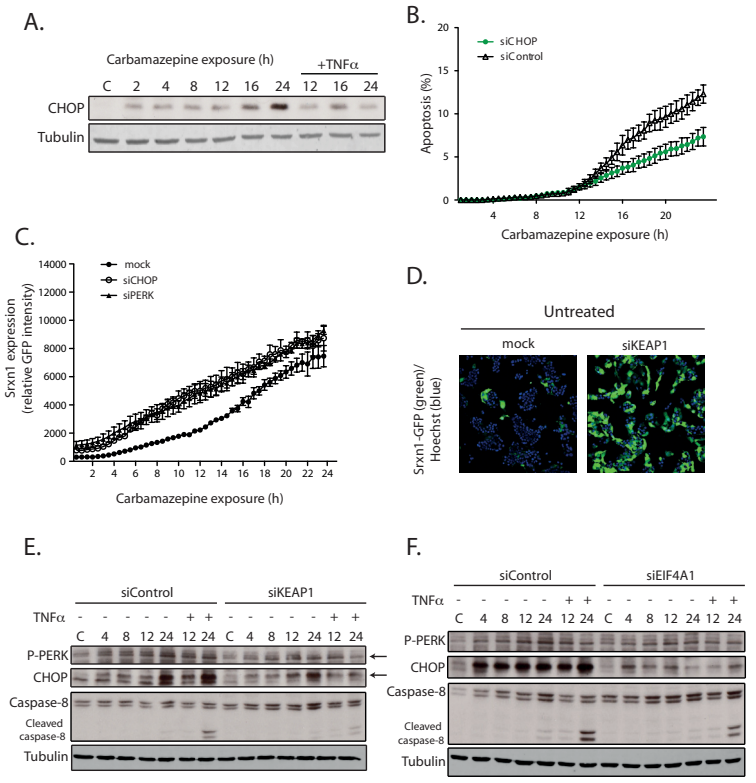

Figure 7. *CHOP-expression and apoptosis is dependent on EIF4A1.* (A) CHOP protein levels were followed in time by western blotting after CBZ (500 μM) exposure +/- addition of TNFα (10 ng/mL) after 8 hours. "C", control exposed to vehicle for 12 hours. (B) The effect of CHOP siRNA mediated knockdown on CBZ/TNFα-induced apoptosis was investigated using AnxV-labelling and automated microscopy. (C) The effect of PERK and CHOP siRNA mediated knockdown on Srxn1-GFP induction after CBZ exposure was investigated using automated confocal microscopy. GFP intensities were normalized to the area occupied by nuclei as determined by Hoechst33342 staining. (D) Shown are representative images of GFP intensity (green) after KEAP1 knockdown in Srxn1-GFP expressing HepG2 cells 72 hours after transfection under non-exposed conditions. Nuclei are labelled with Hoechst33342 (blue) (E and F) ER-stress activation, as measured by protein expression of phosphorylated PERK and CHOP using western blot, was investigated after KEAP1 (E) and EIF4A1 (F) knockdown and a time series of CBZ (500 μM) exposure +/- TNFα (10 ng/mL) addition. Cleavage of caspase-8 is shown for assessment of extrinsic apoptosis induction. Tubulin serves as loading control. "C", control exposed to vehicle for 12 hours. The data are presented as means of three independent experiments +/- SEM or representative for three independent experiments when applicable.

mediated ATF4 activation leads to expression of the pro-apoptotic transcription factor CHOP (15). In line with this, both CBZ and DCF induced the expression of CHOP in parallel to the activation of PERK (compare Fig. 6 C and 7 A and Supporting Data S10). Importantly, knockdown of CHOP strongly protected against both CBZ/TNFα and DCF/TNFα apoptosis (Fig. 7 B and Supplemental Data S11).

Since ER stress can activate the Nrf2 pathway (27) we wanted to determine the link between ER stress and oxidative stress. While PERK and CHOP knockdown protected against cell death (Fig. 6 E and 7 B), neither PERK nor CHOP knockdown inhibited the expression of the Nrf2 target gene Srxn1 (Fig. 7 C). Vice versa, knockdown of Keap1, causing stabilization of Nrf2 (Supporting Data S6 B), in association with strong

Srxn1 expression (Fig. 7 D) and cytoprotection against CBZ/TNFα and DCF/TNFα (Fig. 5 E and 7 E), did not block the activation of PERK and the expression of CHOP (Fig. 7 E).

Given the critical role of the RNA helicase EIF4A1 in the onset of apoptosis, we wondered whether the cytoprotection mediated by EIF4A1 knockdown was directly linked to the control of CHOP expression. Interestingly, EIF4A1 knockdown blocked CHOP protein expression after CBZ treatment, thereby also inhibiting activation of caspase-8 (Fig. 7 F), indicating a central role for the translational machinery in the ER stress signaling-mediated induction of CBZ/TNFα and DCF/TNFα synergy towards death receptor-mediated apoptosis.

DISCUSSION

Here we studied in detail the underlying molecular mechanisms of the synergistic apoptotic response between hepatotoxic drugs and the pro-inflammatory cytokine TNFα using transcriptomics and siRNA-mediated knockdown approaches. Using gene expression analysis of HepG2 cells exposed to different hepatotoxic drugs we identified endoplasmic reticulum stress/EIF2 signaling, Nrf2-related oxidative stress and death receptor signaling as critically activated toxicity pathways. Further functional analysis of the role of critical determinants of these pathways using siRNA approaches support a model in which drug-induced PERK/CHOP-mediated ER-stress and oxidative stress sensitizes hepatocytes to TNFα-induced pro-apoptotic signaling resulting in caspase-8 and subsequent mitochondria-dependent apoptosis (Fig. 8).

Our current data support a general role for a death receptor-mediated apoptosis pathway that act together with Bid and Bim triggered mitochondrial-mediated apoptosome activation in the CBZ and DCF mediated synergy with TNFα to induce apoptosis. At the gene expression level the death receptor signaling/apoptosis pathway was significantly regulated in DCF and CBZ treated cells, but not in cells treated with the non-toxic MTX. This included induction of caspase-8, Bim and APAF1 expression, all of which are critical in the onset of apoptosis (Fig. 4).

The hepatotoxicant/TNFα synergy is for a major part dependent on the pro-oxidant properties of both CBZ and DCF. Indeed, our gene expression profiling showed strong upregulation of Nrf2 target genes by both DCF and CBZ, which correlated with strong Nrf2-dependent induction of Srxn1. A role for DCF and/or CBZ induced oxidative stress induction is supported by gene expression data from mouse liver hepatocytes (Supplemental Data S2), and in vivo DCF treated rat liver (28) and DCF treated mouse liver (29). Importantly, both the anti-oxidant DPPD as well as knockdown of the endogenous Nrf2-inhibitor Keap1 led to protection against DCF/TNFα and CBZ/TNFα-induced apoptosis. In addition, hepatocyte cell death induced by DCF and CBZ alone are oxidative stress dependent (30,31). In our hands, the CBZ- and DCF-mediated oxidative stress was largely controlled by the glutathione peroxidase and reductase system, since knockdown of glutathione reductase (GSR) and glutathione peroxidase (GPX4) strongly enhanced the synergy-based cell killing.

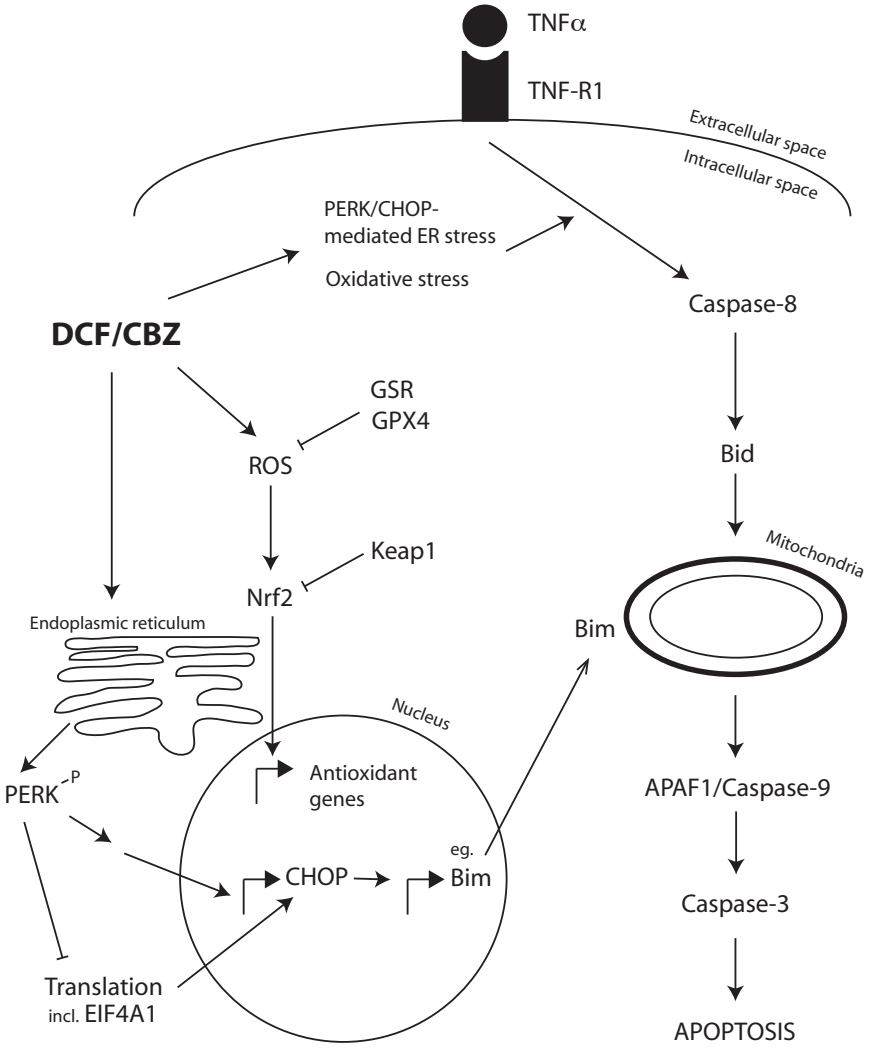

Figure 8. *Working model for drug/TNFα-induced apoptosis.* Reactive metabolites formed by diclofenac (DCF) and carbamazepine (CBZ) metabolism induce both oxidative and endoplasmic reticulum (ER) stress. The ER stress induced is solely dependent on the PERK-pathway, which results in the transcription of CHOP that in turn transcribes for example pro-apoptotic BIM. In the absence of translation less CHOP protein is expressed. Both PERK/CHOP-mediated ER stress and oxidative stress enhances the apoptotic effect of TNFα addition, an event dependent on a caspase-8 initiated Bid/Bim/APAF1/caspase-9/caspase-3 pathway.

Our data indicate that ER stress signaling through the PERK/CHOP pathway is a critical determinant for the hepatotoxicant/TNFα synergy response towards hepatocyte apoptosis. Endoplasmic reticulum (ER) stress and the UPR have been implicated in several different liver diseases including DILI (32). Here we present a more selective activation of the PERK-arm of the ER stress/UPR following DCF and CBZ exposure (Fig. 6), which was directly related to expression of CHOP (Fig. 7), a downstream target of ATF4. In contrast, we did not observe enhanced BiP (HSPA5) expression, despite the

fact that prior UPR-mediated upregulation of BiP protected against cell death. Given the critical role of CHOP in the onset of apoptosis, we propose that CHOP is a critical player in liver toxicity including sensitization for death receptor-mediated apoptosis. Upregulation of CHOP may lead to apoptosis via upregulation of pro-apoptotic Bcl-2 family members, including Bim (33). In our system Bim (BCL2L11) was up-regulated after DCF and CBZ exposure and siRNA mediated knockdown of this gene led to rescue of CBZ/TNFα and DCF/TNFα-induced cytotoxicity, thus supporting a link between ER stress-mediated CHOP induction followed by Bim expression and mitochondrial-mediated apoptosis induction.

The reduction of apoptosis after CBZ/TNFα and DCF/TNFα exposure by the use of siRNA mediated knockdown of translation initiation factors EIF4A1 and EIF4G3 and the use of an inhibitor of eIF2α dephosphorylation, salubrinal, highlight the need for translation in the hepatotoxicant-induced stress response. EIF4A1 and EIF4G3 together with cap-binding protein EIF4E are part of the EIF4F complex that unwinds secondary structures of the 5' untranslated region (UTR) of mRNA to allow ribosomal binding, scanning and thereby translation. The 5' UTR of mRNA can be more or less structured, determining its translation efficiency (34). EIF4A and EIF4G have been implicated with cap-independent translation (34). Interestingly, the translation of several anti- and pro-apoptotic genes such as XIAP, and APAF1 can occur via cap-independent mechanisms (35,36). Since depletion of EIF4A1 reduced the expression of pro-apoptotic CHOP (Fig. 7C), CHOP protein expression could be regulated by EIF4A1 cap-independent translation. While our results emphasize a role of translational control in xenobiotic toxicity, more research is required in this area.

In summary, we show that DCF and CBZ, drugs linked to idiosyncratic DILI with activation of the inflammatory system, sensitize HepG2 cells to TNFα-induced apoptosis in our in vitro system. We propose a mechanism where CBZ and DCF by inducing oxidative and PERK/CHOP-dependent ER stress, enhance the activation of the apoptotic signaling downstream of the TNF receptor, involving caspase-8, Bid, Bim and APAF1, possibly via translationally regulated induction of pro-apoptotic proteins (Fig. 8). This work sheds new light on the mechanism behind the - so far – unpredictable nature of idiosyncratic DILI. Possibly genetic polymorphisms in functionally critical determinants of the cytotoxic response are candidate susceptibility genes that predispose for idiosyncratic DILI.

ACKNOWLEDGEMENTS

We thank Harry Vrieling for kindly offering the Srxn1-GFP BAC-construct.

REFERENCES

1. Lee WM. Etiologies of acute liver failure. Semin Liver Dis 2008;28:142–152.
2. Fredriksson L, Herpers B, Benedetti G, Matadin Q, Puigvert JC, de Bont H, et al. Diclofenac inhibits tumor necrosis factor-α-induced nuclear factor-κB activation causing synergistic hepatocyte apoptosis. Hepatology 2011;53:2027–2041.
3. Roth RA, Ganey PE. Animal models of idiosyncratic drug-induced liver injury--current status. Crit Rev Toxicol 2011;41:723–739.
4. Shaw PJ, Hopfensperger MJ, Ganey PE, Roth RA. Lipopolysaccharide and trovafloxacin coexposure in mice causes idiosyncrasy-like liver injury dependent on tumor necrosis factor-alpha. Toxicol Sci 2007;100:259–266.
5. Barton CC, Barton EX, Ganey PE, Kunkel SL, Roth RA. Bacterial lipopolysaccharide enhances aflatoxin B1 hepatotoxicity in rats by a mechanism that depends on tumor necrosis factor alpha. Hepatology 2001;33:66–73.
6. Lu J, Jones AD, Harkema JR, Roth RA, Ganey PE. Amiodarone exposure during modest inflammation induces idiosyncrasy-like liver injury in rats: role of tumor necrosis factor-alpha. Toxicol Sci 2012;125:126–133.
7. Roberts RA, Ganey PE, Ju C, Kamendulis LM, Rusyn I, Klaunig JE. Role of the Kupffer cell in mediating hepatic toxicity and carcinogenesis. Toxicol Sci 2007;96:2–15.
8. Jaiswal AK. Nrf2 signaling in coordinated activation of antioxidant gene expression. Free Radic Biol Med 2004;36:1199–1207.
9. Kobayashi A, Kang M-I, Okawa H, Ohtsuji M, Zenke Y, Chiba T, et al. Oxidative stress sensor Keap1 functions as an adaptor for Cul3-based E3 ligase to regulate proteasomal degradation of Nrf2. Mol Cell Biol 2004;24:7130–7139.
10. Copple IM, Goldring CE, Kitteringham NR, Park BK. The Nrf2-Keap1 defence pathway: role in protection against drug-induced toxicity. Toxicology 2008;246:24–33.
11. Copple IM, Goldring CE, Jenkins RE, Chia AJL, Randle LE, Hayes JD, et al. The hepatotoxic metabolite of acetaminophen directly activates the Keap1-Nrf2 cell defense system. Hepatology 2008;48:1292–1301.
12. Okawa H, Motohashi H, Kobayashi A, Aburatani H, Kensler TW, Yamamoto M. Hepatocyte-specific deletion of the keap1 gene activates Nrf2 and confers potent resistance against acute drug toxicity. Biochem Biophys Res Commun 2006;339:79–88.
13. Hetz C. The unfolded protein response: controlling cell fate decisions under ER stress and beyond. Nat Rev Mol Cell Biol 2012;13:89–102.
14. Woehlbier U, Hetz C. Modulating stress responses by the UPRosome: a matter of life and death. Trends Biochem Sci 2011;36:329–337.
15. Harding HP, Novoa I, Zhang Y, Zeng H, Wek R, Schapira M, et al. Regulated translation initiation controls stress-induced gene expression in mammalian cells. Mol Cell 2000;6:1099–1108.
16. Puigvert JC, de Bont H, van de Water B, Danen EHJ. High-throughput live cell imaging of apoptosis. Curr Protoc Cell Biol 2010;Chapter 18:Unit 18.10.1–13.
17. Benjamini Y, Hochberg Y. Controlling the false discovery rate: a practical and powerful approach to multiple testing. J Royal Statist Soc, B 1995;57:289–300.
18. Saeed A, Sharov V, White J, Li J, Liang W, Bhagabati N, et al. TM4: a Free, Open-Source System for Microarray Data Management and Analysis. Biotechniques 2003;34:374–378.
19. Poser I, Sarov M, Hutchins JRA, Hériché J-K, Toyoda Y, Pozniakovsky A, et al. BAC TransgeneOmics: a high-throughput method for exploration of protein function in mammals. Nat Methods 2008;5:409–415.
20. Hendriks G, Atallah M, Morolli B, Calléja F, Ras-Verloop N, Huijskens I, et al. The ToxTracker assay: novel GFP reporter systems that provide mechanistic insight into the genotoxic properties of chemicals. Toxicological Sciences 2012;125:285–298.
21. Soriano FX, Baxter P, Murray LM, Sporn MB, Gillingwater TH, Hardingham GE. Transcriptional regulation of the AP-1 and Nrf2 target gene sulfiredoxin. Mol Cells 2009;27:279–282.
22. Soriano FX, Léveillé F, Papadia S, Higgins LG, Varley J, Baxter P, et al. Induction of sulfiredoxin expression and reduction of peroxiredoxin hyperoxidation by the neuroprotective Nrf2 activator 3H-1,2-dithiole-3-thione. J Neurochem 2008;107:533–543.
23. Oyake T, Itoh K, Motohashi H, Hayashi N, Hoshino H, Nishizawa M, et al. Bach proteins belong to a novel family of BTB-basic leucine zipper transcription factors that interact with MafK and regulate transcription through the NF-E2 site. Mol Cell Biol 1996;16:6083–6095.
24. Dhakshinamoorthy S, Jain AK, Bloom DA, Jaiswal AK. Bach1 competes with Nrf2 leading to negative regulation of the antioxidant response element (ARE)-mediated NAD(P)H:quinone oxidoreductase 1 gene expression and induction in response to antioxidants. J Biol Chem 2005;280:16891–16900.
25. Boyce M, Bryant KF, Jousse C, Long K, Harding HP, Scheuner D, et al. A selective inhibitor of eIF2alpha

dephosphorylation protects cells from ER stress. Science 2005;307:935–939.
26. van De Water B, Wang Y, Asmellash S, Liu H, Zhan Y, Miller E, et al. Distinct endoplasmic reticulum signaling pathways regulate apoptotic and necrotic cell death following iodoacetamide treatment. Chem Res Toxicol 1999;12:943–951.
27. Cullinan SB, Diehl JA. Coordination of ER and oxidative stress signaling: the PERK/Nrf2 signaling pathway. Int J Biochem Cell Biol 2006;38:317–332.
28. Deng X, Liguori MJ, Sparkenbaugh EM, Waring JF, Blomme EAG, Ganey PE, et al. Gene expression profiles in livers from diclofenac-treated rats reveal intestinal bacteria-dependent and -independent pathways associated with liver injury. J Pharmacol Exp Ther 2008;327:634–644.
29. Cantoni L, Valaperta R, Ponsoda X, Castell JV, Barelli D, Rizzardini M, et al. Induction of hepatic heme oxygenase-1 by diclofenac in rodents: role of oxidative stress and cytochrome P-450 activity. J Hepatol 2003;38:776–783.
30. Gómez-Lechón MJ, Ponsoda X, O'Connor E, Donato T, Castell JV, Jover R. Diclofenac induces apoptosis in hepatocytes by alteration of mitochondrial function and generation of ROS. Biochem Pharmacol 2003;66:2155–2167.
31. Santos NAG, Medina WSG, Martins NM, Rodrigues MAC, Curti C, Santos AC. Involvement of oxidative stress in the hepatotoxicity induced by aromatic antiepileptic drugs. Toxicol in Vitro 2008;22:1820–1824.
32. Dara L, Ji C, Kaplowitz N. The contribution of endoplasmic reticulum stress to liver diseases. Hepatology 2011;53:1752–1763.
33. Puthalakath H, O'Reilly LA, Gunn P, Lee L, Kelly PN, Huntington ND, et al. ER stress triggers apoptosis by activating BH3-only protein Bim. Cell 2007;129:1337–1349.
34. Jackson RJ, Hellen CUT, Pestova TV. The mechanism of eukaryotic translation initiation and principles of its regulation. Nat Rev Mol Cell Biol 2010;11:113–127.
35. Holcik M, Lefebvre C, Yeh C, Chow T, Korneluk RG. A new internal-ribosome-entry-site motif potentiates XIAP-mediated cytoprotection. Nat Cell Biol 1999;1:190–192.
36. Coldwell MJ, Mitchell SA, Stoneley M, MacFarlane M, Willis AE. Initiation of Apaf-1 translation by internal ribosome entry. Oncogene 2000;19:899–905.

SUPPORTING MATERIALS AND METHODS

Isolation and culture of primary mouse hepatocytes

Primary mouse hepatocytes were isolated from 8-10 weeks old male C57BL/6 mice by a modified two-step collagenase perfusion technique (collagenase type IV, Sigma-Aldrich, Zwijndrecht, The Netherlands), as described previously (1). In short, hepatocytes suspensions with at least 80 % viability were seeded onto plates coated with collagen gel and after attachment overlayed with a second layer of collagen gel, to form a sandwich configuration. Cells were kept in serum-free medium and the culture medium was changed daily until exposures were performed.

Gene expression profiling

Forty-six hours after isolation, hepatocytes were exposed to either 300 μM DCF or the solvent DMSO. After 24 hours of exposure, cells were collected in 1 ml RNAprotect (QIAgen, Venlo, The Netherlands) and stored at -80˚C for RNA isolation. RNA was extracted using QIAzol and purified using the miRNeasy mini kit and the QIAcube (Qiagen), according to the manufacturer's protocol. For both the DCF and vehicle-control groups, four biological replicates were used. RNA concentrations were measured using the NanoDrop ND-1000 Spectrophotometer (Nanodrop Technologies, Wilmington, DE, USA) and RNA quality was assessed with the Agilent 2100 Bioanalyzer (Agilent Technologies, Amstelveen, The Netherlands). Labeled RNA was prepared using the Affymetrix gene chip 3'IVT express kit and hybridized to the Affymetrix Mouse Genome 430 2.0 GeneChip arrays, according to the manufacturer's instructions. After hybridization the array chips were washed and stained with a Genechip Fluidics Station 450 and scanned using the Affymetrix gene chip scanner 3000.

Data analysis

Affymetrix CEL files were each checked on quality, including RNA degradation control, correlation and clustering. All quality checks were within acceptable limits, according to Affymetrix standards. After quality control the files were normalized with the Multichip Average (RMA) procedure (2), using the custom chip description files (CDFs) as previously described (3). For detecting significantly regulated genes, the microarray analysis of variance (MAANOVA) package in R was used (R version 2.9.2, www.r-project.org). For the analyses on significantly regulated genes per compound between treated and control samples, an F1-test was used. Gene-specific P-values were corrected with a Benjamini- Hochberg false discovery rate (FDR) with a cut-off at 0.1 (Benjamini and Hochberg, 1995).

SUPPORTING REFERENCES

1. Van Kesteren PC, Zwart PE, Pennings JL, Gottschalk WH, Kleinjans JC, et al. Deregulation of cancer-related pathways in primary hepatocytes derived from DNA repair-deficient Xpa-/-p53+/- mice upon exposure to benzo[a]pyrene. Toxicol Sci 2011:123:123-132.
2. Irizarry RA, Hobbs B, Collin F, Beazer-Barclay YD, Antonellis KJ, et al. Exploration, normalization, and summaries of high density oligonucleotide array probe level data. Biostatistics 2003:4:249-264.
3. De Leeuw WC, Rauwerda H, Jonker MJ, Breit TM. Salvaging Affymetrix probes after probe-level re-annotation. BMC Reserch Notes 2008:1:66.
4. Benjamini, Y. and Hochberg, Y. Controlling the false discovery rate: a practical and powerful approach to multiple testing. Journal of the Royal Statistical Society, Series B (Methodological). 1995;57:289–300.

Supporting Data S1. *Genes representing significantly regulated canonical signaling pathways.* The genes representing the significantly regulated canonical signaling pathways after 8 hours of diclofenac (DCF) and/or carbamazepine (CBZ) exposure as determined using the Ingenuity Pathway Analysis (IPA®) software (Fig. 3A) are presented. Up-regulated genes after CBZ and/or DCF treatment are marked in red and down-regulated genes in green. In the case of two-colored gene names, the left part represents DCF and the right CBZ.

IPA Canonical Pathways	Involved genes in DCF and CBZ at 8h
EIF2 signaling	AKT1; AKT2; EIF1; EIF5; EIF1AX; EIF2A; EIF2AK1; EIF2AK3; EIF2AK4; EIF2B1; EIF2C2; EIF2C3; EIF2C4; EIF2S1; EIF2S2; EIF3A; EIF3B; EIF3C; EIF4A1; EIF4A2; EIF4G1; EIF4G3; GSK3B; HRAS; INSR; KRAS; MRAS; NRAS; PDPK1; PIK3C2A; PIK3CA; PIK3CD; PIK3R1; PIK3R2; PIK3R3; PPP1CB; PPP1R15A; RRAS2; SOS1; SOS2
NRF2-mediated Oxidative Stress Response	ABCC4; ACTA1; AKT1; ATF4; BACH1; CBR1; CUL3; DNAJA1; DNAJA2; DNAJA3; DNAJB1; DNAJB4; DNAJB6; DNAJB9; DNAJB14; DNAJC5; DNAJC6; DNAJC7; DNAJC8; DNAJC9; DNAJC10; DNAJC11; DNAJC15; DNAJC18; DNAJC21; EIF2AK3; FOS; GCLC; GCLM; GPX2; GSK3B; GSTO2; GSTT1; HERPUD1; HRAS; JUN; JUNB; JUND; KRAS; MAFF; MAFG; MAFK; MAP2K3; MAP2K5; MAP2K6; MAP3K7; MAPK8; MAPK14; MRAS; NFE2L2; NQO1; NRAS; PIK3C2A; PIK3CA; PIK3CD; PIK3R1; PIK3R2; PIK3R3; PRKCA; PRKCI; PRKD3; PTPLAD1; RBX1; RRAS2; SOD2; SQSTM1; TXNRD1; UBE2K; USP14; VCP
Cell Cycle Control of Chromosomal Replication	CDC6; CDC7; CDK2; CDK5; CDK6; CDK7; CDT1; MCM3; MCM4; MCM5; MCM6; MCM7; ORC1; ORC6; RPA1; RPA2
Role of BRCA1 in DNA Damage Respnse	BARD1; BRIP1; CHEK1; E2F1; E2F2; E2F5; FANCB; FANCC; FANCF; FANCG; FANCL; FANCM; GADD45A; MSH2; MSH6; POU2F1; RAD50; RAD51; RBL1; RFC2; RFC3; RFC4; RFC5; RPA1; SLC19A1; STAT1; TP53
14-3-3-mediated Signaling	AKT1; AKT2; CBL; CDKN1B; FOS; FOXO1; GSK3B; HRAS; JUN; KRAS; MAPK8; MRAS; NRAS; PDCD6IP; PIK3C2A; PIK3CA; PIK3CD; PIK3R1; PIK3R2; PIK3R3; PLCD1; PLCG1; PRKCA; PRKCI; PRKD3; RPS6KA1; RRAS2; SRC; TNFRSF1A; TSC1; TUBA1A; TUBA1B; TUBA1C; TUBA3C; TUBA4A; TUBB; TUBB1; TUBB3; TUBB6; TUBB2A; TUBB2C; TUBG1; YAP1; YWHAB; YWHAQ
HMGB1 Signaling	AKT1; AKT2; FNBP1; FOS; HAT1; HMGB1; HRAS; ICAM1; IFNGR2; IL8; IL1R1; JUN; KRAS; MAP2K3; MAP2K5; MAP2K6; MAPK8; MAPK13; MAPK14; MRAS; MYST4; NRAS; PIK3C2A; PIK3CA; PIK3CD; PIK3R1; PIK3R2; PIK3R3; PLAT; RBBP7; RELA; RHOB; RHOQ; RHOT2; RHOU; RRAS2; SERPINE1; SP1; TNFRSF1A
Pyrimidine Metabolism	CMPK2; CTPS; CTPS2; DCTPP1; DPYSL2; DTYMK; DUT; ENPP1; ENTPD4; ENTPD5; ENTPD7; NME3; POLA1; POLA2; POLD1; POLD3; POLE; POLE2; POLE3; POLE4; POLG; POLH; POLK; POLQ; POLR1B; POLR1D; POLR1E; POLR2A; POLR2E; POLR2F; POLR2H; POLR2L; POLR3A; POLR3D; POLR3H; POLR3K; REV3L; RFC5; RRM1; RRM2; RRM2B; TK1; TK2; TXNRD1; TYMS; UCK1; UCK2; UNG; UPP1
Apoptosis Signaling	ACIN1; AIFM1; APAF1; BCL2L1; BCL2L11; BID; CAPN10; CASP2; CASP6; CASP8; CASP10; CYCS; DFFA; ENDOG; FAS; HRAS; HTRA2; IKBKG; KRAS; LMNA; MAP4K4; MAPK8; MCL1; MRAS; NRAS; PARP1; PLCG1; PRKCA; RELA; ROCK1; RPS6KA1; RRAS2; TNFRSF1A; TP53; XIAP
FLT3 Signaling in Hematopoietic Progenitor Cells	AKT1; AKT2; ATF2; ATF4; CBL; CREB3L4; EIF4EBP1; GAB2; HRAS; KRAS; MAPK13; MAPK14; MRAS; NRAS; PDPK1; PIK3C2A; PIK3CA; PIK3CD; PIK3R1; PIK3R2; PIK3R3; RPS6KA1; RPS6KA5; RRAS2; SOS1; SOS2; STAT1; STAT3; STAT6; STAT5B
IGF-1 Signaling	AKT1; AKT2; CSNK2A1; CSNK2A2; CYR61; FOS; FOXO1; FOXO3; GRB10; HRAS; IGF1R; IGFBP1; IGFBP3; IRS1; JUN; KRAS; MAPK8; MRAS; NEDD4; NRAS; PDPK1; PIK3C2A; PIK3CA; PIK3CD; PIK3R1; PIK3R2; PIK3R3; PRKACB; PRKCI; PTK2; RASA1; RRAS2; SOCS6; SOCS7; SOS1; SOS2; SRF; STAT3; YWHAB; YWHAQ
Neurotrophin/TRK Signaling	AKT1; ATF2; ATF4; CREB3L4; FOS; FRS2; GAB1; HRAS; JUN; KRAS; MAP2K3; MAP2K5; MAP2K6; MAPK8; MRAS; NRAS; PDPK1; PIK3C2A; PIK3CA; PIK3CD; PIK3R1; PIK3R2; PIK3R3; PLCG1; RPS6KA1; RRAS2; SOS1; SOS2
Germ-Cell-Sertoli Cell Junction Signaling	ACTA1; AGGF1; AKT1; CDH1; CTNNB1; EPN2; EPN3; FER; FNBP1; HRAS; ITGA2; ITGB1; KRAS; MAP2K3; MAP2K6; MAP3K7; MAP3K11; MAPK8; MAPK14; MRAS; NRAS; PAK2; PDPK1; PIK3C2A; PIK3CA; PIK3CD; PIK3R1; PIK3R2; PIK3R3; PTK2; RAB8B; RHOB; RHOQ; RHOT2; RHOU; RRAS2; SORBS1; SRC; TJP1; TNFRSF1A; TUBA1A; TUBA1B; TUBA1C; TUBA3C; TUBA4A; TUBB; TUBB1; TUBB3; TUBB6; TUBB2A; TUBB2C; TUBG1
Erythropietin Signaling	AKT1; AKT2; CBL; EPO; FOS; HRAS; JUN; KRAS; MRAS; NRAS; PDPK1; PIK3C2A; PIK3CA; PIK3CD; PIK3R1; PIK3R2; PIK3R3; PLCG1; PRKCA; PRKCI; PRKD3; RELA; RRAS2; SOS1; SOS2; SRC; STAT5B
FAK Signaling	ACTA1; AKT1; AKT2; ARHGAP26; ARHGEF7; ASAP1; CAPN10; GIT2; HRAS; ITGA2; ITGB1; KRAS; MRAS; NRAS; PAK2; PDPK1; PIK3C2A; PIK3CA; PIK3CD; PIK3R1; PIK3R2; PIK3R3; PLCG1; PTEN; PTK2; RRAS2; SOS1; SOS2; SRC; VCL
PTEN Signaling	AKT1; AKT2; BCL2L1; BCL2L11; CBL; CDKN1B; CSNK2A1; CSNK2A2; DDR1; FGFR1; FOXO1; FOXO3; GSK3B; HRAS; IGF1R; IKBKG; INSR; ITGA2; ITGB1; KRAS; MAGI1; MRAS; NRAS; PDPK1; PIK3CA; PIK3CD; PIK3R1; PIK3R2; PIK3R3; PTEN; PTK2; RELA; RRAS2; SOS1; SOS2
Factors Promoting Cardiogenesis in Vertebrates	ACVR1; ACVR1B; ACVR2B; ATF2; BMP4; CCNE1; CCNE2; CDC6; CDK2; CTNNB1; DKK1; FZD3; FZD4; FZD5; FZD6; FZD7; GATA4; GSK3B; HNF1A; LRP6; MAP3K7; MAPK14; PRKCA; PRKCI; PRKD3; SMAD1; SMAD2; SMAD4; SMAD9; TCF3; TCF7L2
"Glycin, Serine and Threonine Metabolism"	ALAS2; CBS; CHDH; CHKA; CHKB; CTH; DBT; ELOVL2; GARS; GLDC; GLYCTK; GOT1; MAOA; MAOB; PLCD1; PLCG1; PSAT1; PSPH; SARDH; SARS; SHMT1; SHMT2; SMOX; SRR
Death Receptor Signaling	APAF1; BID; CASP2; CASP6; CASP8; CASP10; CFLAR; CYCS; FAS; HSPB1; HTRA2; IKBKG; MAP4K4; MAPK8; RELA; TANK; TNFRSF21; TNFRSF10B; TNFRSF1A; TNFSF10; XIAP
ERK/MAPK Signaling	ARAF; ATF2; ATF4; BRAF; CREB3L4; DUSP1; EIF4EBP1; ELF2; ELF3; FOS; H3F3A/H3F3B; HRAS; HSPB1; ITGA2; ITGB1; KRAS; MKNK2; MRAS; MYC; NRAS; PAK2; PIK3C2A; PIK3CA; PIK3CD; PIK3R1; PIK3R2; PIK3R3; PLA2G12A; PLA2G12B; PLCG1; PPARG; PPP1CB; PPP1R7; PPP1R14B; PPP2R1B; PPP2R2A; PPP2R2C; PPP2R5A; PPP2R5C; PRKACB; PRKCA; PRKCI; PTK2; RPS6KA1; RPS6KA5; RRAS2; SOS1; SOS2; SRC; SRF; STAT1; STAT3; VRK2; YWHAB; YWHAQ
Ovarian Cancer Signaling	AKT1; AKT2; BRAF; CTNNB1; E2F1; FZD3; FZD4; FZD5; FZD6; FZD7; GSK3B; HNF1A; HRAS; KRAS; MRAS; MSH2; MSH6; NRAS; PA2G4; PGF; PIK3C2A; PIK3CA; PIK3CD; PIK3R1; PIK3R2; PIK3R3; PMS2; PRKACB; PTEN; RAD51; RB1; RRAS2; SIN3A; SRC; SUV39H1; TCF3; TCF7L2; TFDP1; TP53; VEGFA
FcγRIIβ Signaling in B Lymphocytes	AKT1; HRAS; KRAS; MAPK8; MRAS; NRAS; PDPK1; PIK3C2A; PIK3CA; PIK3CD; PIK3R1; PIK3R2; PIK3R3; RRAS2; SOS1
Estrogen Receptor Signaling	CCNH; CDK7; CTBP2; DDX5; GTF2H3; GTF2H4; GTF2H5; GTF2H2/LOC100510744; H3F3A/H3F3B; HNRNPD; HRAS; IGFBP1; KRAS; MED6; MED10; MED13; MED14; MED17; MED30; MED31; MED13L; MRAS; NCOA3; NR0B2; NR3C1; NRAS; PCK1; POLR2A; POLR2E; POLR2F; POLR2H; POLR2L; PPARGC1A; RRAS2; SOS1; SOS2; SRC; TAF3; TAF15; TAF4B; TAF9B
Endoplasmic Reticulum Stress Pathway	ATF4; ATF6; EIF2AK3; EIF2S1; ERN1; HSPA5; MAPK8; XBP1
Cleavage and Polyadenylation of Pre-mRNA	CPSF6; CSTF2; CSTF3; NUDT21; PABPN1; WDR33
IL-6 Signaling	CEBPB; CSNK2A1; CSNK2A2; FOS; HRAS; HSPB1; IKBKG; IL8; IL1R1; IL1RAP; IL6R; IL6ST; JUN; KRAS; MAP2K3; MAP2K6; MAP3K7; MAP4K4; MAPK8; MAPK13; MAPK14; MRAS; NRAS; RELA; RRAS2; SOS1; SOS2; SRF; STAT3; TNFRSF1A
IL-8 Signaling	AKT1; AKT2; ARAF; BCL2L1; BRAF; CCND3; CDH1; EIF4EBP1; FNBP1; GNA13; GNAS; GNB5; GNB2L1; GNG4; GPLD1; HBEGF; HRAS; ICAM1; IKBKG; IL8; IRAK2; KRAS; MAP4K4; MAPK8; MRAS; NAPEPLD; NRAS; PAK2; PGF; PIK3C2A; PIK3CA; PIK3CD; PIK3R1; PIK3R2; PIK3R3; PLD1; PRKCA; PRKCI; PRKD3; PTK2; RELA; RHOB; RHOQ; RHOT2; RHOU; ROCK1; ROCK2; RRAS2; SRC; VEGFA

Supporting Data S2 (Not shown). *Hierarchical clustering of significantly regulated genes.* The genes listed in Supporting Data S1 were clustered using Pearson correlation and average linkage in the MultiExperiment Viewer software. Expression values, here presented as fold change of control, from all time points, 8 and 14 hours +/- TNFα, and exposure conditions, diclofenac (DCF), carbamazepine (CBZ), ketoconazole (KTZ), nefazodone (NFZ) and methotrexate, (MTX) were used. The clusters identified as interesting (1-3) contained genes up-regulated after 8 hours DCF and CBZ exposure but down- or non-regulated after MTX treatment. The genes that could also be found to represent the interesting IPA®-defined canonical pathways presented in Figure 3 were labeled according to their respective pathways; yellow highlight = EIF2-signaling/Endoplasmic Reticulum Stress Pathway; green highlight = Nrf2-mediated Oxidative Stress Response; blue highlight = Apoptosis Signaling/Death receptor Signaling.

		HepG2, DCF 8h	Primary hepatocytes, mouse C57/BL6, DCF 24h	
Human symbol	Mouse symbol	FC	FDR	FC
SQSTM1	Sqstm1	4.14	0.043	1.27
SRXN1	Srxn1	2.08	0.014	2.27
DDIT3	Ddit3	8.14	0.001	2.54
TNFRSF10B	Tnfrsf10b	2.78	0.005	1.41
ATF4	Atf4	1.7	0.086	1.15
XBP1	Xbp1	1.33	0.007	-1.22
DNAJB6	Dnajb6	1.55	0.064	1.35
ABCC4	Abcc4	1.54	0.014	3.15
DNAJB1	Dnajb1	1.67	0.022	1.22
HSPA5	Hspa5	-1.6	0.001	1.44
ATF6	Atf6	1.42	0.043	1.20
SOD2	Sod2	3.16	0.054	-1.18
EIF4A1	Eif4a1	1.84	0.020	1.14
TRIB3	Trib3	5.6	0.002	2.02
PPP1R15A	Ppp1r15a	2.53	0.004	2.06

Supporting Data S3. *Genes downstream of oxidative and endoplasmic reticulum stress are significantly regulated in primary mouse hepatocytes.* Primary hepatocytes from C57BL/6 mice were treated with 300 M diclofenac for 24 h before mRNA collection and gene expression analysis. The expression of a selected number of genes, also regulated in HepG2 cells after 8 hours of DCF, downstream of Nrf2-dependent oxidative stress signaling and endoplasmic reticulum stress signaling, was determined. Only the genes that were significantly regulated, false discovery rate (FDR) < 0.1, are presented. Genes related to ER/translational stress are highlighted in orange and Nrf2-related genes in green.

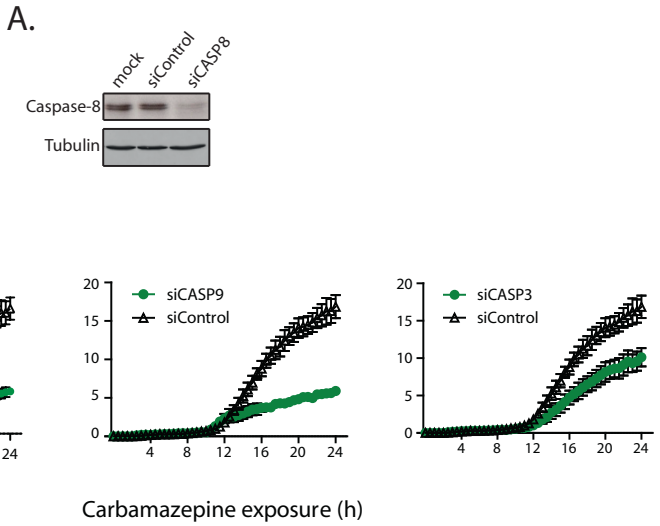

Supporting Data S4. *Knockdown of apoptosis related genes reduce CBZ/TNFα-induced apoptosis.* (A) Knockdown using SMART-pool siRNA targeting caspase-8 was confirmed using western blotting. Tubulin was used as loading control. (B) The apoptosis induced by CBZ/TNFα was followed in time using live cell imaging of apoptosis after SMARTpool siRNA mediated knockdown of Bcl2-family member BID, executioner caspase-3 and initiator caspase-9. TNFα (10 ng/mL) was added after 8 hours of drug exposure. Data presented are means of three independent experiments +/- S.E.M.

	siRNA	CBZ (p-value)	DCF (p-value)	Validation (CBZ)
Gene array	HERPUD1	> 0.05	n.a.	n.a.
	DNAJB1	< 0.001	> 0.05	2/4
	EIF4A2	> 0.05	n.a.	n.a.
	EIF4A1	< 0.001	< 0.001	4/4
	ATF4	> 0.05	n.a.	n.a.
	Bim/BCL2L11	< 0.001	Fredriksson *et al.*	2/4
	FOS	> 0.05	n.a.	n.a.
	JUN	> 0.05	n.a.	n.a.
	MCL1	> 0.05	n.a.	n.a.
	SQSTM1	> 0.05	n.a.	n.a.
	TNFRSF10B	> 0.05	n.a.	n.a.
	XIAP	> 0.05	n.a.	n.a.
	APAF1	< 0.001	Fredriksson *et al.*	3/4
	JUND	< 0.001	< 0.001	3/4
	BACH1	< 0.05	< 0.05	3/4
	KRAS	> 0.05	n.a.	n.a.
	SOD2	> 0.05	n.a.	n.a.
	SOS1	> 0.05	n.a.	n.a.
	CASP10	< 0.001	Fredriksson *et al.*	1/4
	DNAJB6	> 0.05	n.a.	n.a.
	EIF4G3	< 0.001	< 0.01	3/4
	PIK3C2A	> 0.05	n.a.	n.a.
	MRP4/ABCC4	< 0.001	< 0.001	3/4
	GSTO2	< 0.01	< 0.001	2/4
Apoptosis	CASP8	< 0.001	Fredriksson *et al.*	4/4
	CASP3	< 0.001	Fredriksson *et al.*	4/4
	CASP9	< 0.001	Fredriksson *et al.*	2/4
	BID	< 0.001	Fredriksson *et al.*	2/4
ER stress	CHOP/DDIT3	< 0.001	< 0.05	2/4
	PERK/EIF2AK3	< 0.01	< 0.05	4/4
	IRE1α/ERN1	< 0.001	< 0.001	2/4
	ATF6	< 0.001	< 0.001	2/4
Oxidative stress	SOD1	> 0.05	n.a.	n.a.
	GSR	< 0.001	< 0.001	2/4
	GPX4	< 0.001	< 0.001	3/4
	KEAP1	< 0.001	< 0.001	2/4
	NRF2	< 0.001	< 0.001	3/4

Supporting Data S5. *List of siRNAs and their effect on apoptosis following CBZ and DCF exposure.* HepG2 cells were transfected with siRNAs targeting genes up-regulated after 8 hours of CBZ and/or DCF exposure and involved in apoptosis/death receptor signalling (blue highlights), Nrf2-mediated oxidative stress response (green highlights) or ER stress/translation initiation (yellow highlights), and hand-picked from the three respective pathways. 72 hours after transfection the cells were exposed to CBZ (500 µM) with 10 ng/mL TNFα added after 8 hours of drug exposure and the apoptosis was assessed using AnxV-labelling and automated microscopy. The siRNAs that gave a significant difference in apoptosis compared to siControl (using 2-way ANOVA) were also assessed under DCF (500 µM)/TNFα-exposure conditions. The effect of the siRNAs found significant after CBZ exposure was also validated using the 4 single siRNA sequences that consisted the initial SMART-pool. A knockdown effect that could be confirmed with ≥ 2 of the single sequences (AUC = siControl ± 2-3 S.D.) was considered "on target".

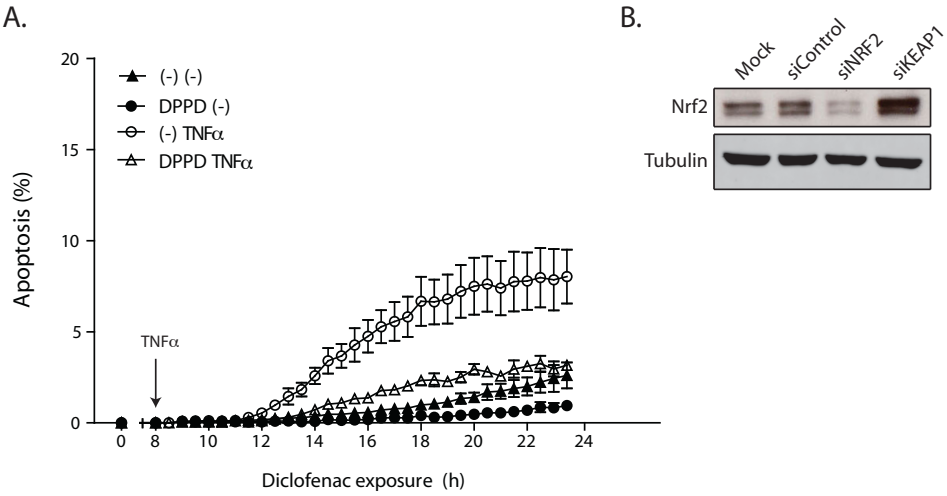

Supporting Data S6. *Modulation of the oxidative stress response.* (A) HepG2 cells were pre-treated with 10 µM N,N'-diphenylbenzene-1,4- diamine (DPPD) before adding 500 µM DCF or vehicle. TNFα (10 ng/mL) was added after 8 hours of drug exposure. The apoptosis induction was followed in time using AnnexinV (AnxV)-Alexa633 and automated microscopy. Data presented are means of three independent experiments +/- S.E.M. (B) Effect of NRF2 and KEAP1 siRNA-mediated knockdown on Nrf2 protein levels was assessed using westernblotting. Tubulin served as loading control.

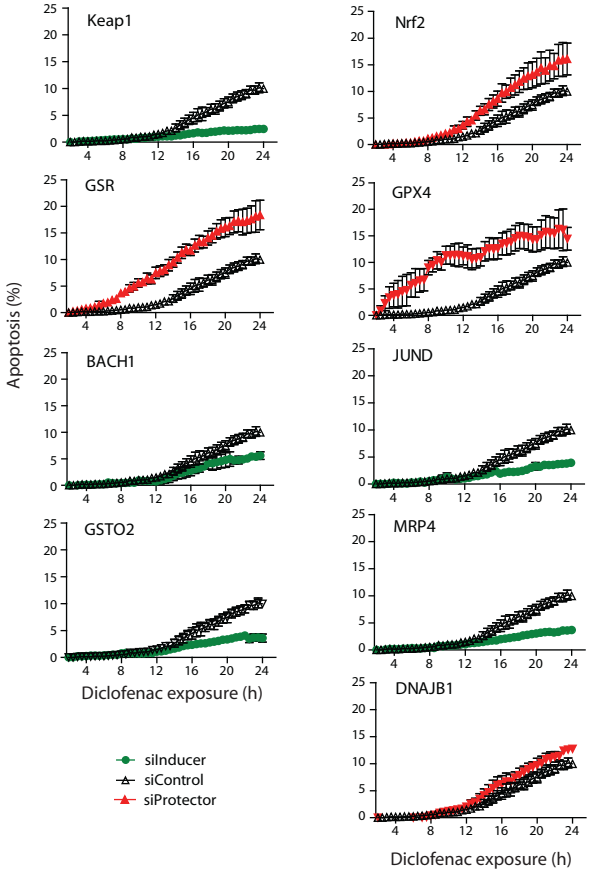

Supporting Data S7. *Knock-down of oxidative stress related genes affects apoptosis induced by DCF/TNFα.* The apoptosis induced by DCF/TNFα was followed in time using live cell imaging of apoptosis after SMARTpool siRNA mediated knockdown of genes involved in oxidative stress and found to give a significant effect on CBZ/TNFα-induced apoptosis. TNFα (10 ng/mL) was added after 8 hours of drug exposure.

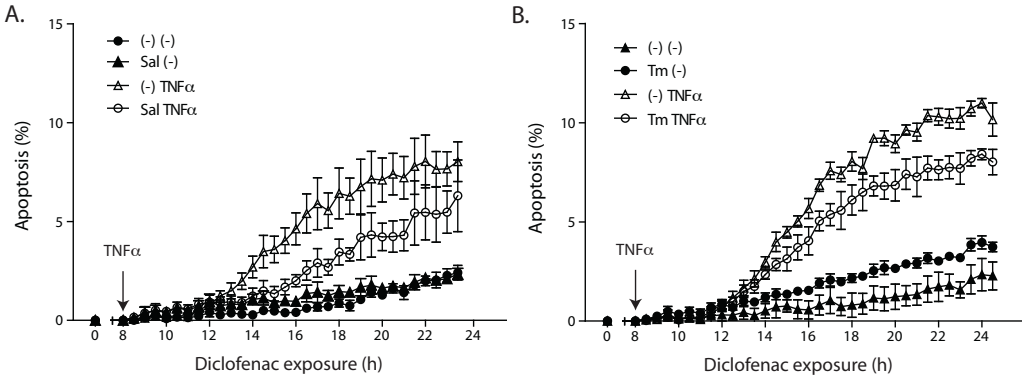

Supporting Data S8. *Inhibition of endoplasmic reticulum stress reduces DCF/TNFα-induced apoptosis.* HepG2 cells were pre-treated with 50 µM Salubrinal (Sal; A) or 5 µg/mL tunicamycin (Tm; B) before replacing the medium with 500 µM DCF. Salubrinal was kept in the medium where indicated. After 8 hours of DCF exposure, TNFα (10 ng/mL) was added. The apoptosis was determined in time using AnnexinV (AnxV)-Alexa633 staining and automated imaging. Data presented are means of three independent experiments +/- S.E.M.

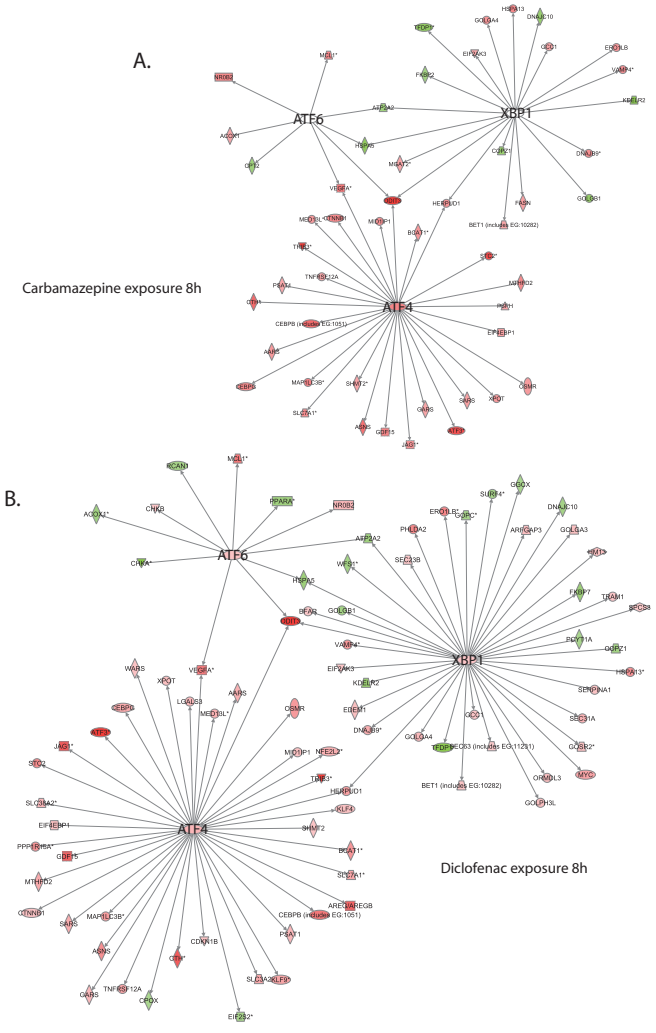

Supporting Data S9. *DCF and CBZ exposure induced mainly ATF4 mediated transcription.* Using the IPA® software the genes up- or down-regulated by the transcription factors downstream of the three distinct unfolded protein response pathways, PERK (ATF4), IRE-1α (XBP1) and ATF6 were determined after 8 hours DCF (A) or CBZ (B) exposure. Red colouring of the shapes indicate up-regulation of the target genes, while green indicated down-regulation. The intensity reflects the fold-change gene expression compared to vehicle-exposed cells.

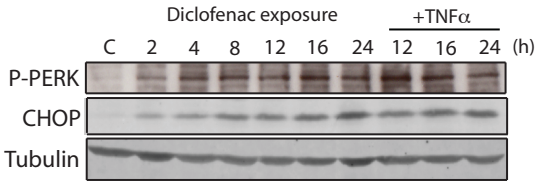

Supporting Data S10. *DCF induces PERK phosphorylation and CHOP expression.* The expression of phosphorylated PERK (P-PERK) and CHOP were followed in time by western blot after DCF+/- TNFα (500 µM/10 ng/mL) exposure.

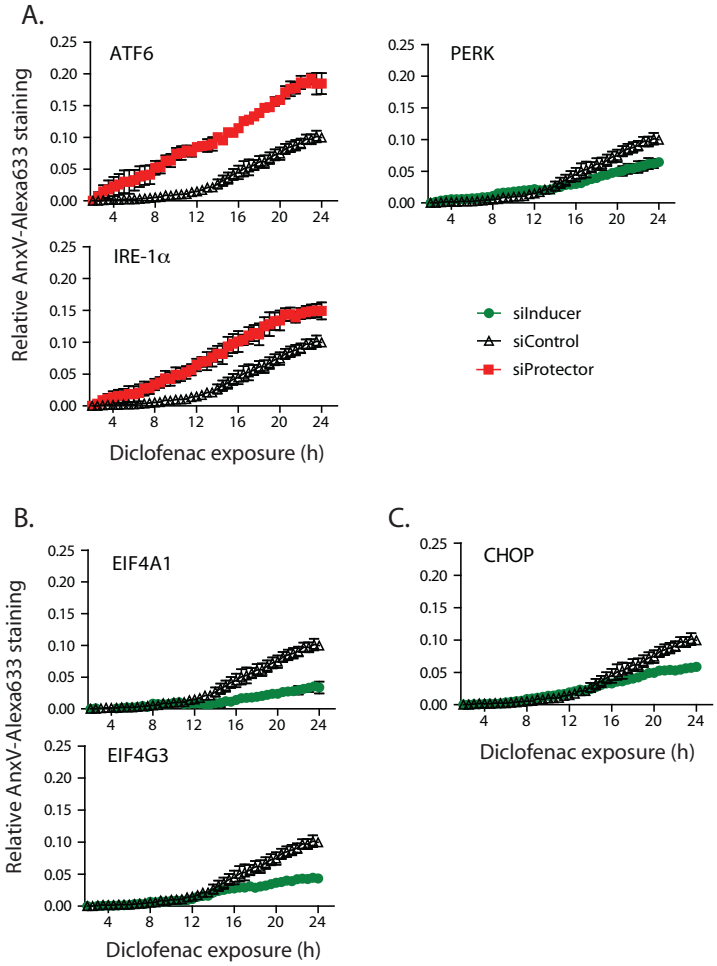

Supporting Data S11. *Knockdown of ER stress related genes affects apoptosis induced by DCF/TNFα.* (A-C) The apoptosis induced by DCF/TNFα was followed in time using live cell imaging of apoptosis after SMARTpool siRNA mediated knockdown of genes involved in ER stress and found to give a significant effect on CBZ/TNFα-induced apoptosis. TNFα (10 ng/mL) was added after 8 hours of drug exposure. Data presented are means of three independent experiments +/- S.E.M.

A live-cell imaging-based NF-κB nuclear translocation RNAi screen identifies novel regulators of TNFα-induced apoptosis through control of the (de)ubiquitinase A20

Lisa Fredriksson*, Bram Herpers*, Giulia Benedetti*, Zi Di, Hans de Bont, John Meerman, Marjo de Graauw and Bob van de Water

Manuscript in preparation

ABSTRACT

Stimulation of cells with the cytokine tumor necrosis factor alpha (TNFα) triggers cytoplasmic-to-nuclear oscillation of the dimeric transcription factor NF-kappaB (NF-κB). In the nucleus, NF-κB stimulates transcription of its own response inhibitors, IkappaBalpha (IκBα) and the (de)ubiquitinase A20. The concerted induction of IκBα and A20 functions to prevent over-activation of the response and the time-dependent inactivation is observed as a dampened NF-κB nuclear oscillation pattern. The number of nuclear oscillations dictates the transcription of downstream pro-inflammatory, anti-oxidant and anti-apoptotic genes. The number of nuclear translocation events is markedly reduced under hepatotoxic drug (diclofenac) exposure conditions in association with enhanced apoptosis. To understand the mechanism of the perturbed oscillatory response, we used a live-cell imaging-based siRNA screen to identify individual kinases, (de)ubiquitinases and sumoylases that control the NF-κB oscillatory response. We applied high content confocal laser scan microscopy in combination with multiparametric image analysis to follow the NF-κB oscillation in ~300 individual cells per condition simultaneously. Out of the ~1500 genes screened, we identified 115 that significantly affected the NF-κB oscillatory response. Using 4 individual siRNAs, we confirmed the action for 46 genes, which affected: (i) the amplitude or duration of nuclear oscillations; (ii) the time between oscillations, leading to an increase or decrease of the number of nuclear translocations; or (iii) an inhibition of the response altogether. In this last category we identified five genes, three novel, whose reduced expression protected against the diclofenac/TNFα-induced apoptosis. Interestingly, the knockdown of four of these genes led to a basic up-regulation of A20 expression. In accordance, A20 knockdown promoted the NF-κB oscillation and enhanced apoptosis. Double knockdown experiments indicated a direct relationship between these four genes and A20 in the control of the NF-κB activation. These findings indicate that the (de)ubiquitinase A20 is a master regulator in the life-death decision upon TNFα stimulation in drug-induced hepatotoxic responses, which, in turn, is kept under control by a network of genes that control its expression level.

INTRODUCTION

The dimeric transcription factor nuclear factor-κB (NF-κB) controls the expression of a wide array of genes that play an important role in many stages of both physiology and disease. The activity of NF-κB is crucial in the host-pathogen response by transcribing anti-oxidant and pro-inflammatory genes and thereby activating the innate and adaptive immune response (1). In addition, the activity of NF-κB has been associated with disease states such as cancer, chronic inflammatory diseases and atherosclerosis (2). The malignant role of NF-κB arises from improper regulation of its activation. Enhanced activation of NF-κB leads to over-expression of genes responsible for proliferation, angiogenesis, metastasis, tumor promotion, inflammation and suppression of apoptosis, which gives the transcription factor its tumorigenic properties (3,4). Yet on the other hand, inhibition of NF-κB activity has been associated to toxicity of drugs (5,6).

NF-κB is activated by canonical and atypical signaling pathways. The canonical pathway is typically activated by pro-inflammatory stimuli such as the cytokines tumor necrosis factor-α (TNFα) and interleukin-1β (IL-1β) that bind to their respective receptors TNFR and IL-1R. Receptor activation is followed by the assembly of a signaling complex composed of several adaptor molecules, ubiquitin ligases and kinases to promote activation of the IKK-complex, the rate-limiting step of NF-κB pathway signaling. The IKK-complex consists of the catalytic subunits CHUK (IKKα) and IKBKB (IKKβ) and the regulatory subunit IKBKG (IKKγ or NEMO) (7). The active IKK complex phosphorylates the inhibitor of NF-κB, IκB, which is subsequently poly-ubiquitinated and degraded by the proteasome. This process unmasks the nuclear localization signal in NF-κB, allowing its nuclear translocation and initiation of NF-κB driven gene transcription (8). De-regulation of the IKK-complex is observed in different cancers, for example through activating mutations in NF-κB signaling promoting genes such as the NF-κB inducing kinase (NIK; MAP3K14) or inactivating mutations in NF-κB signaling repressors such as the deubiquitinase cylindromatosis (CYLD) (9), indicating that NF-κB activity requires tight regulation to control normal cellular physiology.

To understand this regulatory control, the NF-κB pathway has been subject to different screening approaches to further decipher its intracellular signaling. Gain- and loss-of-function screens based on NF-κB luciferase reporter constructs (10,11) were performed using cDNA (10) or RNA-interference (siRNA) screens (11,12). These end-point assay screens focused on the prolonged NF-κB activity, and were unable to unravel the complex regulatory mechanisms involved in NF-κB activity that determine the spatial and temporal behavior of NF-κB after receptor stimulation.

The nuclear translocation of NF-κB is an oscillatory response that is controlled by feedback control mechanisms and varies between individual cells. Importantly, these NF-κB oscillations determine the extent and levels of gene transcription (13-15). These oscillatory responses varies within a cell population and is dependent on regulation by post-translational modifications such as phosphorylation, (de)ubiquitination and sumoylation (16). TNFα-induced activation requires K63 and linear (poly-)ubiquitination chains to

allow (auto-)phosphorylation of the IKK kinases to promote K48 linked poly-ubiquitination of IκB (8). Termination depends on deubiquitination as well as ubiquitination processes, as exemplified by the protein A20 (TNFAIP3). A20 deubiquitinates the activating K63 chains from receptor-interacting protein 1 (RIP1), a TNFR associated kinase upstream of the IKK-complex, and replaces these by K48 chains, marking RIP1 for proteasomal degradation (17,18). As TNFAIP3 and NFKBIA (IκBα) are two of the principle early target genes of NF-κB, this provides a very important negative feedback loop to control NF-κB activation and constitutes the reason for the dampened oscillatory translocation pattern of NF-κB (19). Also drugs that cause liver failure in patients strongly affect the NF-κB oscillatory response (5).

In the current manuscript we searched for novel regulatory components of the oscillatory nuclear translocation response of the canonical NF-κB subunit p65 (RelA) upon exposure to the pro-inflammatory cytokine TNFα. We studied this in the context of drug-induced liver injury responses. By combining RNAi and using live high content confocal imaging of green fluorescent protein tagged p65 (GFP-p65), in a HepG2 cell background, we here present an advanced screening approach to quantitatively determine the effect of individual gene knockdowns on the temporal and spatial behavior of NF-κB in single cells as well as at the population level. We identified several genes that are essential for the regulation of the A20 protein levels, which thereby not only control NF-κB oscillation, but also the susceptibility of TNFα-mediated enhancement of drug-induced toxicity.

MATERIALS AND METHODS

Reagents and antibodies

Human recombinant TNFα was acquired from R&D Systems (Abingdon, UK). Diclofenac sodium and the antibody against tubulin were from Sigma-Aldrich (Zwijndrecht, The Netherlands). AnnexinV-Alexa633 and AnnexinV-Alexa561 were made as described (20). The antibody against phospho-specific IκBα was from Cell Signaling (Bioké, Leiden, The Netherlands). The antibody against A20 was from Santa Cruz (Tebu-Bio, Heerhugowaard, The Netherlands). The bromo phenol blue solution was from Merck (Merck Millipore, Amsterdam Zuidoost, The Netherlands).

Cell culture

Human hepatoma HepG2 cells were obtained from American Type Culture Collection (clone HB-8065, ATCC, Wesel, Germany). HepG2 cells stably expressing GFP-p65 (NF-κB subunit) were created by 400 μg/ml G418 selection upon pEGFP-C1-p65 transfection using Lipofectamine™ 2000 (Invitrogen, Breda, Netherlands). HepG2 BAC IκBα-GFP cells were generated by bacterial artificial chromosome (BAC) recombineering (21,22). Upon validation of correct C-terminal integration of the GFP-cassette by PCR, the BAC-GFP construct was transfected using Lipofectamine™ 2000. Stable HepG2 BAC IκBα-GFP cells were obtained by 500 µg/ml G418 selection. For all experiments the cells were cultured in Dulbecco's modified Eagle's medium (DMEM) supplemented with 10%

(v/v) fetal bovine serum (FBS), 25 U/ml penicillin, and 25 μg/ml streptomycin between passages 5 and 20.

RNA interference

Transient knockdowns of individual target genes were achieved using siGENOME SMARTpool siRNA reagents in the primary screen or single siRNA sequences in the secondary deconvolution screen (50 nM; Dharmacon Thermo Fisher Scientific, Landsmeer, Netherlands). HepG2 cells were transfected using INTERFERin siRNA transfection reagent according to the manufacturer's procedures (Polyplus transfection, Leusden, Netherlands) and left for 72 hours to achieve maximal knockdown before treatment. The negative controls were siGENOME non-targeting pool #1, caspase-8 and mock (INTERFERin only) transfection.

Exposures

Prior to imaging, nuclei were stained with 100 ng/ml Hoechst 33342 in complete DMEM for 45 minutes. The cells were then exposed to Diclofenac 500 μM or DMSO 0.2% for 8 hours. The cells were then challenged with human TNFα (10 ng/ml).

Live Cell Imaging of GFPp65 and GFP-IκBα in HepG2 Cells

The GFP-p65 nuclear translocation response and IκBα-GFP level response upon 10 ng/ml human TNFα challenge was followed for a period of 6 hours by automated confocal imaging every 6 minutes (Nikon TiE2000, Nikon, Amstelveen, Netherlands). Quantification of the nuclear/cytoplasmic ratio of GFPp65 intensity in individual cells was performed using an algorithm for ImageJ (Z. Di, B. Herpers, L. Fredriksson, K. Yan, B. van de Water, F.J. Verbeek and J.H.N. Meerman, submitted).

Translocation response class definition and hit definition

For the primary screen, the amplitudes of the individual translocation response tracks were normalized to their intrinsic response maxima (=1) and minima (=0) to be able to compare the timing of the nuclear translocation events versus the plate average. For the secondary screen, non-normalized data were used. Four different classes were defined according to the type of nuclear p65 oscillation response: increased, no oscillation, decreased and different compared to the oscillation observed with control siRNA. Each class used a different set of five specific parameters (Fig. 1A). For each targeted gene, a Pearson's chi-squared cumulative statistic was calculated from the set of five parameters of each class and p-values were obtained by comparing the value of the statistic to a chi-squared distribution. Targeted genes obtaining a p-value lower than or equal to 0.001 were considered as hits.

Apoptosis measurements

Apoptosis was determined by the live cell apoptosis assay previously described (5,20). The relative Annexin V fluorescence intensity per image was quantified using Image Pro

(Media Cybernetics, Bethesda, MD) and normalized to the number of nuclei or cell area to obtain the estimated percentage of apoptosis.

Western Blot

Cells were harvested in sample buffer (6 times diluted bromo phenol blue solution with β-mercaptoethanol). The samples were subjected to protein separation, blotted on Immobilon-P (Millipore, Amsterdam, The Netherlands). Phosphorylated IκBα was detected using the Tropix Western-Star kit™ (Applied Biosystems) following manufacturer's protocol. For tubulin and A20, the membranes were blocked for 1h at room temperature in milk powder 5% (w/v) in Tris-buffered saline/Tween 20 (TBS-T). Primary antibody incubation was done overnight at 4°C followed by incubation with cy5-labeled secondary or horseradish peroxidase-conjugated antibodies (Jackson Immunoresearch, Newmarket, UK) in 1% BSA in TBS-T for 1 h at room temperature. Protein signals were detected with ECL (GE Healthcare) followed by film detection for A20 or by visualization on the Typhoon 9400 imager (GE Healthcare, Diegem, Belgium) for tubulin.

Statistical procedures

All numerical results are expressed as mean ± standard error of the mean (SEM). Statistical significance was determined by GraphPad Prism using an unpaired t-test, * $P \leq 0.05$, ** $P \leq 0.01$, *** $P \leq 0.001$. Heatmap representations and hierarchical clustering (using Pearson correlation) were performed using the MultiArray Viewer software.

RESULTS

NF-κB nuclear oscillation phenotype siRNA screening in HepG2 cells

Stimulation of cells with TNFα initiates nuclear translocation oscillation of the NF-κB transcription factor. To follow the dynamics of this process, we created a stable GFP-tagged HepG2 reporter line for the NF-κB subunit p65/RelA. Time-lapse confocal microscopy showed that the nuclear translocation of GFP-p65 is transient and follows a dampened oscillation at set time intervals, largely due to NF-κB-dependent transcription of IκBα (19). Under control conditions, the initial translocation peaks at 30 minutes after TNFα (10 ng/mL) stimulation, followed by a second and third peak at 120 minute intervals (Figure 1 A, top). In HepG2 cells this effect was maximal at 10 ng/mL (data not shown). Successful knockdown with siRNAs targeting A20 (Supporting Data S1) slightly decreased the time-interval between oscillations, leading to faster oscillation, whereas knockdown of IκBα (Supporting Data S1) almost completely inhibits NF-κB oscillation in association with enhanced levels of p65-GFP expression (Fig. 1 A, middle). Pre-incubation of HepG2 cells with 500 μM diclofenac for 8 hours increased the time interval between peaks (Fig. 1 A, bottom; (5)). To distinguish these four phenotypes (control, increased oscillation, decreased oscillation and no oscillation) from each another, we established a pipeline of automated image segmentation and GFP-p65 nuclear/cytoplasmic ratio quantification for

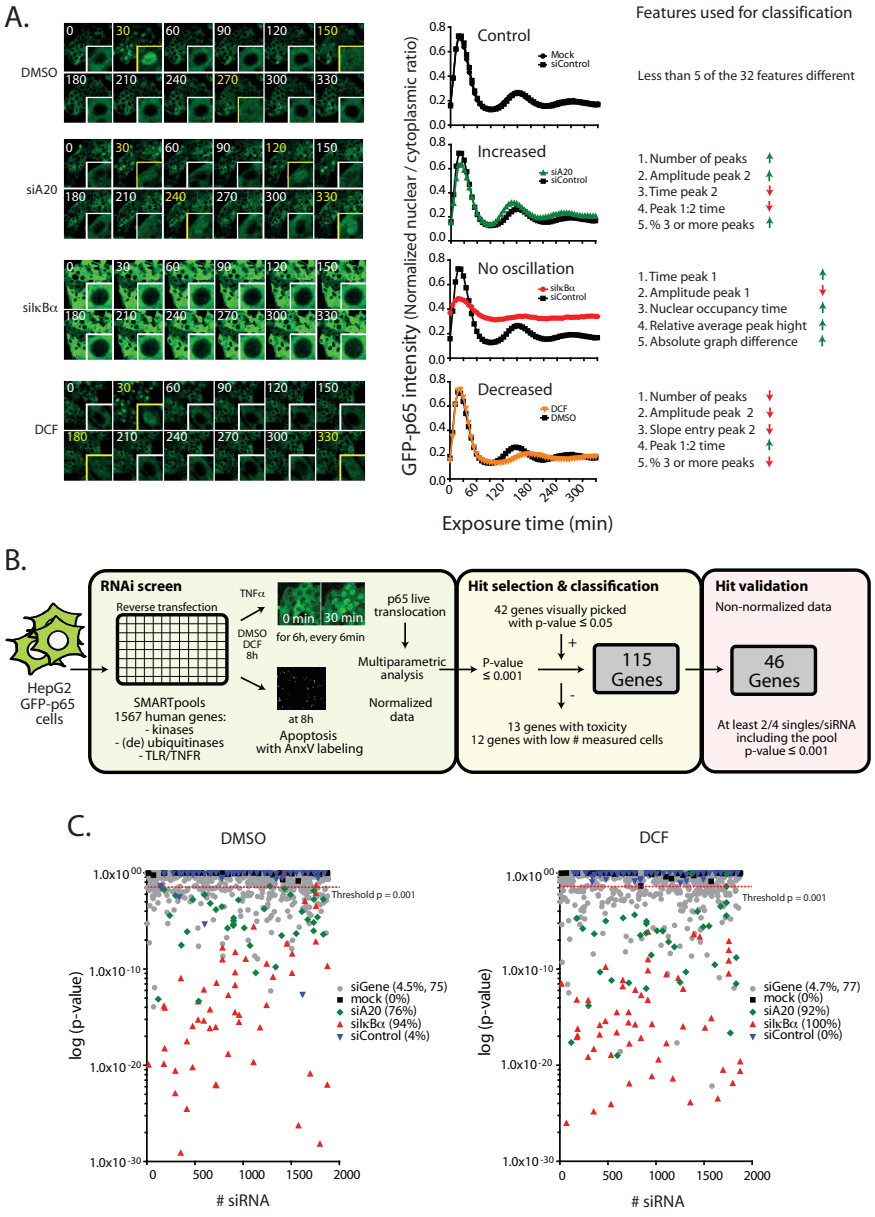

Figure 1. *NF-κB oscillation phenotype siRNA screening in HepG2 cells.* (A) Representative images of GFP-p65 translocation after TNFα (10 ng/mL) challenge in HepG2 cells by automated confocal microscopy. Insets: zooms of single cells with an average response in respect to the imaged population. The nuclear translocation events are marked by yellow boxes and the numbers indicate the time in minutes after TNFα exposure. The nuclear translocation track of each cell was quantified and normalized to its own highest nuclear-to-cytoplasmic ratio (value of 1) and its lowest ratio (0). The average response of the total cell population is presented in the middle panel. The features and their directions that define the response classes (different, increased, decreased and no oscillation) compared to control are shown in the panel to the right. (B) Flowchart of the siRNA screen. (C) P-value distribution of the hits and the positive and negative controls. Under DMSO conditions the true discovery rate was 0.94 and 0.76 for siIκBα and siA20 respectively while the false discovery rate was 0.04. Under DCF conditions the corresponding values were, 1, 0.92 and 0 respectively. 4.5% of the screened genes were found to have an effect on the oscillation under DMSO conditions while 4.7% were determined to give a significant effect after DCF pre-exposure.

all individual cells within one time-series, followed by extraction of 32 distinct oscillation features (Di *et al.*, submitted). We classified the phenotypes based on the direction versus control for at least five oscillation features, e.g. number of peaks, time between peaks and amplitude of peaks (Fig. 1 A). If more than 5 of the 32 measured oscillation features were distinct from control and the oscillation phenotype did not match any of the other categories, the response was marked as “different oscillation”.

Having established an automated system to track, segment and categorize the NF-κB oscillation pattern in individual cells, we set out to identify the genes that are responsible for the timely activity of the NF-κB response by siRNA screening (Figure 1 B). We screened 779 kinases, 107 de-ubiquitinases and sumoylases, 580 ubiquitin ligases and 123 pre-described players in the TNFR/TLR-driven NF-κB response, under DMSO (control) and diclofenac (DCF) conditions. 22 siRNAs were overlapping in either of the libraries. Annexin-V-Alexa633 labeling of the cells allowed us to omit the genes that induce apoptosis upon knockdown. For all target genes the oscillation of the GFP-p65 reporter was followed for 6 hours at 6 minute intervals, directly after TNFα stimulation. Because we were mainly interested in the time between oscillations under control and DCF conditions, we normalized the nuclear/cytoplasmic GFP intensity ratio and separated the analysis for both conditions. Within each condition, we considered genes a potential hit at a p-value below or equal to 0.001, a minimum of in total 35 cells analyzed (average number of cells was 184 per condition) and absence of apoptosis. Within this p-value cut-off we could trace back the effect of A20 knockdown under control and DCF conditions in 76% and 92% of the samples, respectively; and the effect of IκBα knockdown in 94% and 100% of the samples (Fig. 1 C). Another 42 genes were added from the “different” category, based on visual inspection of the translocation phenotype and taking the p-value into consideration ($P \leq 0.05$). In total we re-screened 115 genes by using 4 single siRNAs targeting the same gene, of which 46 genes were confirmed to affect the GFP-p65 oscillation with 2 or more single siRNAs in addition to the pooled siRNAs in either or both DMSO and DCF conditions.

Functional and phenotypic classification of the siRNA screen hits that control NF-κB oscillation

Out of the 46 confirmed hits, 5 genes, including the known inhibitor of NF-κB activation, UCHL1 (23), decreased the oscillation after knockdown; 7 increased the oscillation, also confirming the inhibitory role for TNFAIP3 (A20) for the activation of NF-κB; 24 showed no oscillation, including the essential activators of NF-κB IKBKG (IKKγ) and ubiquitin ligase CUL1, needed for the polyubiquitination of IκBα (24), and 4 did not fall in the previous three categories, but were significantly different from the controls under DMSO conditions (Figure 2 A-B and Table 1). Despite the oscillation-decreasing effect of DCF, 2 siRNAs targeting splicing factor PHF5A and th receptor TNFRSF18, led to a further decrease in oscillation under this condition. Twelve increased the oscillation, 22 stopped the oscillation, including knockdown of the cyclin-dependent kinase CDK12 that was

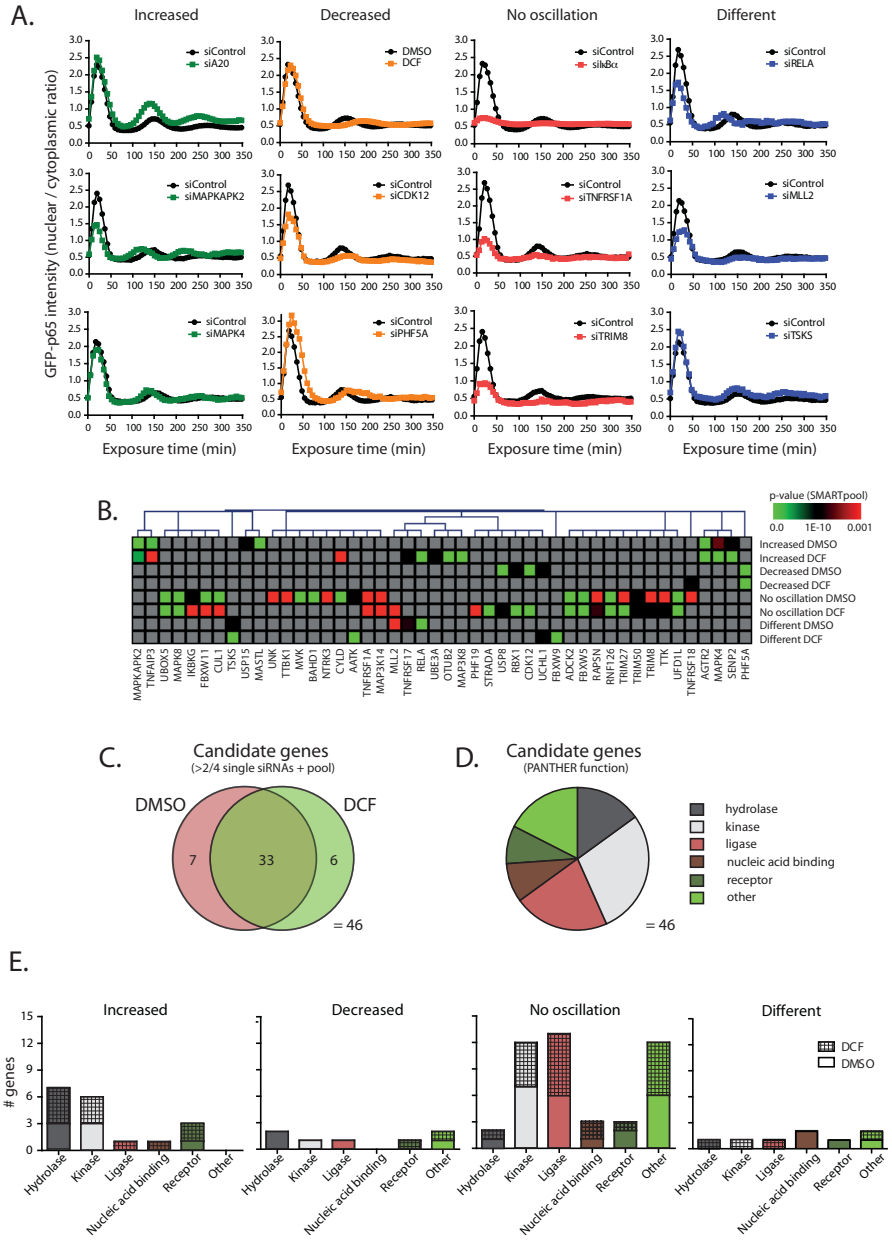

Figure 2. *Functional and phenotypic profiling of the siRNA screen hits that control NF-κB oscillation.* (A) Typical non-normalized NF-κB oscillation averages acquired in the deconvolution screen, including examples of knockdowns that led to a phenotype similar to the classification controls; siA20, diclofenac (DCF) and siIκBα. The "different" class is defined by having five or more features significantly different from the siControl. (B) Heatmap of the SMARTpool classification P-values for the hits confirmed by 2 or more single siRNAs in the deconvolution screen, clustered for their corresponding classification on the right. The overlap of the hits under DMSO and DCF conditions are additionally presented in (C). (D) Most of the hits under both DMSO and DCF conditions are described as kinases, (ubiquitin) ligases and hydrolases (mostly deubiquitinases). (E) Knockdown of hydrolases led to a predominantly "increased" phenotype under both DMSO and DCF conditions, while knockdown of kinases and ligases in general lead to "no oscillation" phenotype. The "decreased" phenotype was predominantly detectable under DMSO conditions. The functionality of the target genes was evenly distributed. The "different" phenotype was evenly distributed over functionality as well as exposure condition.

Table 1. Confirmed hits from the deconvolution screen arranged by classification. DCF = diclofenac.

Gene Symbol	Name (also known as)	Function	DMSO	DCF	# singles DMSO	# singles DCF	Regulator of NF-κB	Reference
		Decreased						
PHF5A	PHD finger protein 5A	splicing factor	Decreased	Decreased	4/4	3/4	(-)	
UCHL1	ubiquitin carboxyl-terminal esterase L1	hydrolase	Decreased	Different pattern	2/4	4/4	Inhibitor	(1)
		Increased						
AGTR2	angiotensin II receptor type 2 (AT2)	receptor	Increased	Increased	3/4	3/4	Activator/Inhibitor	(2,3)
MAPK4	mitogen-activated protein kinase 4 (ERK-4)	kinase	Increased	Increased	3/4	2/4	(-)	
MAPKAPK2	mitogen-activated protein kinase-activated protein kinase 2 (MK2)	kinase	Increased	Increased	2/4	2/4	Inhibitor	(4)
SENP2	SUMO1/sentrin/SMT3 specific peptidase 2	hydrolase	Increased	Increased	2/4	4/4	Inhibitor/Activator	(5,6)
TNFAIP3	tumor necrosis factor alpha-induced protein 3 (A20)	hydrolase/ligase	Increased	Increased	2/4	3/4	Inhibitor	(7)
RELA	v-rel reticuloendotheliosis viral oncogene homolog A (p65)	nucleic acid binding	Different pattern	Increased	3/4	4/4	Inhibitor	(8)
TNFRSF17	tumor necrosis factor receptor superfamily, member 17 (BCMA)	receptor	Different pattern	Increased	3/4	3/4	Activator	(9,10)
		No oscillation						
CDK12	cyclin-dependent kinase 12 (CRK7; CrkRS)	kinase	Decreased	No oscillation	3/4	3/4	(-)	
RBX1	ring-box 1	ligase	Decreased	No oscillation	2/4	2/4	Inhibitor	(11,12)
USP8	ubiquitin specific peptidase 8	hydrolase	Decreased	No oscillation	2/4	3/4	(-)	
TNFRSF18	tumor necrosis factor receptor superfamily member 18 (GITR)	receptor	No oscillation	Decreased	4/4	3/4	Activator	(13)
ADCK2	aarF domain containing kinase 2	unclear	No oscillation	No oscillation	4/4	2/4	(-)	
CUL1	cullin 1	liagse	No oscillation	No oscillation	3/4	3/4	Activator	(14)
FBXW11	F-box and WD repeat domain containing 11 (BTRCP2)	ligase	No oscillation	No oscillation	4/4	4/4	Activator	(15)
FBXW5	F-box and WD repeat domain containing 5	ligase	No oscillation	No oscillation	3/4	2/4	Inhibitor	(16)
IKBKG	inhibitor of kappa light polypeptide gene enhancer in B-cells kinase gamma (NEMO)	enzyme regulator	No oscillation	No oscillation	4/4	4/4	Activator	(17)
MAP3K14	mitogen-activated protein kinase kinase kinase 14 (NIK)	kinase	No oscillation	No oscillation	2/4	2/4	Activator	(18)
MAPK8	mitogen-activated protein kinase 8 (JNK1)	kinase	No oscillation	No oscillation	4/4	3/4	Inhibitor	(19)
RAPSN	receptor-associated protein of the synapse (rapsyn)	receptor adaptor protein	No oscillation	No oscillation	3/4	3/4	(-)	
RNF126	ring finger protein 126	unclear	No oscillation	No oscillation	3/4	3/4	(-)	
TNFRSF1A	tumor necrosis factor receptor superfamily member 1A (TNFR1)	receptor	No oscillation	No oscillation	4/4	4/4	Activator	(8)
TRIM27	tripartite motif containing 27 (RFP)	ligase	No oscillation	No oscillation	3/4	2/4	Inhibitor	(20)
TRIM50	tripartite motif containing 50	ligase	No oscillation	No oscillation	3/4	2/4	(-)	
TRIM8	tripartite motif containing 8	ligase	No oscillation	No oscillation	2/4	2/4	Activator	(21,22,23)
TTK	TTK protein kinase (PYT)	kinase	No oscillation	No oscillation	3/4	3/4	(-)	
UBOX5	U-box domain containing 5	enzyme modulator	No oscillation	No oscillation	3/4	3/4	(-)	
UFD1L	ubiquitin fusion degradation 1 like	enzyme modulator	No oscillation	No oscillation	4/4	3/4	(-)	
		Miscellaneous						
TSKS	testis-specific serine kinase substrate	unclear	Different pattern	Different pattern	3/4	2/4	(-)	
MLL2	myeloid/lymphoid or mixed-lineage leukemia 2	nucleic acid binding	Different pattern	No oscillation	3/4	2/4	(-)	
AATK	apoptosis-associated tyrosine kinase (AATYK)	kinase	No oscillation	Different pattern	4/4	3/4	(-)	
CYLD	cylindromatosis	hydrolase	No oscillation	Increased	4/4	2/4	Inhibitor	(24)
NTRK3	neurotrophic tyrosine kinase receptor type 3 (TRKC)	kinase	No oscillation	not different	3/4	(-)	(-)	
BAHD1	bromo adjacent homology domain containing 1	nucleic acid binding	No oscillation	not different	3/4	(-)	(-)	
MVK	mevalonate kinase	kinase	No oscillation	not different	3/4	(-)	(-)	
TTBK1	tau tubulin kinase 1	kinase	No oscillation	not different	3/4	(-)	(-)	
UNK	unkempt homolog (unkempt)	ligase	No oscillation	not different	3/4	(-)	(-)	
FBXW9	F-box and WD repeat domain containing 9	ligase	not different	Different pattern	(-)	3/4	(-)	
MAP3K8	mitogen-activated protein kinase kinase kinase 8 (COT; TPL2)	kinase	not different	Increased	(-)	2/4	Activator	(25)
OTUB2	OTU domain ubiquitin aldehyde binding 2	hydrolase	not different	Increased	(-)	2/4	Inhibitor	(26,27)
UBE3A	ubiquitin protein ligase E3A	ligase	not different	Increased	(-)	2/4	(-)	
PHF19	PHD finger protein 19	nucleic acid binding	not different	No oscillation	(-)	3/4	(-)	
STRADA	STE20-related kinase adaptor alpha (STRADalpha)	kinase	not different	No oscillation	(-)	2/4	(-)	
MASTL	microtubule associated serine/threonine kinase-like (greatwall)	kinase	Increased	not different	2/4	(-)	(-)	
USP15	ubiquitin specific peptidase 15	hydrolase	Increased	not different	3/4	(-)	Inhibitor	(28)

shown to only decrease the oscillation under DMSO conditions, and 4 had a different oscillation phenotype (Fig. 2 B and Table 1). Between the two conditions, 33 hits were overlapping, 7 were unique for DMSO and 6 for the diclofenac condition at a p-value cut-off of $p<0.001$ (Fig. 2 B-C and Table 1). Most hits were kinases and (ubiquitin) ligases, which most often contributed to the "no oscillation" or "decreased" response phenotype (Fig. 2 D and 2 E).

The strength of our siRNA screening approach is the analysis of the dynamics of the NF-κB response at the single cell level within an entire population of cells. This allows measurement of the population dynamics upon knockdown of our candidate genes (Fig. 3 A and 3 B). Under control conditions the majority of the cells showed three nuclear translocation events within the imaging period. Yet the siRNA conditions that blocked the oscillation led to profiles with either no, or one shallow oscillation event, as shown with our positive control IκBα and knockdown of the genes necessary for NF-κB activation, IKBKG (IKKγ) and TNFRSF1A (TNFR1) (Fig. 3 Bi). The decreased phenotype exhibited mainly 2 or 3 oscillation events, as shown by knockdown of CDK12 and PHF5A, whereas the increased class, best illustrated by knockdown of our positive control TNFAIP3 (A20), showed mostly cells with 3 or 4 oscillations (Fig. 3 Bii). Within the profile class of "no oscillation" the number of peaks was vastly reduced and any observable translocation event occurred later than in control cells, at lower amplitude and with a reduced nuclear entry slope. Within the remaining fraction of cells (~30%) that showed more than one nuclear translocation event, the peaks remained shallow, which leads to a reduced dampening between the peaks (Fig. 3 Ci). The group of siRNAs that decreased the oscillation also decreased the number of oscillations and increased the time of the first translocation event. Differently from the "no oscillation" class, the profiles within the "decreased" class that included CDK12, RBX1, PHF5A and USP8, all showed an increase in the duration of the initial translocation event including a delayed time for the maximum. This suggests a role in the regulation of the NF-κB nuclear export, which subsequently affects the timing of the second peak (Figure 3 Cii). Finally, the increased class, including our positive control TNFAIP3 (A20), the inhibitor of NF-κB activation MAPKAPK2 (25), AGTR2 and MAPK4, were hallmarked by an increase in the number of oscillations, with a decreased time interval between peaks, that exhibit an elevated NF-κB nuclear translocation amplitude (Figure 3 Ciii).

Genes that prevent the NF-κB oscillation protect against TNFα/hepatotoxicant-induced cell death.

Diclofenac (DCF) and carbamazepine (CBZ) are two drugs that are associated with idiosyncratic liver injury in humans, in which the innate immune system-based TNFα is an important component. Indeed, we have previously reported that diclofenac sensitizes liver cells to apoptosis caused by an otherwise non-toxic dose of TNFα (5). Since this was directly linked to inhibition of NF-κB signaling (5), we questioned whether inhibition of the 22 candidate genes that showed a "no oscillation" phenotype after knockdown,

would affect the cytotoxic response upon DCF/TNFα and CBZ/TNFα exposure. Since knockdown of caspase-8 completely inhibited the apoptotic response induced by both DCF/TNFα and CBZ/TNFα, we further used this as a positive control (Fig. 4 A and B). The majority of the knockdowns that displayed a "no oscillation" phenotype significantly inhibited the drug/TNFα-induced apoptotic response (12 out of 21; including CDK12,

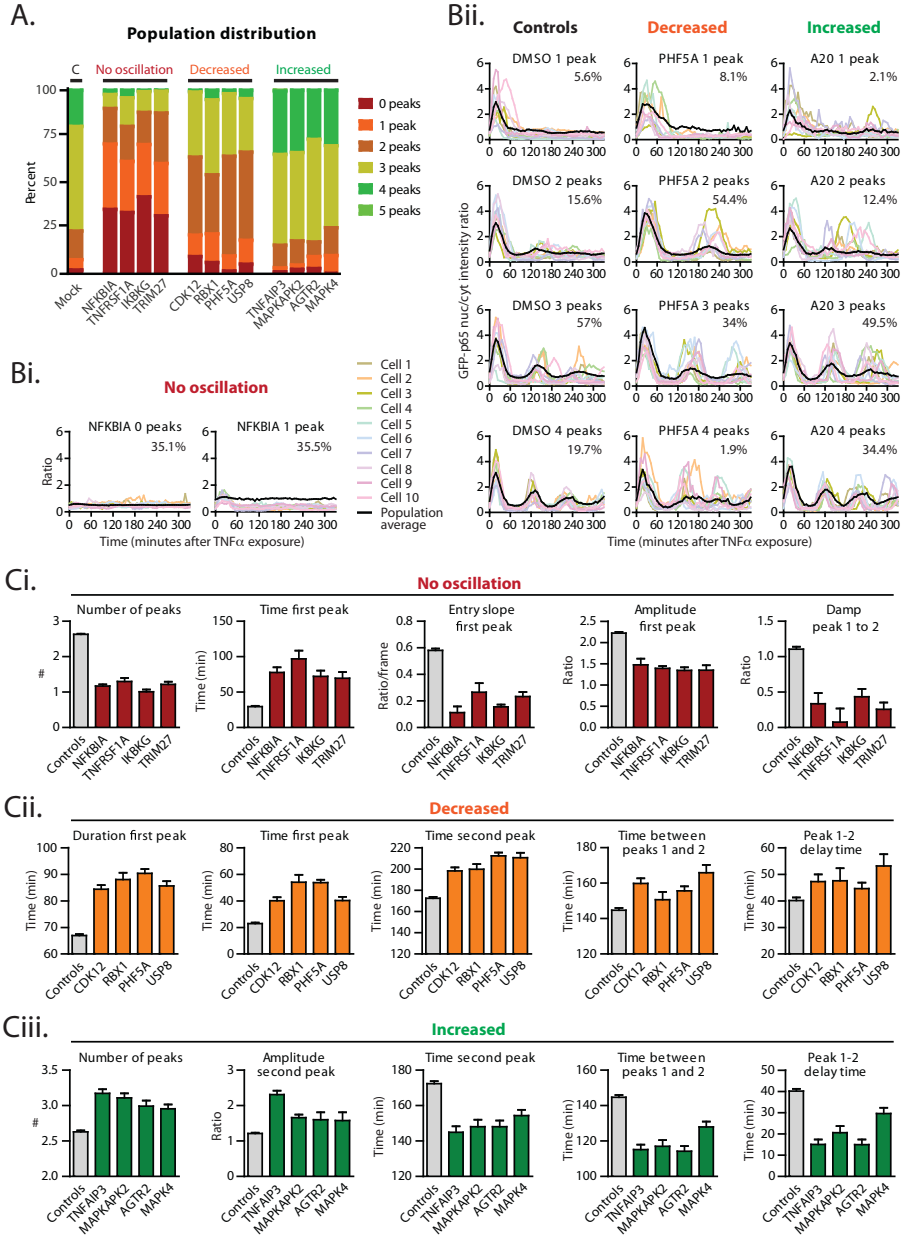

Figure 3. *Population statistics.* (A) The population distribution of NF-κB oscillations in HepG2 GFPp65 cells upon indicated siRNA treatments. (B) Examples of how each phenotypic class is distributed in relation to the number of translocation peaks. (C) The translocation features that define the different classes: "no oscillation" (Ci), "decreased" (Cii) and "increased"(Ciii) are exemplified by their representative siRNAs.

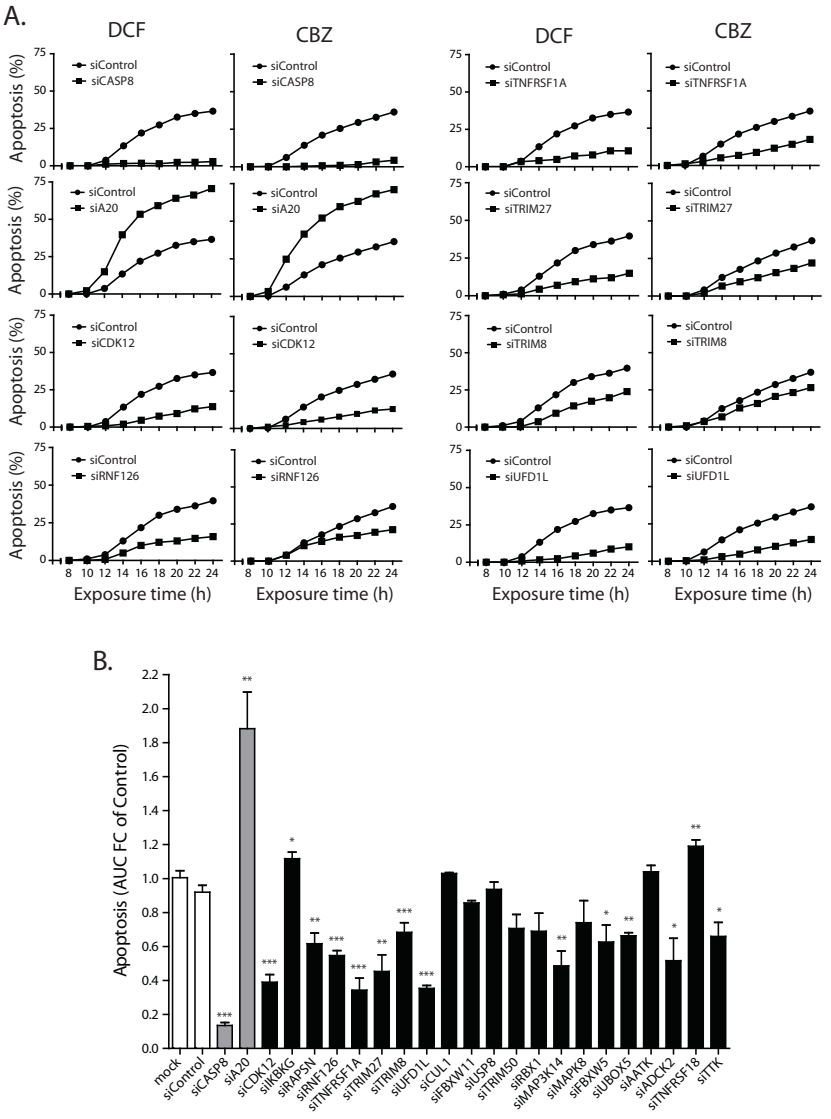

Figure 4. *A "no oscillation" phenotype correlates to decreased drug/TNFα-induced apoptosis.* (A) Live apoptosis imaging of wild type HepG2 cells with knockdowns resulting in a "no oscillation" phenotype in GFP-p65 cells after 500μM diclofenac (DCF) or 500μM carbamazepine (CBZ) pre-incubation for 8 hours followed by addition of TNFα (10 ng/mL) The amount of apoptosis is presented as a percentage after normalization to the number of Hoechst33342-positive cells. (B) The area under the curves (AUC) depicted in A was calculated and an average of the fold change (FC) compared to siControl for three independent experiments was determined. The difference in FC AUC compared to siControl was defined using Student's t-test where * P≤0.05, ** P≤0.01 and ***P≤0.001.

RNF126 and TNFRSF1A), while others did not significantly affect the response (7 out of 21; including CUL1, USP8 and AATK); only IKBKG (IKKγ) and TNFRSF18 knockdowns slightly, but significantly, increased the sensitivity towards apoptosis (Fig. 4 B). Interestingly, knockdown of the important negative regulator of TNFα-induced apoptosis, A20, strongly enhanced the apoptotic response (Fig. 4 A and B).

Protection against apoptosis is correlated to A20 expression and not IκBα activation

IκBα is a direct phosphorylation target for the IKK complex after TNF receptor activation and subsequently targeted for proteasomal degradation, a prerequisite for NF-κB nuclear translocation. In addition, IκBα constitutes the earliest induced negative feedback mechanism for the attenuation of NF-κB activity. We wondered whether genes showing the most significant reduction in drug/TNFα-induced apoptosis (p-value < 0.001 in Figure 4B: including CDK12, RNF126, TNFRSF1A, TRIM8 and UFD1L) would affect IκBα levels. We used BAC-NFKBIA-GFP (IκBα-GFP) HepG2 cells that phosphorylate and degrade IκBα-GFP with the same kinetics as non-tagged IκBα (Supporting Data S2). We knocked down above genes individually and followed the IκBα-GFP levels by live cell imaging. Depletion of the TNFRSF1A, UFD1L, and RNF126 strongly increased the initial levels of IκBα-GFP compared to mock treatment (Fig. 5 A), which was associated

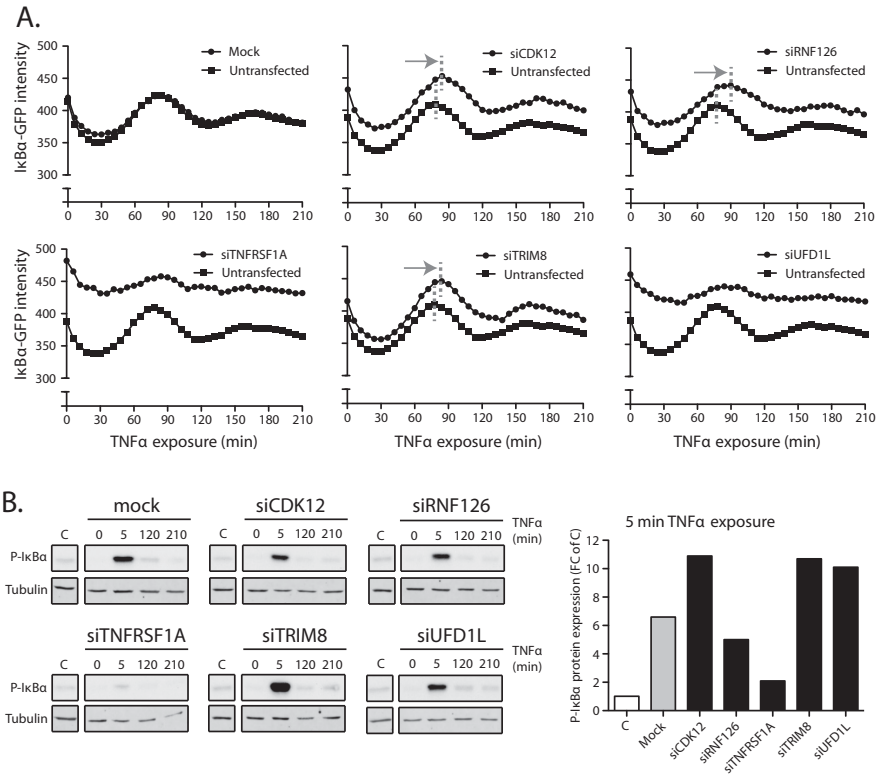

Figure 5. *IκBα levels are elevated and the re-expression is delayed while phosphorylation status remains the same after knockdown of the candidate genes.* (A) Quantification of GFP expression in HepG2 cells expressing a BAC-NFKBIA-GFP construct. TNFα stimulation induces degradation and re-synthesis of the IκBα-GFP protein, which is altered after knockdown of the indicated candidate genes. (B) The amount of IκBα phosphorylation (P) after knockdown of the indicated candidate genes in HepG2 GFP-p65 cells followed by TNFα exposure for 0, 5, 120 and 210 minutes was determined by western blotting. The tubulin-normalized intensities of P-IκBα for the same knockdowns after 5 minutes of TNFα exposure is shown in the right panel.

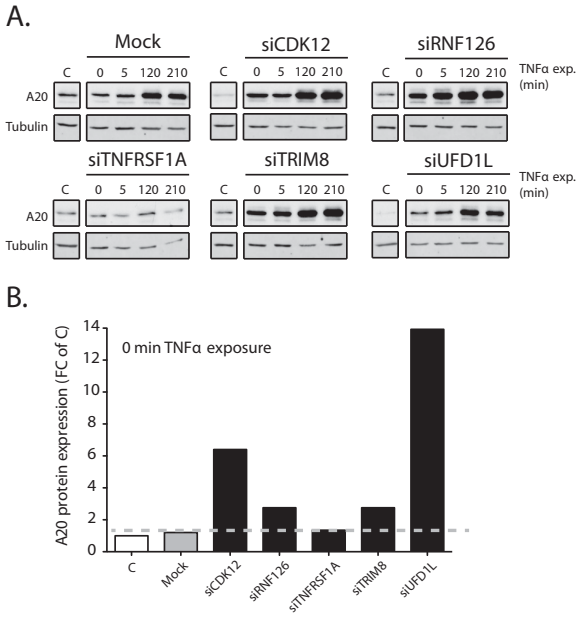

Figure 6. *Knockdown of the candidate genes leads to basic upregulation of (de) ubiquitinase A20.* (A) Western blot for the A20 expression levels after knockdown of the indicated candidate genes in HepG2 GFP-p65 cells exposed to 10ng/ml TNFα for 0, 5, 120 and 210 minutes. (B) Quantification of the A20 protein levels at time-point 0 in A.

with an essential complete inhibition of the NF-κB translocation response (see Fig. 2 B). Importantly, TNFα treatment caused an oscillatory response of IκBα-GFP at the population level, corresponding to the western blot data. As expected, depletion of the TNF receptor inhibited an IκBα-GFP oscillatory expression. Yet, CDK12, TRIM8 and RNF126 did not affect the initial breakdown of IκBα-GFP, but slightly delayed the newly translated IκBα-GFP. In line with this CDK12, TRIM8 and RNF126 did not inhibit the early phosphorylation of IκBα upon TNFα stimulation; as expected, TNFRSF1A knockdown prevented this phosphorylation event (Fig. 5 B). Knockdown of UFD1L showed a different response: despite the fact that TNFα could initiate a phosphorylation of IκBα, the degradation of IκBα-GFP was reduced, suggesting a role for UFD1L in the degradation of this protein (Fig. 5 A and B).

As differences in IκBα phosphorylation and breakdown were not the major contributors to the effect of CDK12, RNF126, TRIM8 and UFD1L, we turned our attention to a second important negative feedback mechanism for NF-κB activity, A20 (TNFAIP3) (17,18). Intriguingly, the A20 levels after knockdown of CDK12, RNF126, TRIM8 or UFD1L were increased at control situation, prior to TNFα treatment (Fig. 6 A and B). Regardless, TNFα was still capable to further induce A20 after TNFα exposure (Fig. 6 A) most likely since the first NF-κB nuclear entry peak is not affected by these knockdowns. Again, as expected, depletion of the TNFα-receptor (TNFRSF1A) did not affect A20 levels under control or TFNα treatment.

A20 was an important regulator of the oscillatory NF-κB response in HepG2 cells. The above data suggested that the effects of CDK12, RNF126, TRIM8 and UFD1L depletion on the reduced NF-κB oscillation was a direct result of the increased A20 levels. Therefore, we performed double knockdown experiments by combining A20 siRNAs with the siRNA against CDK12, RNF126, TRIM8 or UFD1L, again using TNFRSF1A as a

positive control. Importantly, depletion of TNF receptor together with A20 did not induce any oscillatory response, indicative for the effectiveness of our double knockdown. Yet, simultaneous knockdown of A20 with either CDK12, RNF126, UFD1L or TRIM8, (partially) recovered the NF-κB oscillatory response (Fig. 7 A), which was further quantified with respect to the average number of nuclear entry peaks at the cell population level (Fig. 7 B).

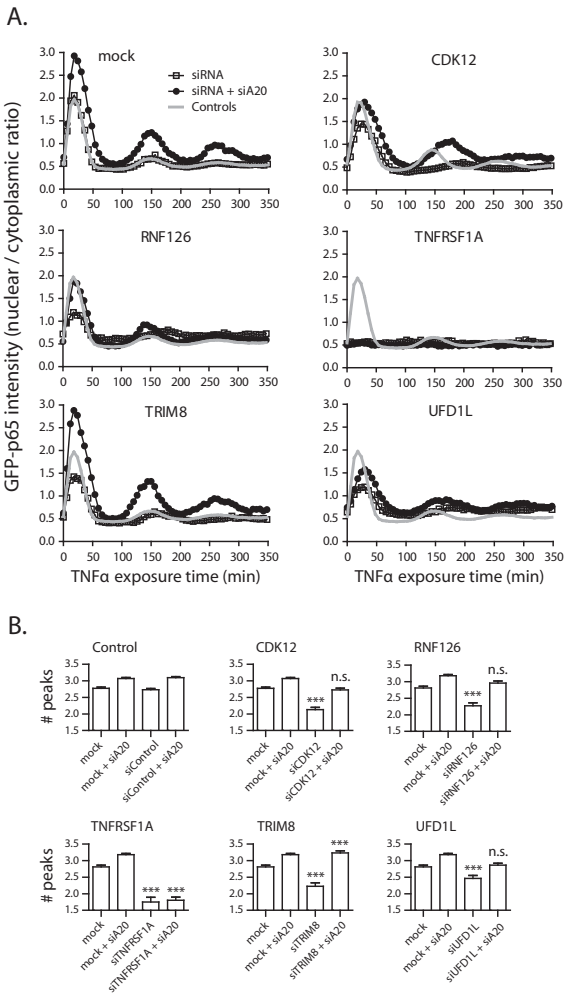

Figure 7. *Double knockdown with candidate genes and siA20 leads to restoration of the translocation response.* (A) The average oscillatory response in HepG2 GFP-p65 cells upon TNFα addition under double candidate gene and A20 knockdown conditions. Increased oscillation could be observed compared to knockdown of the candidate genes alone. (B) Quantification of the average number of peaks with and without A20 double knockdown. The data represent the average of 3 independent experiments +/- S.E.M. The difference in the number of peaks compared to mock was defined using Student's t-test where *** P≤0.001.

DISCUSSION

The transcription factor NF-κB is an important player in both physiology and disease, and its (enhanced) activity has been implicated in cancer as well as chronic inflammatory diseases (2). In addition, inhibition of NF-κB signaling has been implicated in the toxicity of drugs (5). The NF-κB translocation response is tightly controlled by different types of posttranslational modifications such as phosphorylation and especially (de)ubiquitination,

which has received much attention in recent years (16,17). In the current manuscript we have investigated the role of individual kinases, (de)ubiquitinases and sumoylases in the nuclear translocation of the transcription factor NF-κB following TNFα stimulation using siRNA-mediated knockdowns. For accuracy to determine the dynamics of the response, we employed a high content imaging method including a recently developed image analysis technique to quantify 32 different parameters describing the NF-κB oscillatory response. Using at least 5 of these features we could distinguish and classify siRNA knockdowns that result in a "no oscillation", "decreased", "increased" and significantly "different" translocation phenotype. An siRNA deconvolution screen confirmed 46 of the 115 hits from the primary screen of which the majority showed a "no oscillation" phenotype, and are thus likely to be positive regulators of NF-κB oscillation (Fig. 2). Many of these positive regulators also control the apoptotic outcome after hepatotoxicant/TNFα-exposure, by regulating the expression levels of the (de)ubiquitinase A20.

We successfully applied an advanced high content imaging approach to identify novel regulators of NF-κB signaling. So far RNA interference screens for NF-κB signaling mainly involved endpoint assays that mimic NF-κB transcriptional activity using luciferase reporter assays (11,12), precluding mechanistic insight in the dynamics of the NF-κB activation response. Our method allowed us to identify candidate genes that regulate the oscillatory response of NF-κB. Some of the 46 candidate genes have already been implicated in the regulation of NF-κB signaling (Table 1). This overlap was primarily observed in the target genes that upon knockdown increased or inhibited an NF-κB oscillatory response: genes with an "increased" phenotype were previously described as inhibitors of the NF-κB signaling response, and genes with "no oscillation" phenotypes are associated with promoters of NF-κB signaling (Table 1).

There is increasing evidence for a role of the oscillatory response of NF-κB in the control of gene expression. The total duration of nuclear localization and promoter association is likely to define the spatiotemporal control of epigenetic modulation of genes, and thereby their expression. Indeed, the differential expression of early, mid and late NF-κB target genes seems proportional to the strength and duration of the NF-κB nuclear occupancy (14,15). IκBα and A20 are classical early NF-κB target genes that are also regulated tightly in our model systems and provide early feedback control of NF-κB activation. At this point we do not know whether our candidate genes that affect the oscillatory response of NF-κB will also affect the overall target gene expression. We anticipate that such a dynamic transcriptional activity of NF-κB is likely to differ within the cell population. Indeed, we observed a differential response of the NF-κB oscillation in our cell population, with around 80% of the cells demonstrating 3 to 4 oscillations in control situations, and only 10% demonstrating one single peak. Depletion of for example TRIM27 completely shifted this response with 80% showing either 0 or 1 oscillation peak. Reversely, MAPKAPK2, AGTR2 and MAPK4 increased the percentage of cells with 4 peaks. These effects will likely determine NF-κB mediated gene transcription.

Various novel candidates that regulate NF-κB signaling were identified. We described the splicing factor PHF5A as a promoter of the NF-κB oscillatory response.

PHF5A is implicated in processing of pre-mRNA (26). We suggest that this gene is required for proper processing of the mRNA of the protein needed for nuclear export of NF-κB, i.e. IκBα, after transcriptional activation. Furthermore we implicated the atypical mitogen activated protein kinase (MAPK) 4 (also known as ERK4), in the attenuation of the NF-κB signaling, since knockdown of this protein resulted in an "increased" translocation phenotype. ERK4 acts as a kinase for the substrate MAPKAPK5 (MK5) (27). We identified MAPKAPK2 (MK2), another protein in the same family as MK5 as an inhibitor of NF-κB translocation. MK2 is known to inhibit the nuclear export of NF-κB by reducing the levels of IκBα (25). MK5 has a similar role as MK2 and both phosphorylate HSP27 (28). Interestingly, HSP27 was previously implicated in the regulation of IKK activity as well as IκBα function (25,29,30). More research is required to investigate this link.

Previously we reported that inhibition of the NF-κB translocation is linked to enhanced cytotoxicity following exposure to the hepatotoxicant diclofenac in combination with TNFα (5). Therefore, we focused on the knockdowns that resulted in a "no oscillation" phenotype. As expected, knockdown of known activators of the NF-κB signaling response, such as IKBKG (IKKγ; NEMO) and TNFRSF18 (GITR) (Table 1) enhanced the apoptotic response under diclofenac/TNFα and carbamazepine/TNFα exposure conditions (Fig. 4). In addition, knockdown of known inhibitors of the NF-κB response such as FBXW5 and TRIM27 (RFP) as well as the TNF receptor itself (TNFRSF1A) (Table 1) reduced the apoptotic response (Fig. 4). However, surprisingly, most of the knockdowns that lead to a reduced or no oscillatory response, reduced the drug/TNFα-induced apoptosis, including the known activators of NF-κB signaling, MAP3K14 (NIK) and TRIM8. Here we report for the first time that this observation is most likely due to the basal induction of the (de) ubiquitinase A20. Higher A20 levels at the start of TNFα exposure would indeed reduce the induction of NF-κB translocation, as A20 is the most important negative regulator of RIP1 activity (17,18). Furthermore, since A20 also controls apoptosis by deubiquitinating caspase-8 to reduce the activation of this protease (31), the elevated A20 levels might provide cellular protection against drug/TNFα-induced cell death. To our knowledge none of the candidate genes have been previously reported to affect A20 expression.

Since both IκBα as well as A20 levels were enhanced under control conditions (Fig. 5 A and 6), and both are important target genes of NF-κB, it seems likely that the enhanced expression of these proteins results from some initial activity of p65 after knockdown of the candidate genes. Especially in UFD1L knockdowns, the A20 and IκBα levels were exceptionally high. UFD1L is described as part of a complex regulating the proteasomal degradation of polyubiquitinated proteins from the endoplasmic reticulum and implicated in the closure of the nuclear envelope (32). Potentially, lack of UFD1L dismantles the boundary between inactive (cytoplasmic) and active (nuclear) p65, allowing a rise in nuclear p65 presence and thereby transcription of the negative feedback genes A20 and IκBα, an effect similar to IκBα knockdown itself (Supporting Data S1). In addition, the higher expression of A20 together with potential upregulation of NF-κB transcribed anti-apoptotic genes could result in the decreased apoptotic response

observed.

To our knowledge nothing is known about the functions and substrates of the E3 ubiquitin ligase RNF126. However, as discussed earlier, many regulatory steps leading to the translocation of NF-κB involves ubiquitination of RIP1 and therefore RNF126 knockdown possibly prolongs RIP1 polyubiquitination and thereby NF-κB activity, leading to the "no oscillation" phenotype by up-regulation of A20 as well as IκBα (Fig. 5 A and 6). To determine whether the elevated IκBα and A20 expression is indeed caused by enhanced NF-κB activity before TNFα stimulation, the basal transcriptional activation of NF-κB should be addressed during the pre-stimulation knockdown period.

Similar to PHF5A described earlier, cyclin dependent kinases such as CDK12 have been implicated in the processing of pre-mRNA (33). Although not yet described, knockdown of CDK12 could have a similar effect on the processing of IκBα pre-mRNA as suggested for PHF5A above, resulting in the "delayed" phenotype (Fig. 2 A), and delayed re-expression of IκBα protein (Fig. 5 A). The delay of IκBα pre-mRNA processing and thus prolonged nuclear p65 presence would also explain the enhanced expression of A20.

TRIM8 is an E3 ubiquitin ligase that has been reported to activate the NF-κB pathway by ubiquitinating the activating kinase TAK1 (34) as well as SOCS-1, a negative regulator of transcriptionally active NF-κB (35,36). Reduction of TRIM8 thereby resulted in a non-responsive, "no oscillation" phenotype with basic enhanced levels of A20 protein (Fig. 6). Of all candidate gene knockdowns leading to the "no oscillation" phenotype, the effect of TRIM8 knockdown seems to rely most on A20 upregulation as double knockdown for TRIM8 and A20 completely restored and even increased the NF-κB oscillatory response (Fig. 7).

In summary, using an advanced systems microscopy approach involving high content imaging and RNA interference screening, we identified novel regulators of NF-κB signaling. Some of these regulators were essential to control the TNFα-dependent cell death by controlling the expression levels of A20, a negative feedback regulator of TNF receptor signaling. Besides in cytotoxicity, our candidate genes are likely to have important functions in inflammation and in the development or progression of different diseases including cancer, rheumatoid arthritis and pathogen infection. This needs further exploration.

ACKNOWLEDGEMENTS

This work was performed under the framework of the Dutch Top Institute Pharma project D3-201 and the Netherlands Toxicogenomics Center supported by the Netherlands Genomics Initiative.

REFERENCES

1. Hayden MS, West AP, Ghosh S. NF-kappaB and the immune response. Oncogene 2006;25:6758–6780.
2. Courtois G, Gilmore TD. Mutations in the NF-kappaB signaling pathway: implications for human disease. Oncogene 2006;25:6831–6843.
3. Karin M, Lin A. NF-kappaB at the crossroads of life and death. Nat Immunol 2002;3:221–227.
4. Shen H-M, Tergaonkar V. NFkappaB signaling in carcinogenesis and as a potential molecular target for cancer therapy. Apoptosis 2009;14:348–363.
5. Fredriksson L, Herpers B, Benedetti G, Matadin Q, Puigvert JC, de Bont H, et al. Diclofenac inhibits tumor necrosis factor-α-induced nuclear factor-κB activation causing synergistic hepatocyte apoptosis. Hepatology 2011;53:2027–2041.
6. Zhang L, Jiang G, Yao F, He Y, Liang G, Zhang Y, et al. Growth inhibition and apoptosis induced by osthole, a natural coumarin, in hepatocellular carcinoma. PLoS ONE 2012;7:e37865.
7. Israël A. The IKK complex, a central regulator of NF-kappaB activation. Cold Spring Harb Perspect Biol 2010;2:a000158.
8. Hayden MS, Ghosh S. Shared principles in NF-kappaB signaling. Cell 2008;132:344–362.
9. Staudt LM. Oncogenic activation of NF-kappaB. Cold Spring Harb Perspect Biol 2010;2:a000109.
10. Halsey TA, Yang L, Walker JR, Hogenesch JB, Thomas RS. A functional map of NFkappaB signaling identifies novel modulators and multiple system controls. Genome Biol 2007;8:R104.
11. Chew J, Biswas S, Shreeram S, Humaidi M, Wong ET, Dhillion MK, et al. WIP1 phosphatase is a negative regulator of NF-kappaB signalling. Nat Cell Biol 2009;11:659–666.
12. Li S, Wang L, Berman MA, Zhang Y, Dorf ME. RNAi screen in mouse astrocytes identifies phosphatases that regulate NF-kappaB signaling. Mol Cell 2006;24:497–509.
13. Ashall L, Horton CA, Nelson DE, Paszek P, Harper CV, Sillitoe K, et al. Pulsatile stimulation determines timing and specificity of NF-kappaB-dependent transcription. Science 2009;324:242–246.
14. Tian B, Nowak DE, Brasier AR. A TNF-induced gene expression program under oscillatory NF-kappaB control. BMC Genomics 2005;6:137.
15. Nelson DE, Ihekwaba AEC, Elliott M, Johnson JR, Gibney CA, Foreman BE, et al. Oscillations in NF-kappaB signaling control the dynamics of gene expression. Science 2004;306:704–708.
16. Perkins ND. Post-translational modifications regulating the activity and function of the nuclear factor kappa B pathway. Oncogene 2006;25:6717–6730.
17. Iwai K. Diverse ubiquitin signaling in NF-κB activation. Trends Cell Biol 2012;22:355–364.
18. Wajant H, Scheurich P. TNFR1-induced activation of the classical NF-κB pathway. FEBS J 2011;278:862–876.
19. Werner SL, Kearns JD, Zadorozhnaya V, Lynch C, O'Dea E, Boldin MP, et al. Encoding NF-kappaB temporal control in response to TNF: distinct roles for the negative regulators IkappaBalpha and A20. Genes Dev 2008;22:2093–2101.
20. Puigvert JC, de Bont H, van de Water B, Danen EHJ. High-throughput live cell imaging of apoptosis. Curr Protoc Cell Biol 2010;Chapter 18:Unit 18.10.1–13.
21. Poser I, Sarov M, Hutchins JRA, Hériché J-K, Toyoda Y, Pozniakovsky A, et al. BAC TransgeneOmics: a high-throughput method for exploration of protein function in mammals. Nat Methods 2008;5:409–415.
22. Hendriks G, Atallah M, Morolli B, Calléja F, Ras-Verloop N, Huijskens I, et al. The ToxTracker assay: novel GFP reporter systems that provide mechanistic insight into the genotoxic properties of chemicals. Toxicol Sci 2012;125:285–298.
23. Takami Y, Nakagami H, Morishita R, Katsuya T, Cui T-X, Ichikawa T, et al. Ubiquitin carboxyl-terminal hydrolase L1, a novel deubiquitinating enzyme in the vasculature, attenuates NF-kappaB activation. Arterioscler Thromb Vasc Biol 2007;27:2184–2190.
24. Tan P, Fuchs SY, Chen A, Wu K, Gomez C, Ronai Z, et al. Recruitment of a ROC1-CUL1 ubiquitin ligase by Skp1 and HOS to catalyze the ubiquitination of I kappa B alpha. Mol Cell 1999;3:527–533.
25. Gorska MM, Liang Q, Stafford SJ, Goplen N, Dharajiya N, Guo L, et al. MK2 controls the level of negative feedback in the NF-kappaB pathway and is essential for vascular permeability and airway inflammation. J Exp Med 2007;204:1637–1652.
26. Rzymski T, Grzmil P, Meinhardt A, Wolf S, Burfeind P. PHF5A represents a bridge protein between splicing proteins and ATP-dependent helicases and is differentially expressed during mouse spermatogenesis. Cytogenet Genome Res 2008;121:232–244.
27. Kant S, Schumacher S, Singh MK, Kispert A, Kotlyarov A, Gaestel M. Characterization of the atypical MAPK ERK4 and its activation of the MAPK-activated protein kinase MK5. J Biol Chem 2006;281:35511–35519.
28. Shiryaev A, Dumitriu G, Moens U. Distinct roles of MK2 and MK5 in cAMP/PKA- and stress/p38MAPK-induced heat shock protein 27 phosphorylation. J Mol Signal 2011;6:4.
29. Parcellier A, Schmitt E, Gurbuxani S, Seigneurin-Berny D, Pance A, Chantôme A, et al. HSP27

is a ubiquitin-binding protein involved in I-kappaBalpha proteasomal degradation. Mol Cell Biol 2003;23:5790–5802.
30. Park K-J, Gaynor RB, Kwak YT. Heat shock protein 27 association with the I kappa B kinase complex regulates tumor necrosis factor alpha-induced NF-kappa B activation. J Biol Chem 2003;278:35272–35278.
31. Jin Z, Li Y, Pitti R, Lawrence D, Pham VC, Lill JR, et al. Cullin3-based polyubiquitination and p62-dependent aggregation of caspase-8 mediate extrinsic apoptosis signaling. Cell 2009;137:721–735.
32. Bays NW, Hampton RY. Cdc48-Ufd1-Npl4: stuck in the middle with Ub. Curr Biol 2002;12:R366–71.
33. Loyer P, Trembley JH, Katona R, Kidd VJ, Lahti JM. Role of CDK/cyclin complexes in transcription and RNA splicing. Cell Signal 2005;17:1033–1051.
34. Li Q, Yan J, Mao A-P, Li C, Ran Y, Shu H-B, et al. Tripartite motif 8 (TRIM8) modulates TNFα- and IL-1β-triggered NF-κB activation by targeting TAK1 for K63-linked polyubiquitination. Proc Natl Acad Sci U S A 2011;108:19341–19346.
35. Toniato E, Chen XP, Losman J, Flati V, Donahue L, Rothman P. TRIM8/GERP RING finger protein interacts with SOCS-1. J Biol Chem 2002;277:37315–37322.
36. Strebovsky J, Walker P, Lang R, Dalpke AH. Suppressor of cytokine signaling 1 (SOCS1) limits NFkappaB signaling by decreasing p65 stability within the cell nucleus. FASEB J 2011;25:863–874.

References in Table 1

1. Takami Y, Nakagami H, Morishita R, Katsuya T, Cui T-X, Ichikawa T, et al. Ubiquitin carboxyl-terminal hydrolase L1, a novel deubiquitinating enzyme in the vasculature, attenuates NF-kappaB activation. Arterioscler Thromb Vasc Biol 2007;27:2184–2190.
2. Rompe F, Artuc M, Hallberg A, Alterman M, Stroder K, Thone-Reineke C, et al. Direct angiotensin II type 2 receptor stimulation acts anti-inflammatory through epoxyeicosatrienoic acid and inhibition of nuclear factor kappaB. Hypertension 2010;55:924–931.
3. Guo R-W, Yang L-X, Wang H, Liu B, Wang L. Angiotensin II induces matrix metalloproteinase-9 expression via a nuclear factor-kappaB-dependent pathway in vascular smooth muscle cells. Regul Pept 2008;147:37–44.
4. Gorska MM, Liang Q, Stafford SJ, Goplen N, Dharajiya N, Guo L, et al. MK2 controls the level of negative feedback in the NF-kappaB pathway and is essential for vascular permeability and airway inflammation. J Exp Med 2007;204:1637–1652.
5. Lee MH, Mabb AM, Gill GB, Yeh ETH, Miyamoto S. NF-kappaB induction of the SUMO protease SENP2: A negative feedback loop to attenuate cell survival response to genotoxic stress. Mol Cell 2011;43:180–191.
6. Fenner BJ, Scannell M, Prehn JHM. Expanding the substantial interactome of NEMO using protein microarrays. PLoS ONE 2010;5:e8799.
7. Shembade N, Harhaj EW. Regulation of NF-kappaB signaling by the A20 deubiquitinase. Cell Mol Immunol 2012;9:123–130.
8. Hayden MS, Ghosh S. NF-κB, the first quarter-century: remarkable progress and outstanding questions. Genes Dev 2012;26:203–234.
9. Hatzoglou A, Roussel J, Bourgeade MF, Rogier E, Madry C, Inoue J, et al. TNF receptor family member BCMA (B cell maturation) associates with TNF receptor-associated factor (TRAF) 1, TRAF2, and TRAF3 and activates NF-kappa B, elk-1, c-Jun N-terminal kinase, and p38 mitogen-activated protein kinase. J Immunol 2000;165:1322–1330.
10. Alexaki V-I, Pelekanou V, Notas G, Venihaki M, Kampa M, Dessirier V, et al. B-cell maturation antigen (BCMA) activation exerts specific proinflammatory effects in normal human keratinocytes and is preferentially expressed in inflammatory skin pathologies. Endocrinology 2012;153:739–749.
11. Thu KL, Pikor LA, Chari R, Wilson IM, Macaulay CE, English JC, et al. Genetic disruption of KEAP1/CUL3 E3 ubiquitin ligase complex components is a key mechanism of NF-kappaB pathway activation in lung cancer. J Thorac Oncol 2011;6:1521–1529.
12. Lee D-F, Kuo H-P, Liu M, Chou C-K, Xia W, Du Y, et al. KEAP1 E3 ligase-mediated downregulation of NF-kappaB signaling by targeting IKKbeta. Mol Cell 2009;36:131–140.
13. Placke T, Kopp H-G, Salih HR. Glucocorticoid-induced TNFR-related (GITR) protein and its ligand in antitumor immunity: functional role and therapeutic modulation. Clin Dev Immunol 2010;2010:239083.
14. Tan P, Fuchs SY, Chen A, Wu K, Gomez C, Ronai Z, et al. Recruitment of a ROC1-CUL1 ubiquitin ligase by Skp1 and HOS to catalyze the ubiquitination of I kappa B alpha. Mol Cell 1999;3:527–533.
15. Suzuki H, Chiba T, Suzuki T, Fujita T, Ikenoue T, Omata M, et al. Homodimer of two F-box proteins betaTrCP1 or betaTrCP2 binds to IkappaBalpha for signal-dependent ubiquitination. J Biol Chem 2000;275:2877–2884.
16. Minoda Y, Sakurai H, Kobayashi T, Yoshimura A, Takaesu G. An F-box protein, FBXW5, negatively

regulates TAK1 MAP3K in the IL-1beta signaling pathway. Biochem Biophys.Res Commun 2009;381:412–417.
17. Israël A. The IKK complex, a central regulator of NF-kappaB activation. Cold Spring Harb Perspect Biol 2010;2:a000158.
18. Sun S-C. The noncanonical NF-kappaB pathway. Immunol Rev 2012;246:125–140.
19. Tan J, Kuang W, Jin Z, Jin F, Xu L, Yu Q, et al. Inhibition of NFkappaB by activated c-Jun NH2 terminal kinase 1 acts as a switch for C2C12 cell death under excessive stretch. Apoptosis 2009;14:764–770.
20. Zha J, Han K-J, Xu L-G, He W, Zhou Q, Chen D, et al. The Ret finger protein inhibits signaling mediated by the noncanonical and canonical IkappaB kinase family members. J Immunol 2006;176:1072–1080.
21. Li Q, Yan J, Mao A-P, Li C, Ran Y, Shu H-B, et al. Tripartite motif 8 (TRIM8) modulates TNFα- and IL-1β-triggered NF-κB activation by targeting TAK1 for K63-linked polyubiquitination. Proc Natl Acad Sci U S A 2011;108:19341–19346.
22. Toniato E, Chen XP, Losman J, Flati V, Donahue L, Rothman P. TRIM8/GERP RING finger protein interacts with SOCS-1. J Biol Chem 2002;277:37315–37322.
23. Strebovsky J, Walker P, Lang R, Dalpke AH. Suppressor of cytokine signaling 1 (SOCS1) limits NFkappaB signaling by decreasing p65 stability within the cell nucleus. FASEB J 2011;25:863–874.
24. Kovalenko A, Chable-Bessia C, Cantarella G, Israël A, Wallach D, Courtois G. The tumour suppressor CYLD negatively regulates NF-kappaB signalling by deubiquitination. Nature 2003;424:801–805.
25. Gewurz BE, Towfic F, Mar JC, Shinners NP, Takasaki K, Zhao B, et al. Genome-wide siRNA screen for mediators of NF-kappaB activation. Proc Natl Acad Sci U S A 2012;109:2467–2472.
26. Li S, Zheng H, Mao A-P, Zhong B, Li Y, Liu Y, et al. Regulation of virus-triggered signaling by OTUB1- and OTUB2-mediated deubiquitination of TRAF3 and TRAF6. J Biol Chem 2010;285:4291–4297.
27. Komander D, Barford D. Structure of the A20 OTU domain and mechanistic insights into deubiquitination. Biochem J 2008;409:77–85.
28. Schweitzer K, Bozko PM, Dubiel W, Naumann M. CSN controls NF-kappaB by deubiquitinylation of IkappaBalpha. EMBO J 2007;26:1532–1541.

SUPPORTING DATA

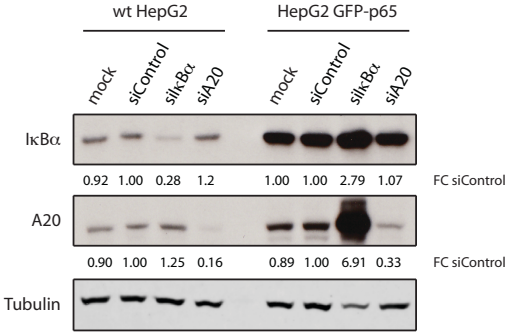

Supporting Data S1. *siRNA-mediated knockdown is successful in wildtype and GFP-p65 HepG2 cells.* 50 nM siRNA SMARTpool transfection on positive controls, siA20 and siIκBα results in successful knockdown using INTERFERin tranfection reagent, as determined by western blotting. In GFP-p65 cells the siIκBα results in higher IκBα levels after 72 hours of knockdown, since knockdown of this inhibitor leads to enhanced p65 activity during this period and thereby increased IκBα transcription.

Supporting Data S2. *Expression of IκBα-GFP does not enhance the levels of the protein.* Stable expression of BAC-IκBα-GFP does not result in overexpression of this protein. Furthermore, the GFP-tagged version of this protein behaves as the endogenous protein following TNFα (10 ng/mL) exposure, as determined by western blotting.

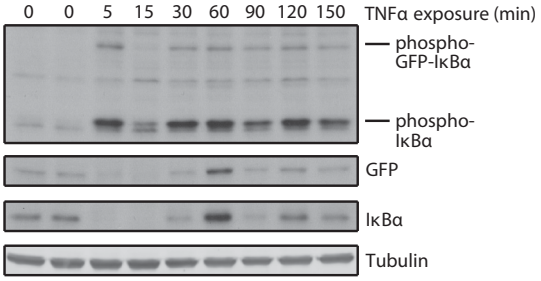

6

Discussion and conclusion

Lisa Fredriksson

The occurrence of adverse drug reactions (ADRs) is a significant problem both for society and for the drug-industry. A few decades ago, the biggest challenge during drug development was poor bioavailability and pharmacokinetics. This has now shifted towards issues related to ADRs, of which idiosyncratic drug-induced liver injury (iDILI) is the most common.

To tackle the ADR problems in drug development, there is need to better understand the underlying molecular mechanisms of ADRs. An improved mechanistic foundation of iDILI would open doors to establish new pre-clinical *in vitro* and *in vivo* tests that represent the most important programs that underlie iDILI. These would allow the removal of candidate drugs with a high likelihood of iDILI-inducing potential from further development at an early stage. In addition, such mechanistic insight could allow individualization of drug therapy by avoiding certain drug therapies for susceptible individuals, while maintaining access of these same drugs for patients that benefit from its actions without any demonstration of ADR. Finally, such a mechanistic understanding could help patients already suffering from ADRs, by providing candidate therapeutic strategies for protection, adaption or recovery.

In this thesis I have investigated the involvement of the pro-inflammatory cytokine tumor necrosis factor-alpha (TNFα), in the toxicity of drugs that are known to cause iDILI in humans. I have given special attention to the non-steroidal anti-inflammatory drug diclofenac (DCF) and the anticonvulsant carbamazepine (CBZ). A variety of techniques including high content imaging of cell toxicity, cell based fluorescent reporters of drug-induced and inflammatory stress, and toxicogenomics, allowed me to present in depth understanding of the mechanisms that could be involved in iDILI.

The role of TNFα-signaling in DILI

The immune system is known to play a major role in the development of adverse drug reactions, and especially of DILI. In relation to this, both the innate and the adaptive immune system have been shown to play an important role. However, irrespective of which part of the immune system gets activated, the main mediators of their activity are cytokines.

The role of inflammatory stress in iDILI has been most extensively studied in the group of Patricia Ganey and Robert Roth. They have developed an animal model in which the severity of human iDILI has been replicated the best thus far (1). In this model, non-toxic doses of drugs like diclofenac, sulindac, trovafloxacin and amiodarone have been rendered toxic by the addition of a non-toxic dose of the bacterial endotoxin lipopolysaccharide (LPS). Although LPS, when absorbed from the intestines to the circulation, and thereby reaching the liver, causes activation of the liver stationary macrophages (Kupffer cells), the main source of injury in this model is infiltrating neutrophils (2-4). However, importantly, TNFα, a cytokine secreted by both macrophages and neutrophils, has been shown to be indispensible for the liver injury seen in these models (5,6). In **chapter 2**, for the first time, I show that this cytokine can significantly

enhance the toxicity of diclofenac in an *in vitro* model using HepG2 cells, providing a good cell system for the study of the detailed mechanism(s) behind the role of inflammatory stress in DILI.

The unique role of the TNF receptor in the decision between life and death

The TNF receptor 1 (TNFR1) is unique among other cytokine receptors in the sense that it can induce both pro-survival and pro-apoptotic signaling. In **chapter 2**, I demonstrated that diclofenac and TNFα co-exposure leads to an enhanced amount of apoptosis, compared to exposure to the drug or the cytokine alone. Next, I showed that this apoptosis is strictly dependent on caspase-8 activity. This suggests that diclofenac is sensitizing the cells to TNFα-induced apoptosis rather than the other way around. Necroptosis is a novel mechanism by which TNFα can induce cell killing in a caspase independent manner (7). However, I show that the DCF/TNFα-induced cytotoxicity, in these cells, is solely dependent on apoptosis and seems not to involve necroptosis, since z-VAD-fmk, a pan-caspase inhibitor, could completely inhibit the cytotoxicity induced.

In **chapter 2**, I also show an important role for c-Jun N-terminal kinase (JNK) in the induction of DCF/TNFα-induced apoptosis. JNK is known to induce apoptotic signaling after prolonged activation by the disruption of mitochondrial membrane integrity. Since the apoptosis is completely caspase-8 dependent, I propose that the pro-apoptotic role of JNK most likely occurs upstream of the mitochondria by controlling proteins at the proximity of casaspe-8 activity control. Indeed, JNK regulates the expression of cellular FLICE-like inhibitory protein (c-FLIP), the endogenous inhibitor of caspase-8, by phosphorylation of the E3 ubiquitin ligase Itch (8). Furthermore, more recently, TRAF7 was described as an inducer of JNK activity downstream of the TNFR1 and additionally as a regulator of c-FLIP by inducing its degradation (9). This provides another common factor between the stress kinase JNK and the anti-apoptotic protein c-FLIP. Interestingly, the gene encoding the c-FLIP protein (CFLAR), was down-regulated after DCF and CBZ exposure of HepG2 cells (**chapter 4**), further supporting the potential role for c-FLIP in the survival of drug/TNFα co-exposed cells. Additionally, siRNA-mediated knockdown of CFLAR led to induction of DCF/TNFα-induced apoptosis, as shown in **chapter 2**. Recently, a mouse model with a conditional liver specific c-FLIP deletion was described (10). This mouse presented enhanced liver injury upon exposure to D-galactosamine and LPS, which induces liver cell death by activation of TNFR1. The cell death was also dependent of JNK activity, which suggests a bidirectional regulation of JNK and c-FLIP. A role for c-FLIP expression levels in regulating DILI under in vivo conditions needs further investigation.

CFLAR is one of the anti-apoptotic target genes of nuclear factor kappaB (NF-κB), the most important transcription factor induced down-stream of the TNFR1 upon TNFα exposure. In **chapter 2** I described how diclofenac pre-exposure leads to a delay in the cytosol-to-nuclear translocation pattern of NF-κB using high content imaging of a GFP-tagged canonical NF-κB subunit, p65 (RelA). The strength, duration and type

of oscillatory pattern of NF-κB determines the set of NF-κB target genes that will be transcribed after TNFR1 activation (11-13). Thus, a delay in the NF-κB translocation response may very well lead to a differential regulation of the crucial target genes and thereby affect the activation of the pro-apoptotic pathway downstream of TNFR1. This provides a potential explanation to why pre-exposure to certain drugs result in a greater sensitivity to TNFα; however it needs further detailed investigations.

A shift in the NF-κB translocation response upon drug exposure does not *per se* result in enhanced apoptosis by any hepatotoxicant. This was observed in **chapter 3**, where three different high content imaging methods were used to assess apoptotic synergism with TNFα, induction of oxidative stress and ability to cause a shift in the TNFα-induced NF-κB nuclear translocation response. A panel of 15 drugs, including several iDILI-inducing compounds, was used. Interestingly, the majority of the compounds that were able to induce an oxidative stress response as monitored by the Nrf2-dependent expression of Srxn1, also caused an inhibition of NF-κB activation. This is in agreement with other reports (14,15). Yet, a conclusive link between oxidative stress induction, NF-κB nuclear translocation shift and TNFα apoptotic synergism could not be made for all compounds.

Translation initiation and mRNA processing - crucial determinants of TNFα-signaling

The lack of a direct link between oxidative stress-induction and increased sensitivity to TNFα calls for an alternative mechanism. Glutathione depletion (especially mitochondrial) also causes sensitization to TNFα-induced apoptosis (16,17). In this thesis I did not assess (mitochondrial) GSH after drug exposure, which could be an explanation for the differences in the TNFα-synergism. However, to explain the DCF/TNF and CBZ/TNF synergism, in **chapter 4** we applied a toxicogenomics approach and determined the gene transcription profiles after exposure to synergizing drugs DCF and CBZ compared to the hepatotoxicants ketoconazole, nefazodone and the far less toxic methotrexate. For the first time, I in this chapter describe translation initiation as a crucial process for the control of TNFα-induced hepatocyte-toxicity. The translation initiation factor EIF4A1 was selectively up-regulated after diclofenac and carbamazepine exposure. Intriguingly, knockdown of this RNA helicase using transient siRNA gene silencing led to a marked protection against drug/TNFα-induced apoptosis. Also the transcription of other translation initiation factors was affected, including a close family member of EIF4A1, EIF4A2. Yet, knockdown of EIF4A2 did not affect apoptosis. Only until recently, there was no difference in action described between EIF4A1 and EIF4A2 and they were presumed to have redundant functions. However, interestingly, selective knockdown of EIF4A1 can apparently increase the expression of EIF4A2. Yet, this did not completely compensate for the loss of EIF4A1, possibly due to differences in enzymatic activity or substrate specificity (18). This could also form the basis for the discrepancy between the two isoforms in our hands.

Inhibition of EIF4A in general (without isoform specificity) using the pharmacological inhibitor hippuristanol, has been described to result in selective inhibition of translation of injurious proteins, while translation of protective proteins remained intact (19). A similar scenario could be set in our case, where selective inhibition of EIF4A1 by knockdown, would result in decreased translation of crucial apoptotic proteins including CHOP, as was described in **chapter 4**, while translation of essential anti-apoptotic proteins would remain intact or even enhanced, due to increased activity of EIF4A2 upon EIF4A1 inhibition. The role for translation initiation in drug-induced liver injury is an unexplored area. My data indicate that this clearly deserves more attention both in the context of DILI but also in relation to other liver pathological conditions.

I searched for novel regulators of NF-κB nuclear translocation in **chapter 5**. Interestingly, two of the candidate genes whose knockdown had a significant effect on the TNFα-induced nuclear translocation of NF-κB are involved in mRNA splicing: splicing factor PHF5A and the cyclin dependent kinase CDK12 (20,21). Despite the fact that CDK12 has also been implicated in gene-set specific transcription by its phosphorylation of RNA polymerase II (22), this further emphasizes the important role for post-transcriptional regulation of protein expression in a situation of cellular stress. Interestingly, depletion PHF5A or CDK12 led to a "delayed" translocation phenotype under DMSO conditions, much like the one seen by diclofenac pre-treatment. Additionally, knockdown of PHF5A led to a slight enhancement of apoptosis induced by TNFα under DMSO conditions (observation not shown). This suggests aberrant mRNA splicing as a mechanism for diclofenac-induced inhibition of NF-κB translocation as well as induction of apoptosis after TNFα exposure. The description of similar substrate specificity between EIF4A1 initiated translation and PHF5A and CDK12 mediated mRNA splicing, would provide further mechanistic insight to how certain drugs can sensitize towards TNFα-induced apoptosis and thereby induce DILI. It would be relevant to investigate the expression of c-FLIP after knockdown of EIF4A1, PHF5A and CDK12.

A central role for A20 in regulating cell death and survival in TNFα-signaling

I demonstrated that perturbations in NF-κB signaling are critical in drug-induced hepatocyte cell death. NF-κB is well known for its involvement in the transcription of genes involved in for example inflammation, survival and proliferation. However, inappropriate activity of NF-κB signaling has been linked to the development of (liver) cancer, but also of autoimmune and inflammatory diseases (23). Therefore, the identification of novel regulators of the NF-κB signaling would provide improved insight for both hepatotoxicity as well as (liver) carcinogenesis. We focused on the NF-κB translocation response for our siRNA screen. Interestingly, most of our hits from the screen inhibited the NF-κB translocation response (described as "no oscillation"). Additionally, we were able to link this "no oscillation" phenotype to inhibition of drug/TNFα-induced apoptosis. "No oscillation" could be explained by inhibition of TNFR1 activation, which would also result in inhibition of TNFR1-mediated apoptosis. This suggests that the knockdown of these

candidate genes would affect the assembly of TNFR1 downstream signaling complexes, thereby preventing the pro-survival NF-κB signaling, but also preventing the pro-apoptotic caspase-8 activation. We showed that a common denominator for the knockdowns that inhibited both processes was the expression of the protein A20.

A20, or TNFAIP3, is a target gene of NF-κB and constitutes, together with IκBα (NFKBIA), the most important transcriptionally regulated feedback mechanisms to down-regulate NF-κB activation (24). A20 inhibits NF-κB signaling by deubiquitinating receptor-interacting protein 1 (RIP1) and subsequently targeting this protein for proteasomal degradation by ubiquitin ligation (25). However, apart from its role in terminating the NF-κB signaling, A20 has a crucial role in regulating the apoptotic response after TNFα exposure as demonstrated in an A20-deficient mouse model (26). The inhibition of apoptosis has been shown to occur via deubiquitination of caspase-8 downstream of the death receptor 4 and 5 (27). Further research in this topic is however needed to clarify the exact role of A20 in repression of the pro-apoptotic signaling downstream of the TNFR1. One possibility is that A20 is involved in the direct switching from anti-apoptotic complex I formation, to pro-apoptotic complex II initiation, and thereby regulating the apoptosis induced by TFNα.

Because of its dual role in the regulation of TNFα and other immune-mediated signaling, A20 has been thoroughly investigated as a key mediator in cancer and chronic- as well as autoimmune disease. Moreover this gene has been described as a susceptibility locus for the development of such diseases (28). Together with its protecting role in drug/TNFα-induced liver cell death, further studies on the regulation of A20 expression in DILI is needed. In **chapter 5** I describe four novel regulators of A20 expression, CDK12, UFD1L, TRIM8 and RNF126. Importantly, knockdown of these genes resulted in an enhanced expression of A20 leading to the inhibition of TNFα-induced NF-κB nuclear translocation, as well as apoptosis under drug pre-exposure conditions. Further investigation on how this regulation occurs is relevant to exploit this pathway to treat chronic inflammatory and autoimmune diseases as well as cancer, in which A20 has been shown to play an important role (28).

The future for *in vitro* hepatotoxicity assessment

A golden standard for human liver toxicity testing in a pre-clinical setting is the use of primary or cryo-preserved human hepatocytes. However, this cell system has been proven difficult to work with, as the batch-to-batch variability in the cellular responses is large, and as the cells go through rapid dedifferentiation. The use of HepG2 cells is then an attractive option since these cells, as an immortal cell line, show low variability in between experiments and allow detailed mechanistic research using techniques such as the functional genomics screening in this thesis. Granted an important drawback of using a transformed cell line such as HepG2 is its low drug-metabolizing capacity. Yet, while HepG2 cells show low phase I metabolizing activity (29), its phase II metabolism is more adequate, leaving them as an acceptable cellular system for the study of drug-toxicity

induced by certain drug-metabolites (30). Furthermore, and critically importantly for our research, the acyl-glucuronide metabolite for the induction of idiosyncratic diclofenac-mediated liver injury, could be readily identified in our culture system (chapter 2).

An additional advantage of the HepG2 cells is that they can be easily engineered to express for example GFP-tagged proteins as reporters for different types of intracellular stress. This was first introduced in **chapter 2** using a GFP-p65 reporter cell line, and further expanded in more detail in **chapter 3**. Here it is nicely illustrated how the combination of a few different cellular assays, can be used to estimate the toxicity potential of novel drug candidates. Although in the end not proven to result in apoptosis in our cellular system, the capability of a drug to induce oxidative stress as detected by the Srxn1-GFP reporter, or its ability to inhibit the nuclear translocation response of NF-κB, can provide enough information from a toxicological perspective. Especially since both these events have been linked to enhanced drug toxicity *in vivo* (see chapter 1).

Multi-parametric analysis of cells stained with different dyes to assess different drugs' hepatotoxic potential has recently been described as a high throughput method for fast assessment of (mode of) toxicity (31). However, such a method involves different sample preparation steps as well as the limitation of a fixed-time-point. Instead an extended panel of *in vitro* reporters of different types of cellular stresses known to be involved in drug-induced liver injury, similar to the stress reporters described in **chapter 3**, would constitute an important asset to the pharmaceutical safety assessment. These would provide minimal amount of wet-work, resulting in reduced variability. Since GFP-based reporter systems allow live cell imaging of stress responses, kinetic information about the toxicity onset on a cell-to-cell basis provides additional valuable information. In addition, different GFP stress reporter cell lines would provide important mechanistic information about the pathways of toxicity that are induced by drug exposure. When considering the results from **chapter 4**, I would additionally suggest reporters for CHOP and EIF4A1-induction, as a part of the pre-clinical *in vitro* tox-screening panel. These proteins were both up-regulated after liver-toxic drug exposure and functionally critical for the drug/TNFα-induced synergistic toxicity.

The use of induced pluripotent stem cells (iPSCs) that are later differentiated into hepatocytes is becoming an increasingly attractive alternative for *in vitro* toxicity testing. These newly differentiated cells seem more "hepatocyte-like" than HepG2 cells when it comes to for example drug metabolism capacity (32). In an ideal world, these could also be used for stress reporter construction, as this background would be even more relevant to the human situation compared to the HepG2 cells. Interestingly, considering the individual variances in drug responses, projects are underway to generate iPSCs, and subsequently hepatocytes, from patients experiencing iDILI (33). This would provide very important information on the hepatocyte-based molecular mechanisms underlying ADRs in highly susceptible patients.

CONCLUSION

In this thesis I used an *in vitro* model to study the role of inflammatory stress in idiosyncratic DILI. I have described in detail the interplay between hepatotoxicant- and cytokine-induced signaling in liver cell death. Two drugs, diclofenac and carbamazepine, which have been associated with inflammatory DILI in humans, showed an exceptionally strong synergistic response with the pro-inflammatory cytokine TNFα. This response was linked to the inhibition of NF-κB signaling (chapter 2 and 3) and the induction of oxidative as well as to onset of endoplasmic reticulum and translation-dependent stress (chapter 3 and 4). Finally in chapter 5, I described novel regulators of A20 expression and indirectly of NF-κB signaling as well as apoptosis induction. Potentially these genes could be used as markers for inflammatory diseases as well as susceptibility markers for the development of DILI. Moreover, I anticipate that more detailed studies of post-transcriptional regulation will provide further important information about the mechanisms behind drug-induced liver injury.

The findings reported in this thesis provide important contributions to the understanding of the mechanisms behind drug-induced liver-injury. This deeper understanding may aid in the development of advanced pre-clinical drug safety assessment models for novel candidate drugs. Furthermore, I anticipate that the novel findings regarding the regulation of NF-κB activation can contribute to areas beyond drug-induced liver injury, including inflammatory and autoimmune diseases, as well as cancer.

REFERENCES

1. Roth RA, Ganey PE. Animal models of idiosyncratic drug-induced liver injury--current status. Crit Rev Toxicol. 2011;41:723–739.
2. Deng X, Stachlewitz RF, Liguori MJ, Blomme EAG, Waring JF, Luyendyk JP, et al. Modest inflammation enhances diclofenac hepatotoxicity in rats: role of neutrophils and bacterial translocation. J Pharmacol Exp Ther. 2006;319:1191–1199.
3. Barton CC, Barton EX, Ganey PE, Kunkel SL, Roth RA. Bacterial lipopolysaccharide enhances aflatoxin B1 hepatotoxicity in rats by a mechanism that depends on tumor necrosis factor alpha. Hepatology. 2001;33:66–73.
4. Waring JF, Liguori MJ, Luyendyk JP, Maddox JF, Ganey PE, Stachlewitz RF, et al. Microarray analysis of lipopolysaccharide potentiation of trovafloxacin-induced liver injury in rats suggests a role for proinflammatory chemokines and neutrophils. J Pharmacol Exp Ther. 2006;316:1080–1087.
5. Tukov FF, Luyendyk JP, Ganey PE, Roth RA. The role of tumor necrosis factor alpha in lipopolysaccharide/ranitidine-induced inflammatory liver injury. Toxicol Sci 2007;100:267–280.
6. Shaw PJ, Hopfensperger MJ, Ganey PE, Roth RA. Lipopolysaccharide and trovafloxacin coexposure in mice causes idiosyncrasy-like liver injury dependent on tumor necrosis factor-alpha. Toxicol Sci 2007;100:259–266.
7. Vandenabeele P, Galluzzi L, Vanden Berghe T, Kroemer G. Molecular mechanisms of necroptosis: an ordered cellular explosion. Nat Rev Mol Cell Biol. 2010;11:700–714.
8. Chang L, Kamata H, Solinas G, Luo J-L, Maeda S, Venuprasad K, et al. The E3 ubiquitin ligase itch couples JNK activation to TNFalpha-induced cell death by inducing c-FLIP(L) turnover. Cell. 2006;124:601–613.
9. Scudiero I, Zotti T, Ferravante A, Vessichelli M, Reale C, Masone MC, et al. Tumor necrosis factor (TNF) receptor-associated factor 7 is required for TNFα-induced Jun NH2-terminal kinase activation and promotes cell death by regulating polyubiquitination and lysosomal degradation of c-FLIP protein. J Biol Chem. 2012;287:6053–6061.
10. Schattenberg JM, Zimmermann T, Wörns M, Sprinzl MF, Kreft A, Kohl T, et al. Ablation of c-FLIP in hepatocytes enhances death-receptor mediated apoptosis and toxic liver injury in vivo. J Hepatol. 2011;55:1272–1280.
11. Ashall L, Horton CA, Nelson DE, Paszek P, Harper CV, Sillitoe K, et al. Pulsatile stimulation determines timing and specificity of NF-kappaB-dependent transcription. Science. 2009;324:242–246.
12. Tian B, Nowak DE, Brasier AR. A TNF-induced gene expression program under oscillatory NF-kappaB control. BMC Genomics. 2005;6:137.
13. Nelson DE, Ihekwaba AEC, Elliott M, Johnson JR, Gibney CA, Foreman BE, et al. Oscillations in NF-kappaB signaling control the dynamics of gene expression. Science. 2004;306:704–708.
14. Nagai H, Matsumaru K, Feng G, Kaplowitz N. Reduced glutathione depletion causes necrosis and sensitization to tumor necrosis factor-alpha-induced apoptosis in cultured mouse hepatocytes. Hepatology. 2002;36:55–64.
15. Han D, Hanawa N, Saberi B, Kaplowitz N. Hydrogen peroxide and redox modulation sensitize primary mouse hepatocytes to TNF-induced apoptosis. Free Radic. Biol. Med. 2006;41:627–639.
16. Lou H, Kaplowitz N. Glutathione depletion down-regulates tumor necrosis factor alpha-induced NF-kappaB activity via IkappaB kinase-dependent and -independent mechanisms. J Biol Chem 2007;282:29470–29481.
17. Matsumaru K, Ji C, Kaplowitz N. Mechanisms for sensitization to TNF-induced apoptosis by acute glutathione depletion in murine hepatocytes. Hepatology. 2003;37:1425–1434.
18. Galicia-Vázquez G, Cencic R, Robert F, Agenor AQ, Pelletier J. A cellular response linking eIF4AI activity to eIF4AII transcription. RNA. 2012;18:1373–1384.
19. Bottley A, Phillips NM, Webb TE, Willis AE, Spriggs KA. eIF4A Inhibition Allows Translational Regulation of mRNAs Encoding Proteins Involved in Alzheimer's Disease. PLoS ONE. 2010;5:e13030.
20. Rzymski T, Grzmil P, Meinhardt A, Wolf S, Burfeind P. PHF5A represents a bridge protein between splicing proteins and ATP-dependent helicases and is differentially expressed during mouse spermatogenesis. Cytogenet. Genome Res. 2008;121:232–244.
21. Loyer P, Trembley JH, Katona R, Kidd VJ, Lahti JM. Role of CDK/cyclin complexes in transcription and RNA splicing. Cellular Signalling. 2005;17:1033–1051.
22. Blazek D, Kohoutek J, Bartholomeeusen K, Johansen E, Hulinkova P, Luo Z, et al. The Cyclin K/Cdk12 complex maintains genomic stability via regulation of expression of DNA damage response genes. Genes Dev. 2011;25:2158–2172.
23. Hayden MS, Ghosh S. Shared principles in NF-kappaB signaling. Cell. 2008;132:344–362.
24. Renner F, Schmitz ML. Autoregulatory feedback loops terminating the NF-kappaB response. Trends Biochem. Sci. 2009;34:128–135.
25. Heyninck K, Beyaert R. A20 inhibits NF-kappaB activation by dual ubiquitin-editing functions. Trends

Biochem. Sci. 2005;30:1–4.
26. Lee EG, Boone DL, Chai S, Libby SL, Chien M, Lodolce JP, et al. Failure to regulate TNF-induced NF-kappaB and cell death responses in A20-deficient mice. Science. 2000;289:2350–2354.
27. Jin Z, Li Y, Pitti R, Lawrence D, Pham VC, Lill JR, et al. Cullin3-based polyubiquitination and p62-dependent aggregation of caspase-8 mediate extrinsic apoptosis signaling. Cell. 2009;137:721–735.
28. Vereecke L, Beyaert R, van Loo G. The ubiquitin-editing enzyme A20 (TNFAIP3) is a central regulator of immunopathology. Trends Immunol. 2009;30:383–391.
29. Westerink WMA, Schoonen WGEJ. Cytochrome P450 enzyme levels in HepG2 cells and cryopreserved primary human hepatocytes and their induction in HepG2 cells. Toxicol In Vitro. 2007;21:1581–1591.
30. Westerink WMA, Schoonen WGEJ. Phase II enzyme levels in HepG2 cells and cryopreserved primary human hepatocytes and their induction in HepG2 cells. Toxicol In Vitro. 2007;21:1592–1602.
31. Tolosa L, Pinto S, Donato MT, Lahoz A, Castell JV, O'Connor JE, et al. Development of a multiparametric cell-based protocol to screen and classify the hepatotoxicity potential of drugs. Toxicol Sci. 2012;127:187–198.
32. Kia R, Sison R, Heslop J, Kitteringham NR, Hanley N, Millis JS et al. Stem cell-derived hepatocytes as a predictive model for drug-induced liver injury: are we there yet? Br J Clin Pharmacol. Epub 2012 Jun 15.
33. Opar A. Overtaking the DILI Model-T. Nat Rev Drug Discov. 2012;11:585–586.

Nederlandse samenvatting
English summary
Sammanfattning på svenska
List of abbreviations
Curriculum vitae
List of publications
Acknowledgements

NEDERLANDSE SAMENVATTING

Bijwerkingen van medicijnen zijn een groot probleem voor zowel de maatschappij als voor de farmaceutische industrie. Bij ernstige bijwerkingen zijn de kosten hoog; voor de farma-bedrijven in de financiële zin omdat hun product (vroegtijdig) van de markt gehaald moet worden en voor de maatschappij omdat de betrokken individuen mogelijk additionele behandelingsmethodes moeten ondergaan. Dit is nog afgezien van de last voor de patiënten in kwestie.

Leverschade door medicijngebruik is de meest voorkomende bijwerking en zo ook onderliggende reden voor het verwijderen van een medicijn. Dit type bijwerking, in het engels afgekort tot DILI (drug-induced liver injury), schaadt de lever in die zin dat de lever ophoudt met functioneren, met mogelijk dodelijke gevolgen. De lever is één van de meest kwetsbare organen bij medicijngebruik vanwege diens functie: het bloed, dat langs de darmen stroomde, ontdoen van lichaamsvreemde stoffen, inclusief medicijnen. Daarbij worden deze stoffen omgezet naar makkelijk af te voeren stofjes die uitgescheiden kunnen worden via de urine of de gal. Dit omzetten gaat vaak goed en het medicijn wordt navenant afgevoerd. Echter, soms worden ook schadelijke nevenproducten gevormd die de lever kunnen schaden. Of en waarom ernstige leverschade optreedt lijkt af te hangen van het individu.

Voor een aantal medicijnen kan DILI worden verklaard. Paracetamol bijvoorbeeld wordt gedeeltelijk omgezet tot een reactief bijproduct, wat normaliter efficiënt wordt weggevangen door de verdedigingsmechanismen in de lever zolang de inname niet overmatig is, anders leidt het tot leverfalen met dodelijke afloop. Het bijproduct kan worden weggevangen en daarom is de ernstige schade relatief makkelijk te voorkomen. Echter, de oorzaak en het mechanisme van DILI door andere medicijnen is vaak nog niet bekend. Omdat DILI niet vaak voorkomt maar wel zeer ernstig kan zijn, is het wenselijk om te weten te komen hoe dit proces zich ontwikkelt om het uiteindelijk te kunnen voorkomen. Een beter inzicht in de toedracht leidt mogelijk tot testsystemen die gebruikt kunnen worden door de farmaceutische industrie om te voorkomen dat dit type schadelijke medicijnen nooit op de markt gebracht worden. Mijn proefschrift gaat over dit belangrijke probleem; waarom treden deze onverklaarbare bijwerkingen op in de lever en welke testsystemen kunnen we opzetten om nieuwe kandidaat-medicijnen op veiligheid te testen?

Het is al bekend dat niet alleen het omzetten van of het metabolisme van een stof de lever kan beschadigen, maar ook dat het immuunsysteem een belangrijke rol speelt in dit proces. Met deze kennis hebben we in **Hoofdstuk 2** de synergie-hypothese getest: het tegelijkertijd blootstellen van gekweekte levercellen aan een stof die DILI veroorzaakt en een cytokine die ontstekingen bevordert, leidt tot meer celdood dan beide componenten an sich. We testten deze hypothese voor de modelstof diclofenac, de niet-schadelijke controlestof naproxen en de cytokine TNFα: tumor necrosis factor α. Met dit model ontdekten we dat TNFα inderdaad de celdood bevordert in aanwezigheid van diclofenac, maar niet op zichzelf of in aanwezigheid van naproxen. Dit effect bleek in gang

te worden gezet door diclofenac, dat de levercellen gevoelig maakt voor de schaduwzijde van TNFα, en niet andersom. TNFα stimuleert namelijk overlevingsmechanismen binnen een cel, maar tegelijkertijd ook celdood. De balans tussen deze tegenovergestelde signaalcascades helt normaliter over naar overleving, maar deze wordt dusdanig verstoord door diclofenac dat de celdood-respons de overhand krijgt, met meer leverschade tot gevolg.

Als medicijnen worden omgezet tot metabolieten leidt dit tot stress in levercellen. In **Hoofdstuk 3** laten we een combinatie van drie microscopie-gebaseerde benaderingen zien om medicijnen op leverschade potentie te testen. Blootstelling aan medicijnen kan oxidatieve stress induceren. Daarom testten we eerst een aantal stoffen, inclusief die medicijnen die onverklaarbare leverschade kunnen veroorzaken, in een reporter systeem voor oxidatieve stress. Hiermee konden we aantonen dat het gros van de stoffen, zo ook diclofenac, oxidative stress veroorzaakt. Dit drukt mogelijk de overlevingsmechanismen die normaliter aangezet worden na TNFα. Daarom onderzochten we de dynamiek van de signaal-cascade volgend op TNFα stimulatie in een toegewijde assay. De mate waarop oxidatieve stress werd geïnduceerd voorspelde echter niet of een medicijn de respons op TNFα negatief zou beïnvloeden. Desalniettemin, zodra we de verkregen informatie combineerden met een derde assay die de celdood meet door toedoen van een combinatie van cytokine en medicijn, vonden we dat de stoffen die zowel oxidatieve stress induceerden en de TNFα-afhankelijke overlevingsresponsen negatief beïnvloedden juist degenen zijn die tot meer celdood leiden in combinatie-condities. Hiermee konden we aantonen dat een combinatie van meetmethodes ingezet kan worden om het leverschadelijke potentiëel van medicijnen te indexeren.

Omdat het optreden van oxidatieve stress niet voorspellend was voor het optreden van leverschade na medicijn en cytokine, is het aannemelijk dat ook andere stress-routes een belangrijke rol spelen. In **Hoofdstuk 4** hebben we dit aangepakt door te kijken naar het genexpressie patroon dat door blootstelling aan DILI-gerelateerde medicijnen wordt geïnduceerd. De focus lag op twee medicijnen waarvan de celdood flink versterkt wordt door TNFα: diclofenac en carbamazepine. Met software die signaalcascades helpt analyseren hebben we de verschillende typen celstress nagelopen. We konden bevestigen dat deze twee stoffen oxidatieve stress induceren en vonden vervolgens ook dat beide de eiwitproductie beïnvloeden. Vooral een specifiek gen, EIF4A1, werd sterk aangezet na blootstelling aan diclofenac en carbamazepine, maar minder door stoffen waarbij TNFα de celdood niet specifiek verergerde. Wat verder interessant is, is dat het specifiek voorkomen dat dit eiwit aangemaakt kan worden voorkomt de celdood. Dit toont aan dat dit eiwit zeer belangrijk is bij de versterking van de celdood na medicijn-blootstelling door TNFα. Mogelijkerwijs kan dit eiwit dienen als merker voor het leverschadelijk effect van stoffen. Anders zou het ook kunnen dienen als een additionele merker voor translationele stress in een microscopische setup vergelijkbaar met het oxidatieve stress reporter-systeem zoals beschreven in hoofdstuk 3, om medicijnen te kunnen monitoren op ernstig DILI-potentiëel.

In hoofdstuk 2 lieten we zien dat diclofenac een verschuiving veroorzaakt in de

overlevingsrespons na TNFα om uit te monden in celdood. Diclofenac voorkomt namelijk de gerichte activiteit van de transcriptie-factor NF-κB waarmee de stof voorkomt dat de genen die voor overleving zorgen niet (goed) aangezet worden. In **Hoofdstuk 5** hebben we systematisch de rol van individuele genen getest in de dynamiek van NF-κB. NF-κB dient in een voorgeprogrammeerde cyclus de kern in en uit te gaan om de juiste genetische respons aan te zetten. We konden enkele nieuwe eiwitten identificeren die deze locatie-wisseling beïnvloeden en ook aantonen dat dit direct invloed heeft op de celdood. Het uitbreiden van de kennis rondom NF-κB regulatie is niet alleen van belang bij het begrijpen van bijwerkingen, maar ook op gebied van celgroei en ontstekingsreacties, processen waarbij NF-κB een belangrijke rol speelt en kennis bijdraagt bij het begrijpen van kanker en chronische ontstekingsziekte.

Samenvattend, het werk dat in dit proefschrift is gepresenteerd is dieper ingegaan op hoe bijwerkingen optreden in de lever en focuste op de rol van ontstekingsreacties in dit proces. De kennis die we hebben verzameld kan mogelijk ingezet worden om nieuwe en betere testmethodes voor toxiciteit te ontwerpen en ontwikkelen om in te zetten voor medicijn-ontwikkeling. Verder denk ik dat het werk dat in hoofdstuk 5 staat, aangaande NF-κB, bij zal dragen aan de kennis op andere onderzoeksgebieden, zoals kanker.

ENGLISH SUMMARY

Adverse drug reactions, more commonly called side effects, are very problematic for both society and pharmaceutical industry. The costs are high in severe cases: for pharmaceutical companies due to the loss of intended income if a drug needs to be removed from the market; for society due to the extra healthcare that is required to treat the affected individuals. And, not to be forgotten, the burden to the patient in question.
Liver damage upon drug intake is the most common type of adverse drug reaction and reason for drug withdrawal. Drug-induced liver injury (DILI) may affect the liver to such an extent that the liver fails to function, which is potentially fatal. One of the major functions of the liver is drug clearance, meaning that it monitors the blood coming from the intestines for foreign substances, including drugs, takes these up and modifies them to species (metabolites) that can be removed via the urine or bile. Often this drug clearance process runs without trouble; however, sometimes drug metabolites are formed that actively damage the liver. Whether and why severe liver damage occurs seems to depend on the individual.

Sometimes DILI can be explained. For example, paracetamol is partially modified to form a harmful side product. Under normal circumstances this is detoxified by the liver's own defense systems, but upon overdose the concentrations exceed the defense potential, resulting in acute liver failure. This process can be counteracted and by that avoided. However, the cause and mechanism of DILI by various other drugs is not (yet) known. Although infrequent, but severe, it is of major interest to prevent unexplainable DILI. Understanding how and why will therefore be very important. The knowledge could result in creating tests for drug safety that can be used by the pharmaceutical industry, to prevent the marketing of harmful drugs. My thesis dealt with this important problem: why does DILI occur and would it be possible to create tests to screen new drug-candidates for (liver) safety?

For some time it is known that not only the drug transformation or metabolism can damage the liver, but there is also a role for the immune system in DILI. Based on this knowledge, we tested in **Chapter 2** the synergy hypothesis: simultaneous exposure to a drug that can cause DILI and a cytokine that promotes inflammation is more harmful to liver cells that are grown in a culture dish, than either of the two components alone. We tested this hypothesis for the model-drug diclofenac, the safe control drug naproxen and combined these with the cytokine TNFα: tumor necrosis factor α. Using this model we could confirm our hypothesis, TNFα indeed enhanced the cell-death response when combined diclofenac, but not by itself or when combined with naproxen. In this chapter we further show that this effect occurs because diclofenac sensitizes the liver cells to the dark side of TNFα, rather than the other way around. TNFα namely stimulates both pro-death as well as pro-survival signals in a cell. Under normal conditions, the balance between these opposites is favored towards survival. However, diclofenac shifts this balance by inhibiting the pro-survival signaling and thus promotes the cell-death response, resulting in enhanced liver cell damage.

The formation of drug metabolites induces stress in liver cells. In **Chapter 3** we demonstrate the combination of three imaging methods to address the liver-injury potential of drugs. First, drug exposure may cause so called oxidative stress. Several drugs, including those that can cause unexplainable DILI, were tested in a imaging-based system to be able to detect this type of stress. This showed that many drugs, including diclofenac, cause oxidative stress. It is known that this might affect the survival-response to TNFα and therefore the activation of this response was monitored. The induction of oxidative stress by itself did not accurately predict the effect on the survival response. However, when this information was combined with the third assay, the cell-death assay to investigate the potential of TNFα to enhance the drug-induced liver cell death, we found that the drugs that both induced oxidative stress and inhibited the TNFα-induced survival signaling, caused more cell death. This demonstrated that a combination of readouts can be used to indicate the liver injury-inducing potential of drugs.

Since the induction of oxidative stress by drugs alone does not fully predict the enhancement of liver cell injury when combined with TNFα, other stress pathways must be involved. In **Chapter 4** we took a gene expression approach to identify the types of signaling that are induced upon drug exposure. For the analysis we focused on two drugs whose toxicity is exceptionally enhanced when combined with TNFα: diclofenac and carbamazepine. Using signaling pathway analysis software we investigated the stress types that are induced by these drugs. This confirmed our earlier findings that these two drugs induce oxidative stress, but additionally indicated that they both affect genes controlling the protein synthesis machinery. Especially one gene, EIF4A1, was enhanced in expression under diclofenac and carbamazepine conditions, but not by drugs whose toxicity is not enhanced by TNFα. Interestingly, preventing this protein from being expressed reduced the amount of dying cells under these conditions. This shows its vital importance in the TNFα-enhanced drug-induced cell death response. Potentially, this gene could be used as a marker for the liver injury potential of drugs. Additionally, it might serve as a marker that can be used in an imaging setup, next to the oxidative stress reporter presented in chapter 3, to identify drugs that cause severe DILI.

In chapter 2 we reported that diclofenac leads to a shift in the survival response to TNFα to favor cell death. Diclofenac does this by inhibiting the activity of the TNFα-responsive transcription factor NF-κB, and thereby prevents the induction of pro-survival genes. In **Chapter 5** we systematically investigated the role of individual proteins in the response dynamics of NF-κB. NF-κB needs to move in and out of the nucleus in a pre-determined manner in order to induce the appropriate genetic response. We identified several novel proteins as being important in controlling this movement, and were able to show that this had a direct impact on the cell death response under drug and TNFα conditions. This expansion of the knowledge about NF-κB regulation is not only important for understanding adverse drug reactions, but also in relation to cell growth and inflammation, which are responses important in areas such as cancer and chronic inflammatory diseases.

In summary, the work presented in this thesis provides a deeper understanding of how adverse drug reactions occur in the liver and emphasized on the role of inflammation in this process. The knowledge we gathered can be used to design and develop novel and better tests for toxicity assessment during drug development and I think that the work presented in chapter 5, the NF-κB screen, will prove useful to other fields of research, including cancer.

SAMMANFATTNING PÅ SVENSKA

Läkemedelsbiverkningar utgör ett stort problem både för samhället och för läkemedelsindustrin. Om biverkningarna som uppstår är mycket allvarliga blir kostnaderna höga: för läkemedelsbolagen på grund av förlorad inkomst om läkemedlet i fråga måste tas bort från marknaden; för samhället i form av sjukvårdskostnader om biverkningarna leder till sjukhusintagning. Biverkningar medför också mycket lidande för patienten i fråga, vilket inte får glömmas.

Leverskada till följd av läkemedelsanvändning är den vanligaste formen av läkemedelsbiverkan och det är också den vanligaste orsaken till att ett läkemedel måste tas bort från marknaden. Läkemedelsorsakad leverskada kan påverka levern till en sådan grad att den slutar att fungera, kallat leversvikt, något som kan leda till döden. En av leverns viktigaste funktioner är att rena blodet från främmande ämnen, också läkemedel, genom att modifiera dem på ett sådant sätt att de lätt kan utsöndras från kroppen, antingen med urinen eller gallan. Oftast fungerar den här oskadliggörande utsöndringsprocessen som den ska, men ibland kan skadliga biprodukter bildas. Om och varför en allvarlig leverskada inträffar eller inte tros bero på omständigheter rörande individen.

Ibland kan den läkemedelsorsakade leverskadan förklaras, givet att man vet vad som vållar den. Till exempel paracetamol är ett läkemedel som delvis omvandlas till en skadlig biprodukt i levern. Normalt sett kan leverns eget försvarssystem ta hand om den här biprodukten men vid överdosering resulterar detta i att försvarssystemet överhettas, vilket i sin tur leder till akut leversvikt. Detta är i många fall dödligt om den överdoserade inte behandlas snabbt. För andra läkemedel finns det däremot (ännu) ingen förklaring till varför vissa individer får leverskador vid en normal dosering. Leverskadorna uppkommer sällan, men det är mycket allvarligt när de väl inträffar, vilket gör att det är väldigt eftertraktat att försöka undvika dem. Att förstå ”varför?” och ”hur?” är därför väldigt angeläget, och den kunskapen skulle kunna användas för att designa tester som kan användas inom läkemedelsindustrin för att undvika att skadliga mediciner kommer till försäljning. Min doktorsavhandling handlar just om detta viktiga problem: varför uppkommer läkemedelsrelaterad leverskada och är det möjligt att ta fram tester som kan användas för att se om ett potentiellt läkemedel riskerar att orsaka detta?

Sedan en tid tillbaka vet man att inte bara läkemedelsmetabolism/-modifikation kan skada levern, men också immunsystemet har visat sig spela en viktig roll. Med denna kunskap i åtanke testade vi i **Kapitel 2** hypotesen att samtidig exponering för ett läkemedel som orsakar oförklarlig leverskada, och en cytokin som orsakar inflammation, leder till mer skada av isolerade leverceller än exponering för de två komponenterna var för sig. Vi testade den här hypotesen med hjälp av det sällan leverskadande läkemedlet diklofenak, det ”säkra” läkemedlet naproxen och den inflammationsorsakande cytokinen TNFα. Med hjälp av den här modellen kunde vi bevisa vår hypotes. Samtidig exponering av leverceller för diklofenak och TNFα ledde till fler döda leverceller jämfört med exponering för de två faktorerna var för sig. Kombinationen TNFα och naproxen resulterade inte

heller i förhöjd celldöd. I samma kapitel presenterar vi också att den ökade celldöden beror på att diklofenak gör levercellerna mer känsliga för TNFα, snarare än det motsatta: att TNFα gör levercellerna mer känsliga för den skadliga effekten av diklofenak. TNFα är intressant på så sätt att den både kan skicka både överlevnads- och dödssignaler till den cell som är utsatt. Normalt sett väger överlevnadssignalerna över, men diklofenak hämmar dem på ett sådant sett att dödssignalerna tar över istället, vilket leder till ökad leverskada.

Då levern bryter ner läkemedel i sitt försök att oskadliggöra och utsöndra dem, kan som redan sagts, skadliga biprodukter bildas. Dessa orsakar stress inne i cellerna. I **Kapitel 3** beskriver vi att kombinationen av tre olika mikroskoperingsmetoder kan användas för att förutspå om ett läkemedel kommer att ha en leverskadande effekt eller inte. Läkemedel kan orsaka så kallad oxidativ stress. Flera läkemedel, inklusive de som kan medföra oförklarlig leverskada, testades för att se om de kunde orsaka sådan typ av stress med hjälp av ett mikroskop. Det visade sig att många läkemedel, inklusive diklofenak, orsakar just oxidativ stress. Det har redan bevisats av andra att detta kan hämma överlevnadssignalerna som skickas av den inflammatoriska cytokinen TNFα, så därför valde vi att också följa aktiveringen av det här svaret med hjälp av ett mikroskop. Det visade sig att bildandet av oxidativ stress i sig själv inte kunde förutspå om överlevnadssignalerna skulle hämmas. Däremot märkte vi att om de här två metoderna kombinerades med en tredje mikroskoperingsmetod som gör det möjligt att övervaka framkallandet av celldöd, så var det möjligt att säga att de läkemedel som båda orsakade oxidativ stress och hämmade TNFαs överlevnadssignaler, orsakade mer celldöd. Detta demonstrerar att en kombination av olika metoder kan användas för att förutspå möjligheten för ett läkemedel att orsaka leverskada.

Eftersom metoden att övervaka uppkomsten av oxidativ stress själv inte kunde förutspå om mer celldöd skulle bli resultatet av samtidig exponering för läkemedel och TNFα, undersökte vi i **Kapitel 4** om läkemedel också kan orsaka annan typ av stress. För att kunna svara på denna fråga använde vi oss av en metod som mäter genuttrycket hos celler vid en given tidpunkt och ett givet tillstånd. För denna analys använde vi oss återigen av diklofenak, men också av karbamazepin som också orsakar mycket celldöd om det kombineras med TNFα, och som också visats vara allvarligt leverskadande i sällsynta fall. Genom att använda en programvarubaserad analysmetod kunde vi bestämma vilken typ av stress som de här två läkemedlen orsakade i levercellerna. Vi kunde därmed bekräfta att både diklofenak och karbamazepin orsakar oxidativ stress, men det visade sig också att de påverkar uttrycket av gener som är involverade i cellens förmåga att producera nya proteiner. Speciellt en gen, EIF4A1, nådde högre nivåer i levercellerna efter behandling med diklofenak och karbamazepin. Om vi förhindrade uttrycket av den här genen kunde vi intressant nog förhindra de förhöjda nivåerna av celldöd som vi såg vid exponering för diklofenak/TNFα och karbamazepin/TNFα. Detta betyder att uttrycket av den här genen är ytterst viktigt för att cellerna ska dö under dessa förhållanden. EIF4A1 skulle möjligtvis kunna användas som en markör för ett läkemedels möjlighet att orsaka leverskada. Alternativt skulle en mikroskoperingsmetod, liknande den som presenterades i kapitel 3 för att mäta oxidativ stress, kunna designas som

ytterligare ett test för att förutspå blivande läkemedels förmåga att orsaka leverskada.

I kapitel 2 beskrev vi att diklofenak hämmar överlevnadssignalerna från TNFα så att dödssignalerna väger över. Sättet som diklofenak gör detta på är genom att hämma transkriptionsfaktorn NF-κB som aktiveras till följd av TNFα-exponering, och på så sätt förhindrar uttrycket av de gener som är ansvariga för överlevnadssignalerna. I **Kapitel 5** undersökte vi systematiskt vilka gener som är ansvariga för att aktiveringen av NF-κB fungerar som den ska. NF-κB måste röra sig in och ut från kärnan av cellen för att se till att rätt sorts gener uttrycks vid rätt tidpunkt. Genom vår systematiska undersökning fann vi flera nya gener som är involverade i NF-κBs rörelsemönster och vi kunde också visa att de påverkar överlevnadssignalerna som skickas från TNFα vid samtidig exponering för läkemedel. Den utökade kunskapen som vi därmed fått om hur NF-κB regleras, är inte bara viktig för att förstå varför läkemedelsbiverkningar i levern uppstår, men den är också viktig i relation till tillväxt av celler och inflammation, vilka är två processer som är betydande i uppkomst av cancer och kroniskt inflammatoriska sjukdomar, till exempel reumatism.

Sammanfattningsvis presenteras i den här avhandlingen, data som ger en djupare förståelse för varför läkemedelsbiverkningar uppstår i levern, med betoning på den roll inflammation har i processen. Kunskapen som vi har fått kan användas för att designa nya tester som läkemedelsföretag kan använda sig av för att bedöma nya läkemedels förmåga att orsaka leverskada. Dessutom tror jag att de data som presenteras i kapitel 5 kommer visa sig användbara inom andra forskningsområden, inklusive cancer.

LIST OF ABBREVIATIONS

ADR	Adverse drug reaction
AIF	Apoptosis-inducing factor
AMAP	3'-hydroxyacetanilide
AMI	Amiodarone
AnxV	Annexin V
APAF1	Apoptosis protease-activating factor 1
APAP	Acetaminophen; paracetamol
ATF4	Activating transcription factor 4
ATF6	Activating transcription factor 6
AUC	Area under curve
BAC	Bacterial artificial chromosome
CBZ	Carbamazepine
cFLIP	Cellular FLICE inhibitory protein
CHOP	C/EBP-homologous protein
CLZ	Clozapine
CYLD	Cylidromatosis
CYP450	Cytochrome P450
DCF	Diclofenac
DILI	Drug-induced liver injury
DMSO	Dimethyl sulfoxide
EIF	Eukaryotic translation initiation factor
ESI	Electrospray ionization
ER	Endoplasmic reticulum
FADD	Fas-associated death domain
GFP	Green fluorescent protein
GPX	Glutathione peroxidase
GRP	Glucose-regulated protein
GSH	Glutathione
GST	Glutathione S-transferase
HLA	Human leukocyte antigen
HMGB1	High mobility group box 1
HSP	Heatshock protein
IAP	Inhibitor of apoptosis protein
iDILI	idiosyncratic drug-induced liver injury
IFN-γ	Interferon-γ
IκB	Inhibitor of κB
IKK	IκB kinase
IL-1β	Interleukin-1β
IL-6	Interleukin-6
INH	Isoniazid

IPA®	Ingenuity Pathway Analysis
IRE-1α	Inositol-requiring enzyme 1α
JNK	c-Jun N-terminal kinase
Keap1	Kelch-like ECH-associated protein 1
KTZ	Ketoconazol
LDH	Lactate dehydrogenase
LPS	Lipopolysaccharide
MAPK	Mitogen activated protein kinases
MHC	Major histocompatibility complex
MOMP	Mitochondrial outer membrane permeabilization
mPT	Mitochondrial membrane permeability transition
MTX	Methotrexate
NEMO	NF-κB essential modifier
NF-κB	Nuclear factor κB
NFZ	Nefazodone
NIK	NF-κB inducing kinase
NPX	Naproxen
Nrf2	Nuclear factor-erythroid 2 (NF-E2)-related factor 2
NSAID	Non-steroidal anti-inflammatory drug
NTF	Nitrofurantoin
OFX	Ofloxacin
PARP	Poly (ADP)-ribose) polymerase
PERK	Protein kinase R-like ER kinase
PUMA	p53 up-regulated modulator of apoptosis
RAIDD	RIP-associated protein with a death domain
RIP	Receptor-interacting protein
RNAi	RNA interference
ROS	Reactive oxygen species
shRNA	short hairpin RNA
siRNA	short interfering RNA
SN	Simvastatin
SOD	Superoxide dismutase
SRXN1	Sulfiredoxin 1
TAK1	TGFβ-activated kinase 1
TGZ	Troglitazone
TNFα	Tumor necrosis factor α
TNFR	TNF receptor
TRADD	TNF receptor-associated death domain
TRAF	TNF receptor associated factor
UGT	Uridine diphosphate glucuronosyl-transferase
UPR	Unfolded protein response
XBP1	X-box binding protein 1

CURRICULUM VITAE

Lisa Fredriksson was born the 1st of January 1984 in Uppsala, Sweden. In June 2002 she completed her secondary education at Katedralskolan in Uppsala, with a major in natural science. A bit more than half a year later, in January 2003, she began her university studies to become a pharmacist. In 2007 she obtained her Master of Science in Pharmacy degree at the University of Uppsala after a six-month internship at the Division of Toxicology, Leiden University, under the supervision of Dr. Erik Danen. During this internship she investigated the role of integrins and oncogenes in chemosensitivity, work that later inspired to a publication. After another six-month internship at a pharmacy in Malmö, Sweden, she obtained her license to work as a pharmacist in 2008. However, the internship in Leiden had made her interested in pharmaceutical research and in April 2008 she began her PhD under the supervision of Prof. Bob van de Water. During her PhD she has investigated the role of inflammatory and drug-induced intracellular stress in the development of drug-induced liver injury. She has throughout this period learnt to master several new techniques such as high content confocal microscopy, high throughput siRNA screening as well as pathway analysis of gene expression data. Currently, she is working as a postdoc in the same lab to finalize the publications that will come as a result of her work.

LIST OF PUBLICATIONS

A live-cell imaging-based NF-κB nuclear translocation RNAi screen identifies novel regulators of TNFα-induced apoptosis through control of the (de)ubiquitinase A20
Fredriksson L*, Herpers B*, Benedetti G*, Di Z, de Bont H, Meerman JHN, de Graauw M, van de Water B.
Manuscript in preparation

Translation initiation factor EIF4A1 determines TNFα-mediated apoptosis in drug-induced liver injury through the stress protein CHOP
Fredriksson L*, Herpers B*, Wink S, Benedetti G, de Bont H, Danen EH, Luijten M, de Graauw M, Meerman JHN, van de Water B.
Submitted to Hepatology

High content imaging of Nrf2 and NF-κB activation as markers for the prediction of adverse drug-induced liver toxicity
Fredriksson L*, Herpers B¬*, Di Z, Hendriks G, Vrieling H, de Bont H, van de Water B.
Ready to be submitted to Journal of Hepatology

Automated analysis of NF-κB nuclear translocation kinetics in high-throughput screening
Di Z, Herpers B, **Fredriksson L**, Yan K, van de Water B, Verbeek FJ, Meerman JHN.
Under revision, PlosONE

TNFα-mediated NF-κB survival signaling impairment by cisplatin enhances JNK activation allowing synergistic apoptosis of renal proximal tubular cells
Benedetti G, **Fredriksson L**, Herpers B, Meerman JHN, van de Water B, de Graauw M
Accepted for publication, Biochemical Pharmacology

Diclofenac inhibits tumor necrosis factor-α-induced nuclear factor-κB activation causing synergistic hepatocyte apoptosis
Fredriksson L*, Herpers B*, Benedetti G, Matadin Q, Puigvert JC, de Bont H, Dragovic S, Vermeulen NP, Commandeur JN, Danen E, de Graauw M, van de Water B.
Hepatology. 2011

Cross-talk between integrins and oncogenes modulates chemosensitivity
Puigvert JC, Huveneers S, **Fredriksson L**, op het Veld M, van de Water B, Danen EH.
Molecular Pharmacology, 2009

* These authors contributed equally to the study.

ACKNOWLEDGEMENTS

It has now been a bit more than 4 years since I started this journey, a journey towards a PhD diploma, and now I have reached the final destination.

When I had half a year left of my masters to become a pharmacist, I had no plans to pursue a career in research. After only a few hours in the lab per week, with doing mostly pure chemistry work, there was nothing about research that attracted me. However, my determination to do the internship for my master thesis abroad, made me change my mind. At first I knew that I wanted to go to a big city, but when my professor in Toxicology told me about a cute little town in the Netherlands, a country that I barely heard about before, let alone visited, I thought that this option sounded even better. The fact that my present professor, Bob van de Water, was so quick and friendly in his way of answering the e-mails we exchanged made the choice even easier. Going for my master internship to Leiden was the best thing that I could ever have done, and this decision literally changed my life.

My first supervisors were Stephan Huveneers and Erik Danen. Without them agreeing with taking on a Swedish master student, I would never have made it to Leiden, and if that had not happened I would never have written this thesis. Thank you for accepting me as a student, for including parts of my work in your thesis Stephan, and for publishing the same work, together with Jordi Carreras Puigvert, leading to my first scientific article.

In relation to the above I would also like to show my gratitude to the complete "old" TOX-team for making my master experience so nice that I in the end decided that I wanted to do a PhD in the same lab. Marja Moerkens Noordzij, I am so very grateful for you being such great support, both in and outside the lab, already back then!

When coming back to the lab not much was like it had been. There were a lot of new people, but nice people. Giulia Benedetti, it has been great working so close with you. Always full of action. Thank you for sharing the burden of the early mornings and late nights to be able to perform the NF-κB screen. And thank you for your company. It is for sure not the same now when I do not have you in my room anymore. I miss our discussions about work, but also about non-work-related things. Bram Herpers, thank you for starting up our shared project so nicely! It made it very easy to get into the work quickly. Thanks to you the NF-κB screen was even made possible and also with you the inconvenient working hours were shared. I am, additionally, very thankful for the knowledge that you have transferred to me about everything that has to do with imaging. This was undoubtly helpful during the production of the data presented in this thesis, but I am sure that it will also help me in my future career.

Louise von Stechow, what a difference it made when you entered the lab! You have been such an inspiration and such an encouragement when it comes to everything and anything. You have been there and supported me for all the important decisions…all. You are always there for excellent advice, also when it comes to how to produce the best lentiviruses, but especially for discovering the wonderful world of translation initiation

together with me. With you I have made a true friend!

All the other TOX-members, old and new, thank you for helping me when I needed it, either if it was regarding calibrations of the pH-meter or for discussing disappearing proteins on the western blots. But also for keeping up the good spirits in the coffee corner, at the lunch table and in the lab.

Without the support of my family, none of this would have been possible. Mamma och pappa, I cannot imagine what you thought when I said that the 6 months that I had spent abroad was not enough, but that I would go away for another 4 years. I do not know what your secret is for getting such ambitious children, but I would guess that giving support, trust and the freedom to be independent has played a big role in it. I cannot thank you enough for this!! Peter, min käre bror, you are my biggest role model, also when it comes to an academic career. I was so impressed when you got your PhD and later professorships, and I for sure did not believe that I would have my own PhD one day. Thank you for your inspiration! La meva nova família i amics. Moltes gràcies per la vostra càlida benvinguda. Que significa molt per a mi. Ramon, a special thanks to you for the wonderful cover!

And last but not least, Jordi, my mentor, my inspiration, my biggest fan, my life, amor meu, without you nothing would have been the same. You were always there for support and you were the one that convinced me that I could do anything as long as I really wanted it, including a PhD. You have always, always, been there for me and I will always be there for you. This is the beginning of the rest of our lives, and I cannot wait to share it with you!! T'estimo tant!!